

The
University
Of
Sheffield.

**Department of
Chemical & Biological
Engineering**

Network Modelling of the Formation and Fate of Hydrogen Sulfide and Methane in Sewer Systems

By:

Moran Wang

A thesis submitted in partial fulfilment of the requirements for the degree of
Doctor of Philosophy

Supervisors:

Dr. Henriette Jensen, Dr. Rachel Smith

The University of Sheffield

Faculty of Engineering

Department of Chemical & Biological Engineering

March 2017

Abstract

Hydrogen sulfide is produced by sulfate reducing bacteria, which are mainly associated with the biofilms covering the surfaces in rising mains. Sulfide control strategies commonly used such as chemical dosage are costly for long-term management. The effect of physical and hydraulic conditions of sewers on sulfide formation has been investigated in recent years. One of the key parameters in modelling the formation of hydrogen sulfide is the pipe area-volume ratio (A/V), as this indicates the relative contribution between biofilm and wastewater processes. The A/V is naturally related to the pipe diameter. A high A/V is associated with small pipe diameter, and would lead to a high contribution from the biofilms and hence the potential for high hydrogen sulfide formation. However, it would also decrease the residence time of the wastewater, which would tend to decrease the amount of hydrogen sulfide formed. Based on the results of in-sewer process modelling, this study quantifies the importance of the pipe diameter and pumping strategy for optimal design for rising mains, to minimise hydrogen sulfide production, either to improve the life time for the downstream sewer structures or to minimise the potential chemical dosing needed in the rising mains. The model results from this study show optimal diameter options for both existing rising mains in terms of minimum hydrogen sulfide formation. The sensitivity analysis on model parameter based on the case studies also indicates the most uncertain parameters and COD fractions.

Methane is a problem acknowledged in some sewer networks around the world and is particularly of concern in China where sewer explosions can occur. Septic tanks are integrated parts of many Chinese sewer systems and methane is believed to be produced not only in sewer pipes, but also in septic tanks. Work has been done to look at how the anaerobic digestion model can be applied in combinations with sewer processes models to describe such a system. Model simulation results on methane formation in rising mains is similar to reported literature. The field measurements in the Chinese sewer system demonstrated high gas phase hydrogen sulfide and methane concentrations both in gravity systems and rising mains due to the surcharging sewer conditions. Future work has been proposed according to the local problems by discussing the benefits of applying sewer process and anaerobic digestion models based on this study.

Acknowledgments

First and foremost, I would like to express my deepest gratitude to Dr. Henriette S. Jensen, my supervisor, for her excellent supervision, persistent support, and valuable advice for my research and writing within the last five years (include obtaining my master's degree). I would like to thank Dr. Jensen for the patient guidance, encouragement, and advice she has provided throughout my study, whenever and wherever I face challenges and difficulties in my researches.

A very special gratitude goes out to Prof. Yanchen Liu and all the staff and colleagues in the group from School of Environment, Tsinghua University, Beijing, for providing field measurements data and supporting laboratory work. I would also like to thank Tsinghua University for offering me the postdoctoral researcher job opportunity after my study.

I am very grateful to Dr. Will Shepherd for constructing the sewer hydraulic model and providing hydraulic field measurements data for the two study catchments in the UK. Chapter 3 would not have been conducted without his technical support.

With a special mention to my friend, Dr. Xueyan Zhao, who helped and directed me learning MATLAB and other programming tools at the beginning of my study; and my colleague, Afifah Abd Rahim, who assisted me completing the lab work and experiments for Chapter 5.

I am also grateful to my friends, Dr. Xueyan Zhao, Dr. Wen Qiu, Dr. Yuan Chen, Dr. Kewei Duan, Shirui Chai, I-tung Chan for their companionship and support since I am living in Sheffield.

In addition, a special gratitude goes to the Department of Chemical & Biological Engineering for providing the scholarship.

And finally, last but by no means least, also to my parents, who always support and encourage me for my study. Thanks for all your encouragement!

Contents

Abstract.....	2
Acknowledgments	3
Nomenclatures	7
List of Figures	12
List of Tables	15
Chapter 1. Introduction	16
Chapter 2. Literature Review	19
2.1 Urban drainage system and urban wastewater - general background.....	19
2.1.1 Urban drainage system	19
2.1.2 General wastewater constituents	20
2.2 Sewer system and in-sewer processes.....	23
2.3 Hydrogen sulfide in sewers and sulfide related problems	26
2.3.1 Sulfide induced sewer corrosion.....	28
2.3.2 Sulfide and odour in sewers	30
2.4 Mitigation strategies on the formation of hydrogen sulfide in sewers	33
2.5 Methane in sewers a review	35
2.6 Sewer processes modelling and process models review.....	38
2.7 Parameters for modelling and the uncertainties and sensitivities	44
2.8 Sewer hydraulic conditions and hydraulic models	46
2.9 Summary of Literature Review.....	50
Chapter 3, Impact of sewer hydraulic condition on sulfide formation and build-up.	52
3.1 Introduction	52
3.2 Materials and Methodologies	55
3.2.1 Objectives, catchments information and concept for model set-up	55
3.2.2 Infoworks flow data and the pump operations	58
3.2.3 The selection of rising main pipe diameter	60
3.2.4 Flow Chart of Model Implementations	61
3.2.5 Model implementation and integrations.....	62
3.2.6 Comparison between sulfide formation kinetic equations in process models.....	63
3.3 Results and Discussion	64
3.3.1 Flow variations for Catchment A and B	64
3.3.2 Sulfide formation in different diameter pipes	67
3.3.3 The effect of COD fractions on sulfide formation	71

3.3.4 <i>Total sulfide production and pump operations</i>	72
3.3.5 <i>COD mass balance</i>	74
3.4 <i>Conclusions</i>	76
3.5 <i>Future work</i>	77
Chapter 4, <i>Global sensitivity analysis on model parameters.</i>	79
4.1 <i>Introduction</i>	79
4.2 <i>Methodology</i>	82
4.2.1 <i>Monte Carlo Simulation and data generation</i>	82
4.2.2 <i>Sensitivity analysis on model parameters</i>	86
4.3 <i>Results and Discussion</i>	87
4.3.1 <i>Model results on selected parameters</i>	87
4.3.2 <i>Comparison between sampling data and literature dataset</i>	94
4.4 <i>Conclusions and Discussions</i>	100
Chapter 5, <i>Methane formation in sewers and the relative contribution from septic tanks and sewer pipes.</i>	102
5.1 <i>Introduction</i>	102
5.1.1 <i>Septic tanks</i>	102
5.1.2 <i>Anaerobic digestion and the anaerobic digestion model (ADM)</i>	104
5.1.3 <i>SeweX model for methane production</i>	107
5.2 <i>Methodologies</i>	109
5.2.1 <i>Field measurements on selected septic tank</i>	110
5.2.2 <i>COD analysis method (Potassium Dichromate Method)</i>	110
5.2.3 <i>Solids settlement experiment</i>	112
5.2.4 <i>COD analysis method (spectrophotometric method)</i>	113
5.2.5 <i>ADM model implementation on the septic tank</i>	114
5.2.6 <i>SeweX model application for methane production</i>	114
5.3 <i>Results and Discussion</i>	115
5.3.1 <i>Septic tank COD removal rate</i>	115
5.3.2 <i>Solids settlement and mass transfer rate</i>	116
5.3.3 <i>ADM model results on the septic tank</i>	120
5.3.4 <i>SeweX model results on methane formation in rising mains</i>	123
5.4 <i>Conclusions</i>	125
Chapter 6, <i>Field measurements and modelling approach of a sewer catchment in China.</i>	126
6.1 <i>Introduction</i>	126
6.1.1 <i>Impact of urban development and realities of sewer systems in China</i>	127
6.1.2 <i>Methane induced sewer explosions</i>	128

6.1.3 <i>TU sustainable wastewater management centre</i>	130
6.2 Methodologies.....	131
6.2.1 <i>Gas monitoring in a residential gravity system</i>	132
6.2.2 <i>Gas monitoring in two pumping-rising main systems</i>	134
6.2.3 <i>Modelling approach on the gravity system</i>	135
6.3 Results and Discussion	137
6.3.1 <i>Gas concentrations in the gravity system</i>	137
6.3.2 <i>Gas concentrations in the pumping-rising main systems</i>	140
6.3.2.1 Hydrogen sulfide concentrations in the pumping-rising main systems.....	140
6.3.2.2 Methane concentrations in the pumping-rising main systems.....	144
6.3.3 <i>Modelling approach results on the gravity sewer pipe</i>	147
6.4 Conclusions and Future Work	149
Chapter 7, Conclusions	151
Publications	153
Appendices	154
Appendix A: Typical values for selected parameters in WATS model	154
Appendix B: Typical values for selected parameters in SeweX model	155
Appendix C: Suggested values for selected parameters in ADM 1 model	156
Appendix D: Suggested stoichiometric parameters in ADM 1 model.....	157
Appendix E: Matlab script for modelling the operation of pumping stations	158
Appendix F: Matlab script of WATS model for rising main and gravity sewers.....	159
Appendix G: Matlab script of SeweX model for rising main and gravity sewers.....	160
Appendix H: Matlab script of hydraulic and process model integration	161
Appendix I: Matlab script of SeweX model for methane formation.....	162
Appendix J: Matlab script of ADM 1 model for methane formation	163
References	164

Nomenclatures

Model parameters in WATS:

r_a	Hydrogen sulfide formation rate
X_{HW}	Heterotrophic active biomass in the water phase
X_{Hf}	Heterotrophic active biomass in the biofilm
X_{S1}	Hydrolysable substrate, fast biodegradable
X_{S2}	Hydrolysable substrate, slowly biodegradable
S_F	Fermentable substrate
S_A	Fermentable products (i.e. VFAs)
S_S	Readily biodegradable substrates ($S_F + S_A$)
S_O	Dissolved oxygen
COD	Total COD
S_{H_2S}	Total sulfide
α_w	Temperature coefficient for heterotrophic, aerobic water phase processes
α_f	Temperature coefficient for aerobic biofilm processes
α_r	Temperature coefficient for reaeration
α_{sf}	Temperature coefficient for sulfide formation in the biofilm
μ_{HW,O_2}	Maximum specific aerobic growth rate for heterotrophic biomass in the water phase (day^{-1})
μ_{HW,NO_3}	Maximum specific anoxic growth rate for heterotrophic biomass in the water phase (day^{-1})
ε_f	Relative efficiency constant for hydrolysis of the biofilm biomass
k_{h1}	Hydrolysis rate constant, fraction 1 (fast) (day^{-1})
k_{h2}	Hydrolysis rate constant, fraction 2 (slow) (day^{-1})
K_O	Saturation constant for DO ($\text{g O}_2 \text{ m}^{-3}$)
K_{NO_3}	Saturation constant for nitrate (g N m^{-3})
K_{Sw}	Saturation constant for readily biodegradable substrates in the water phase (g COD m^{-3})
K_{X1}	Saturation constant for hydrolysis, fraction 1 (fast) ($\text{g COD (g COD)}^{-1}$)
K_{X2}	Saturation constant for hydrolysis, fraction 2 (slow) ($\text{g COD (g COD)}^{-1}$)

q_{m,O_2}	Maintenance energy requirement rate constant for aerobic respiration in the water phase (day^{-1})
Y_{HW,O_2}	Yield constant for aerobic growth of heterotrophic biomass in the water phase ($\text{g COD (g COD)}^{-1}$)
Y_{HW,NO_3}	Yield constant for anoxic growth of heterotrophic biomass in the water phase ($\text{g COD (g COD)}^{-1}$)
Y_{Hf,O_2}	Yield constant for aerobic growth of heterotrophic biomass in the biofilm ($\text{g COD (g COD)}^{-1}$)
$S_{(-II)}$	Total $C_{H_2S} + C_{HS^-}$ in the water phase (g S m^{-3})
S_{SO_4}	Concentration of sulfate in the water phase (g S m^{-3})
MeS	Precipitated metal sulfide expressed in units corresponding to a water phase concentration (g S m^{-3})

Model parameters in SeweX:

S_{H_2}	Total hydrogen
S_{AC}	Concentration of acetate
$\frac{A}{V}$	Area-volume ratio
q_{ACETOG}	Acetogenesis rate coefficient
q_{ACIDOG}	Acidogenesis rate coefficient
k_{H_2S,H_2}	Hydrogenotrophic sulfidogenesis rate coefficient
$k_{H_2S,AC}$	Acetate-based sulfidogenesis rate coefficient
$k_{H_2S,PROP}$	Propionate-based sulfidogenesis rate coefficient
k_{CH_4,H_2}	Hydrogenotrophic methanogenesis rate coefficient
$k_{CH_4,AC}$	Acetoclastic methanogenesis rate coefficient
K_F	Saturation constant for fermentable substrates
$K_{H_2,SRB}$	Saturation constant for hydrogen in Hydrogenotrophic sulfidogenesis
$K_{AC,SRB}$	Saturation constant for acetate in Acetate-based sulfidogenesis
K_{PROP}	Saturation constant for propionate
K_{SO_4}	Saturation constant for sulfate
$K_{S_{AC,MA}}$	Saturation constant for acetate in acetoclastic methanogenesis
$K_{H_2,MA}$	Saturation constant for hydrogen in Hydrogenotrophic methanogenesis
K_{sf}	Saturation constant for S_s in biofilm
S_{FCOD}	Fermentable COD

S_{VFA} Volatile fatty acids

Model parameters in ADM1

C_i	Carbon content of component i
i	Component index
I	Inhibition function
j	Process index
$K_{A/B,i}$	Acid-base rate constant for component i
K_{dec}	First order decay rate for biomass death
$K_L a$	Gas-liquid transfer coefficient
K_m	Specific Monod maximum uptake rate
K_a	Acid-base equilibrium constant
K_H	Henry's law coefficient
K_I	Inhibition constant
K_S	Monod half saturation constant
N_i	Nitrogen content of component
p_{gas}	Pressure of gas
pH	$-\log_{10}[S_{H^+}]$
pK_a	$-\log_{10}[K_a]$
q	Flow
S_I	Inhibition component
t	Time
T	Temperature
V	volume
$Y_{substrate}$	Yield of biomass on substrate
$v_{i,j}$	Rate coefficient for component i on process j
$f_{product,substate}$	Yield (catabolism only) of product on substrate
p_i	Rate for process j
X_c	Composite/Particulate material
X_{ch}	Carbohydrates

X_{pr}	Proteins
X_{li}	Lipids
X_I	Particulate inerts
S_I	Soluble inerts
S_{su}	Monosaccharides
S_{aa}	Amino acids
S_{fa}	Total LCFA (long chain fatty acids)
S_{va}	Total valerate
S_{bu}	Total butyrate
S_{pro}	Total propionate
S_{ac}	Total acetate
S_{h2}	Hydrogen
S_{ch4}	methane
S_{IC}	Inorganic carbon
S_{IN}	Inorganic nitrogen
X_{su-h2}	Biomass
S_{cat}	Cations
S_{an}	Anions
$f_{sl,xc}$	Soluble inerts from composites
$f_{xl,xc}$	Particulate inerts from composites
$f_{ch,xc}$	Carbohydrates from composites
$f_{pr,xc}$	Proteins from composites
$f_{li,xc}$	Lipids from composites
N_{xc}, N_I	Nitrogen content of composites and inerts
$f_{fa,li}$	Fatty acids from lipids
$f_{h2,su}$	Hydrogen from sugars
$f_{bu,su}$	Butyrate from sugars
$f_{pro,su}$	Propionate from sugars
$f_{ac,su}$	Acetate from sugars
$f_{h2,aa}$	Hydrogen from amino acids

N_{aa}	Nitrogen in amino acids and proteins
$f_{va,aa}$	Valerate from amino acids
$f_{bu,aa}$	Butyrate from amino acids
$f_{pro,aa}$	Propionate from amino acids
$f_{ac,aa}$	Acetate from amino acids

List of Figures

Figure 2.1, Aerobic and anaerobic biological sulfur cycle in a sewer.....	28
Figure 2.2, Schematic of sulphur cycle in gravity sewers and concrete corrosion.....	29
Figure 2.3, Concentration-pH / Percentage-pH diagram of sulphur species in wastewater.	31
Figure 2.4, Hydrogen sulfide control methods in sewer systems	33
Figure 2.5, Schematic of sewer biofilm penetration by MA and SRB	37
Figure 2.6, Schematic of wastewater anaerobic transformations and biofilm process sulfide formation.....	41
Figure 2.7, Sketches of fully filled rising main and partially filled gravity sewers	47
Figure 3.1, Relationship between A/V ratio and pipe diameter.....	53
Figure 3.2, Methane production with A/V and HRT variation.....	54
Figure 3.3, Satellite images of Catchment A and Catchment B	56
Figure 3.4, Layout of study catchment area and rising mains with flow recording locations.....	57
Figure 3.5, Screenshot intercepted section of Catchment A in Infoworks CS.	58
Figure 3.6, Wet well, gravity flow, pump operations in Catchment A collection point.....	59
Figure 3.7, A/V ratio with selected pipe diameter range for rising main A and B.....	60
Figure 3.8, Variability of weekday flows at Catchment A flow recording location.....	65
Figure 3.9, Average daily dry weather flow variability in 7 days a week.....	66
Figure 3.10, Average of all DWF in Catchment A and B before rising mains	66
Figure 3.11, The variations of H ₂ S concentration in a day on different diameter pipes at the end of the rising main in Catchment A (a is WATS, b is SeweX).	68
Figure 3.12, Typical modelled sulfide concentration from WATS and SeweX model	69
Figure 3.13, Selected diameter pipes on sulfide formation	69
Figure 3.14, The variations of H ₂ S concentration in a day on different diameter pipes at the end of the rising main in Catchment B.....	70
Figure 3.15, Lowest and highest sulfide generation pipes in figure 2.14b	70
Figure 3.16, Sulfide formation on extreme organic substrates concentrations in different diameter pipes	71
Figure 3.17, Total sulfide production in different diameter pipes.....	72
Figure 3.18, Variation of sulfide production with different pump operation frequencies for rising main A.....	74
Figure 3.19, Transformation of organic substrates in the rising mains.....	75

Figure 3.20, Total COD mass balance in the rising main	76
Figure 4.1, Comparison between COD fractions (percentage).	80
Figure 4.2, Empirical CDF curves for the selected parameters based on 1000 random draws from the random number generator, Dataset B	85
Figure 4.3, Monte Carlo simulation results of hydrogen sulfide distribution	88
Figure 4.4, Monte Carlo simulation results on selected model parameters for rising main A in 6h	90
Figure 4.5, Coefficients related hydrogen sulfide concentration distribution curves.....	91
Figure 4.6, COD related hydrogen sulfide concentration distribution curves	92
Figure 4.7, Coefficient related hydrogen sulfide distribution curves.....	93
Figure 4.8, COD related hydrogen sulfide distribution curves.....	93
Figure 4.9, Annually COD variations in wastewater at the inlet of WwTP.....	94
Figure 4.10, The annually variation of inflow rate and rainfall at the wastewater treatment plant	95
Figure 4.11, The annual variation of COD against flow rate in the WWTP	96
Figure 4.12, Empirical cumulative distribution curve of the measured COD concentrations	97
Figure 4.13, Hydrogen sulfide concentration as function of temperature variation	98
Figure 4.14, Weather and wastewater temperature variations at the wastewater treatment plant	99
Figure 5.1, Schematic of septic tank layers, processes, and HRT.....	103
Figure 5.2, COD fraction and anaerobic digestion processes in ADM No 1 model	105
Figure 5.3, Potassium dichromate method COD analysis instruments	111
Figure 5.4, Spectrophotometer and COD vials used for COD analysis	113
Figure 5.5, Wastewater solids settlement experiments results	117
Figure 5.6, Solids layers of the four wastewater samples in the solids settlement experiments ..	117
Figure 5.7, Change of COD fractions within 10 days of anaerobic digestion transformation in the sludge layer.....	120
Figure 5.8, Change of COD fractions after first 7 days of transformations	121
Figure 5.9, Variation of COD fractions after a stabilized concentration, 30 days transformation .	122
Figure 5.10, Methane production in wastewater in rising mains	124
Figure 6.1, The Fushougou ditch sewer system in Ganzhou City, China	126
Figure 6.2, Surcharged manholes on dry weather flow days in the study catchment in the TUSWMC	128
Figure 6.3, CCTV footage and the scenes photos of methane induced sewer explosions in China	129
Figure 6.4, Schematic of a selected catchment in the TUSWMC centre	130
Figure 6.5, Change of annual flow rate at the WwTP in the selected catchment.....	131

Figure 6.6, Schematic of the residential gravity sewer systems for gas monitoring	132
Figure 6.7, Gas sensors and the installations in the manholes.....	133
Figure 6.8, Schematic of two pumping rising main systems in the catchment	134
Figure 6.9, Gas phase hydrogen sulfide concentrations in the gravity sewer system	137
Figure 6.10, Wastewater temperature variations vs. sulfide concentration in the manholes.....	138
Figure 6.11, Methane concentrations in manhole 5	139
Figure 6.12, Hydrogen sulfide gas concentrations at the two pumping stations	142
Figure 6.13, Hydrogen sulfide concentrations at the wastewater treatment plant and the flow rates.....	143
Figure 6.14, Methane gas concentrations in the two pumping stations.....	145
Figure 6.15, Methane gas concentrations at the wastewater treatment plant	146
Figure 6.16, Change of COD fractions in the gravity sewer pipe within 10 minutes.....	147
Figure 6.17, Change of methane concentration in the gravity sewer pipe within 10 minutes	147
Figure 6.18, Sampling data of wastewater COD in the main trunk sewer pipe.....	148

List of Tables

Table 2.1, Aerobic and Anaerobic transformations in WATS model.....	41
Table 2.2, Comparison between different process models reviewed.....	44
Table 3.1, WATS model matrix expression of the processes in rising mains.....	62
Table 3.2, Two sets of COD fractions and literature standard COD fraction	63
Table 3.3, Kinetic equations and rate coefficients for the formation of hydrogen sulfide	64
Table 3.4, Average hydraulic residence time and A/V ratio on two rising mains with different diameter pipes	67
Table 4.1, Sewer process model parameters and distribution data	83
Table 4.2, Different ratio of standard deviation over average on parameter and sulfide	87
Table 4.3, Comparison of COD fractions between datasets	98
Table 5.1, COD fractions in Anaerobic Digestion Model ADM No.1	106
Table 5.2, Stoichiometry and kinetics of SeweX model describing methanogenesis and sulfidogenesis processes – model matrix	108
Table 5.3, Chemicals and instruments used in the COD analysis.....	110
Table 5.4, The variation of wastewater quality before and after septic tank	115
Table 5.5, Total COD analysis results of wastewater solids settlement samples	118
Table 5.6, Wastewater COD mass transfer rates	119

Chapter 1. Introduction

Sewer systems are important parts of the urban infrastructure and play an essential role in collecting and conveying wastewater safely. Simultaneously, complex chemical and biological transformations are taking place in wastewater (Hvitved-Jacobsen et al., 2013). This, for example, leads to the formation of noxious or hazardous gases such as hydrogen sulfide and methane through the biochemical transformations of wastewater in sewers. Hydrogen sulfide is a universal problem existing in almost all sewer systems in the world, due to hydrogen sulfide causing in odour nuisance and sewer corrosion, and consequently of air pollution and damage to sewer structures (Jensen et al., 2009). Severe corrosion, especially concrete corrosion, is observed and reported in many studies. Methane is considered to be a major source of green-house gas emissions (Liu et al., 2015b), and is highly flammable and explosive. The formation of methane and its related problems is only being reported in a few countries and regions such as US, Australia and China (Guisasola et al., 2008). Significant methane production has also been reported in septic tanks in the US (Diaz-Valbuena et al., 2011). Intensive methane concentration has been measured in rising mains in Australia (Guisasola et al., 2009). High methane concentration has been reported in both sewer pipes and septic tanks in China, and hundreds of methane induced sewer explosion occur in China each year which results in many casualties as well as economic loss (Li, 2007).

Hydrogen sulfide and methane are produced by sulfate reducing and methanogenic bacteria, respectively, which are mainly associated with the biofilms and sediments. This means the area-volume ratio (A/V) is one of the key parameters affecting the model description of the formation of hydrogen sulfide and methane, because it defines the relative contribution from biofilm and wastewater (Sharma et al., 2008). Other parameters include temperature, pH, and organic matter, often represented by total COD, sulfate and hydraulic condition has been identified as the most influencing parameters (Donckels et al., 2014). Among all these parameters, the hydraulic condition is the only physical mechanical factor which is influenced by water consumption, pump operations, sewer system dimensions, and layouts. Not only can the flow control the wastewater residence time, but also the growth and deposition of

biofilm and sediments which contributes to the processes of hydrogen sulfide and methane formation.

The operation of a septic tank is similar to that of an anaerobic digester. Hence, septic tanks have a high potential for methane formation. Methane is believed to be produced through anaerobic digestion process in the sludge layer in septic tanks. In for example the UK and US, septic tanks are normally only being used as treatment facilities in remote areas and farming communities. However, in China, septic tanks are used as additional systems before wastewater is discharged into the sewer network for pre-treatment (Su et al., 2011). This is done as a response to rapid urbanisation and pressure on the systems. Hence, it is important to understand the relative contribution and individual processes in sewer pipes and septic tanks.

The aim of this thesis is to investigate the hydraulic mechanics associated hydrogen sulfide formation and sulfide induced corrosion, and to look at methane formation in septic tanks and sewer pipes. One of the main objectives is to understand the influence of pipe dimension, area-volume ratio and hydraulic residence time on the formation of hydrogen sulfide by using sewer processes modelling approach. The current WATS in-sewer process model has been extended to the scope of the studies to examine the formation and fate of methane in sewers with real time field network monitoring and supporting laboratory work to investigate the relative contribution from septic tanks and sewer pipes, from biofilm, wastewater, and sediments. It has also been focused on the adaptation of the in-sewer process models to different physical structures in the sewer networks to allow for a more holistic approach to system modelling. The sources of uncertainty in the application of the WATS model to the simulation of hydrogen sulfide in case study sewers have been investigated, and the uncertainty in the model simulations has been quantified.

This thesis consists of seven chapters. Chapter 1 gives a background introduction and Chapter 2 summarises literature review on the current situations related to the topics. Chapter 3 works on the effect of hydraulic condition in sewer pipes on sulfide formation. Chapter 4 investigates the most sensitive model parameters especially COD fractions on sulfide formation as an extension for previous uncertainty studies. Chapter 5 illustrates the

transformation processes involved with septic tanks, and methane formation in septic tanks and sewer pipes. Chapter 6 reviews the sewer systems and current situations in China with some field measurements, which provides an outlook on finding possible solutions and proposing for future work. Lastly, Chapter 7 gives an over-arching conclusion of the studies and results for the whole thesis.

Chapter 2. Literature Review

2.1 Urban drainage system and urban wastewater - general background

2.1.1 *Urban drainage system*

Urban drainage system is the infrastructure for the interactions between human water consumption activities and natural water cycle in urban areas. The urban drainage system is the combined term for three main components, namely sewer systems, wastewater treatment plants, and receiving waterbodies (Butler and Davies, 2010). Urban drainage system is one of the most fundamental elements of urban infrastructure, which becomes more important with the development and improvement of technology and life quality. In urban areas there are two main types of water requiring drainage: wastewater from domestic, commercial and industrial activities; and stormwater run-off from precipitation. Both types of wastewater are handled through urban drainage systems, to reduce the risk of spreading of diseases and to reduce the risk of flooding (Butler and Davies, 2010).

With a focus on in-sewer processes, this thesis will mainly focus on wastewater during dry weather flows and hence stormwater runoff will not be discussed further. Wastewater generally contains a complex mixture of soluble substrates and solids, which are either organic and inorganic (Butler and Davies, 2010). Fresh wastewater which has just been discharged from sources is normally a light grey colour with a soapy and musty smell (Marleni et al., 2012). Due to the physical, chemical and biological processes that occur in sewer systems and wastewater treatment plants, the character of wastewater changes gradually with time during transport. At the downstream end of sewer systems, it is usually called aged wastewater or stale wastewater, which is a dark grey colour or sometimes completely black. The smell of aged wastewater has a strong odour of “rotten eggs” which is particularly easy to spot at treatment works (Marleni et al., 2012).

The concentrations of dissolved substrates and insoluble materials are assessed as wastewater quality. Significant quality changes take place during the transport in sewer systems before wastewater reaches treatment plants (Marsalek et al., 2008). However, the chemical and physicochemical aspects of wastewater can be described by a small proportion

of substances (Butler and Davies, 2010). Which means it is the constituents such as organic matter, oxygen, sulfate, which affects the transformation processes.

2.1.2 General wastewater constituents

Solids, dissolved oxygen (DO), organic matter, together with other important contents such as nitrate, phosphorus, and sulphur are defined as wastewater quality parameters (Butler and Davies, 2010). These parameters are very important for understanding the wastewater transformation processes and for modelling approach.

Solids is one of the three states of matter, which is structural rigidly in wastewater and resistance to shape or volume changes. Four categories of solids have been classified in wastewater based on particle size: gross ($>6000\mu\text{m}$); grit ($6000\mu\text{m} - 150\mu\text{m}$); suspended ($150\mu\text{m} - 0.45\mu\text{m}$); dissolved ($<0.45\mu\text{m}$), with the former two fractions contribute to the growth of biofilm and sediments, and the dissolved fraction in particular contributing to the biochemical transformation processes (Butler and Davies, 2010). The amount of solids in wastewater varies in different sewer systems, and the larger particles can easily build up and causing blockages (Laplace et al., 1992). It is the flow rate, velocity and shear stress that control the movement and build-up of solids, hence for combined sewers the occasional high storm water flows are often required to move the solid load through the systems in order to prevent clogging (Arthur and Ashley, 1998, Suarez and Puertas, 2005). However, in most situations, having combined sewers can result in more sediments to be found in the sewers which originate from such as road wash-off, ingress leaves, and street materials (Ashley and Crabtree, 1992). Therefore, the use of combined sewers is not the specific solution to prevent sediment in sewers even with peak flows due to stormwater inflows. Self-cleaning sewers are ideal for the design of sewers under different conditions (May et al., 1989).

Oxygen is partially soluble in water and hence oxygen in wastewater is referred to as dissolved oxygen (DO) (Butler and Davies, 2010). Oxygen is one of the most important parameters of wastewater which determines the aerobic, anaerobic or anoxic processes of wastewater transformation (Hvitved-Jacobsen et al., 2013). The influencing factors on DO saturation concentration in wastewater are complex, and mainly depend on temperature, pressure, pH, flow rate and biochemical transformations in the sewer systems (Li et al., 2013). The DO

saturation concentrations of dissolved oxygen vary due to different locations and flow conditions along a sewer system and is dependent on the reaeration rate and the uptake processes (Huisman et al., 2004a). The DO concentration in wastewater decreases with the increase of temperature and the decrease of atmospheric pressure. Typical DO saturation concentration in water is between 11.33mg/l and 10.15mg/l at 10°C to 15°C (Butler and Davies, 2010), while typical average DO concentration in wastewater is around 4g/m³ in most situations at joints and connection locations, which is important to maintain the aerobic condition (Hvitved-Jacobsen et al., 2013). However, the DO concentration is likely to be higher near the house connections and sewer falls and drops structures (Mourato et al., 2003), and can get much lower further in the downstream systems (less than 0.1 g/m³) or even can get anaerobic condition (Gudjonsson et al., 2002). Thus, to understand the sewer processes and investigate the transformations of wastewater in sewers the first and foremost task is to measure or model the DO concentrations (Gudjonsson et al., 2002), because it directly defines aerobic or anaerobic/anoxic conditions, which controls a lot of the processes of interest for in-sewer process model predictions.

Organic matter or organic compounds in wastewater can occur as particulate matter or as solutes (Butler and Davies, 2010). Both particulate and soluble organic matter contributes to the transformations of wastewater and the simulation of model processes (Batstone et al., 2002b, Sharma et al., 2008, Hvitved-Jacobsen et al., 2013). Carbohydrates and proteins are the main forms of organic compounds in wastewater (Nielsen et al., 1992). The organic matter in wastewater typically consists of protein (40-60%), carbohydrates (25-50%), oil and fats (8-12%) (Safoniuk, 2004). Similarly summarized in other studies: protein (28%), carbohydrates (28%), lipids (31%)(Raunkjær et al., 1994); protein (30%), carbohydrates (30%), lipids (30%) (Batstone et al., 2002a). A portion of organic compounds are reactive and, can be easily transformed by means of biochemical reactions such as hydrolysis and fermentation. Other compounds are to a certain extent inactive and stable in physical and chemical aspects within the normal residence time of sewer networks (Vollertsen and Hvitved-Jacobsen, 2002).

The chemical oxygen demand (COD), total organic matter (TOC), and volatile solids (VS) are normally used to characterize the concentration of organic compounds in wastewater (Hvitved-Jacobsen et al., 2013), while the biochemical oxygen demand (BOD) is used to

indicate the amount of biodegradable organic matter (Orhon et al., 1997). The biodegradability of wastewater is defined by BOD/COD ratio, where a high BOD/COD ratio means readily biodegradable wastewater, and a low ratio indicates it is comparatively slowly biodegradable (Vollertsen and Hvitved-Jacobsen, 2002). It is all the particle and soluble, readily and slow biodegradable organic matter participate in the transformations. They are specified to individual fractions in sewer processes models. The biodegradability of wastewater needs to determine some model parameters. This can be done by means of analysing oxygen utilization rate (OUR) (Xu and Hasselblad, 1996). The calculation of COD fractions and the determination of particle size distribution is also part of the standard method for the measurement of wastewater biodegradability (Dulekgurgen et al., 2006). The degradation of large particle size organic substrates requires more oxygen than that of small particle size ones (Karahan et al., 2008). The concentration of organic matter in wastewater is very important for both the chemical and biological transformations and the modelling approaches on in-sewer processes (Nielsen et al., 1992).

Other important parameters are nitrogen, phosphorus and sulphur, which also play a significant role in in-sewer processes. Protein and ammonia nitrogen are the main forms of nitrogen and organic nitrogen, they are normally expressed as ammonia (NH_3) and ammonium (NH_4^+); nitrate and nitrite (NO_3 , NO_2). The ammonia biological oxidation is the major process associated with nitrogen in sewer systems, involving further oxidation from nitrite to nitrate (Baban and Talinli, 2009). Nitrogen oxides such as amino acids also contribute to the formation of hydrogen, which further results in methane production (Batstone et al., 2002a). Phosphorus in wastewater mainly occurs in the form of phosphates. It is one of the most important elements initiating eutrophication when discharged to natural water bodies without appropriate treatment (Gutierrez et al., 2010). Sulfide and sulfate are the main forms of sulphur elements existing in wastewater which include sulfate (SO_4^{2-}), sulfite (SO_3^{2-}) and sulfides (S^{2-}), and hydrogen sulfide (H_2S) both in water and gas phase. Sulfate, sulfite and sulfides influence the formation of hydrogen sulfide in sewers, and hydrogen sulfide released from water is the leading cause of odour, corrosion and health risks in sewer systems (Hvitved-Jacobsen et al., 2013).

2.2 Sewer system and in-sewer processes

Sewer systems are the drainage systems for collecting and conveying wastewater and stormwater to treatment plants or discharging it to the environment in appropriate conditions (Read, 2004). Foul sewage comes from domestic, industrial and commercial water consumption; stormwater includes flows from urban areas such as roofs, streets, and paved surfaces. Sewer systems consist of a large number of sub-components for instance pipes, manholes, pumping systems, wells, septic and storage tanks, channels and tunnels (Butler and Davies, 2010). There are two main types of sewer pipes; pressure sewer and gravity sewer (Butler and Davies, 2010). Pressure sewer is also called pressure main, rising main, or force main, in which the wastewater is always full flow but discontinuously. Wastewater flow in a rising main is driven by external forces such as pumped systems, while the flow in gravity sewers follows the gravitational force. A rising main is normally filled with bulk water phase plus biofilms covering the inner pipe surfaces, while a gravity sewer contains sediment, bulk water, biofilm, and an upper atmosphere (Hvitved-Jacobsen et al., 2013).

There are currently three types of sewer systems in towns and cities: the combined system, separated system and partially separated system (Read, 2004). In many countries, almost all sewer system was constructed as combined system in the past (except in some specific countries such as tropical areas with significant amounts of precipitation), and they are still commonly existing in older towns and cities (Metcalf, 2003). In early 20th century, the separated system (sanitary sewer) was introduced. Foul sewage and stormwater were discharged separately to treatment plants and natural watercourses without interactions. The partially separated system is generally a separated system, only backyards and back roofs surface water is occasionally drained into sanitary sewers for convenience and to reduce site costs (Read, 2004). At current time, the separate system is mostly considered to be the best option for new construction and for replacement of old combined system with combined sewer overflows (CSO) pollution problems (Butler and Davies, 2010). Separate sewer systems are also more effective for downstream wastewater treatment than combined sewer system with diluted wastewater (U.S. Environmental Protection Agency (EPA), 2004). However, the combined sewer is still required for some situations with polluted stormwater or runoff from foul catchment surfaces where treatment is desired before discharging. Most the towns and cities today are hybrid systems where the combined system is located in the town centre or

the old part of city area; the newly constructed residential area and suburban industrial area are often all separated systems (Butler and Davies, 2010).

Up to 90% of the sewer system consists of pipes which are normally of circular shape with a diameter from 200 mm onwards for gravity pipes, and 100 mm onwards for rising mains. In the UK, clay, concrete, PVC, iron and steel are the most common materials for sewer pipes construction (Butler and Davies, 2010). Manholes provide manual work access point for inspection, testing and cleaning purposes. Manholes are also normally built as circular shapes with metal or precast concrete covers for protection (Melnick and Melnick, 1994). A manhole is typically installed for every 100 meters of sewer line (Read, 2004), however, the average distance between manholes are normally less because they are also placed at junctions, drops and at locations where pipe diameter and slope changes. Pumping systems consist of pumping stations, pumping wells/tanks and rising mains. A pumping system is required to overcome geographical obstructions and to avoid deep excavation that would be needed for gravity sewers (Jones Jr, 1970). Gully inlets which are also called gully pots are for stormwater runoff from urban surfaces. Water seals are installed for gully pots if they are connected to combined sewer systems to prevent odour emission (Authorities, 2013). Sewer ventilation is very important for keeping the relative humidity down and controlling the transport of gasses. It is also required for either foul sewer or combined sewer to avoid noxious and explosive gases build up (Pomeroy, 1945).

Transformations of wastewater quality occur during the transport in the sewer systems. The physical, chemical and biological in-sewer processes are complex and associated with not only the concentration of wastewater constituents such as solids, oxygen, organic matter, but also the redox transformation conditions. In general, there are two major transformation conditions in sewers: aerobic and anaerobic (Hvitved-Jacobsen et al., 2013). When there is no presence of oxygen or the DO concentration in wastewater is extremely low, the anoxic respiration process dominates, where nitrate or other oxidized nitrogen compounds acts as electron acceptor instead of oxygen in the oxidation of organic matter (Hvitved-Jacobsen et al., 2013). Some basic processes under aerobic and anaerobic conditions include hydrolysis, degradation and fermentation (Vollertsen and Hvitved-Jacobsen, 2000). Both aerobic and anaerobic hydrolysis are processes where large compounds are decomposed to small

molecules with the presence of enzymes for better utilization by bacteria (Vollertsen et al., 1999). Fermentation is a metabolic process of converting large compounds to small molecules such as acids and gases under the absence of oxygen (Prescott et al., 2005). The major products through fermentation processes in wastewater are mainly VFAs (volatile fatty acids or short-chain fatty acids), hydrogen sulfide and methane gases (Lee et al., 2013).

Aerobic processes in sewers are relatively fast compared to anaerobic due to the activity of bacteria and long residence time. Wastewater quality changes during the transport in sewers with a reduction in the concentration of biodegradable organic substrates together with the production of heterotrophic biomass (Hvitved-Jacobsen et al., 2013). The flows in gravity sewers consist of the water phase and the upper sewer atmosphere. Reaeration is a dynamic process at the free water surface with gas-liquid mass transfer, where oxygen is constantly entering the water phase from the upper sewer atmosphere (Huisman et al., 2004b). The reaeration rate is influenced by many factors and mainly dependent on Froude number; the reaeration rate can be calculated by models with empirical equations (Lahav et al., 2006a). Ventilation is important for reaeration, but also to maintain good conditions for sewer workers. However, the ventilation in sewers is complex and hard to quantify in model simulations (Ward et al., 2011). The effect of aerobic process on wastewater quality is specifically significant during dry weather flows when the compounds in the wastewater is not diluted by stormwater (Flamink et al., 2005). The aerobic process prominently decreases the soluble and biodegradable organic matter in wastewater. However, the removal of phosphorus and the denitrification process are reduced simultaneously, the low organic matter content has a negative effect on the potential removal efficiency in the downstream wastewater treatment plants (Almeida et al., 1999). This problem has also regularly been reported at field site sewers and treatment works (Abdul-Talib et al., 2002a). Hence, it is important to understand the transformations of wastewater constituents, not only for investigating the in-sewer processes, but also for better performance for the downstream wastewater treatment works. The aerobic condition of wastewater, along with temperature and pH are the vital parameters contribute to the organic matter transformation process and sulfide related problem in sewers (Nielsen et al., 2006b). Aerobic conditions also relate to the emission of hydrogen sulfide gas and sulfide oxidation, which is relatively high particularly under turbulent flow conditions (Nielsen et al., 2008a).

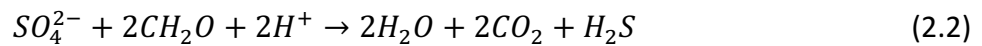
The concept of anoxic process had rarely been studied in the past (Schmitt and Seyfried, 1992). It now has been investigated in a number of studies since the sulfide control strategies have been implemented for sewer management, especially with the introduction of nitrate dosage (Mathioudakis and Aivasidis, 2009). In order to control sulfide related problems, anoxic processes is usually established on purpose (Yang et al., 2005). Both the anoxic sulfide oxidation and the denitrification processes are very important for the potential removal efficiency on downstream treatment plants (Abdul-Talib et al., 2002b). Process models have been developed for anoxic transformations in wastewater focused on the simulation of nitrate and nitrite utilization rate (Abdul-Talib et al., 2005). When the nitrite concentration in wastewater fairly matches the nitrate concentration, the anoxic process in bulk water phase can be simplified as the nitrate reduction to nitrogen (Abdul-Talib et al., 2002a).

To sum up, it is important to understand the difference between aerobic, anaerobic and anoxic processes. Hydrolysis, fermentation, methanogenesis, and sulfate reduction are the dominant processes under anaerobic conditions (Hvitved-Jacobsen et al., 2013). Anaerobic hydrolysis is the transformation of hydrolysable substrates to biodegradable and fermentable substrates through the effect of enzymes (Vavilin et al., 2008). The fermentation process means the organic matter is both electron donor and electron acceptor. It normally involves the formation of hydrogen sulfide and methane. Fermentation products are produced by the transformation of readily biodegradable substrates, fermentable substrates, and VFAs (Ting and Lee, 2007). Methane production from fermentation products is described as methanogenesis. Methane formation in sewers is hazardous due to the explosion risk and methane is also a green-house gas contributing to climate change (Guisasola et al., 2008). Hydrogen sulfide formation from sulfide reduction processes is one of the main sewer gases involved with in-sewer processes (Transfer and Pomeroy, 1974).

2.3 Hydrogen sulfide in sewers and sulfide related problems

Hydrogen sulfide has been recognised as a universal and ubiquitous problem in sewer systems due to the odour and corrosion problems, and it has fuelled the investigations of the in-sewer processes for many decades (Pomeroy, 1959, Transfer and Pomeroy, 1974, Boon, 1995,

Hvitved-Jacobsen et al., 2013). In general, hydrogen sulfide is produced by sulfide reducing bacteria (SRB), primarily *Desulfovibrio* and *Desulfotomaculum* mainly associated with biofilms and sediments in sewer pipes (Firer et al., 2008, Jensen et al., 2009, Jiang et al., 2013). The production of hydrogen sulfide mainly comes from two routes in wastewater. Firstly, the fermentation of organic compounds such as proteins and amino acids, as equation 2.1 shows an example of amino acid degradation. Secondly, the redox reaction of sulfate reduction as equation 2.2 shows (Hvitved-Jacobsen et al., 2013):



Where equation 2.1 shows an example of amino acids degradation – the anaerobic hydrolysis of cysteine, one of the major source of sulfide production with the participant of heterotrophic bacteria. Equation 2.2 indicates the complete redox reaction of sulfate reduction and hydrogen sulfide formation, where CH_2O signifies an example of organic composition.

The sulfur cycle in a sewer system is involved with the transformations of organic matter and the transfer between sulfur, sulfide and sulfate. Figure 2.1 shows the aerobic and anaerobic biological sulfur cycle in sewers.

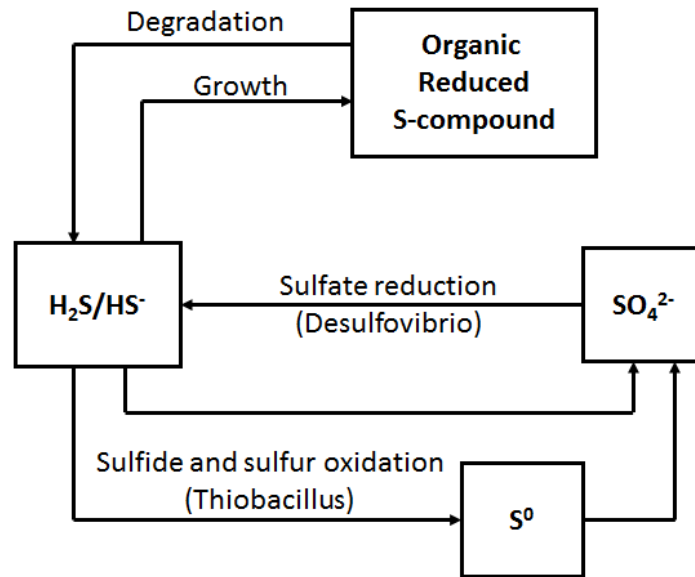


Figure 2.1, aerobic and anaerobic biological sulfur cycle in a sewer (Hvitved-Jacobsen et al., 2013).

The formation of hydrogen sulfide occurs in wastewater phase, biofilms, and sediments. The growth of sulfate reducing bacteria SRBs is a slow process, and it is more retained and kept in the biofilms and sediments than in the water phase, where it is flushed away with the flow. That is why the formation of hydrogen sulfide is mainly associated with the biofilms and sediments (Hvitved-Jacobsen et al., 2013). The growth and degradation processes are also involved with a series of heterotrophic bacteria.

2.3.1 Sulfide induced sewer corrosion

Sewer corrosion, especially concrete corrosion, is caused by hydrogen sulfide build-up in the sewer atmosphere. The build-up is controlled by air-water mass transfer of hydrogen sulfide from the wastewater to the sewer atmosphere and insufficient ventilation (Nielsen et al., 2012). Figure 2.2 gives a simple illustration of the emission process of hydrogen sulfide from water phase, the oxidation of hydrogen sulfide and concrete corrosion.

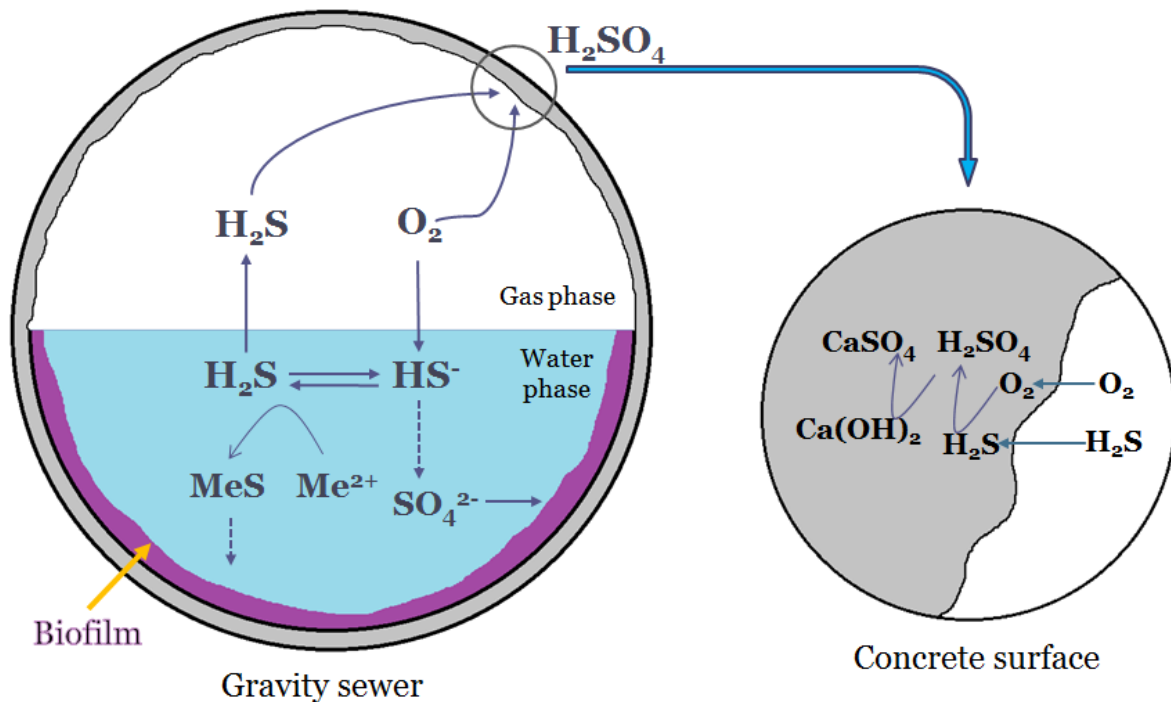
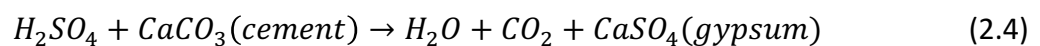


Figure 2.2, schematic of sulphur cycle in gravity sewers and concrete corrosion.

As illustrated in Figure 2.2 in gravity sewers, hydrogen sulfide gas is released from the free water surface and entering into the sewer atmosphere above, where it makes contact with the moist sewer walls and is oxidized to sulfuric acid as shown in eq. 2.3. Once the pH of concrete surface is reduced to 9, the sulfide oxidizing bacteria (SOB) starts to grow and form biofilms on the concrete surface which continuously absorb hydrogen sulfide and produce sulfuric acid. Sulfuric acid easily reacts with the concrete or iron materials of sewer pipe which further produces metal sulphates (Vollertsen et al., 2008b). Concrete is a composite material which mainly consists of cement, aggregates and pebbles, and a major component in sewer pipe cement is limestone (Andersson et al., 1989). Biogenic sulfuric acid penetrates into the concrete and reacts with the alkaline materials (chemistry illustrated in Equation 2.4). As equation 2.4 indicates the concrete sewer corrosion process, concrete pipes are severely consumed by hydrogen sulfide in real time situations, only left hard pebbles on the pipe surface and normally in dark black colour (Nielsen et al., 2008b).



Equation 2.4 shows the reaction between sulfuric acid and alkaline cement in the concrete, which is mainly calcium hydroxide or calcium carbonate (Hvitved-Jacobsen et al., 2013). The reaction product calcium sulfate (gypsum) detaches from the surface and leaves with water flow and air movement. For metal material pipes, two main reactions take place as follows:



In Equation 2.5 and 2.6, where Me represents metals in general. Metal corrosion in sewer systems has been observed for example in pumping stations and where electronic equipment is installed (Hvitved-Jacobsen et al., 2013). Equation 2.5 shows the metal corrosion process, the reaction between sulfuric acid and metal produces metal sulfate and hydrogen gas. Due to the chemical properties of metal, it can be the electron donor which directly reacts with hydrogen sulfide in sewer pipes, reaction products include metal sulfide and hydrogen gas as shown in equation 2.6. Hydrogen sulfide induced sewer corrosion results in costly replacement and restoration of sewer systems. It was estimated that the rehabilitation of sewer pipes due to sulfide corrosion costs \$ 430 million a year in Los Angeles in the US (Sydney et al., 1996) and € 5 million per year at the Flanders region in Belgium (Vincke, 2009), which represents 10% of the total costs spend on urban drainage system every year (Vincke, 2009). The costs of sewer pipe replacement due to corrosion for Germany and Australia is €100 billion and \$100 billion a year respectively (Kaempfer and Berndt, 1998, Brongers, 2002).

If sewers are made from different materials, for example, plastic pipes, hydrogen sulfide released from water phase will stay in the sewer air phase and travel with the movement of the air as dragged by the water flow or by ventilation. Hydrogen sulfide will then be released into the atmosphere or be oxidized once it is transported to a location with concrete or metal materials.

2.3.2 Sulfide and odour in sewers

The odour nuisance of sewer system mainly comes from hydrogen sulfide, along with ammonia and volatile fatty acids (VFAs) (Zhou and Zhang, 2003). Hydrogen sulfide is easy to

detect because of its particular “rotten egg” smell. Hydrogen sulfide is toxic, especially harmful to human nervous system (Guidotti, 1996, Reiffenstein et al., 1992). The toxicology of hydrogen sulfide on human is complex and individually different, the most direct reaction is the strong irritation to olfactory sense, eyes and brain (Hughes et al., 2009). When the gas phase hydrogen sulfide concentration reaches 0.5ppm and above, it starts to give the unpleasant smell. The irritation reaction and injury to the respiration system and the eyes begin at a concentration of 10ppm. Concentrations over 50ppm will be life threatening, and concentrations above 700ppm will be fatal (Park et al., 2014).

Hydrogen sulfide release from wastewater involved with air-water mass transfer is a dynamic physical-chemical process in sewer systems (Elmaleh et al., 1998). The influencing factors on sulfide emission in sewers primarily include temperature, pH, flow conditions and ventilation (Yongsiri et al., 2004a, Yongsiri et al., 2004b, Yongsiri et al., 2005). Hydrogen sulfide in wastewater is mainly presents as two species due to pH variation in wastewater (Yongsiri et al., 2003) as Figure 2.3 shows below.

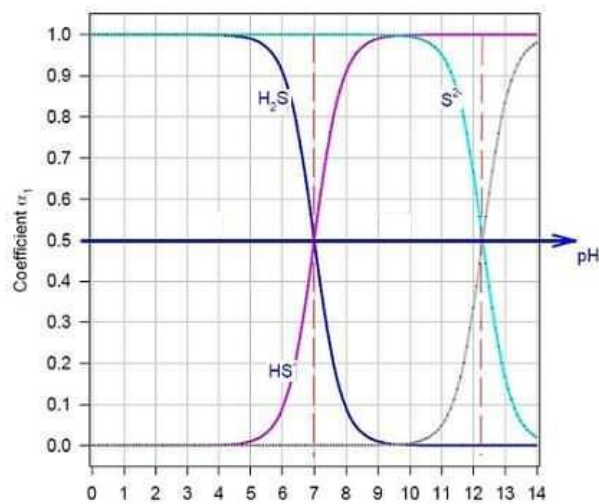


Figure 2.3, Concentration-pH / Percentage-pH diagram of sulphur species in wastewater.

Figure 2.3 illustrates the change of sulphur species concentration-percentage on account of pH variation in wastewater. Where the coefficient α_1 represents fraction of sulfide species. The two species of hydrogen sulfide presented as H_2S and HS^- at a pH around 7 in wastewater (Yang et al., 2005). The sulfide ion S^{2-} is normally not included when looking at sulfide species in wastewater because it only exists at a very high pH, and such a high pH condition is rarely

to be found in sewer systems (Perrin, 2013). From Figure 2.3 it can be seen that the concentration of hydrogen sulfide increases with the decreasing of pH, and reaches equilibrium at pH 7.

Odour nuisance is mainly caused by hydrogen sulfide and volatile organic compounds (VOCs) released from wastewater. Hydrogen sulfide gas released from wastewater phase can accumulate in the sewer atmosphere, and be released again into the urban atmosphere through valves and, access points such as manholes, and even house drain vents (Metcalf, 2003). Odorous gases released from wastewater can cause direct impact on human health and the environment (Jehlickova et al., 2008). Long-term exposure to moderately odorous environment will have negative effects on human health, for example resulting in headaches, nausea and respiration illness (Sucker et al., 2009, Zarra et al., 2008). Regulations regarding odour from wastewater has been set up in places such as Australia, Europe and USA (Lebrero et al., 2011), and odour complaints are frequently being reported all along (Petts and Eduljee, 1994).

Hydrogen sulfide is also flammable, the explosion limits of H₂S in the air is from 4.5% to 45.5% (Patnaik, 2007). It is reported that 80% to 90% of odour gases released from sewer systems consists of sulphur compounds such as hydrogen sulfide and methyl mercaptan (Beghi et al., 2012). Odorous gases generally emerge at hot spots in sewer systems after relatively long residence time, and from downstream structures such as treatment plants (Burlingame, 1999). For instance, the area around a wastewater treatment plant in northwest Philadelphia, US has received 20 years continuous intensive complaints on odour problems before a solution was found (Cheng et al., 2007). Odour problems are also frequently been reported at popular tourists sites such as the City of Sao Paulo in Brazil (Sena, 2013). Another example is that the government authorities of Eugene Springfield, Oregon, USA, had to set up a legal program to manage odour problems after the joint reporting to the environmental agencies by the locals (Collett et al., 2011). It is also reported that a large-scale investigation had to be carried out to identify and eliminate the odour sources followed by thousands of complaints to the environmental protection agencies (Beghi et al., 2012). Therefore, hydrogen sulfide produced from sewer systems not only contributes to sewer corrosion, but also results in great concern for healthcare and odour complaints. Hydrogen sulfide also has an impact on WWTPs. The

oxygen utilization rate (OUR) of activated sludge in WWTP can be reduced by 50% with 1mg/L H₂S concentration. Hence, alkaline agents have often been advised to add into the sludge to raise the pH (Richard et al., 2003).

2.4 Mitigation strategies on the formation of hydrogen sulfide in sewers

Since hydrogen sulfide has been regarded as an inevitable problem associated with sewer processes, mitigation strategies for preventing the formation of hydrogen sulfide and reducing hydrogen sulfide production have been investigated in recent decades (Zhang et al., 2008). The main approaches to sulfide control and management can be summarized as: the initial control of sulfate from sources such as the pre-treatment and source separation; the prevention and decrease of hydrogen sulfide emission from wastewater (Nielsen et al., 2006a); material modification for more resistant concrete pipes to minimize sulfide induced concrete corrosion (Monteny et al., 2001, De Belie et al., 2004); and the improvement of sewer system design for optimized hydraulic condition (USEPA, 1991). Figure 2.4 listed some typical hydrogen sulfide control methods in sewer networks which include: injection of oxidants, chemical precipitation, chemical oxidation, pH increasing, and biocides addition.

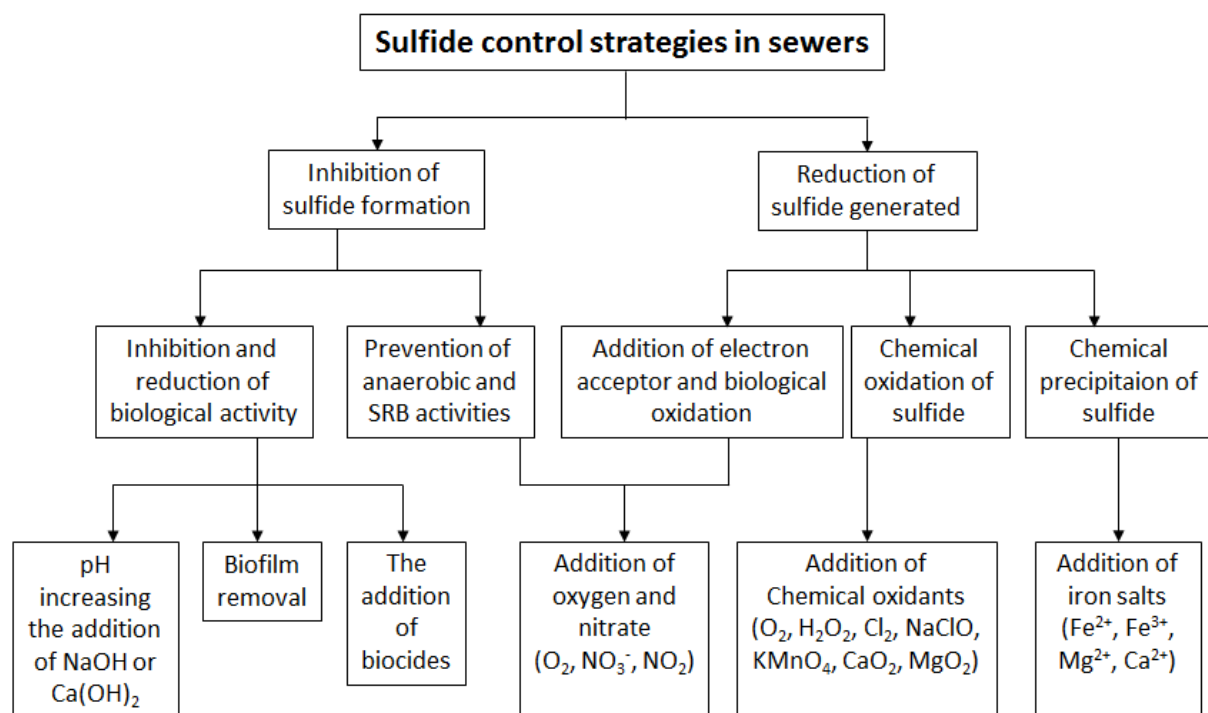


Figure 2.4, Hydrogen sulfide control methods in sewer systems (modified from (De Lomas et al., 2006, Hvitved-Jacobsen et al., 2013)).

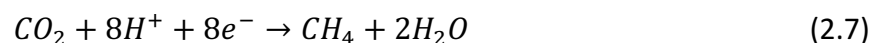
Figure 2.4 sums up some of the typical hydrogen sulfide control methods used in sewer systems. The most commonly used method for both preventing sulfide generation and removing the produced sulfide is chemical dosage, which includes the dosing of oxidants, nitrate, and iron salts (Ganigue et al., 2011, Auguet et al., 2016, Liu et al., 2015d). The chemical dosage is an effective method for sulfide control which can give an average elimination rate of 80% - 100% (Tomar and Abdullah, 1994, Nielsen et al., 2005b). However, the total cost for long-term sulfide control in sewers is not so effective compared to the removal rate. Typical iron salts dosage such as FeCl_2 and KMnO_4 costs \$24-28/kg·S and \$20-23.5/Kg·S (Bowker et al., 1992). The cost for using H_2O_2 is around \$4.5-11.5/kg·S annually (Waltrip and Snyder, 1985). Even the most commonly used nitrates still costs \$2.5-13/kg·S on average (Jenneman et al., 1986, Yang et al., 2005). Although oxygen injection is the most cost-effective approach, it is also least effective on sulfide removal rate compared to other chemicals (Park et al., 2014). There is also a debate whether the expenses for chemical dosage are worthwhile in comparison with the management and replacement costs of corroded pipes. Some studies suggested installing “fat” concrete pipes at sulfide hot spot sections or by using specific sacrificial concrete blocks for corrosion at those locations, gives effective management by increasing the amount of material for the concrete pipes (Nielsen and Vollertsen, 2014).

In recent years, the effect of hydraulic conditions on sewer processes has received closer attention especially driven by a change in legislation and regulations to reduce water consumption in some countries such as Australia (Parkinson et al., 2005, Marleni et al., 2012). It has been found that the impact of reduced water consumption on sewer hydraulics and processes is significant, which gives rise to increased sulfide and methane generation, due to increased wastewater residence time, and amplified biofilm growth and sediment accumulation (Sun et al., 2015, Shypanski et al., 2015). This trend is not a good phenomenon and has negative effects on sewer processes. Further investigation and study are required to have a better understanding on sewer hydraulic performance and to create a more sustainable sewer system for future development.

2.5 Methane in sewers a review

Methane is the main constituent of natural gas which is found in underground and below the sea floor, atmospheric methane comes from the release of methane from earth surface (Khalil, 1999). Methane is regarded as one of the most potent greenhouse gasses (GHG) which has significant effects on global climate change. The actual effect of each methane molecule on warming up earth temperature is 21 times higher than that of carbon dioxide (Liu et al., 2015b). The methane concentration in earth atmosphere has increased by 260% since 1750, and it is expected to increase by a further 150% till 2050 (IPCC, 2006).

Apart from being regarded as a major source of GHG emission, methane in sewers is also a hazardous gas and a severe risk to human because of its highly explosive characteristics (Guisasola et al., 2008). The explosion limits of methane in air at standard pressure (atmosphere pressure) is approximately between 5% and 15% (volume concentration) (Zabetakis, 1965). Some studies also indicated the methane explosion limits is between 5.4% - 17% in air volume percentage (Hensher and Button, 2003). There is an increasing number of sewer methane explosion incidents being reported. One person was killed during sewer explosion in Ottawa, Canada (NYT, 2012). In Chicago, a man was severely burned by methane explosion when using the electric appliance in the bathroom which ignited methane released from the bathtub (Spencer et al., 2006). A methane explosion in a sewer destroyed an entire house in Southern Minnesota (Sarah and Albert Lea, 2012). A similar methane explosion was reported in a residential area in Switzerland (Knoblauch and Steiner, 1999). Hundreds of methane explosions in sewers in China are reported every year.



Equation 2.7 shows the net reaction process of natural methanogenesis, it is also a process of anaerobic respiration used by microorganism as an energy source (Hamilton et al., 2003).

The formation of hydrogen sulfide in sewer system received more attention due to the odour nuisance, toxicity to human health, and the corrosion problems. On the other hand, methane production in sewers had not been investigated and reported until recent years (Guisasola et al., 2008). In some studies, it is believed that the majority of wastewater related methane

production occurs in WWTPs, and the emission of methane from WWTPs is the major source of atmospheric methane contribution (Czepiel et al., 1993, Daelman et al., 2012, Souza et al., 2012, Wang et al., 2011). It was reported by the European Commission that methane released from WWTPs consists of 9% of the world's total methane emission (European Commission, 2011). It was also concluded by the Intergovernmental Panel on Climate Change (IPCC) that the WWTPs is the primary source of methane emission, the sewer system is not assumed to be a substantial methane source (IPCC, 2006). However, these conclusions have been continuously questioned and challenged due to the insufficient investigations and lack of data. Previous studies already indicated domestic sewer system is one of the main methane sources (Minami and Takata, 1997). It has been measured methane concentration in rising mains in Australia can easily build-up to 20 – 25 mg/l (Guisasola et al., 2008). Both experiment results and field analysis showed significant methane formation in sewer systems (Liu et al., 2016b, Liu et al., 2015c).

The formation of hydrogen sulfide and methane in sewers is a simultaneous process, and the coexistence and competition between sulfate reduction bacteria (SRB) and methanogenesis bacteria (MA) are continuously under discussion and investigation. It has been concluded that the utilization rate of acetate and hydrogen by MA is much greater than that of SRB (Guisasola et al., 2009). Although literature indicated that during the coexistence of MA and SRB in an anaerobic environment, SRB is always out of competition (Isa et al., 1986, Yoda et al., 1987). However, this conclusion is against the theory of MA and SRB kinetics and thermodynamics, other parameters such as COD to sulfate ratio, biofilm process should have also been taken into consideration (Nielsen, 1987, Raskin et al., 1996).

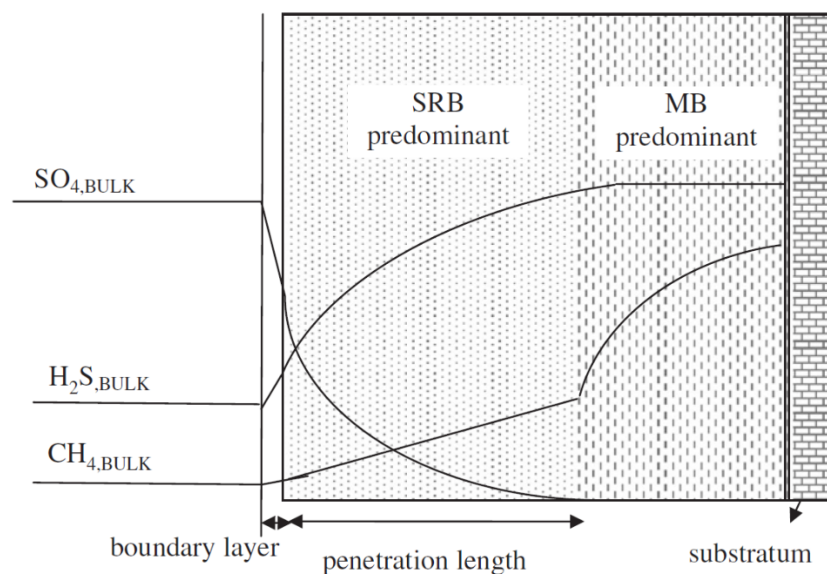


Figure 2.5, Schematic of sewer biofilm penetration by MA and SRB (Guisasola et al., 2008).

Figure 2.5 shows the cross-section of a biofilm area and SRB and MB predominant layers. It can be seen from the figure that the MB predominant layer is below the SRB layer which is closer to the biofilm base and sewer walls. This means the penetration depth of MB layer is much deeper than that of SRB layer, in which the utilization rate of COD, sulfate, acetate and hydrogen should be slower than the upper layer where SRB dominants. Some previous studies also concluded that the COD to sulfate concentration ratio is a key parameter which defines the sulfidogenesis and methanogenesis process (Omil et al., 1998). When the COD/sulfate ratio exceeds 6.08, the MA activities will be predominant and the organic matter will be utilized; the SRB activities and sulfate reduction process will be prevented above this ratio (Rinzema and Lettinga, 1988). The average COD/sulfate ratio of real wastewater is around 13.3, hence it creates a positive and supportive condition for methanogenesis process (Guisasola et al., 2009).

Intensive methane production in sewers has been reported in many studies in mild to hot climate countries such as Australia, China and USA, yet rarely been reported in cold climate places such as north and west Europe. There is a discussion as for whether no methane production happens in these regions, or whether methane is oxidized before it can be released. Several studies have confirmed that methane can be oxidized by microorganisms in biofilm and sediments under anaerobic, aerobic and anoxic conditions (Islas-Lima et al., 2004,

Waki et al., 2005, Schreiber et al., 2010). However, these studies were all based on WWTPs and laboratory conditions, investigations on methane oxidation in sewers have not been found in the literature. The growth rate of methane oxidation microorganism is very slow and difficult (Valentine and Reeburgh, 2000). Studies on marine science indicate an average natural methane oxidation rate in lakes and ocean sediments of $0.02 \text{ g}\cdot\text{CH}_4\cdot\text{m}^2\cdot\text{day}$ (Bastviken et al., 2002), which is far more less compared to the methane production rate in sewer sediments, for example, an average rate of $1.56 \pm 0.14 \text{ g}\cdot\text{CH}_4\cdot\text{m}^2\cdot\text{day}$ (Liu et al., 2015a). One previous study mentioned methane formed in the deep layer in biofilms is found to be oxidized in the upper aerobic layer. However, no detailed calculation or further study on methane oxidation in biofilms have been conducted. In order to have a clear understanding of actual methane oxidation process in sewers, more investigations should be taken place in sewer networks in the future.

2.6 Sewer processes modelling and process models review

The research and study on sewer systems were only limited to lab based analysis and field investigation till the early 1980s, when there came a change that computer modelling was first introduced for the design and management of sewer systems and treatment works (Butler and Davies, 2010). When it comes to the new construction of sewer system or for the redesign and management of existing systems, the purpose of computer models is to provide a preview of the layout and to analyse and troubleshoot current and potential problems with respect to complex design and costly traditional control strategies (Metcalf, 2003). Most models were based on experience equations and database, lab experiments and field work is very important for model validation. Sewer hydrology and hydraulic models are the most available commercial models in the market (Chadwick et al., 2013). It also had a vigorous development of processes models for sewer systems and treatment plants in recent decades.

The first original process model appeared in early 1959, when computer science and technology had not been wide popularized using at that time; Pomeroy *et al* (Pomeroy, 1959) conducted some initial modelling on hydrogen sulfide formation (Sharma et al., 2014). The prediction of hydrogen sulfide formation was limited in this pioneer model because only a

certain few parameters were considered associated with sulfide formation. In the following decades, a number of process models have been developed. For instant, the MOUSTRAP model was developed based on the simulation of constant oxygen uptake rate from biofilms (Garsdal et al., 1995). The prototype of the well-known Activated Sludge Model (ASM) which is currently commonly used in wastewater treatment plants was first developed as ASM No.1 (Hvitved-Jacobsen et al., 1998a). Its succeeded models ASM No.2 and No.3 were tended to appear later with extended developments. The processes of oxygen consumption, nitrification, denitrification and phosphorus accumulating organisms were added compared to ASM No.1 (Gujer et al., 1995, Gujer et al., 1999). While ASM was firstly developed for the purpose of working with wastewater treatment plant processes, following studies has extended its applications based on the ASM No.3; such as the modelling of mass transfer in biofilms (Huisman and Gujer, 2002), specific determination of new model parameters (Jiang et al., 2007), and integrated modelling of wastewater treatment plants with river water quality models (Reichert et al., 2001).

Along with the development of treatment models, a certain number of processes models specific for sewer systems have been developed in recent decades. 7 sewer processes models were reviewed and compared below with sufficient literature background information:

Wastewater Aerobic/Anaerobic Transformations in Sewers – WATS

In the 1970s, Thistlethwayte, Boon, Pomeroy *et al* discovered some sulfide formation rate equations associated with biofilm processes in the sewer pipes (Thistlethwayte, 1972, Boon and Lister, 1975, Pomeroy and Parkhurst, 1977). These equations are as follows:

$$r_a = 0.5 \times 10^{-3} V_s (BOD)^{0.8} (SO_4)^{0.4} 1.139^{(T-20)} \quad (2.8)$$

$$r_a = 0.228 \times 10^{-3} (COD) 1.07^{(T-20)} \quad (2.9)$$

$$r_a = 1.0 \times 10^{-3} (BOD) 1.07^{(T-20)} \quad (2.10)$$

In Equations 2.8, 2.9 and 2.10, where r_a is the sulfide formation rate ($\text{g S m}^{-2} \text{h}^{-1}$), V_s is the flow velocity (m/s), SO_4 is the sulfate concentration (g/m^3), and T is temperature ($^{\circ}\text{C}$). These early sulfide formation equations defines a ratio between COD or BOD concentration. In 1987, (Nielsen, 1987) had done a series of lab investigations on the sulfide formation rate in biofilms with real sewerage. It found the sulfide formation rate is 50% - 75% lower than the rate reported in Equations 2.8 – 2.10. The sulfide formation rate r_a was calculated by:

$$r_a = 0.5 \times 10^{-3} (\text{COD} - 47)^{0.8} 1.07^{(T-20)} \quad (2.11)$$

(Nielsen and Hvitved-Jacobsen, 1988) indicated the sulfide formation rate can be calculated by Equation 2.11 with a wastewater COD concentration lower than 400 mg/L.

Based on the previous studies, In the late 1990s, Hvitved-Jacobsen and his group developed a sewer process model concept, and it was first introduced as the Wastewater Aerobic/Anaerobic Transformations in Sewers model (WATS) (Hvitved-Jacobsen et al., 1998a). The aerobic and anaerobic processes were included in this concept, and therefore incorporated carbon and sulphur cycle into this model. Since then, this model has been continually developed and extended. Compared to early models, the more comprehensive physical chemical and biological processes were presented in the WATS model (Yongsiri et al., 2003). The two-phase model was firstly presented with sulfide generation in gravity sewers and the emission of hydrogen sulfide into sewer atmosphere (Yongsiri et al., 2004b). However, the chemical and biological oxidation of hydrogen sulfide gas in sewers had not been included yet. Later came a major update that (Nielsen et al., 2005a) extended the model with sulphur cycle. Where the sulfide generation, precipitation, chemical and biological oxidation, and mass transfer, hydrogen sulfide emission, reaeration, concrete corrosion were all introduced and provided to the model. In present day, the WATS model has been extended and developed for covering the aerobic, anaerobic, anoxic processes in water phase, biofilms, sediments; and the sulfide emission, ventilation, and concrete corrosion processes (Vollertsen et al., 2008a, Jensen et al., 2009, Rudelle et al., 2012, Nielsen et al., 2012).

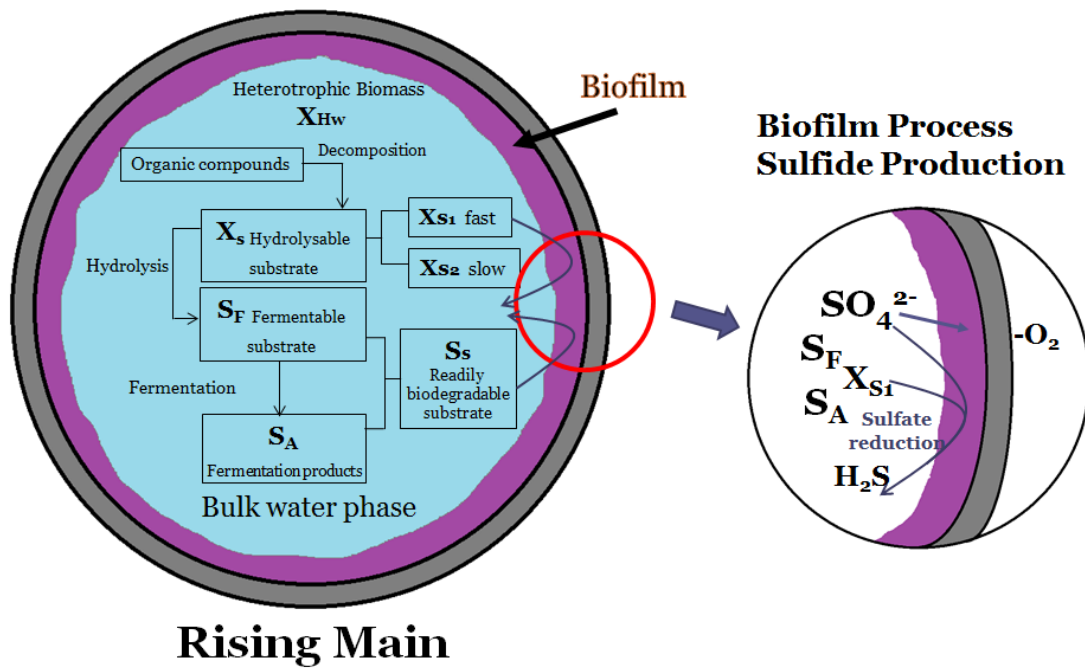


Figure 2.6, schematic of wastewater anaerobic transformations and biofilm process sulfide formation.

Figure 2.6 shows the schematic of WATS model expressions of wastewater anaerobic transformations in a rising main or in a full flow gravity sewer, and the sulfate reduction process in the biofilms. The transformations of organic matter are defined similarly in other process models. The WATS model matrix of aerobic and anaerobic transformations is summarised in Table 2.1:

Table 2.1, Aerobic and Anaerobic transformations in WATS model

Process	X_{Hw}	S_s	X_{S1}	X_{S2}	$-S_O$	S_F	S_A	$S(-II)$	S_{SO4}	Rates
Growth of biomass in bulk water phase	1	$-1/Y_{Hw}$			$(1 - Y_{Hw})/Y_{Hw}$					r_{grw}
Growth of biomass in biofilm	1	$-1/Y_{Hf}$			$(1 - Y_{Hf})/Y_{Hf}$					r_{grf}
Maintenance energy requirement	-1	-1			1					r_{maint}
Hydrolysis, fast		1	-1			1				r_{hydrn}
Hydrolysis, slow		1		-1		1				r_{hydrn}
Reaeration					-1					
Decay of biomass, X_{Hw}	-1			1						r_d
Fermentation in the water phase						-1	1			r_{ferm}
H_2S formation								1	-1	r_a

The rate equations and calculations are introduced in Chapter 3

SeweX model

SeweX model is a commonly used model for in-sewer processes especially for the modelling of hydrogen sulfide formation in Australia, which is developed by (Sharma et al., 2008). It is defined as a new approach for dynamic modelling on hydrogen sulfide formation compared to other process models which depend on limited steady state conditions (Sharma et al., 2008). The transformations of organic matter and COD processes in SeweX model was developed based on the WATS model, SeweX implemented different kinetic equations for the formation of hydrogen sulfide (Donckels et al., 2014). SeweX model provided wide applications in Australian water industries with intensive field investigations. It has been used for testing different sulfide control strategies such as various chemical dosage, oxygen, nitrate, and iron salts (Sharma et al., 2008, Sharma et al., 2012). The growth and activities of sulfate reduction bacteria (SRB) are very important for modelling the sulfide formation process, a biofilm model was developed based on the SeweX model which provided the information on dynamic biofilm growth, change of biofilm thickness, and sulfide reduction related to bacteria activities (Jiang et al., 2009). The SeweX model has also been extended to include the modelling on methane formation which is derived from the IWA Anaerobic Digestion Model (Guisasola et al., 2009). Equation 2.12 is the sulfide formation rate introduced in SeweX.

$$r_a = k_{H_2S} \frac{S_{FCOD+S_{VFA}}}{K_{sf}+(S_{FCOD+S_{VFA}})} \frac{S_{SO_4}}{K_{SO_4}+S_{SO_4}} \frac{K_{O_2}}{K_{O_2}+S_{O_2}} \frac{A}{V} \frac{S_{FCOD}}{S_{FCOD+S_{VFA}}} \quad (2.12)$$

EAST Central Interceptor Sewer (ECIS)

The East Central Interceptor Sewer model (ECIS) was developed and introduced by (Michiels and Salgaonkar, 1994). It was claimed to be a new model for the prediction of hydrogen sulfide concentration in wastewater. The model was modified and extended from the previous SULFBAS and HS program model. However, even with this updating, it was still limited to only predict the sulfide generation rate in wastewater and the relative hydrogen sulfide concentration. There was no consideration of air-water mass transfer, sulfide emission and gas phase hydrogen sulfide concentration. The ECIS model had been added with calculating concrete corrosion by adopting the Pomeroy equation (USEPA, 1991). It is unpredictable to use a single transfer rate to calculate concrete corrosion without proper consideration on the dynamic air-water mass transfer and hydrogen sulfide emission.

AEROSEPT model

In order to calculate and predict sulfide formation in the Costa do Estoril region, Portugal, (Matos and Aires, 1995) presented a model describing the processes in both gravity sewers and rising mains. It indicated the source for gravity sewer and rising main modelling was from (Pomeroy, 1959) and (Pomeroy and Parkhurst, 1977) respectively. The AEROSEPT model had been extended by using some equations and algorithms from the ASM and WATS model to include the anoxic process with experiments data (Mourato et al., 2003). AEROSEPT model has also been applied to many other areas, mainly in Portugal (but references in Portuguese). However, the AEROSEPT model has limited validation by comparing field measurements to model predicted values. The purpose of the development of this model was to highlight the importance of modelling for the design of new systems for the local conditions.

Septicity Prediction and Control Algorithms (SPACA)

The septicity of sewers generally involves with toxicity, odour nuisance, and corrosion of sewers which results from the processes mainly occurring in rising mains (Boon, 1995). The Septicity Prediction and Control Algorithms (SPACA) model was developed for modelling the formation of hydrogen sulfide in rising mains with important parameters such as temperature, pH, COD, DO concentration. The SPACA model even took the influence of flow rate on sulfide formation into consideration (Boon et al., 1998). The SPACA model has also been validated with field measurements. However, there are no available algorithms for this model been provided, and no further development or application on this model found in the literature.

EPA Sulfide and Corrosion Models

The EPA sulfide and corrosion models consist of two separated parts developed by the US EPA: the EPA sulfide model (Pomeroy and Parkhurst, 1977, Kienow et al., 1982) and the EPA corrosion model (Transfer and Pomeroy, 1974). Later on, two parameters called turbulence and crown corrosion factors were introduced to the EPA models to enhance the algorithms (Romer and Kienow, 2004). This model can be used to a wider range of conditions with various sewer structures for a more specific corrosion rate calculation.

INTERCEPTOR Model

The Interceptor model was actually developed based on the EPA sulfide and corrosion models, which incorporated the full cycle mechanisms existed in EPA models with extensions of air-water mass transfer and sulfide oxidation (Witherspoon et al., 2004). The author indicated the calculation and relations to the EPA models but did not provide certain model matrix or algorithms. There is also no further literature available.

Table 2.2, Comparison between different process models reviewed

	WATS	SeweX	INTERCEPTOR	SPACA	ECIS	AEROSEPT	EPAs
Sulfide generation	Y	Y	Y	Y	Y	Y	Y
Sulfide oxidation	Y	Y	Y	Y	Y	Y	N
Mass transfer	Y	Y	Y	N	Y	Y	Y
PH impacts	Y	Y	Y	Y	Y	Y	Y
DO concentration	Y	Y	Y	N	N	Y	Y
Gas phase process	Y	Y	Y	N/A	Y	Y	N
Concrete corrosion	Y	Y	Y	N/A	N	Y	Y

*Y, Yes; N, No; N/A, not available.

Table 2.2 summarized the 7 different sewer processes models reviewed. It can be seen from the table that the WATS, SeweX, AEROSEPT and Interceptor model include the most processes compared to other models. Among them, WATS and SeweX models are the most widely used and referenced models in many studies. The algorithms and matrix for WATS model are open access, and parameters are available from its related papers and books. While SeweX model only released parts of its matrix and algorithms. It also needs analysis when using these models with different local conditions such as temperature and wastewater COD.

2.7 Parameters for modelling and the uncertainties and sensitivities

Concept process model consists of empirical equations and a number of parameters, which have a significant influence on model outputs. The transformations of organic matter and the formation of hydrogen sulfide is highly sensitive to the variation of parameters; typical key

parameters associated with these processes include temperature, pH, COD and flow conditions (Nielsen et al., 2006b).

Firstly, temperature is the basic key parameter which determines the wastewater biological activities and all transformation rates. Wastewater temperature in sewer systems varies in a quite range depends on the time of year and climates. In general, the temperature of sanitary wastewater originated from households ranges between 10 to 20 degrees Celsius throughout a year (Dürrenmatt and Wanner, 2014). To be specific, wastewater temperature normally varies between 10 – 14°C in winter seasons, and 18 – 22°C during summer periods on average (Cipolla and Maglionico, 2014). Temperature directly controls the formation rate of both hydrogen sulfide and methane, and sulfide and methane are reported to be very high especially in warm climate countries such as Australia (Eijo-Río et al., 2015). However, apart from methane production, the sulfide formation rate is still reported to be significant as well as in cold climate countries (Nielsen and Hvitved-Jacobsen, 1988).

Wastewater pH value is also a very important parameter for the formation of hydrogen sulfide in sewers (Sharma et al., 2013). As similar to temperature, wastewater pH varies in different ranges at different locations and countries. For instant, field analysis showed the pH value is around 7.0 – 8.5 in a sewer pipe in Denmark (Nielsen et al., 1998); a pH was observed slightly higher than average in a French sewer within a range of 7.7 – 9.8 (Houhou et al., 2009); and a field test in a gravity sewer indicated a pH variation between 6.2 – 7.4 in Taiwan (Pai et al., 2010). (Hvitved-Jacobsen et al., 2013) summarised a desired wastewater pH condition for sulfate reducing bacteria growth is between 5.5 and 9.0. However, it is still unclear the influence of pH value on sulfidogenesis and methanogenesis in sewers. Hence, modelling and field work had been conducted in order to investigate the pH influence on these processes (Sharma et al., 2013, Sharma et al., 2014). Results show that when the pH was manually increased to 8.6 and 9.0, the sulfate reduction bacteria activities were reduced by 30% and 50% respectively; then the methanogenesis was the main process (Gutierrez et al., 2009). When a pH level is over 10.5, the sulfide formation rate will be reduced by 70% -90%, and methane production rate will be reduced by 95% - 100% as well (Gutierrez et al., 2014). pH value also impacts sulfide oxidation process, for example, at a pH of 6, 7, 8 gives sulfide oxidation rate constant of 0.08, 0.26, 0.45 respectively (Nielsen et al., 2005a). To sum up, in

general, the activities of sulfate reducing bacteria is reduced when the pH is either higher than 9.0 or lower than 4.0. A neutral pH of 6.5 – 7.5 provides the highest hydrogen sulfide formation rate (Sharma et al., 2014).

The chemical oxygen demand (COD) is an indirect index to express the amount of organic compounds in wastewater (Metcalf, 2003). And the wastewater COD concentration is much more fluctuant compared to temperature and pH. Typical COD concentrations in the United States, European and Australian sewer networks have been shown to vary between 200 and 800 gO_2/m^3 , 5 – 15 $\text{gS}\cdot\text{m}^{-3}$ for sulfide concentration in municipal wastewaters (Hvitved-Jacobsen et al., 2013). (Vollertsen et al., 2005) collected 109 wastewater samples in Denmark and Germany in 2005, the average total COD of these samples were 691 mg/L and 439 mg/L respectively. The COD concentration even has a great variation in a single intercepted system with complex biochemical transformation. For instance, the COD in a gravity sewer is 283 g/m^3 , while it changes to 660 g/m^3 in a storage tank connecting to the gravity sewer (Makowska and Spychała, 2014).

The dissolved oxygen (DO) concentration in wastewater mainly depends on temperature, pressure and flow condition; and geographical information of gravity sewers for the reaeration rate (Gudjonsson et al., 2002, Huisman et al., 2004b). It is also very important to investigate and calculate the DO concentration in rising mains, because the DO concentration determines how long it takes to transfer from aerobic process to anaerobic process (Hvitved-Jacobsen et al., 2013). There are normally drop structures in pump stations or wet wells before rising mains, where massive air-water mass transfer occurs and with the reaeration of DO (Matias et al., 2015). Calculations had been provided for these processes, which also referred to the DO saturation concentration in wastewater at different situations (Madsen et al., 2006)

2.8 Sewer hydraulic conditions and hydraulic models

The hydraulic conditions in sewer system are complex because the system consists of small sewer pipelines connecting to larger sewers before joining main trunk sewers which terminate at combined sewer overflows and wastewater treatment plants (Swamee and

Sharma, 2013). The hydraulic characteristics of sewer systems have been summarised as one of the most important factors influencing the in-sewer processes as early in the 1970s. However, the actual impact of sewer hydraulics on in-sewer processes has not been recognised and taken into consideration until recent years. Parameters influencing sewer hydraulic conditions mainly include the area to volume ratio, velocity, shear stress, and velocity gradient (Park et al., 2014).

The area to volume ratio (A/V) is the ratio of total area of biofilms divided by the total volume of wastewater in a sewer pipe (Hvitved-Jacobsen et al., 2013). Hydrogen sulfide is produced by sulfate reducing bacteria, which are mainly associated with the biofilms covering the submerged surfaces in wastewater in sewer pipes (Jiang et al., 2009). The concentration of hydrogen sulfide in wastewater phase depends on the diffusion process of hydrogen sulfide produced in the biofilms. Thus, the A/V ratio defines the relative contribution of biofilm and wastewater processes on the formation of hydrogen sulfide (Hvitved-Jacobsen et al., 2013). Figure 2.7 illustrates two different situations of full filled rising main (A), and partially filled gravity sewers (B & C). Where the blue area shows the total volume of wastewater, and the purple area is the total surface area of biofilms. It has also been found that a low depth to diameter ratio (d/D) can also contribute to a high A/V ratio and low flow velocity (Figure 2.7 C). Hence it is observed higher hydrogen sulfide transfer rate at high A/V ratio sewer pipes (Lahav et al., 2006b).

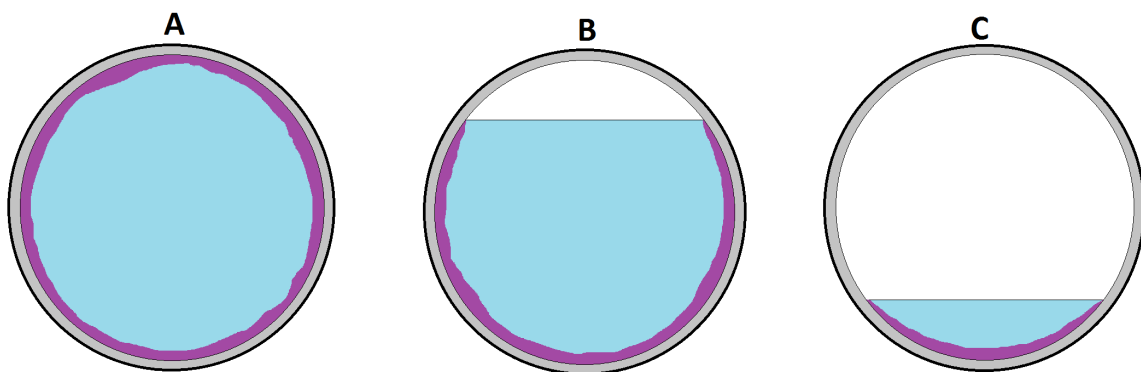


Figure 2.7, sketches of fully filled rising main and partially filled gravity sewers.

The flow velocity of wastewater generally determines the wastewater residence time and the growth of biofilms. The thickness of biofilm can reach up to 50mm and the deepest layer of

biofilm is believed to be permanently in anaerobic condition (Hvitved-Jacobsen et al., 2013). The biofilm thickness can lose 1 - 5mm with the increase of flow velocity every 0.5 – 1m/s (Park et al., 2014). (Santry, 1963) summarised the influence of flow velocity on hydrogen sulfide formation and emission. When the velocity is less than 0.8m/s, it will result in longer wastewater residence time, which further contributes to the increased thickness growth of biofilm and more deposition of sediment. Thus, there will be more hydrogen sulfide generation with the combination of these factors. However, when the flow velocity is greater than 1.5m/s, it does decrease the residence time and biofilm growth; but there will be more hydrogen sulfide release from wastewater, hence, more sulfuric acid production due to the turbulent flow condition. The ideal flow velocity is between 0.8 – 1.5m/s, which provides optimum conditions corresponding to avoid sulfide formation, biofilm growth, and the prevention of sediment accumulation (Santry, 1963). This velocity is ideal for the system to prevent sedimentation, as well as the formation of hydrogen sulfide. Meanwhile, more turbulence is desired in the upstream but not in the downstream of the system, where hydrogen sulfide stripping may occur. When it comes to the hydraulic design of sewer pipes, the self-cleaning velocity which is the minimum flow velocity to prevent the deposit of solids and pipe blockage also needs to be considered. It also needs to consider the type of solids the system normally carries and the pipe diameters (Swamee et al., 1987). The minimum velocity for pipe diameter larger than 0.3m is around 0.6 – 0.75m/s, while it has to be reaching 1m/s for pipe diameter smaller than 0.25m.

Shear stress and velocity gradient are another two important hydraulic parameters in terms of hydrogen sulfide formation, where shear stress is related to flow velocity, flow depth, and pipe slope, while velocity gradient is influenced by flow rate, flow velocity and slope. It was investigated the formation of hydrogen sulfide is reduced with a high shear stress, which also increases the reaeration rate to create aerobic transformation (MMBW, 1989). The velocity gradient is more connected to the sulfide emission process. High sulfide emission rate is believed to be affected by high-velocity gradient (as similar to turbulent flow) rather than other parameters such as the oxidation rate (Lahav et al., 2004).

Wastewater flow and the hydraulic condition is the most important parameter for the design of sewer systems. In the past, the traditional measurements of flow were limited due to the

rough inner sewer environment and complex hydraulic conditions especially during peak and wet weather flows (Nguyen et al., 2009). However, computer programmes were not invented for the design and analysis of sewer drainage system until the 1970s, and those hydraulic models were only developed to be useful and reliable when the computer technology had been improved (Butler and Davies, 2010). In practice, the purpose of using hydraulic models is to represent the sewer system and to analyse its response to various flow conditions. For instance, with a known flow rate at an access point, the model can predict and indicate the flow conditions in the following and downstream sewer pipes (Chadwick et al., 2013).

Most urban drainage models are used for planning, operations and design purposes; and catchment models can be used for event and long-term simulations. Event based model is for short term simulations such as several precipitation events; while long term model which also called continuous model is for an overall seasonal or annual water balance for a catchment (Zoppou, 2001). Hydraulic models are mainly used for flow conditions simulation and sometimes for water quality as well with uncertainty analysis for model evaluation (Mannina et al., 2006, Kalantari et al., 2014). The representative of the first early generation hydraulic models include DR₃M–QUAL, HSPF, QQS, STORM, Wallingford; whereas in the recent decade, more advanced and well-known models were available in the market such as MOUSE, SLAMM, SWMM (Elliott and Trowsdale, 2007). Among those, the MOUSE and SWMM are the most widely used models because both of them are suitable for small catchments flow prediction and capable for large catchments for dynamic hydraulic routing. CFD models are often used to model the flow and sediment movements in sewer systems (Dufresne et al., 2009). CFD models can also be used for specific studies in 3D structures such as, for example, wet wells and retention tanks (Thinglas and Kaushal, 2008).

In recent years, a computer package named Infoworks was available on the market developed by an industrial company Innowyze. It was developed as a more comprehensive management tool, with which more accurate and efficient network solutions can be provided by Infoworks for water distribution system than before (Mitchell et al., 2007). Its sub-models Infoworks ICM (catchment model), Infoworks CS (collection system) and Infoworks WS (water supply together can give an overview on the whole system and provide management strategies and predictions (Cantone and Schmidt, 2009). Infoworks as a system analysis tool has been

frequently used for the evaluation of sewer system capacity and the impact and possibility of flooding events (Rubinato et al., 2013). The Infoworks software is not free and the running cost is relatively high, some studies had done using Infoworks combined with other free software such as SWMM to simplify the model construction and to control the running cost effectively (Koudelak and West, 2008).

The Stormwater Management Model (SWMM) is the most well-known and widely used free software, which was developed by the US Environmental Protection Agency in 1971, and the latest version is SWMM 5 (Rossman, 2010). It can provide dynamic simulation on rainfall runoff for the quantity of water flow in pipes and for the quality of pollutant loads from stormwater (Chadwick et al., 2013). The main purposes of using SWMM is to calculate and predict average and peak flows in the system and evaluate the potential threat of pollutants from rainfall loads to the natural water environment (Liong et al., 1995, Tsihrintzis and Hamid, 1998). SWMM was also used for simulation of the interactions between old and new sewer system to find out the vulnerable locations with the assessment of hydrologic impact in urban areas (Słyś and Stec, 2012, Jang et al., 2007). It has even been used for modelling the quality and quantity of runoff to rivers and watersheds (Lee et al., 2010). Although SWMM was specially designed for stormwater management, however, it can also be used for sanitary sewers as long as the parameters were adjusted accordingly (Lowe, 2010). Infoworks was normally used for the calibration of SWMM model, and detailed GIS (geographic information system) is needed for large catchments (Barco et al., 2008).

2.9 Summary of Literature Review

To sum up, all the key knowledge gaps identified in the literature review and an overview summary section are listed here. Hydrogen sulfide in sewer systems is a well-known problem, which has also been intensively studied in the past several decades. Traditional sulfide control strategies are costly for long term management. In recent year, the influence of sewer hydraulic condition and flow on sewer processes and sulfide formation has been investigated. It has also been taken into consideration to focus more on other sewer gases produced in sewer systems such as methane and oxynitrides. Donckel's (Donckel et al., 2014) global sensitivity analysis study indicated the most influential parameters for sulfide formation such

as the total COD. However, as far as the author is aware the individual influence of COD substrates and COD fractions has not been investigated. Methane is a greenhouse gas emission source, and is highly inflammable and explosive. Intensive methane production has been found in sewer systems in some countries such as US, China and Australia. Relative models have been developed to simulate methane formation in sewer systems. Septic tanks are also found to be a major source for methane production. However, as far as the author is aware no specific models have been developed or designed to simulate methane formation in septic tanks, and the relative contribution from sewer pipes with an integrated view. Future sewer related research will be focused on methane and oxynitrides, as well as hydrogen sulfide to provide a broader view in this area.

Chapter 3, Impact of sewer hydraulic condition on sulfide formation and build-up.

3.1 Introduction

The hydraulic condition in sewer system is complex, and there are two main types of flows in sewer system, namely full pipe flow and open channel flow (Butler and Davies, 2010). In fluid mechanics, a simple approach for describing of fluid flow in a pipe is plug flow modelling, in which an infinitely small section of fluid is intercepted as a plug (Munson et al., 2012). By using “plug flow” modelling which requires uniform flow in a pipe. The flow of wastewater in sewer pipes is generally non-uniform flow, however, it is normally assumed as uniform flow for hydraulic and process modelling in most situations (Butler and Davies, 2010). Basically, in order to use the “plug” modelling approach, it assumes there is no boundary layer between wastewater and pipe surfaces, biofilms and sediments.

The wastewater flow pattern in residential catchments generally peaks in morning and evening periods and comes to a relative low flow at night. It normally results in high sulfide generation overnight and low sulfide production during morning and evening peak times due to the long wastewater residence time at night according to the flow pattern (Vollertsen et al., 2011a, Vollertsen et al., 2011b). The flow of wastewater not only affects hydraulic performance of sewer systems, but also associated with the transformation and transporting processes of wastewater, for instance, more hydrogen sulfide loading occurs under turbulent conditions than stable flows, because turbulent condition creates more air-water mass transfers (Hvitved-Jacobsen et al., 2013). Many studies indicated that the flow of wastewater has been identified as one of the key factors influencing the formation of hydrogen sulfide (Freudenthal et al., 2005, Sharma et al., 2008, Hvitved-Jacobsen et al., 2013). Another flow related hydraulic factor affecting sulfide formation in sewers is the hydraulic retention time which is also called hydraulic residence time (HRT). Longer residence time normally results in higher hydrogen sulfide and methane concentration due to longer time period for the biochemical transformation and accumulation (Eijo-Río et al., 2015). Low flows at night are linked to high hydrogen sulfide formation. (Sun et al., 2015) also confirmed the reduction in morning and evening peaks flows resulted from reduced water consumption, which contributes to increased hydrogen sulfide production by 50-100%. The reduced water

consumption also results in the increase of COD, BOD, TSS in wastewater; which further contributes to the decrease of flow rate and the increase of HRT.

The formation of hydrogen sulfide is a universal and frequent problem in urban drainage systems (Nielsen et al., 2008a). Hydrogen sulfide is produced by sulfate reducing bacteria, which is mainly associated with the biofilms covering the submerged surfaces in wastewater in sewer pipes (Jiang et al., 2009). This means that the area-volume ratio (A/V) is one of the key parameters in defining the formation of hydrogen sulfide as this indicates the relative contribution between biofilm and wastewater processes. For a given wastewater composition, the biological transformations are related to two factors: the A/V ratio and hydraulic residence time. The A/V ratio is naturally related to the dimension of sewer pipe, to be specific – the inner diameter of the pipe. A high A/V ratio is associated with small pipe diameter for full flow rising mains, and would lead to a high contribution from the biofilms and hence potential for high hydrogen sulfide formation. However, it would also decrease the residence time of the wastewater, which would tend to decrease the amount of hydrogen sulfide formed.

The HRT in a rising main sewer pipe is determined by the wastewater flow velocity, which is controlled by the pump operation, the pumping rate, and pump frequency (Guisasola et al., 2009). For a given flow rate and pump operation in a sewer system, by changing the diameter of a rising main sewer pipe which changes both the A/V ratio and HRT; by changing the length of a pipe only changes the HRT. Thus, A/V ratio and HRT makes up the determination of biological transformation.

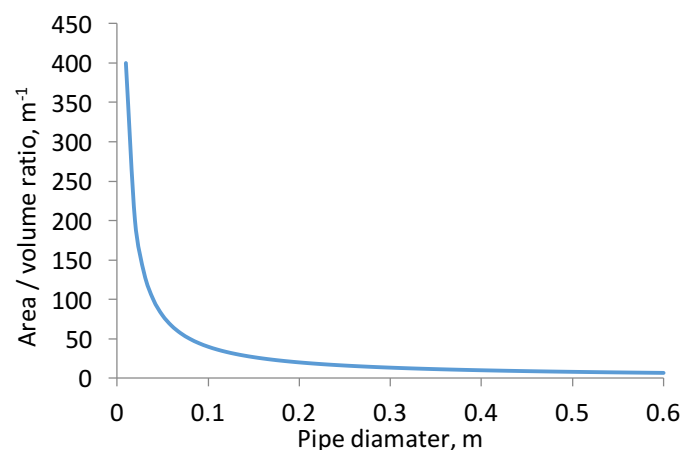


Figure 3.1, the relationship between A/V ratio and pipe diameter.

Figure 3.1 shows the relationship between A/V ratio and pipe diameter. In rising mains, the A/V ratio decreases with the increasing of pipe diameter.

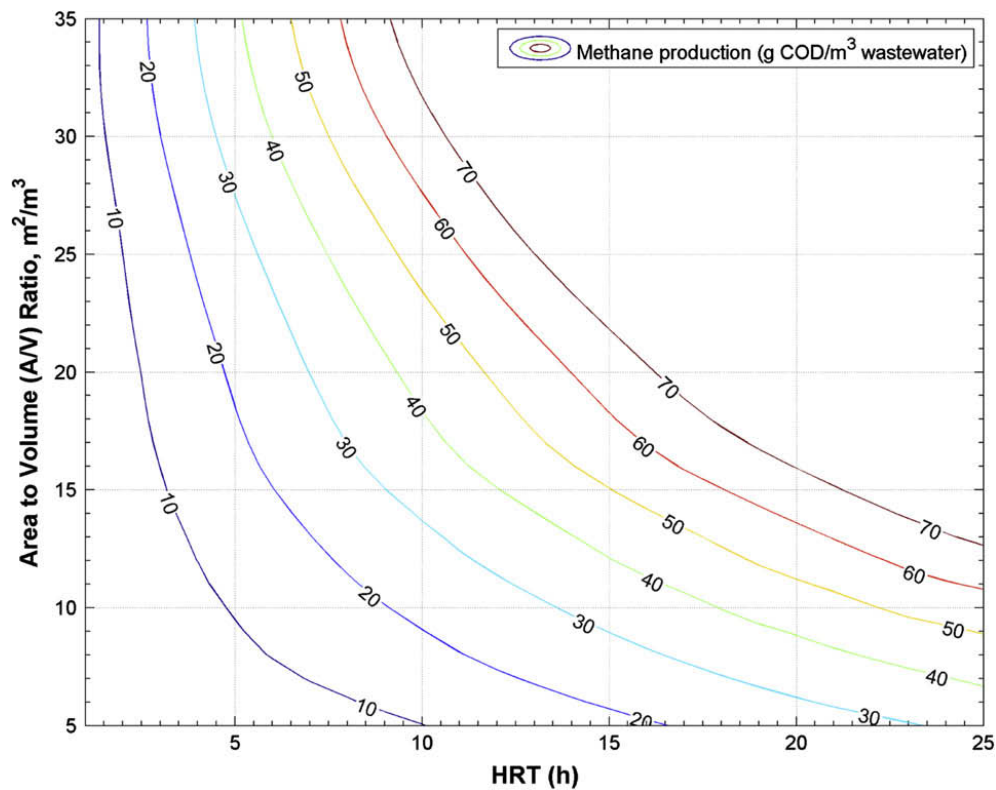


Figure 3.2, Methane production with A/V and HRT variation (Guisasola et al., 2009).

(Guisasola et al., 2009) calculated a graph for methane production in wastewater within a given average methane production rate at a constant temperature. It can be seen from the Figure 3.2 that longer HRT results in longer time period for the biological transformation, which contributes to more methane production. Higher A/V ratio gives a higher percentage of biofilm bacteria activities per volume of wastewater, which leads to higher methane production as well. There are optimal combinations of different A/V ratios and HRTs for the least methane production in sewer pipes. Thus, there should be an optimal pipe diameter selection for each section of pipe in a sewer system with given flow rate and pump operation.

Current commonly used hydrogen sulfide mitigation strategies have been summarised in the literature review. All the typical and traditional mitigation methods are costly for long-term sulfide control and management. New mitigation strategies should be investigated and tested, such as flow manipulating and pump operations. Previous studies showed methods of

changing the wastewater flow conditions in sewers has been used such as the commonly implemented sewer storage tanks (Dufresne et al., 2009) and various pump control strategies (Ostojin et al., 2011). The flow pattern can be manipulated through these methods and simulated by models or be reported by on-site monitoring tools (Nguyen et al., 2009). The fuzzy logic pump control strategies can both improve the pump efficiency and energy cost. In the meantime, these flow control methods can not only be used for improving the hydraulic conditions of sewer systems, but potentially also for hydrogen sulfide mitigation. (Liu et al., 2016a) have done a flow event-based pump controls to give a more optimised distribution of chemical dosage into the system, which can significantly improve the sulfide mitigation rate compared to standard constant dosing.

Modelling of wastewater transformations and the formation of hydrogen sulfide in sewers is considered to be a cost-effective way for sewer process management, for instance, it can provide sulfide hot spot locations and better understanding of the in-sewer processes. As reviewed in literature, WATS and SeweX model are two of the most commonly used sewer processes models at present. SeweX model was developed based on the WATS model which implements different kinetic equations for the formation of hydrogen sulfide (Sharma et al., 2008). The WATS model assumed that the formation of hydrogen sulfide is a static process and does not consume organic substrates. However, the kinetic equation does have a strong dependence on the concentrations of organic substrates, which involves the parameters of organic matter in the equations. (Donckels et al., 2014) developed a model which implemented the WATS model for the transformation of organic matter, and the kinetic equations from SeweX model for the formation of hydrogen sulfide. This study indicated the most sensitive parameters in terms of sulfide formation such as the maximum sulfide formation rate and total COD concentration.

3.2 Materials and Methodologies

3.2.1 Objectives, catchments information and concept for model set-up

The aim of the work in this chapter is to access the effect of pipe diameter (A/V ratio and HRT) and pump operations on the formation and build-up of hydrogen sulfide in rising mains, and the effect of network wide real time control of pump operations on cost-effective hydrogen

sulfide management. It also aims to quantify the importance of the pipe diameter and pumping strategy for optimal design for rising mains, to minimise hydrogen sulfide production, either to improve the life time for the downstream sewer structures or to minimise the potential chemical dosing needed in the rising mains. The simulation is based on the model results from two small catchments in England, UK, which will be termed A and B.



Figure 3.3, Satellite images of Catchment A and Catchment B.

Figure 3.3 shows the satellite images of Catchment A and B. Catchment A has a population of around 15000, a contributing area of approximately 320 Ha. Catchment A lies on the edge of a large city suburb and the residential boundaries are not well defined. It comprises roughly 60 km of predominantly combined sewers. The majority part of catchment B situated to the south of a moderate sized river which has a population of around 17000 with contributing area of 350 Ha and 90 km of predominantly combined sewers. The main flow of Catchment B is draining to a small wastewater treatment plant. There are also two CSOs in Catchment B and the system includes three main pumping stations with several small stations. Verified

Infoworks CS models V7.5 by Yorkshire Water Services were completed for both catchments (WaPUG, 2002).

Catchments output flow data for simulation include gravity inflows into the wet well, upstream wet well flow and flow in the rising mains. The flow data at the downstream outlet from the catchments was generated using verified Infoworks CS hydraulic models. Flows in rising mains were generated based on Infoworks inflows into the wet well and the previously described switching levels and pump flow rates. The chemical and biological transformations of wastewater and the formation of hydrogen sulfide in the rising mains have been modelled in MATLAB Simulink with programmed WATS and SeweX models. The transformation of organic matter in wastewater was simulated in WATS model. The stoichiometric and kinetic equations for hydrogen sulfide formation from WATS and SeweX model were used to compare the effects and results on sulfide generation (Sharma et al., 2008, Hvitved-Jacobsen et al., 2013). There are no wastewater quality samples available for these two catchments. The total COD, fractions, and organic composition using in the process models were collected from sewer networks in Denmark and Germany (Vollertsen et al., 2005). Detailed information on wastewater composition and the sensitivity analysis on COD fraction is discussed in Chapter 4.

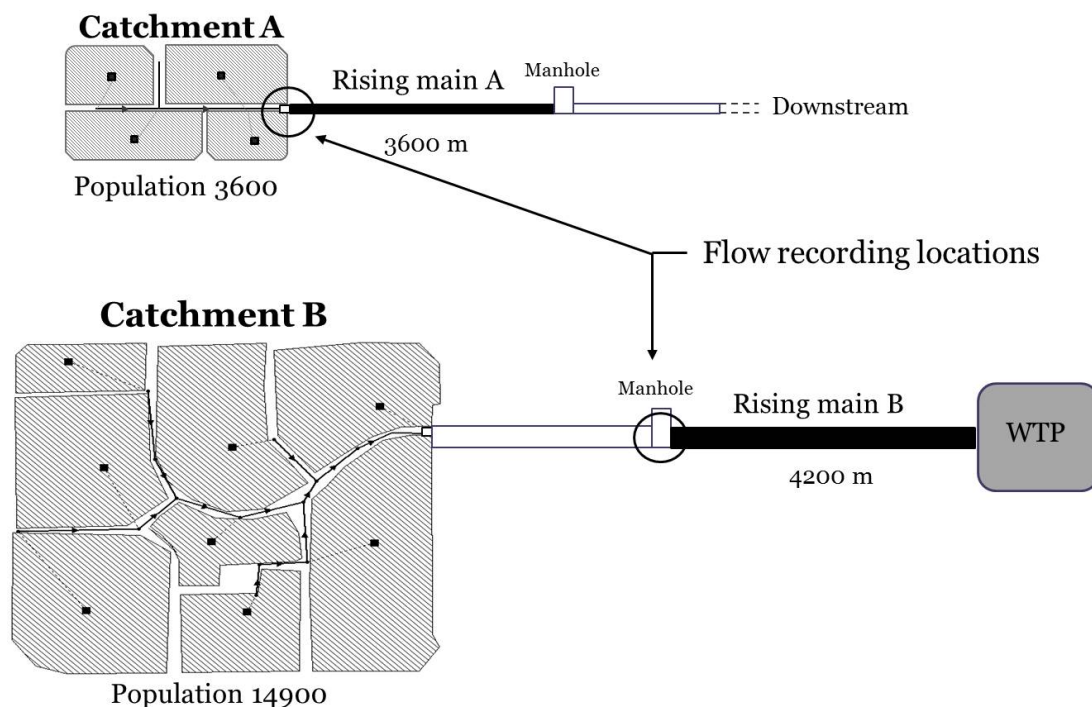


Figure 3.4, the layout of study catchment area and rising mains with flow recording locations.

Figure 3.4 illustrates the two study rising mains in the two catchments. From GIS data, it shows the length of the rising main in Catchment A is 3600m and the rising main in Catchment B is 4200m long. Rising main A follows a pumping station from Catchment A and connects to a gravity sewer in the downstream. Rising main B follows the main trunk sewer from Catchment B and connects to the wastewater treatment plant. The two arrow pointed circles indicate the flow recording locations for Catchment A and B. In Catchment A the flow was recorded in the wet well before the rising main A. In Catchment B the flow was recorded at the end of the gravity sewer before rising main B.

3.2.2 Infoworks flow data and the pump operations

The Infoworks CS model for Catchment A simulates detailed flow information at the flow recording location which includes gravity inflow, wet well flow and pump operations.

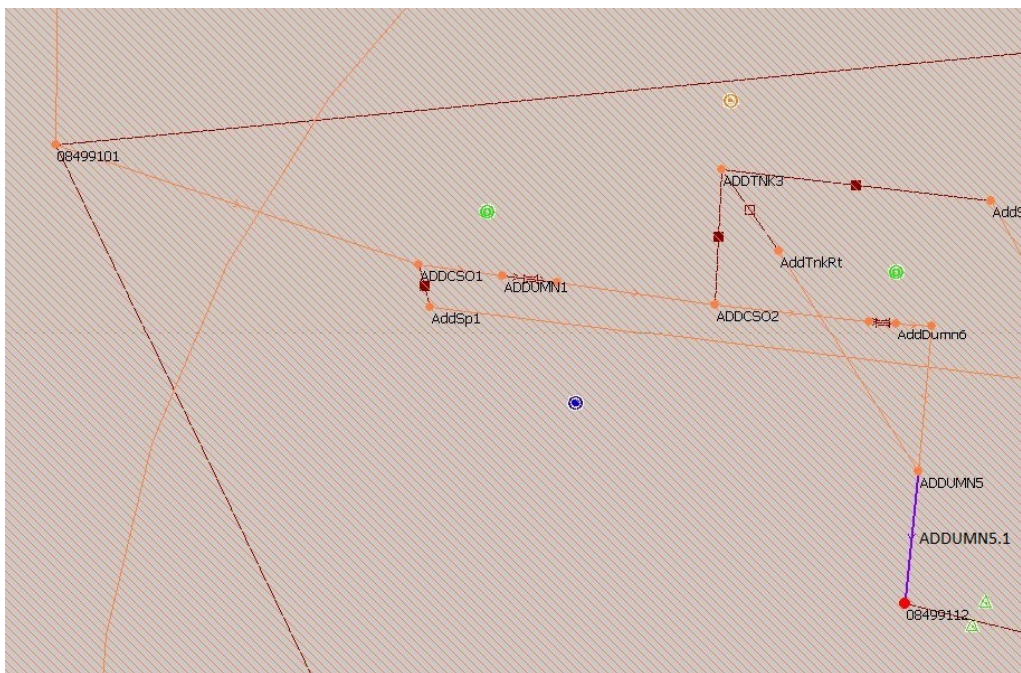


Figure 3.5, Screenshot intercepted section of Catchment A in Infoworks CS.

Figure 3.5 screenshot shows the layout at the pump station in Catchment A. The inlet for output flow is ADDUMN5.1 which is immediately upstream of the wet well. 0849112 node is the wet well. 0849112.1 is the rising main / pump. InfoWorks CS models often don't explicitly model the rising main, it is just modelled as a pump with a remote outlet, which in this case it is a fixed discharge pump. Thus, it can be calculated the velocity manually by assuming a rising main diameter, then the related HRT.

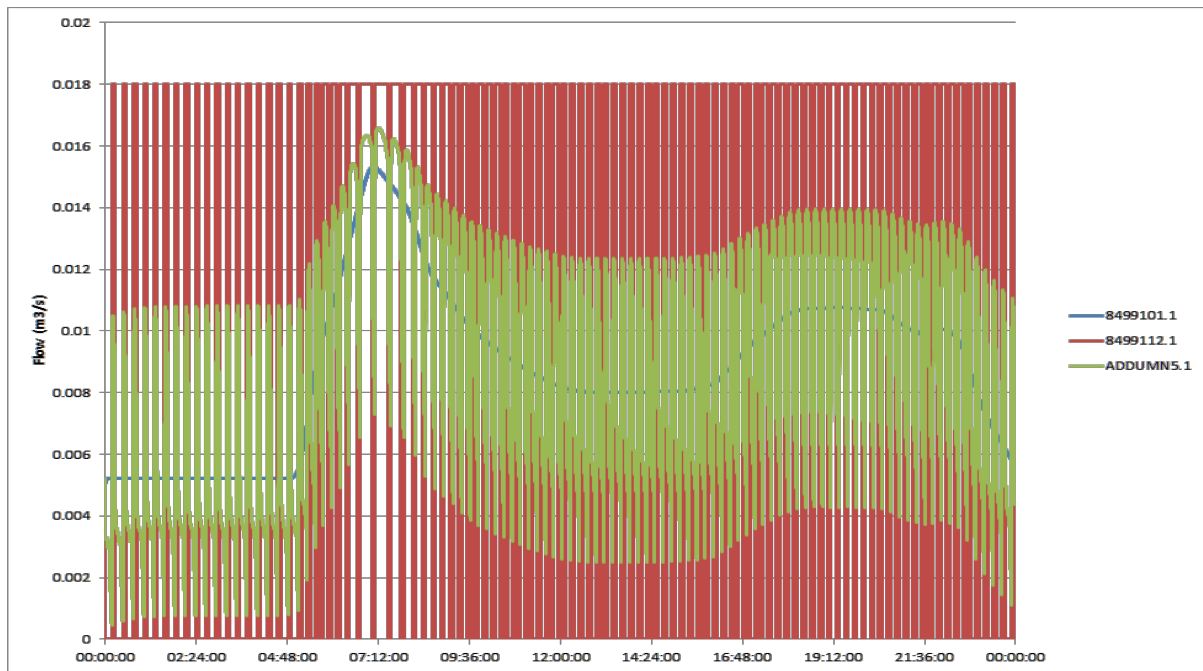


Figure 3.6, wet well, gravity flow, pump operations in Catchment A collection point.

Figure 3.6 shows the flows of the annual average DWF in the intercepted system in Catchment A. There were 349 out of 508 dry weather flow days selected. Pipe 8499101.1 is the gravity inflow into the wet well. Pipe ADDUMN5.1 is also the flow into the wet well, but is immediately upstream, of the wet well and seems to become surcharged when the wet well fills up, hence the spiky flow. 8499112.1 is the flow in the rising main, the pumping seems to be on almost continuously during the morning corresponding with the pump discharge only being a little higher than the peak daily inflow. During the night the residence time would be longer due to the slower frequency from the pump. The Infoworks results indicate the average dry weather flow (DWF) into wet well A and gravity sewer B is $0.0088\text{m}^3/\text{s}$ and $0.056\text{m}^3/\text{s}$ respectively. GIS shows the pump in Catchment A had an original pump switching levels on: 79.55 m AOD (Above Ordnance Datum); off 79.04 m AOD. The pump in Catchment B has a 10.08m^3 switch on/off volume of wastewater. The outflow of the two pumps is $0.018\text{m}^3/\text{s}$ and $0.112\text{m}^3/\text{s}$ respectively. Current on-site pipe diameter of rising main A is 0.1 m; the pipe diameter of rising main B is 0.4 m.

The operation of pumps is essential because it controls all the flows in the rising main which results in the different wastewater residence time and transformation. Different pump switching frequencies were compared for the effects on the formation of hydrogen sulfide. It

was designed different pump operation frequencies with relative pump switching on and off levels. The pump operation has been set to 10 start/stops per hour as standard frequency for modelling (Butler and Davies, 2010). A 5 and 20 start/stops per hour pump operation frequency was also simulated for the redesigned pump station of Catchment A and B pump stations. The three different pump operation frequencies were compared on the influence of hydraulic retention time and sulfide formation. The operation strategies of pumps can be potentially used to interact with the retention capacity of sewer systems and available storage facilities at probable locations.

3.2.3 The selection of rising main pipe diameter

To investigate the effect of different area to volume (A/V) ratios and HRTs, five different diameter pipes were simulated on each of the rising mains. The selection of the pipe diameters was based on the flow velocity of wastewater in sewers which should be greater than $0.7 \text{ m}\cdot\text{s}^{-1}$ to avoid solid accumulation and pipe blockage. The velocity design should also be less than $3 \text{ m}\cdot\text{s}^{-1}$ to avoid hydraulic damage (Read, 2004), which means flow velocity greater than $3 \text{ m}\cdot\text{s}^{-1}$ would significantly reduce the lifetime of sewer structures and results in damage especially for rising mains, and at joints, valves, and bends. Therefore, the selection range of pipe diameter should be in the range of required desirable flow velocity. The diameters investigated were in steps of 0.05 m, for rising main A the range was from 0.1 to 0.3 m, giving an A/V ratio of from 13.3 to 40 m^{-1} ; and for rising main B from 0.25 to 0.45 m, giving an A/V ratio of from 8.89 to 16 m^{-1} .

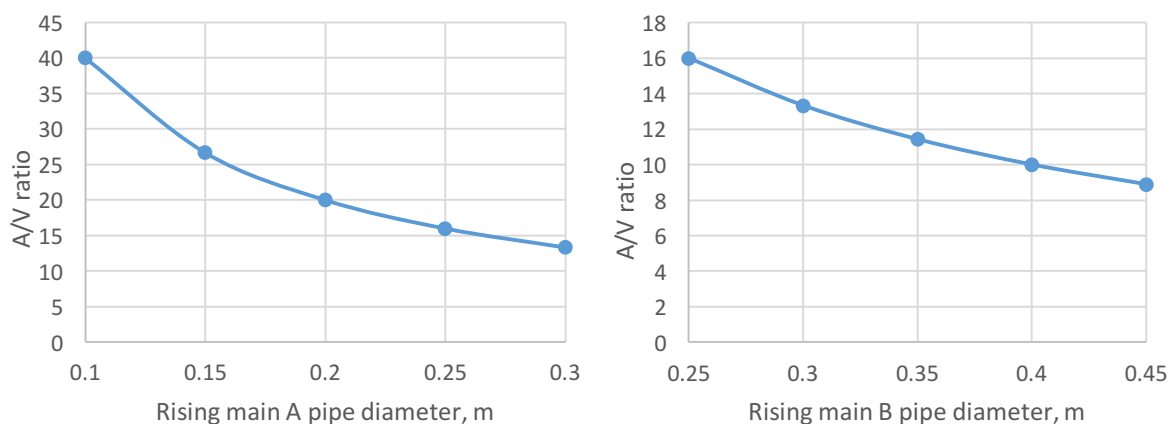
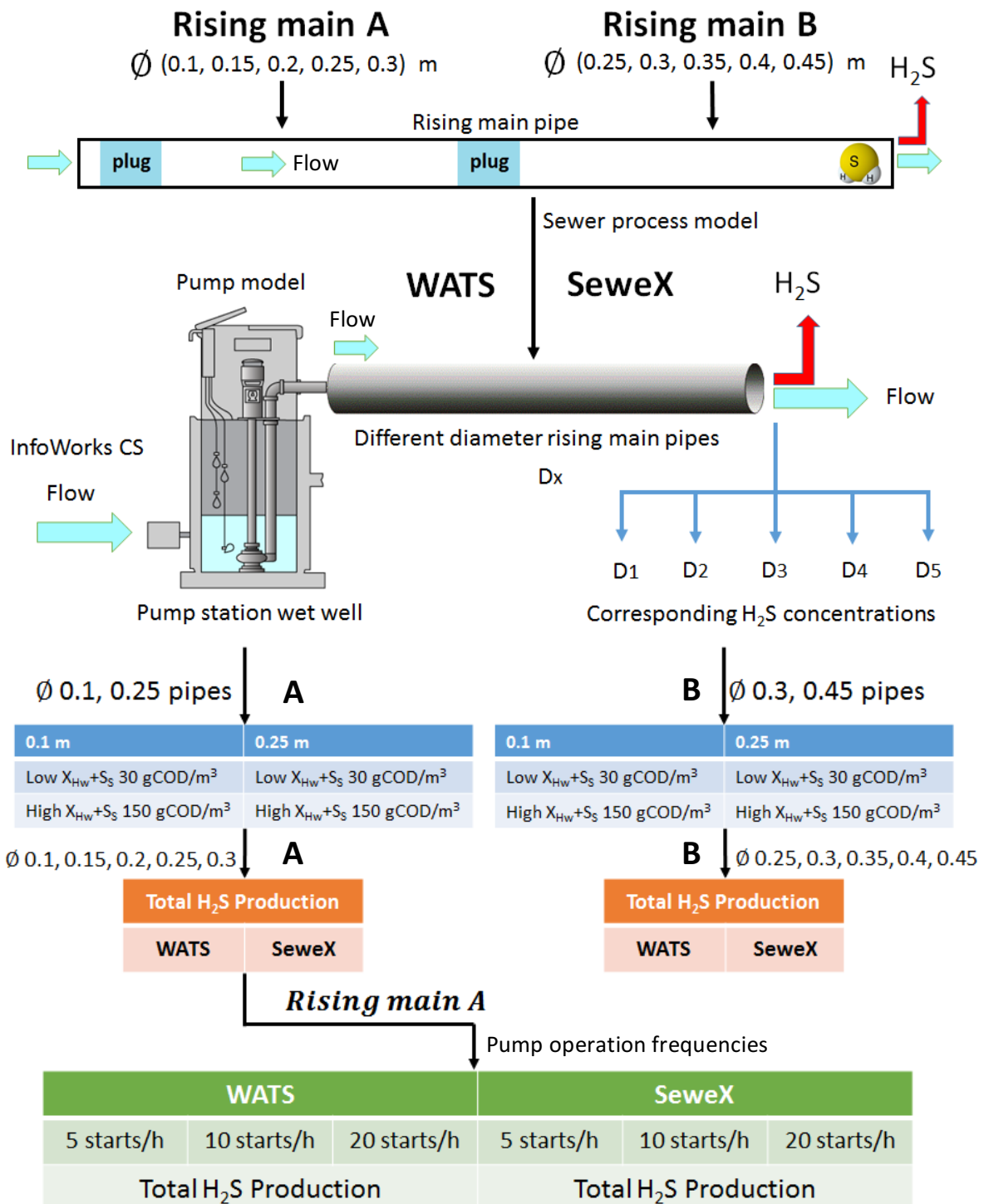


Figure 3.7, A/V ratio with selected pipe diameter range for rising main A and B.

Figure 3.7 shows the A/V ratios corresponding to selected pipe diameters for rising main A and B in the range of required flow velocity. The diameter of 0.25m and 0.3m for rising main A is only for modelling purpose. It won't be selected in practice because the flow is less than 0.5m/s which will result in sedimentation and pipe blockage.

3.2.4 Flow Chart of Model Implementations



3.2.5 Model implementation and integrations

The transformation of organic substrates and the formation of hydrogen sulfide processes were simulated using the WATS and SeweX process models. The full matrix and algorithm of SeweX model are not open access, only a few kinetic equations available in the literature. The aerobic and anaerobic processes matrix and equations of WATS model used in this study are shown in Table 3.1.

Table 3.1, WATS model matrix expression of the processes in rising mains

Process	X_{Hw}	S_s	X_{S1}	X_{S2}	$-S_o$	S_F	S_A	$S(-II)$	S_{SO4}	Rates
Growth of biomass in bulk water phase	1	$-1/Y_{Hw}$			$(1 - Y_{Hw})/Y_{Hw}$					r_{grw}
Growth of biomass in biofilm	1	$-1/Y_{Hf}$			$(1 - Y_{Hf})/Y_{Hf}$					r_{grf}
Maintenance energy requirement	-1	-1			1					r_{maint}
Hydrolysis, fast		1	-1			1				r_{hydrn}
Hydrolysis, slow		1		-1		1				r_{hydrn}
Reaeration					-1					
Decay of biomass, X_{Hw}	-1			1						r_d
Fermentation in the water phase						-1	1			r_{ferm}
H ₂ S formation								1	-1	r_a

r_{grw}	$r_{grw} = \mu_{H,02} \frac{S_F + S_A}{K_{sw} + (S_F + S_A)} \frac{S_o}{K_o + S_o} X_{Hw} \alpha_w^{(T-20)}$
r_{grf}	$r_{grf} = K_{1/2} S_o^{0.5} \frac{Y_{Hf}}{1 - Y_{Hf}} \frac{S_F + S_A}{K_{sf} + (S_F + S_A)} \frac{A}{V} \alpha_f^{(T-20)}$
r_{maint}	$r_{maint} = q_m \frac{S_o}{K_o + S_o} X_{Hw} \alpha_w^{(T-20)}$
r_{hydrn}	$r_{hydrn} = k_{hn} \frac{X_{Sn}/X_{Hw}}{K_{Xn} + X_{Sn}/X_{Hw}} \frac{S_o}{K_o + S_o} (X_{Hw} + \varepsilon X_{Hf} \frac{A}{V}) \alpha_w^{(T-20)}$
r_d	$r_d = d_{H,ana} \frac{K_o}{K_o + S_o} \frac{K_{NO3}}{K_{NO3} + S_{NO3}} X_{Hw} \alpha_w^{(T-20)}$
r_{ferm}	$r_{ferm} = q_{ferm} \frac{S_F}{K_{ferm} + S_F} \frac{K_o}{K_o + S_o} \frac{K_{NO3}}{K_{NO3} + S_{NO3}} (X_{Hw} + \varepsilon X_{Hf} \frac{A}{V}) \alpha_w^{(T-20)}$
r_a	$r_a = a \sqrt{S_F + S_A + X_{S1}} \frac{K_o}{K_o + S_o} \frac{K_{NO3}}{K_{NO3} + S_{NO3}} \frac{A}{V} \alpha_w^{(T-20)}$

Table 3.1 shows the aerobic and anaerobic processes occurring in rising mains. The processes were programmed in MATLAB. The output flow data of the two catchments from Infoworks was fed into the process model respectively to simulate the variation of sulfide concentration with the change of flow. Each of the five selected pipe diameters for two rising mains were simulated separately for the comparison on the formation of hydrogen sulfide. The model simulated the hydrogen sulfide concentration at the end of the rising main for each pipe with

the same input flow data from Infoworks. The change of hydrogen sulfide concentration at the end of the rising main was compared for each pipe with the change of flow for a day/24h. The total amount of hydrogen sulfide production was also calculated for each pipe in a 24h time. The time interval of output flow data from Infoworks is 1 second. The process model has been running on two time intervals for comparison, 1 second as the same as Infoworks for first model integration; then 60 seconds was selected as time interval to improve the model efficiency, this time interval is also needed for model stability. The COD concentration of wastewater used in the process model was collected from a dataset based on 109 samples from five different locations in Denmark and Germany (Vollertsen et al., 2005). All other WATS model parameters used were standard and default value from (Hvitved-Jacobsen et al., 2013)

Table 3.2, Two sets of COD fractions and literature standard COD fraction.

COD Concentration (H-Jacobsen,2013) gCOD/m ³		Fraction	COD Concentration (Vollertsen,2005) gCOD/m ³		Fraction	Standard Fraction(H-Jacobsen,2013)
X _{HW}	80	12.6%	X _{HW}	55	12.5%	10%
S _s	50	8%	S _s	32.4	7.5%	6%
X _{S1}	120	19%	X _{S1}	124	28%	14%
X _{S2}	380	60%	X _{S2}	228	52%	70%
Total COD	630		Total COD	439.4		

Table 3.2 shows the total COD and COD fractions used in the WATS process model, where COD fraction means the percentages of each microbial substrates. An average COD concentration of 450 gCOD·m⁻³·day⁻¹ with a COD fraction (X_{HW} 12.5%; S_s 7.5%; X_{S1} 28%; X_{S2} 52%) was used to investigate the five different pipe diameters. The formation of hydrogen sulfide in different diameter pipes was also simulated under extreme COD scenarios. A high and low COD fraction of biomass X_{HW} and readily biodegradable substrates S_s had been modelled. Where X_{HW} + S_s has a COD of 30 and 150 gCOD·m⁻³·day⁻¹ (Hvitved-Jacobsen et al., 2013). A COD mass balance check had been implemented for model validation at last. The change of individual COD fraction and total COD in wastewater had been calculated and validated for each pipe.

3.2.6 Comparison between sulfide formation kinetic equations in process models

The WATS and SeweX models use very different kinetic equations of sulfide formation rate. It is interesting to compare the results by applying the two different sets of equations. SeweX

model regulates a constant temperature of 25°C for wastewater transformations and sulfide formation (Sharma et al., 2008). In order to meet the same condition, the temperature coefficient in WATS model has been set up to 25°C corresponding with the same temperature in SeweX model.

Table 3.3, Kinetic equations and rate coefficients for the formation of hydrogen sulfide

	Kinetic equations	Rate coefficient
WATS ^a	$r_a = a\sqrt{S_F + S_A + X_{S1}} \frac{K_O}{K_O + S_O} \frac{A}{V} \alpha^{(T-20)}$	$a = 0.001 \sim 0.1$ ^c
SeweX ^b	$r_a = k_{H_2S} \frac{S_{FCOD} + S_{VFA}}{K_{Sf} + (S_{FCOD} + S_{VFA})} \frac{S_{SO_4}}{K_{SO_4} + S_{SO_4}} \frac{K_{O_2}}{K_{O_2} + S_{O_2}} \frac{A}{V} \frac{S_{FCOD}}{S_{FCOD} + S_{VFA}}$	$k_{H_2S} = 1.36 \pm 0.16$ ^d
^a Hvitved-Jacobsen <i>et al.</i> , 2013 ^b (Sharma et al., 2008); ^c (Tanaka et al., 2000); ^d (Guisasola et al., 2009)		

Table 3.3 shows the kinetic equations and rate coefficients for sulfide formation process in WATS and SeweX model, in general, WATS and SeweX model use similar kinetic equations on sulfide formation which considers the fermentation and biodegradable processes. The original sulfide formation equation in WATS model contained a fraction of anoxic processes. However, it was not included in the calculations because there was no nitrate chemical dosage in the current case study sewer system and the nitrate concentration in the wastewater was very low. SeweX model also implements the sulfate process into the rate equation, in which it is theoretically important to calculate the change of sulfate concentration on sulfide formation. WATS model states the sulfate process is not important when the sulfate concentration in wastewater is less than 50 g/m³. Therefore, a comparison has been made on the two model equations and rate coefficients for the formation of hydrogen sulfide.

3.3 Results and Discussion

3.3.1 Flow variations for Catchment A and B

In order to complete the Infoworks model construction and the long-term flow survey, the flow meters were placed in the two catchments for a continuous flow recording for 1 year and 7 months. The two flow recording locations for flow data used in this model simulation are shown in Figure 3.4. The flow data used for two catchments was an annual average DWF

in 1 year and 7 months. The output flow data of Catchment A from InfoWorks include gravity flows, wet well flow, upstream wet well flow and flows in the rising mains. Only the wet well out flow was used for model simulations because it is the flow into the rising mains.

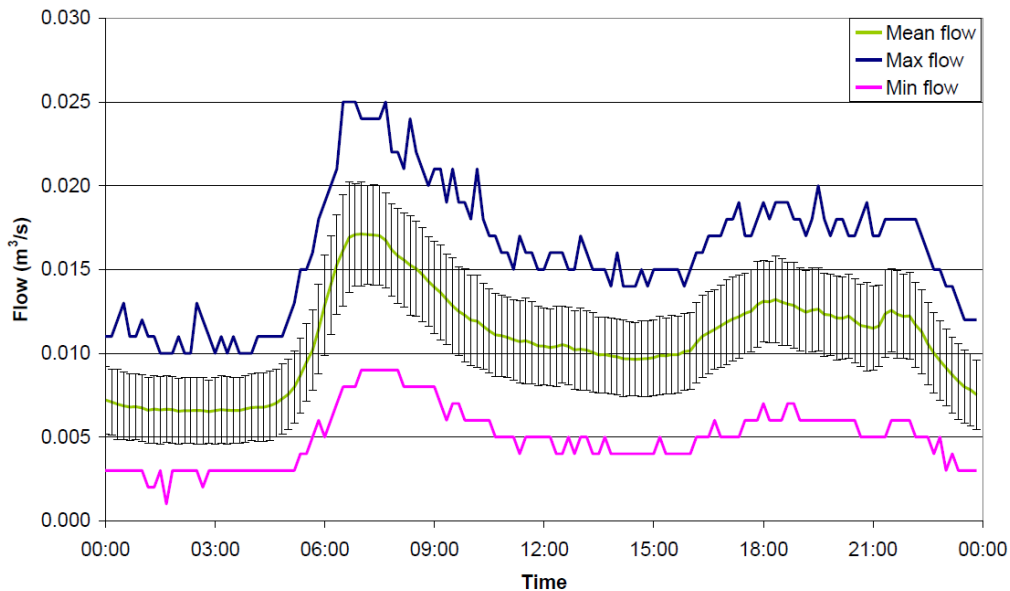


Figure 3.8, Variability of weekday flows at Catchment A flow recording location.

Figure 3.8 shows the average weekday dry weather flows at the flow recording location in Catchment A. The mean flow, minimum flow and maximum flow was plotted. The mean flow indicates 1 standard deviation of the selected DWF dataset at each 10-minute time step, it is interesting to note that through the day the standard deviation remains almost constant at 2 to 3 l/s. The maximum and minimum flows are also seen to follow the diurnal pattern. It is likely that much of the variation in the plotted dry weather flows is a function of long-term trends in infiltration, which tends to be higher in the wetter winter months.

The dry weather flow days were selected and compared for each day of a week based on the weather data along with the flow monitoring survey. 349 out of 508 days have been confirmed as DWF based on the weather data. Figure 3.9 clearly shows the daily flow variability in DWF profiles, which reflects the change of dry weather flow on each day of a week and the drainage characteristics of the local residents. It can be seen that the flow on weekdays is almost the same. Only the peak flows on Saturday and Sunday has a one hour to one-and-a-half-hour delay, where the peak flow is also slightly higher than weekdays.

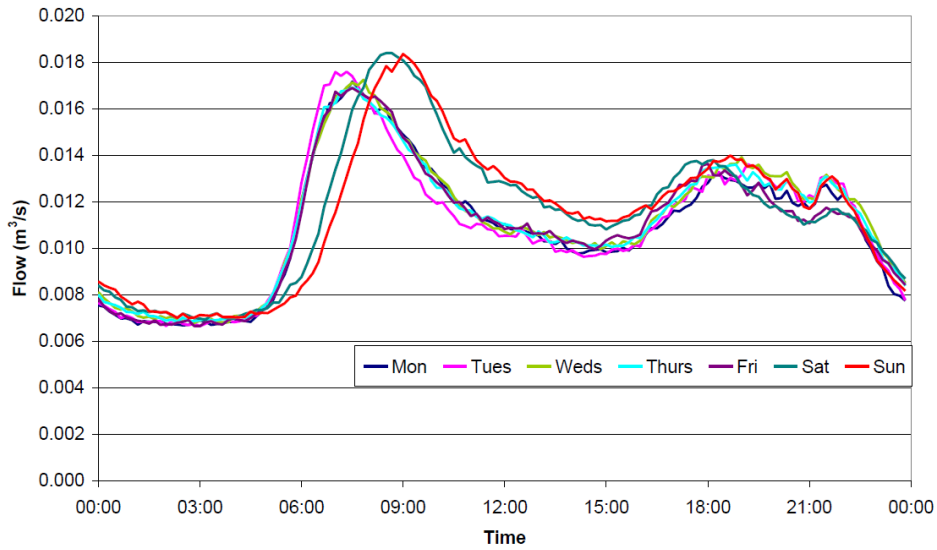


Figure 3.9, Average daily dry weather flow variability in 7 days a week

The flow for Catchment B was recorded in the manhole which contains flows from the upstream gravity sewers. The flow data consists of detailed measured flows and modelled flows from upstream in Infoworks.

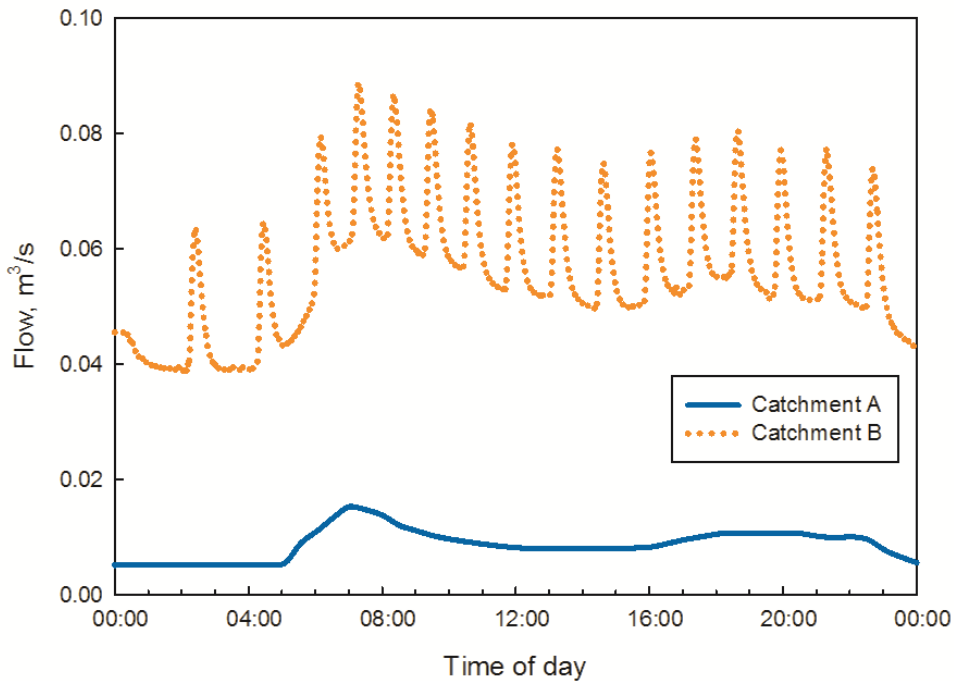


Figure 3.10, Average of all DWF in Catchment A and B before rising mains.

It can be clearly seen from Figure 3.10 that for Catchment B, in addition to gravity flows there is an upstream pump, shown by the spikes in the flow rate curve. The flow in the rising mains

is not constant due to pump operations. The pump is operating almost constantly during the morning, corresponding with the pump discharge outflow only being a little higher than the peak daily inflow. During the night, the average residence times would be longer due to the intermittent flow from the pump. The Catchment B is the flow in the main trunk sewer pipe at the end of the catchment, and which is connected to the rising main before the wastewater treatment plant. The operations of pumps are based on the inflows and which also determines the flow rates and HRTs in the rising mains.

3.3.2 Sulfide formation in different diameter pipes

Table 3.4, Average hydraulic residence time and A/V ratio on two rising mains with different diameter pipes

Rising main Catchment A				Rising main Catchment B			
Pipe diameter	Average HRT	A/V	Flow velocity	Pipe diameter	Average HRT	A/V	Flow velocity
(m)	(hour)	(m ⁻¹)	(m·s ⁻¹)	(m)	(hour)	(m ⁻¹)	(m·s ⁻¹)
0.1	0.68	40.00	2.25	0.25	0.77	16.00	2.29
0.15	1.50	26.67	1.02	0.3	1.10	13.33	1.59
0.2	2.67	20.00	0.56	0.35	1.50	11.43	1.16
0.25	4.20	16.00	0.36	0.4	1.97	10.00	0.89
0.3	6.02	13.33	0.25	0.45	2.51	8.89	0.70

Table 3.4 shows the average hydraulic residence time in rising mains of different diameters with an average pump operation of 10 starts per hour. The diameter selection range for rising main A is only for model purposes, which does not consider the issues of sedimentation or self-cleaning velocity. And the example HRTs are average fictitious values. The real HRT for each pipe varies and depends on the flow and pump operations. It can be seen that the change of residence time in larger pipes is less substantial than that in smaller pipes. The velocity of wastewater in the rising mains are between 0.25 m·s⁻¹ to 2.25 m·s⁻¹ on the pipe diameter from 0.1 m to 0.3 m; and between 0.7 m·s⁻¹ to 2.29 m·s⁻¹ on the pipe diameter from 0.25 m to 0.45 m. The influence of pipe diameter on A/V ratio is significantly decreased for larger pipes. The A/V ratio of 0.1 m, 0.15 m, 0.2 m diameter pipes varies in a quite range. It changes smoothly after 0.25 m pipes.

Figure 3.11 and Figure 3.14 each compares sulfide formation results from the WATS (a) and SeweX (b) models for rising mains A and B respectively for a 24-hour period. It can be seen from Figure 3.11 that the sulfide concentrations predicted by the two models for the rising main in Catchment A is significantly different. This is because the sulfide formation equation

in two models is considerably different, including the rate coefficient and algorithm. It also can be seen that the change of hydrogen sulfide concentration is almost opposite to the change of flow pattern. The sulfide concentration reaches the highest point when the flow was the lowest at night, then it decreased to the lowest concentration during morning peak when the flow rate was the highest.

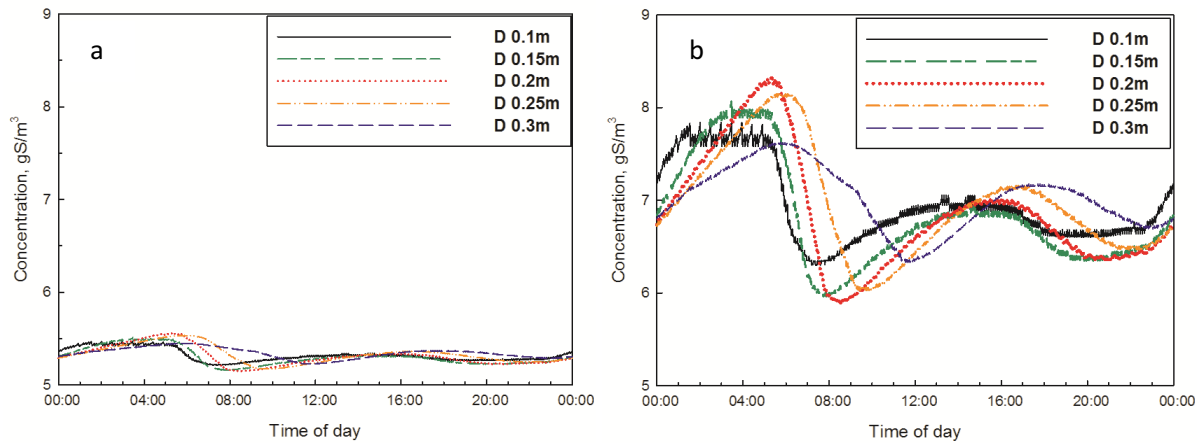


Figure 3.11, the variations of H_2S concentration in a day on different diameter pipes at the end of the rising main in Catchment A (a is WATS, b is SeweX).

Figure 3.11 also illustrates the variation of hydrogen sulfide concentration on different diameter rising mains. Figure 3.11a shows the water phase hydrogen sulfide concentration varying between 5 and 6 $gS \cdot m^{-3}$. Sulfide concentration fluctuates a lot depends on time and location. Hvitved-Jacobsen et al (2013) model results from WATS shows hydrogen sulfide gas concentration varies between 0 – 8 ppm, 0 – 15 ppm, and 15 – 16 ppm in different sewers. A higher sulfide concentration was observed in Figure 3.11b with the SeweX sulfide formation equations. A maximum sulfide production rate of $10 gS \cdot m^{-2} \cdot day^{-1}$ was obtained in the study of Sharma et al (2008) shown in Figure 3.12.

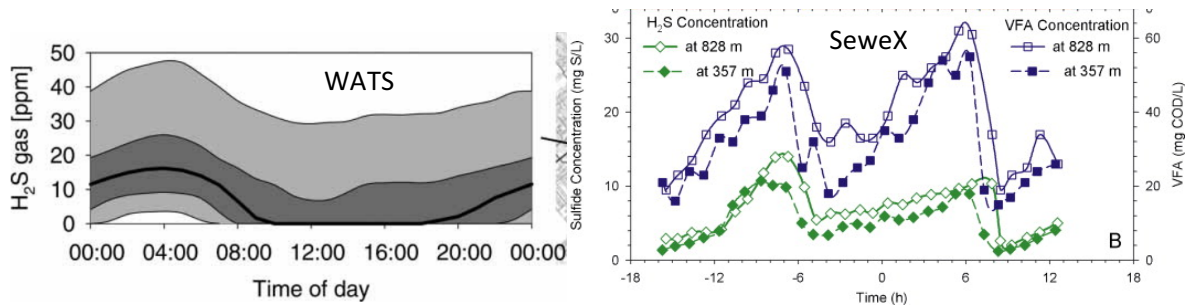


Figure 3.12, typical modelled sulfide concentration from WATS and SeweX model(Hvitved-Jacobsen et al., 2013, Sharma et al., 2008)

Figure 3.12 shows the typical modelled sulfide concentration in rising mains from the two models. The hydrogen sulfide concentration in WATS model is gas phase concentration (ppm). Although it could not reflect the actual concentration in the water phase, it can also indicate the variation trend with the change of flow pattern.

In order to have a clear look on the effect of different diameter pipe on the formation of hydrogen sulfide. The model results of original pipe, lowest and highest total grams of hydrogen sulfide production pipes were selected and plotted separately.

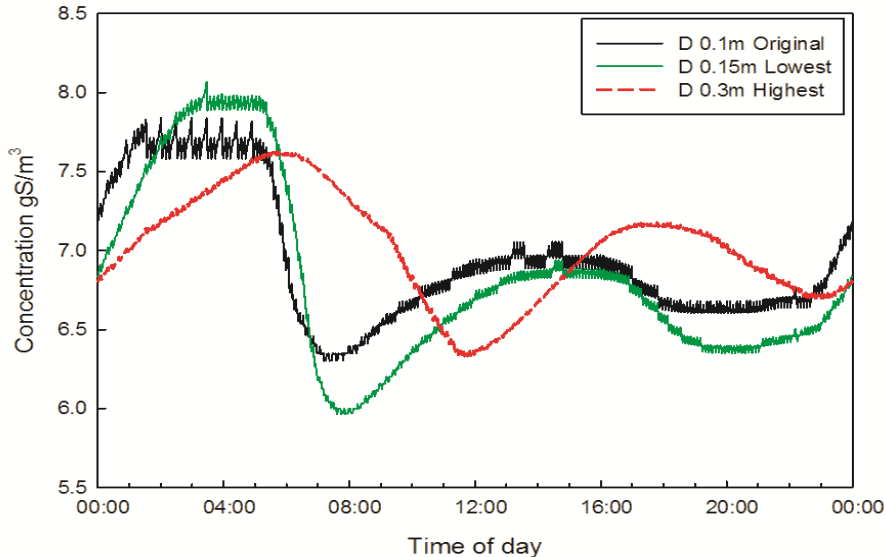


Figure 3.13, selected diameter pipes on sulfide formation.

It can be seen from Figure 3.13 that although the lowest sulfide generation pipe (0.15m) seems to produce the highest hydrogen sulfide concentration at night period compared to the original pipe (0.1m), however, the model results showed that the 0.15m diameter pipe is

the optimal pipe in terms of total hydrogen sulfide production in 24h. The total hydrogen sulfide production is listed in Figure 3.17.

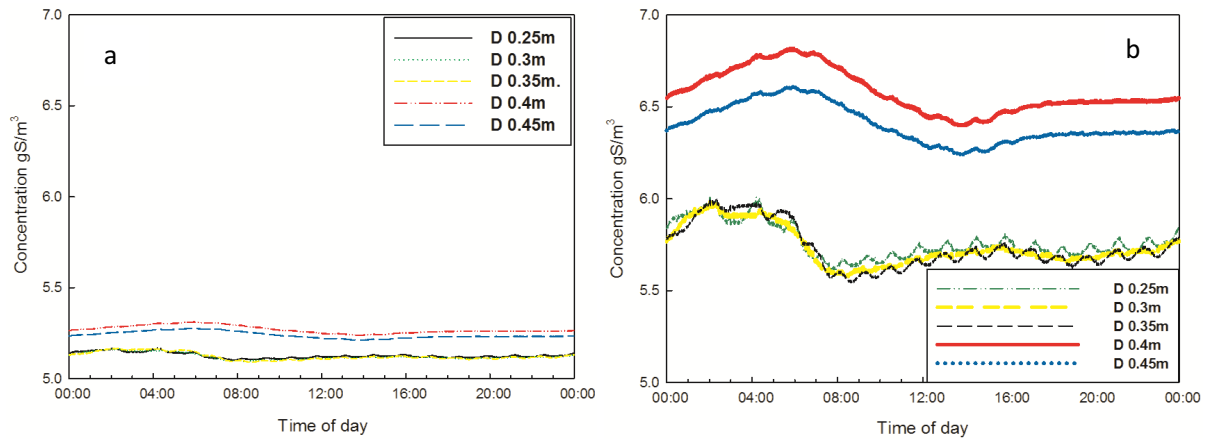


Figure 3.14, the variations of H₂S concentration in a day on different diameter pipes at the end of the rising main in Catchment B (Where a is WATS, b is SeweX).

Figure 3.14 illustrates SeweX model results in rising main B. Apart from the similar variation trend to sulfide concentrations in rising main A, the most significant difference is that the sulfide concentrations in both the 0.4 m and 0.45m diameter pipes simulated to be much higher than that in 0.25 m, 0.3 m and 0.35 m diameter pipes which showed very parallel sulfide concentration variations. This is due to the 0.4m and 0.45m pipes have a combination of relative high A/V ratio and long HRT within the current flow rate from upstream and pump operation.

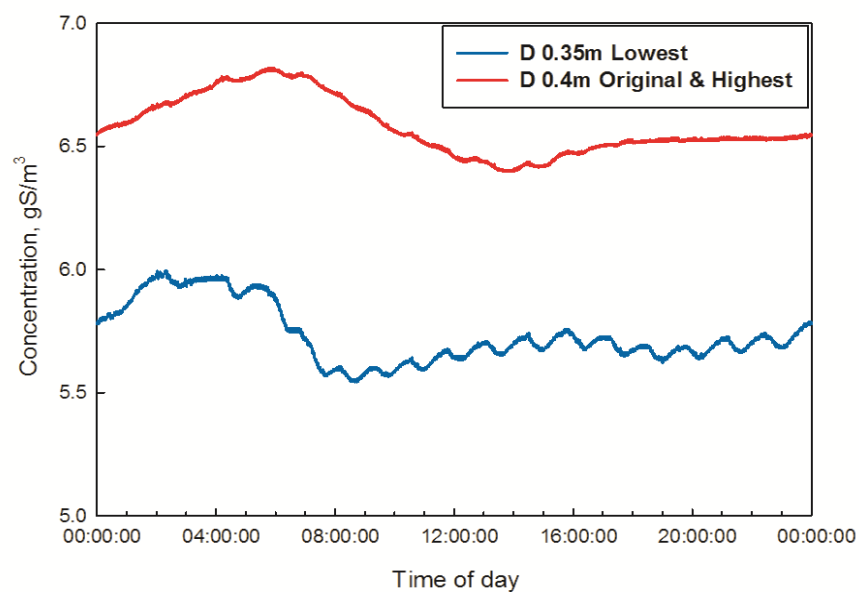


Figure 3.15, Lowest and highest sulfide generation pipes in Figure 3.14b.

The lowest and highest sulfide generation pipes were selected and plotted separately from Figure 3.14b as shown in Figure 3.15. The model results show that the highest hydrogen sulfide production in 0.4m diameter pipe. It is interesting that this is exactly the current on-site pipe with a diameter of 0.4m. It can be estimated from the model results that the A/V ratio and HRT combination of 0.4m pipe creates a more suitable condition for the biological processes in the biofilm, which also contributes a relative low flow velocity for the bacteria activities and biofilm growth.

3.3.3 The effect of COD fractions on sulfide formation

Total COD has been confirmed as one of the most influential parameters on hydrogen sulfide formation in literature. And the COD fraction of biomass and readily biodegradable substrates have been found to be the most influential parameter for sulfide formation in Chapter 4. The formation of hydrogen sulfide under extreme wastewater conditions was also simulated on the smallest and largest pipes for rising main A and B, which is 0.1m and 0.3 m pipes for rising main A; 0.25m and 0.45m pipe for rising main B. The low (30 g-COD/m^3) and high (150gCOD/m^3) COD concentration is the fraction of heterotrophic biomass plus readily biodegradable substrates, which are selected based on the wastewater condition under different weather conditions and flow variation (Hvitved-Jacobsen et al., 2013).

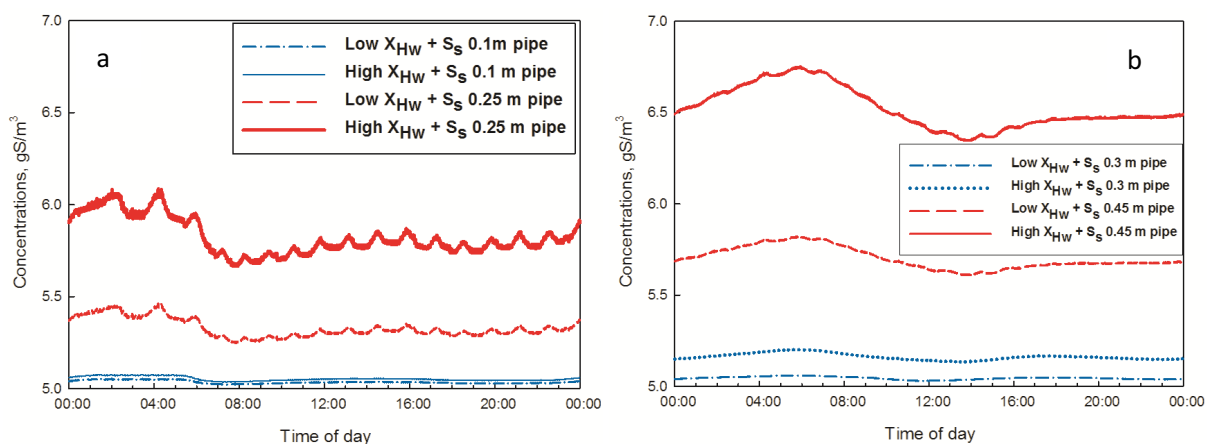


Figure 3.16, Sulfide formation on extreme organic substrates concentrations in different diameter pipes. (Where a is both high and low organic subs. in 0.1m and 0.25m pipes, b is in 0.3m and 0.45m diameter pipes)

Figure 3.16 shows the formation of hydrogen sulfide concentration changes with high and low heterotrophic biomass (X_{HW}) and readily biodegradable substrates (S_S). Within a total COD of 450 gCOD/m^3 , 30 gCOD/m^3 and 150 gCOD/m^3 are the lowest and highest fractions based

on the standard fraction range (Hvitved-Jacobsen et al., 2013). These parameters were identified in the sensitivity analysis to have a high influence on the formation of hydrogen sulfide and both resulted in higher hydrogen sulfide concentration compared to a low concentration of X_{HW} and S_s . Model results showed the effect of S_s was greater than that of X_{HW} . Figure 3.16a also shows the hydrogen sulfide production in 0.1m diameter pipe is similar to that in 0.3 m diameter one in Figure 3.16b when the wastewater is both low in X_{HW} and S_s concentration. While if the wastewater composition is both high in X_{HW} and S_s , a large diameter pipe with small A/V can also result in high hydrogen sulfide formation. The variation trends from Figure 3.16a are all the same as in Figure 3.16b, only the time for maximum and minimum sulfide concentration appears delayed due to longer HRT. Where the average HRTs in larger diameter pipes are 6 hours and 2.5 hours compared to the smaller diameter pipes of 41 minutes and 46 minutes respectively.

3.3.4 Total sulfide production and pump operations

The total daily hydrogen sulfide production in each different diameter pipes for both rising mains was simulated based on the total wastewater flow from the Infoworks hydraulic model. The process model results indicate optimal pipes in terms of least hydrogen sulfide formation. Total sulfide could be potentially removed if it is replaced by optimised diameter pipe.

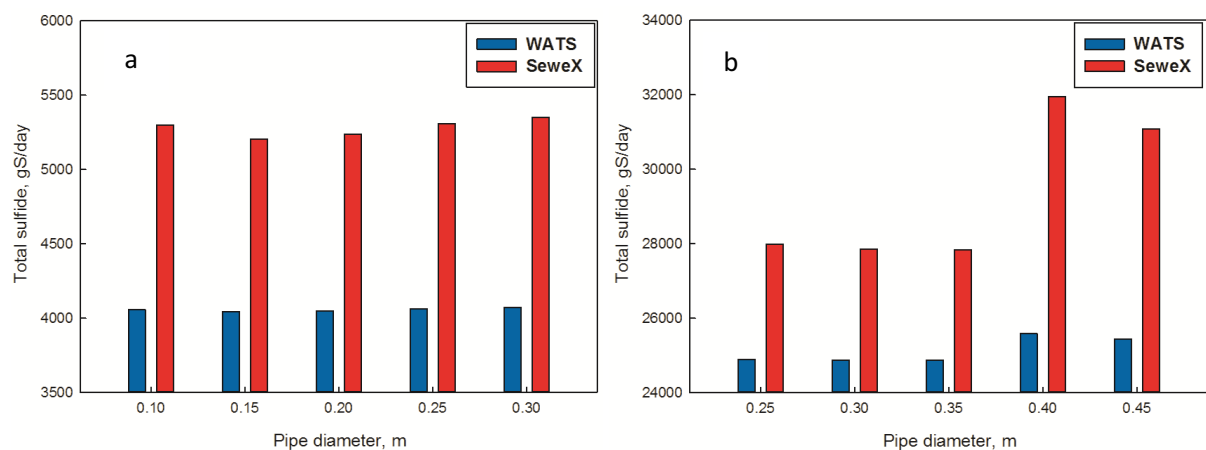


Figure 3.17, Total sulfide production in different diameter pipes. (Where a is rising main A, b is rising main B).

Figure 3.17 shows the total hydrogen sulfide produced in different diameter rising mains. Model results demonstrate rising main B significantly has an optimal option on pipe diameter for less sulfide production. Apart from the differences of sulfide production between different

diameter pipes, the differences between the WATS and SeweX model results are more significant. This is because the model algorithms and parameter conditions are very different. These two models are developed based on two very different climate countries. The model outputs from SeweX model would tend to be much higher due to the hot climate and high temperature. For rising main A, although the differences between different diameter pipes are not obvious, which may also be within the model uncertainties. It still can be seen that for rising main A in catchment A with an original pipe diameter of 0.1 m would have the least sulfide formation if it could be replaced with a 0.15m diameter pipe. It would produce 13 g (WATS) or 91.5 g (SeweX) (1.7%) H_2S less per day than the original 0.1 m pipe. For rising main B, It would significantly reduce 714.8 g (WATS) or 4111.5 g (SeweX) (12.8%) H_2S production per day if the original 0.4 m diameter pipe would be replaced by a 0.35 m one.

For this case study, the two selected rising mains in the catchment didn't provide a desired model simulation scenario. For rising main A, because the pipe diameter is too small, two of the five selected different diameter pipes even cannot meet the velocity requirement. Hence, both model results only showed a 1.7% difference for an optimal diameter pipe. However, for rising main B, the difference significantly increased to 12.8% within an optimal pipe diameter. Thus, a larger pipe with the higher flow can result in more differences even within the model uncertainties. It is advisable to make more comparison on larger pipes in different catchments to understand the genuine effect of pipe diameter on sulfide production. It is noticeable in the catchment B scenario, the model results show that the original 0.4 m diameter rising main got exactly the most sulfide production in a day compared to other diameter pipes due to the combination of relative high residence time and A/V ratio. The effect of pipe diameter on sulfide formation in rising mains is more significant for larger catchments in the aspect of total sulfide production. It is also tended to contribute more hydrogen sulfide emission and sewer corrosion.

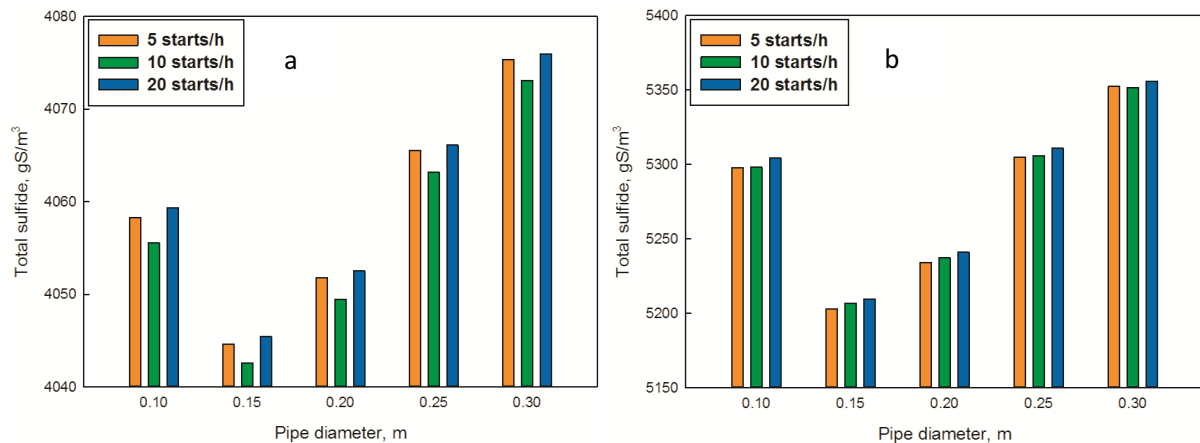


Figure 3.18, Variation of sulfide production with different pump operation frequencies for rising main A. (Where a is WATS model, b is SeweX model).

Figures 3.18 indicates the comparisons on total sulfide production between different pump operations simulated with the WATS and SeweX model. Results show the effect of the pump operation is less substantial than the effect of pipe diameter on sulfide formation. For instance, by replacing the optimal diameter pipe it can significantly reduce 715 g hydrogen sulfide production per day; by changing the pump operation frequency there is only 15 – 20 g different on daily sulfide formation. It is difficult to conclude which is the optimised pump operation frequency, the minor differences are also within the model uncertainties. The discussion and investigation on variable speed pumps and pump operations are recommended for future work. A variable speed pump can reduce peak flows and distribute the excessive water slowly to increase the night flow when the water consumption is very low. It can also reduce high H₂S loads at night with increased flow and shorter HRT.

3.3.5 COD mass balance

The COD balance check was made for the model validation and confirmation. The COD mass balance was checked only with WATS model, because the SeweX model was only used for comparing sulfide formation rate, the organic substrates transformation processes information in SeweX model is unavailable. The change of organic substrates fractions and the total COD has been calculated. The 0.3m diameter pipe for rising main A has been selected for COD mass balance check because it has the longest HRT to investigate the organic matter transformation in the pipe.

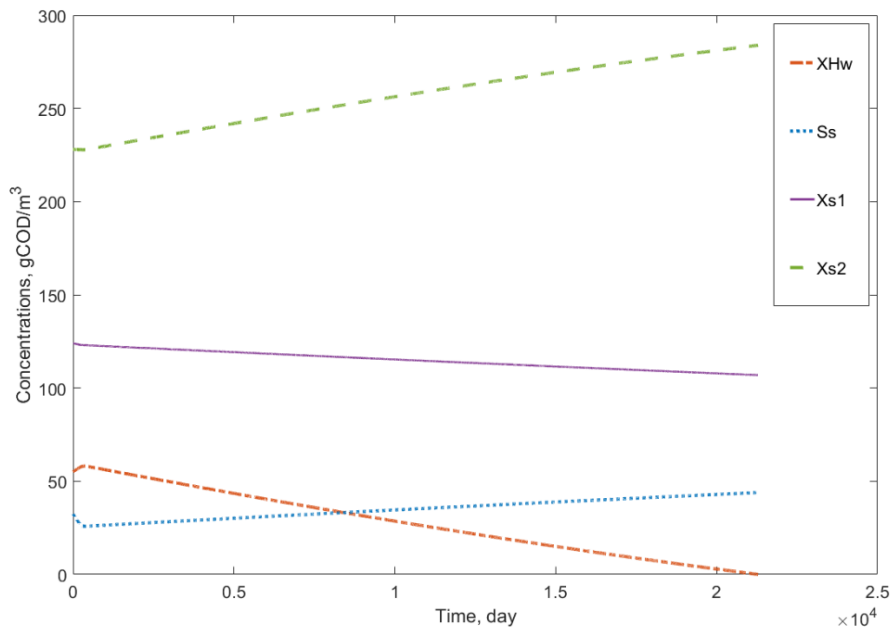


Figure 3.19, Transformation of organic substrates in the rising mains

Figure 3.19 shows the change of organic substrates in rising main A. It can be seen from the figure that around the first 10 minutes it was aerobic process due to the presence of dissolved oxygen which comes from the reaeration and wet well drop in the pump before the rising main. The bulk system transited to anaerobic process when the dissolved oxygen was used up. During the anaerobic process, the decay of heterotrophic biomass contributes to the growth of slow hydrolysable substrates. The hydrolysis of both fast and slow hydrolysable substrates (X_{S1} , X_{S2}) results in the increase of readily biodegradable substrates. The fermentation process on the fermentable substrates fraction also consumes the growth of biodegradable substrates.

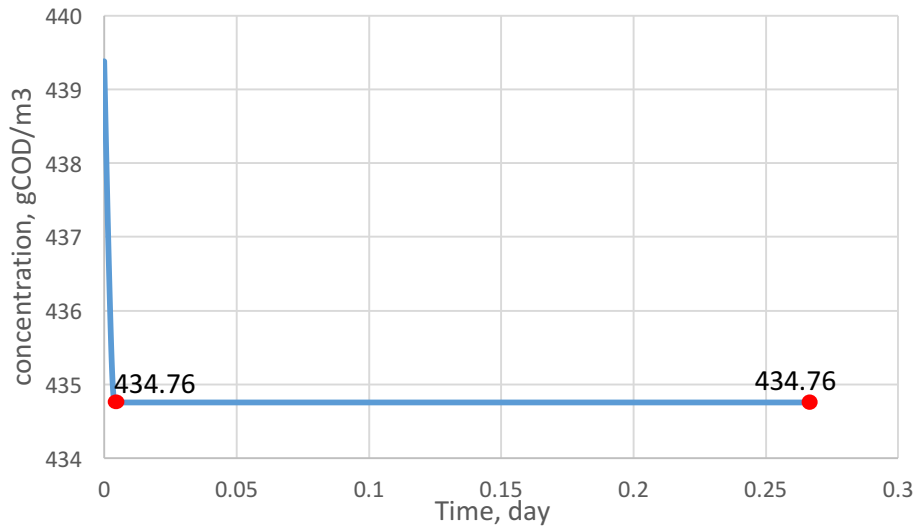


Figure 3.20, Total COD mass balance in the rising main

The total COD mass balance is illustrated in figure 3.20. Before entering the rising main the wastewater had a COD of 439.4 gCOD/m³day. Results showed that the total COD had a decrease at the beginning of the rising main under aerobic condition. The model counted up the organic fraction substrates when the anaerobic process started, it maintained at 434.76 gCOD/m³day till the end of the rising main.

3.4 Conclusions

The studies in this chapter provided theoretical simulation results of the effect of pipe diameter, pumping settings, and COD availability on the formation of hydrogen sulfide in rising mains, which is the effect of A/V ratio, HRT and biofilm processes on sulfide formation. In general, the model results show very little influence on hydrogen sulfide formation for the small rising main; however, more significant influence on the larger pipe. The current model simulation only accounts for sulfide formation in biofilms and water phase, it does not account for the sedimentation effects. The effect of flow on the growth and thickness of biofilms has not been considered. The WATS and SeweX model results on two catchments showed that there potentially is an optimal pipe diameter selection which results in reduced sulfide formation, which was larger than what was currently present in Catchment A, but smaller than the current diameter in Catchment B. Model results suggested to replace the current rising main A (0.1m) with a 0.15m diameter pipe, and the current rising main B (0.4m)

with a 0.35m diameter pipe. Both these optimal pipe diameters provide the desired flow velocity as well.

The WATS and SeweX model show very different results on sulfide formation. This is because the coefficient parameters and sulfide formation rate equations used in these two models are very different. And these two models were developed based on very different conditions. Hence, model validation is very important when using at different locations. The effect of pipe diameter is more significant on large catchment in terms of total hydrogen sulfide formation. It can reduce sulfide production by 4Kg per day from SeweX model results if replaced with optimal pipe for the larger catchment B. This model study delivered a general view that the designers can consider potential hydrogen sulfide formation as well as hydraulic performance when selecting pipe diameter for rising mains. The self-cleaning velocity should always be respected when designing rising mains. However, it also needs to be aware the designing depends on local conditions and wastewater characteristics when considering sulfide formation. For example, a larger optimal diameter pipe cannot be used if the local wastewater contains high solids which will results in blockage with a low velocity. The change of water consumption amount and population growth is also very important for the selection of pipes.

3.5 Future work

This study provided a theoretical simulation on the effect of pipe diameter on the formation of hydrogen sulfide in rising mains. It is interesting and efficient to implement the model investigation; however, it is inconvenient and unpractical to change the on-site rising mains for model validation. Thus, an alternative field test method has been proposed working with the Tsinghua University Sustainable Wastewater Management Centre in China (TUSWMC). Although it is still unpractical to change the on-site pipes, several different diameters rising mains are being selected for different A/V ratios. By changing the pump operation, the outlet flow rate to change the HRTs in the rising mains. This will potentially to provide practical field measurements for model validation.

Variable pump operation control is considered not only to improve sewer hydraulic performance, but also for potential in-sewer processes and wastewater quality management. Some studies had been done on the coordination control of pumping stations for influent and

CSO control. Variable speed pump can reduce peak flows and deliver a more stable daily flow pattern to reduce sulfide formation. The effect of variable speed pump has not been investigated in this study because the current verified Infoworks hydraulic model cannot be adjusted and it is also unavailable to control the on-site pumps. It has been proposed to conduct the variable speed pump testing in the TUSWMC for future work. It is currently working on the system to extend the model with physical, chemical and biological in-sewer processes. The variable pump operation control can potentially benefit for sewer hydraulic performance improvement and wastewater transformations management.

Chapter 4, Global sensitivity analysis on model parameters.

4.1 Introduction

Wastewater in-sewer processes namely the biochemical transformations of organic components are associated with variabilities related to a large number of influencing factors such as parameters and conditions as a fact of modelling approach (Hvitved-Jacobsen et al., 2013). The major concern of in-sewer processes for process modelling is the transformations of organic matter and the formation of hydrogen sulfide. These processes greatly depend on wastewater concentrations such as the total COD and sulfur substrates, and the hydraulic conditions which are mainly flow and residence time in sewer systems. As summarised in literature, many studies revealed COD as one of the five most influential parameters on wastewater transformation and hydrogen sulfide production. However, the total COD consists of COD fractions such as biomass, biodegradable substrates and hydrolysis substrates which vary due to different wastewater source and sewer systems. Therefore, it will be interesting to look at the effect of COD fraction changes on the uncertainty extents of each substrate.

Process models have been divided into different sections correlated to different definitions. For example, the WATS model contains carbon and sulfur cycle which involved with aerobic, anaerobic and anoxic processes (Hvitved-Jacobsen et al., 2013). In terms of hydrogen sulfide, it has been summarised in literature (Freudenthal et al., 2005, Sharma et al., 2008, Hvitved-Jacobsen et al., 2013) that the temperature, pH, flow rate, COD and sulfide concentration has been identified as the key factors controlling the formation of hydrogen sulfide. Among these factors, temperature, pH, flow are all time varying, which means there are no fractions consisted in these parameters. Temperature and pH are the sole physical parameters in a system. Flow velocity is influenced by pipe diameter, pump operation, and also related to A/V ratio when impacting the transformation process. However, these three sole physical parameters control the transformation conditions. While when it comes to COD and sulfide deviations which account on a variety of variables such as the constituents of COD fractions and sulfide, sulfate and all available oxidizing forces.

Organic matter

The composition of wastewater is complex, the majority of COD contents can be classified as biomass, biodegradable, fermentable and hydrolysable substrates (Hvitved-Jacobsen *et al.*, 2013). The COD fraction varies considerably between different model definitions and lab determination methods. For instance, the WWTP based ASM model and sewer system based WATS model define the COD fraction differently. The ASM determines the readily biodegradable substrates (S_s) a percentage of 19%, the fast and slow hydrolysable substrates (X_s) a percentage of 59% (Henze, 2000); while compared to WATS model, in which the S_s and X_s has a fraction of 6% and 84% respectively (Hvitved-Jacobsen *et al.*, 2013, Hvitved-Jacobsen *et al.*, 1998b). Other sewer process models are mostly based on the WATS model COD fraction, such as the Belgian Aqua3S model uses the same fraction from WATS. The COD fraction used in SeweX model is unclear along with all its unknown COD transformation processes. Hence, a comparison on COD fractions of WATS and ASM is listed in below Figure 4.1:

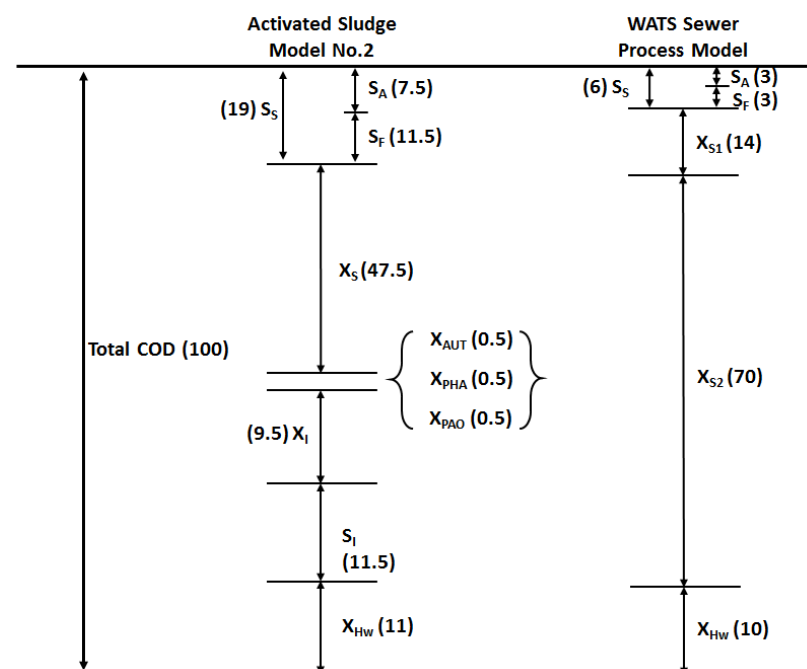


Figure 4.1, Comparison between COD fractions (percentage).

Figure 4.1 shows the comparison of COD fraction between two selected model definitions. If only by applying the percentages here that the transformations of wastewater would be more active in the ASM model description than that of WATS model, especially with a much higher percentage of readily biodegradable substrates. However, this does not mean there will be a

massive difference between these model output results in the same time due to different implemented calculations and algorithm used. An OUR (oxygen uptake rate) test is normally taken for analysing COD fractions in field measurements (Vollertsen et al., 2005).

The stability and credibility of wastewater quality models are decreasing with the increasing of model scale, for example, with the increasing of catchment size, particularly in integrated modelling (Willems, 2006). Most sewer system notes do not get direct measurements, these parameters can be obtained by comparing similar characteristic sewer systems which recorded real time or historical data. It is also not all parameters that can be determined in real time. For example the COD fractions; the measurement takes up to 24 hours. Therefore, either the detail validated model parameters or long term simulation is required to improve model accuracy. In order to test the sensitivity of all organic matter substrates and compared to Donckel's study (Donckels et al., 2014) which only indicated total COD is highly sensitive, a specific modelling on organic substrates sensitivity analysis should be incurred as a further extended analysis. The parameter uncertainties and sensitivities on simple systems require better understanding for dealing with scaling up systems.

Global sensitivity analysis entails applications used for assessing model input parameters and uncertainty on outputs either globally or locally or one factor at a time. It is usually used on empirical, mathematical and concept model testing to review what parameters can be sensitive and the effect on model results, how to identify and understand its impacts on the relationship between modelling and measured data (Saltelli et al., 2008). From Vollertsen's stochastic modelling study (Vollertsen et al., 2005) and Donckel's sensitivity analysis study (Donckels et al., 2014), the results indicated the composition of total COD and the maximum sulfide formation rate has being highly sensitive and influential in terms of aerobic biomass transformation and the anaerobic formation of hydrogen sulfide. The composition of total COD generally consists of heterotrophic biomass (X_{HW}), readily biodegradable substrates (S_S), fermentable substrates (S_F), fermentation products (S_A), fast and slow hydrolysable substrates (X_{S1} and X_{S2}). Hence, it is important to identify the sensitivity of individual COD fractions when dealing with different sewer system conditions. The COD fraction varies between different wastewater samples from different locations.

Donckel's (Donckels *et al.*, 2014) study compared the difference between three models, the ASM, WATS and SeweX model and integrated them to the Aqua3S model. It revealed the most important model input parameters such as total COD and sulfide formation rate for COD transformation, hydrogen sulfide formation and concrete corrosion. However, the influence of each individual COD fraction and some kinetic equation coefficients had not been analysed in Donckel's study, some additional parameters which are important for the process in rising mains had not been tested as well. Total COD in wastewater varies with different time and location, and also with different origins from households or industry (Hvitved-Jacobsen *et al.*, 2013). The total COD even fluctuates significantly in a single system with unstable flow and side connections compared to data from large catchment scale (Vollertsen *et al.*, 2011b). For the development and extension of WATS process model, (Vollertsen *et al.*, 2005, Nielsen *et al.*, 2008a, Tanaka *et al.*, 2000) had done some measurements in real sewer systems, and compared the median value and standard deviation. Based on the results from these studies, it can be seen that there could be a significant difference on model results if by applying the different COD fraction values under different wastewater and sewer conditions.

4.2 Methodology

4.2.1 Monte Carlo Simulation and data generation

In order to test the sensitivity of model parameters, the Monte Carlo simulation has been carried out on the summarised data sets from Denmark and Germany (Vollertsen *et al.*, 2005). Firstly, a group of 13 parameters for rising main process available in literature has been collected and compared of its sensitivity on hydrogen sulfide formation through Monte Carlo simulation. The previous literature paper (Vollertsen *et al.*, 2005) summarised the median and standard deviation value for the selected parameters shown in table 4.1. In table 4.1, where the N in dataset A and B is the number set. For instance, N (3.6; 1.0), means 3.6 is the mean value and 1.0 is the standard deviation. The unit for S_O to $X_{S,slow}$ is gCOD/m³, other parameters are unitless. Data set A is from (Hvitved-Jacobsen *et al.*, 2002), and data set B is from (Vollertsen *et al.*, 2005). The mean value and standard deviation have been justified as normal distributed data in their studies.

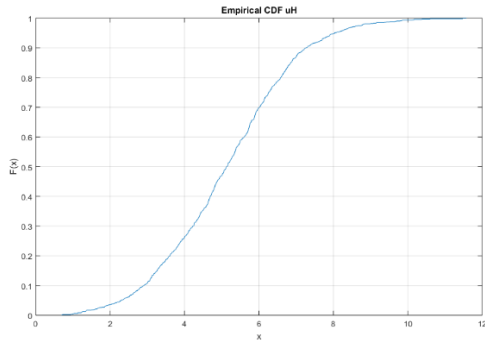
Table 4.1, sewer process model parameters and distribution data.

Parameter	Name	Dataset A (μ, σ)	Dataset B (μ, σ)
uH	Maximum specific growth rate	N (3.6; 1.0)	N (5.17; 1.79)
$K_{1/2}$	Half order rate constant	N (3.0; 1.0)	N (3.0; 1.0)
$K_{h,fast}$	Hydrolysis rate constant fast	N (7.29; 2.76)	N (8.31; 3.29)
$K_{h,slow}$	Hydrolysis rate constant slow	N (1.03; 0.32)	N (0.99; 0.50)
K_O	Saturation constant S_o	N (0.2; 0.05)	N (0.2; 0.05)
K_{Sf}	Saturation constant S_s	N (10.0; 2.0)	N (10.0; 2.0)
$K_{X,fast}$	Saturation constant X_{s1}	0.23 $K_{h,fast}$ N (1; 0.2)	0.34 $K_{h,fast}$ N (1; 0.2)
$K_{X,slow}$	Saturation constant X_{s2}	N (0.91; 1.30)	N (0.94; 1.25)
q_m	Maintenance energy rate constant	N (0.8; 0.2)	N (0.8; 0.2)
S_O	Dissolved oxygen	N (1; 0.5)	N (1; 0.5)
S_S	Readily biodegradable substrates	N (13.5; 11)	N (32.4; 23.3)
X_{Hw}	Heterotrophic biomass	N (51; 16)	N (55; 16)
$X_{S,fast}$	Fast hydrolysable substrate	N (63; 24)	N (124; 19)
$X_{S,slow}$	Slow hydrolysable substrate	N (564; 163)	N (228; 83)
Y_{Hf}	Yield constant biofilm	N (0.43; 0.05)	N (0.43; 0.05)
Y_{Hw}	Yield constant water	N (0.43; 0.05)	N (0.43; 0.05)

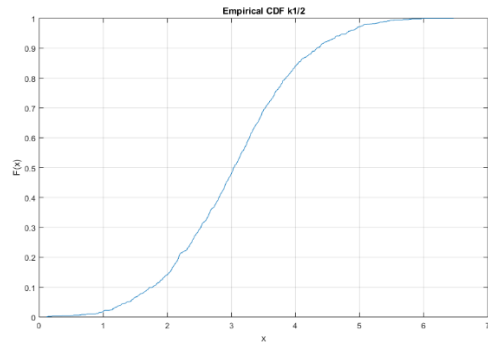
Table 4.1 shows two dataset model parameters for Monte Carlo simulation, dataset A originated from 29 days of dry weather measurements in a gravity sewer in Lisbon, Portugal (Hvitved-Jacobsen *et al.*, 2002); dataset B was obtained from 109 samples collected at 4 different catchments in Denmark and Germany (Vollertsen *et al.*, 2005). From figure 4.1 it can be seen that although two dataset came from North Europe and South Europe with relatively different climate and wastewater conditions, some of the parameters and coefficients even remains the same value; However, COD fractions such as S_S , $X_{S,fast}$, $X_{S,slow}$ did change significantly compared to other parameters. The Monte Carlo Simulation has been implemented within the mean value and standard deviation obtained from these studies, and also compared other constant values based on data from (Hvitved-Jacobsen *et al.*, 2013). In each set of parameter, 1000 value numbers were generated by the normal random number generator function in MATLAB Simulink based on the mean value and standard deviation provided in datasets. Each 1000 value dataset all follows the type of normal distribution.

Figure 4.2 shows the empirical cumulative distribution function s-curves of each parameter dataset generated by normal distribution random generator after 1000 draws Dataset B was used for the Monte Carlo simulation.

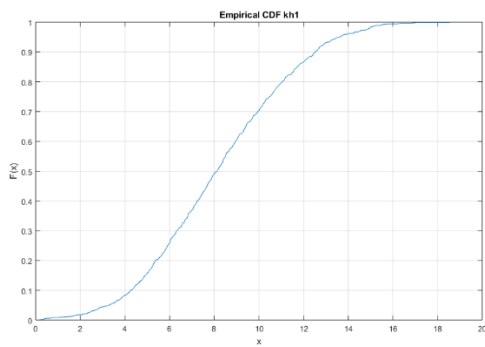
uH Maximum specific growth rate



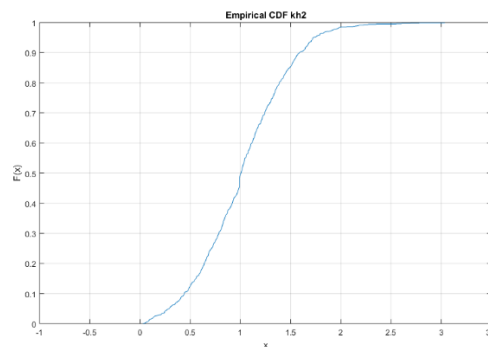
K_{1/2} Half order rate constant



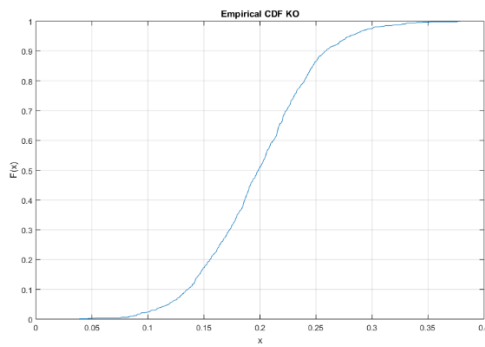
K_{h1} Hydrolysis rate constant fast



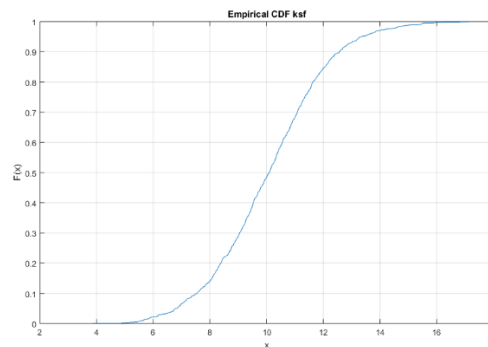
K_{h2} Hydrolysis rate constant slow



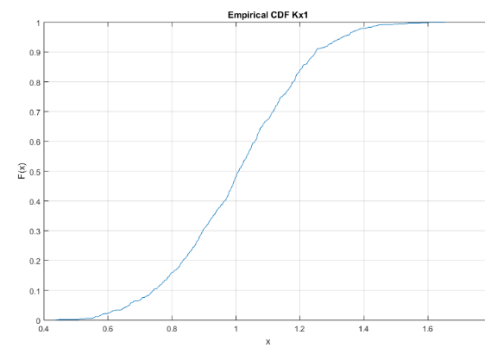
K_O Saturation constant So



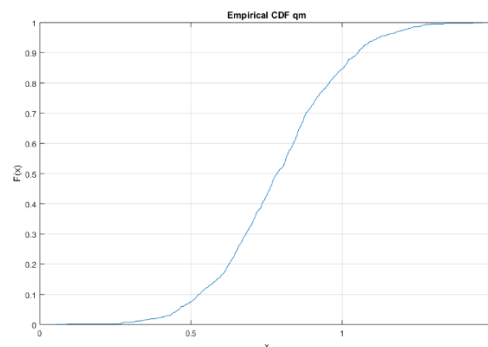
K_{Sf} Saturation constant Ss



K_{x1} Saturation constant Xs1



Q_m Maintenance energy rate constant



S_s Readily biodegradable substrates

X_{HW} Heterotrophic biomass

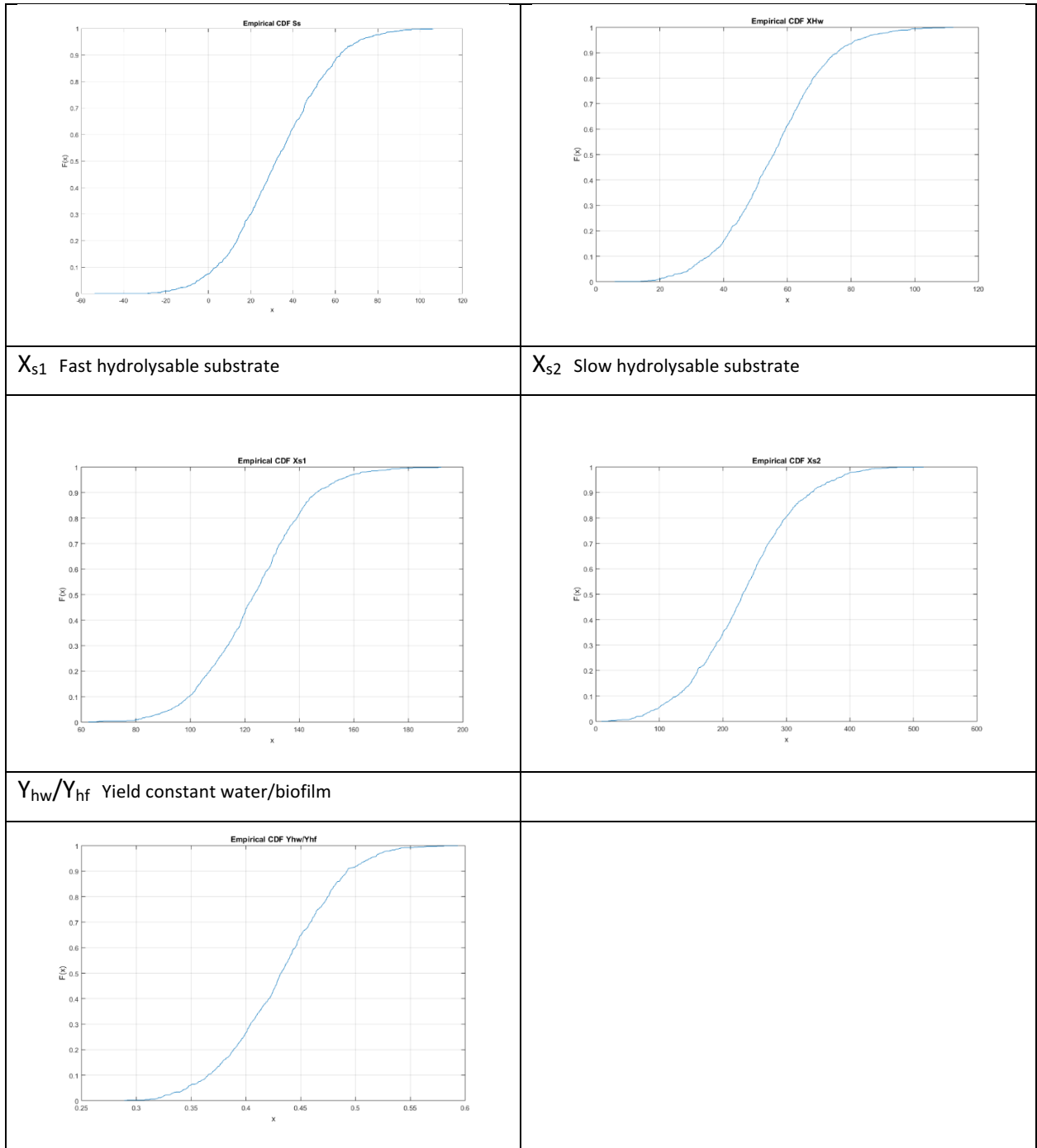


Figure 4.2, Empirical CDF curves for the selected parameters based on 1000 random draws from the random number generator, Dataset B from (Vollertsen et al., 2005).

In order to compare the difference of dataset range and the general performance, the standard deviation divided by average value (μ/σ) has been calculated. The ratio value was increased for each parameter to compare the effect on a wider range of dataset or on more extreme value. Parameters were listed in Table 4.2.

4.2.2 Sensitivity analysis on model parameters

The Monte Carlo simulation was carried out on the rising main in Catchment A introduced in Chapter 3. A scenario of a 0.3m diameter rising main with an average residence time of 6 hours was selected because it has the longest HRT in the rising main diameter ranges. Each dataset containing 1000 data was inputted in the process model which ran 1000 times, It took approximately several hours for running one dataset, and the hydrogen sulfide concentration at the end of the rising main was generated by the WATS process model, results are shown in Figure 4.4 – 4.6.

A long-term wastewater sampling was carried out in Woodhouse Mill WWTP from 12.01.2014 to 02.02.2017 with an average sampling frequency of every two weeks. Wastewater samples were collected at the Woodhouse Mill Wastewater Treatment Plant in South Yorkshire, England. As no wastewater quality was measured at the case study catchment A and B, the samples collected at the WWTP were used as the representative for Catchment A. Samples were collected and transferred to the lab immediately. The COD of wastewater sample was measured using Hach 16mm vials for Chemical Oxygen Demand Analysis and spectrophotometer for reading. The experimental procedure and reading methods are introduced in Chapter 5, Section 5.2.4. Sampling background and results are introduced in Results and Discussion. The COD fraction calculation of WATS model was applied on the samples collected. The total COD and each COD fraction were compared with the literature dataset from several European countries.

The effect of temperature on hydrogen sulfide formation was also compared with model simulation. A range of temperature from 5 – 30°C was simulated in the WATS model. The 3-year long-term wastewater temperature record was also compared with literature dataset. The effect of pH on sulfide formation is reviewed in the literature. However, the effect of pH is only for the release and oxidation of hydrogen sulfide and concrete corrosion. Thus, it is not investigated in this chapter.

4.3 Results and Discussion

4.3.1 Model results on selected parameters

The parameter dataset used for Monte Carlo simulation was based on the mean and standard deviation value from gravity sewers in Denmark and Germany, from the Dataset B in Table 4.1 it can be seen that either the mean value or standard deviation is not significant, and the total COD is relatively low especially compared to the wastewater COD in the UK. It has been manually increased the standard/average (μ/σ) ratio to 0.5 for all parameters, then the concentration of hydrogen sulfide was compared respectively as an amplified sensitivity analysis to look at the influence on a wider range of parameters. The original μ/σ ratio of dataset B and the μ/σ ratio of simulated H₂S was listed at the left of Table 4.2, the increase μ/σ ratio of Dataset B and the related H₂S μ/σ ratio was shown at the right of Table 4.2. The original K_{X1} and S_S had even higher μ/σ ratio in the original Dataset B, hence, the right side value of these two parameters were reduced. It can also indicate the effect on even reduced parameter value.

Table 4.2, different ratio of standard deviation over average on parameter and sulfide

parameters	Dataset B (μ/σ)	H ₂ S (μ/σ)	parameters	0.5 Dataset B (μ/σ)	H ₂ S (μ/σ)
<i>uH</i>	0.3462	0.00005586	<i>uH</i>	0.5	0.00005110
<i>k_{half}</i>	0.3333	0.000007892	<i>k_{half}</i>	0.5	0.00001290
<i>K_{h1}</i>	0.3534	0.000005059	<i>K_{h1}</i>	0.5	0.000002630
<i>K_{h2}</i>	0.5051	0.00001127	<i>K_{h2}</i>	0.5	0.00001104
<i>K_O</i>	0.25	0.0000002544	<i>K_O</i>	0.5	0.000001420
<i>K_{sf}</i>	0.2	0.000001157	<i>K_{sf}</i>	0.5	0.000003320
<i>K_{X1}</i>	1.3298	0.0000008901	<i>K_{X1}</i>	0.5	0.0000008730
<i>q_m</i>	0.25	0.00002829	<i>q_m</i>	0.5	0.00002300
<i>S_O</i>	0.5	N/A	<i>S_O</i>	0.5	N/A
<i>S_S</i>	0.7191	0.001511	<i>S_S</i>	0.5	0.001409
<i>X_{HW}</i>	0.2909	0.004909	<i>X_{HW}</i>	0.5	0.009980
<i>X_{s1}</i>	0.0833	0.0005353	<i>X_{s1}</i>	0.5	0.005528
<i>X_{s2}</i>	0.3640	0.000003046	<i>X_{s2}</i>	0.5	0.000009530
<i>Y_{hf}</i>	0.1163	0.00004932	<i>Y_{hf}</i>	0.5	0.0001280
<i>Y_{hw}</i>	0.1163	0.00004932	<i>Y_{hw}</i>	0.5	0.0001280

Table 4.2 shows the average value divided by standard deviation ratio of the original dataset and the increased wider range of distribution dataset. The left standard/average column

shows the original ratio from the dataset, the right standard/average column shows the increased ratio. It can be seen from the table that the biofilm saturation constant K_{sf} and the readily biodegradable substrate S_s even had a higher original ratio than 0.5, none of them had a significant change on sulfide formation for 6 hours of HRT in rising main A. The probability distribution figures are listed in Figure 4.4 - 4.6. It is also noticeable that the biomass X_{Hw} , biodegradable substrate S_s and fast hydrolysable substrate X_{s1} had a significant increase in sulfide formation with the increased ratio. The results also showed a considerable increase in sulfide formation with the larger ratio of yield constants. The strongest uncertain parameters with high sensitivity can be seen include X_{Hw} , S_s , X_{s1} .

Through the Monte Carlo simulation on each of the testing parameter, the model shows 1000 hydrogen sulfide concentrations distribution based on each parameter. For example, Figure 4.3 shows the hydrogen sulfide concentration distribution of the Monte Carlo simulation results on K_{x1} . All model results distribution is listed in Figure 4.4. A full comparison is listed in Figure 4.5, and the most sensitive parameters are compared in Figure 4.6.

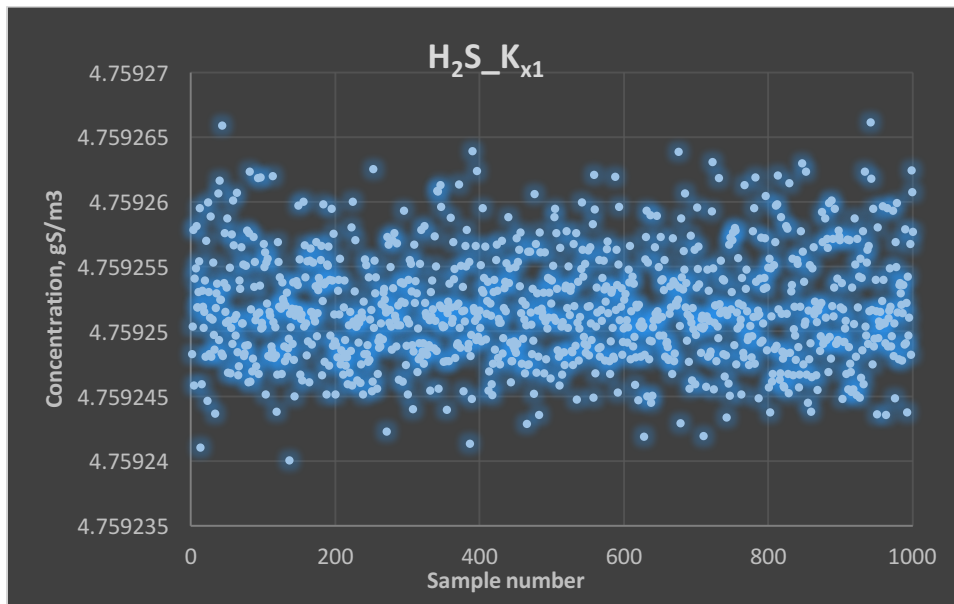
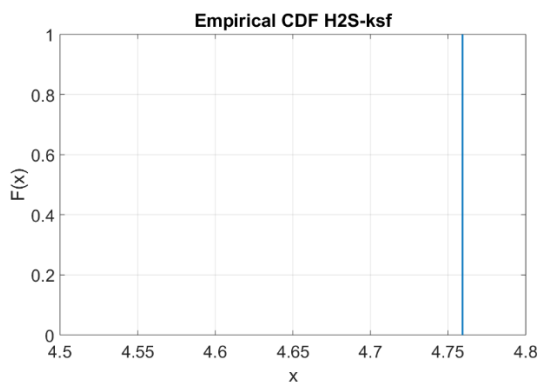
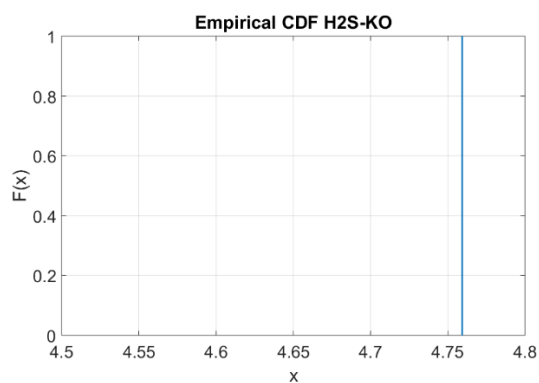
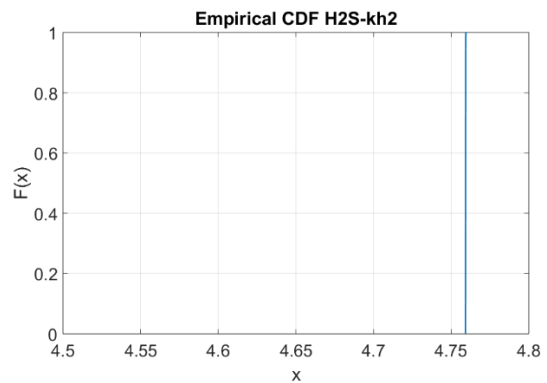
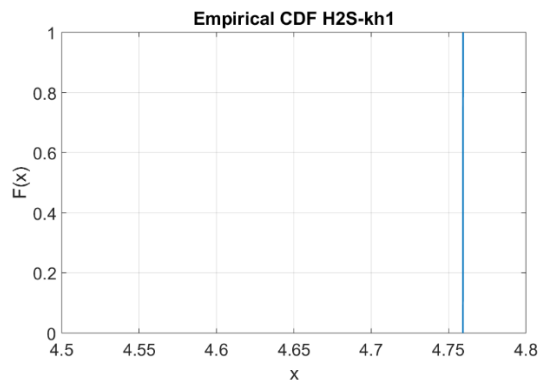
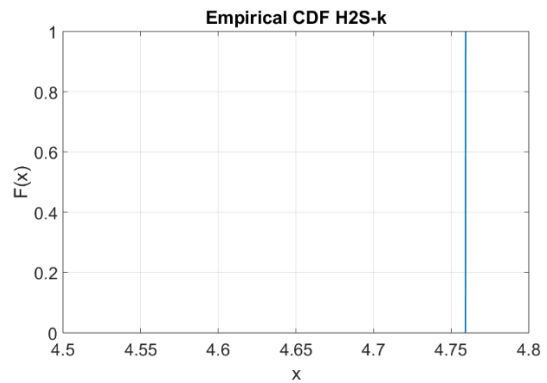
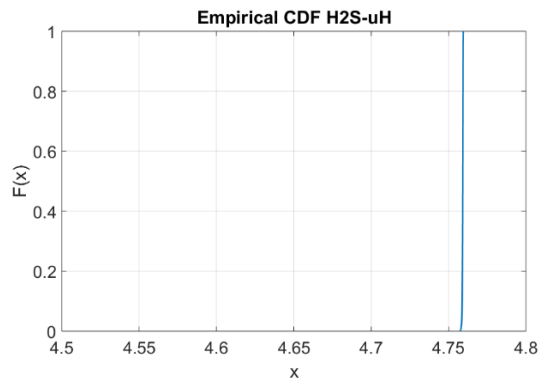


Figure 4.3, Monte Carlo simulation results of hydrogen sulfide distribution

Figure 4.3 shows Monte Carlo simulation model results on hydrogen sulfide concentrations distribution based on 1000 normal distributed K_{x1} value. The hydrogen sulfide concentration values are very close for the coefficient K_{x1} , Figure 4.3 shows a zoomed distribution

concentrations. It can be seen from the figure that the sulfide concentration appears to follow a normal distribution. In order to have a better compare on the distribution of each parameter, all the hydrogen sulfide results distribution is listed in Figure 4.4. In Figure 4.4, where all y axis $F(X)$ is the function of cumulative distribution, and all the X axis is the hydrogen sulfide concentration unit gS/m^3 .



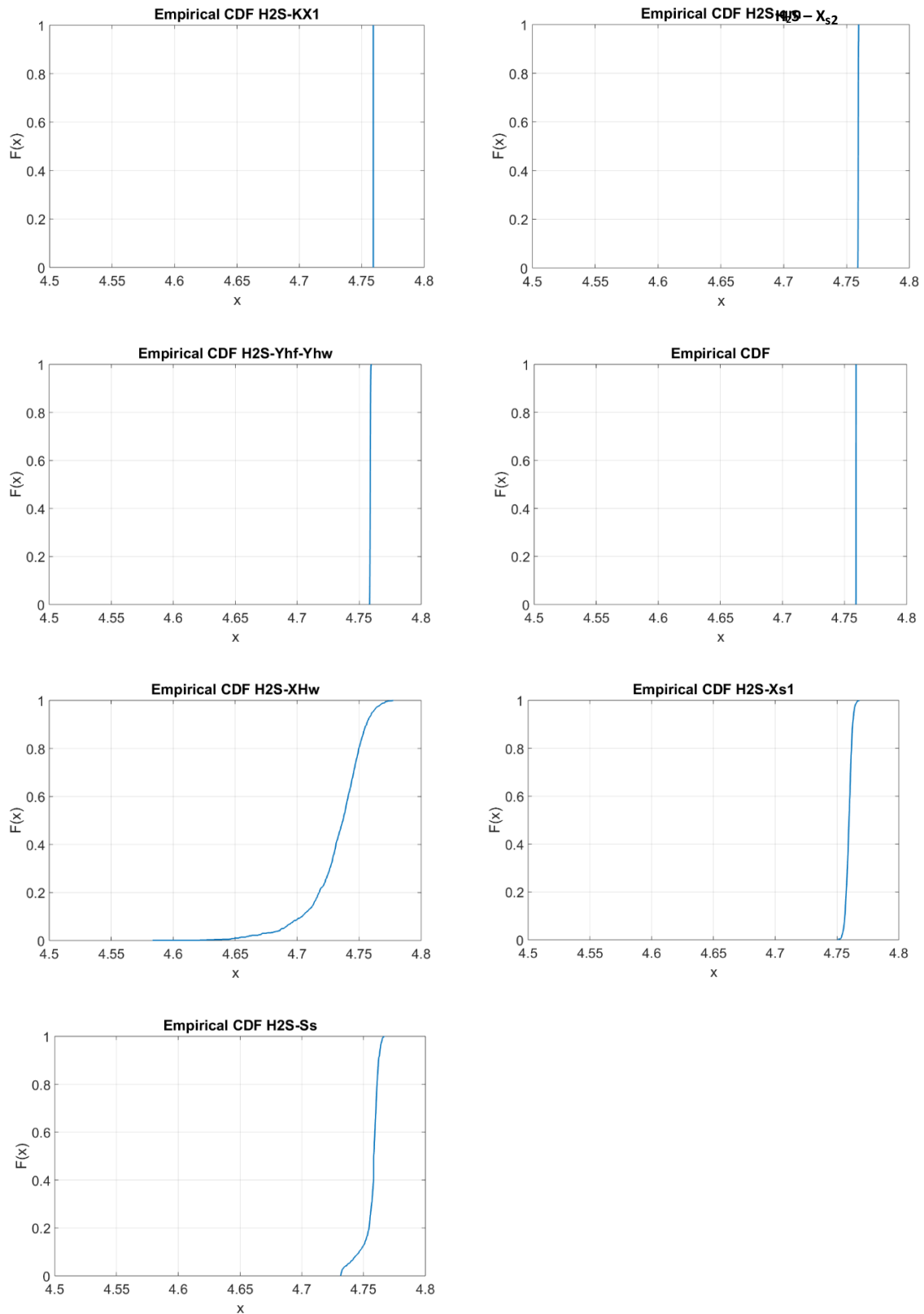


Figure 4.4, Monte Carlo simulation results on selected model parameters for rising main A in 6h.

For all figures in Figure 4.4, from the hydrogen sulfide curve figures, it can be seen that all coefficient parameters plus slow hydrolysable substrates (X_{S2}) have very small standard deviation (due to the same X-axis of COD distribution). While the COD fractions got more fluctuations in terms of hydrogen sulfide production, but there were still not max range difference on the hydrogen sulfide concentration distribution. It can be summarise for several reasons: firstly, the total COD from the database is relative low, which only fell around 500 gCOD/m^3 ; while in real sewer situation it varies greatly, it can reach up to 1500ppm from some systems. Secondly, the sulfide concentration was also very low in the original wastewater. Thirdly, the residence time for the catchment rising main was comparatively short which was around 6 hours, while as summarised before that the sulfide formation highly depends on wastewater residence time for anaerobic transformation. Lastly, the rate coefficient applied in the Monte Carlo simulation was 0.003 which was used in the model study along with the literature sampling dataset, it was also the smallest value in the value range, and hence a similar distribution on rate coefficient is necessary as well to test the influence.

In order to have a closer look on the hydrogen sulfide distribution curves, it was divided into two groups as the coefficient related and COD related Figure 4.5 & 4.6:

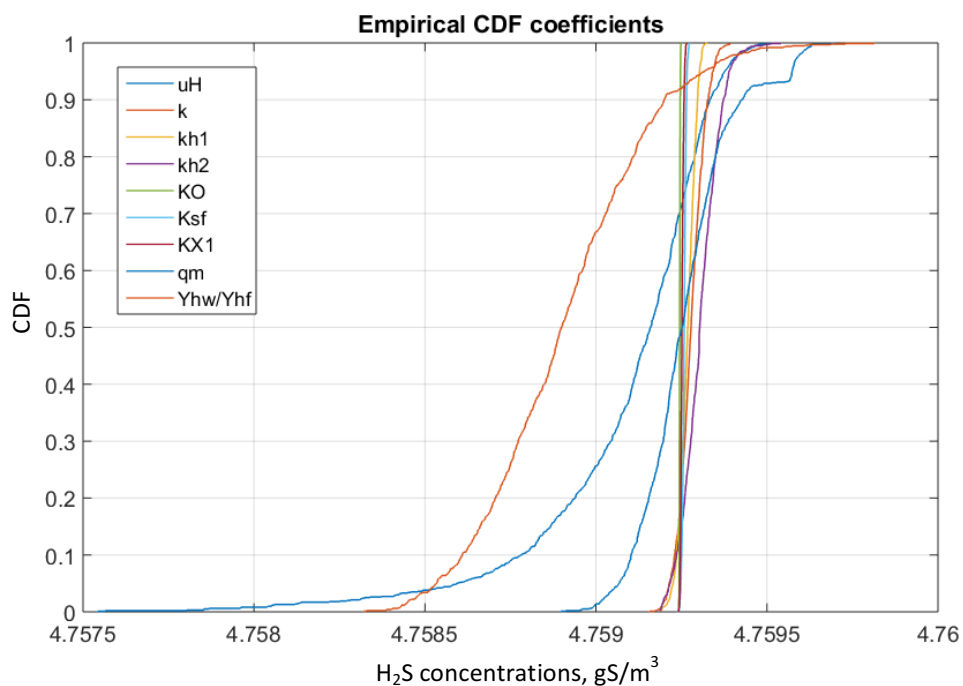


Figure 4.5, coefficients related hydrogen sulfide concentration distribution curves.

Figure 4.5 shows the coefficients related hydrogen sulfide concentration distribution curves. It has a more direct view on the difference with the same X-axis. It can be seen from Figure 4.5, although all coefficient parameters have less influence on hydrogen sulfide production compared to COD parameters, some of them still got more fluctuations such as the maximum specific aerobic growth rate of biomass (μ_H), the maintenance energy requirement rate constant (q_m), and the yield constant for biomass aerobic growth (Y_{hw}). The yield constant even got a higher uncertainty with an increased standard deviation over average ratio.

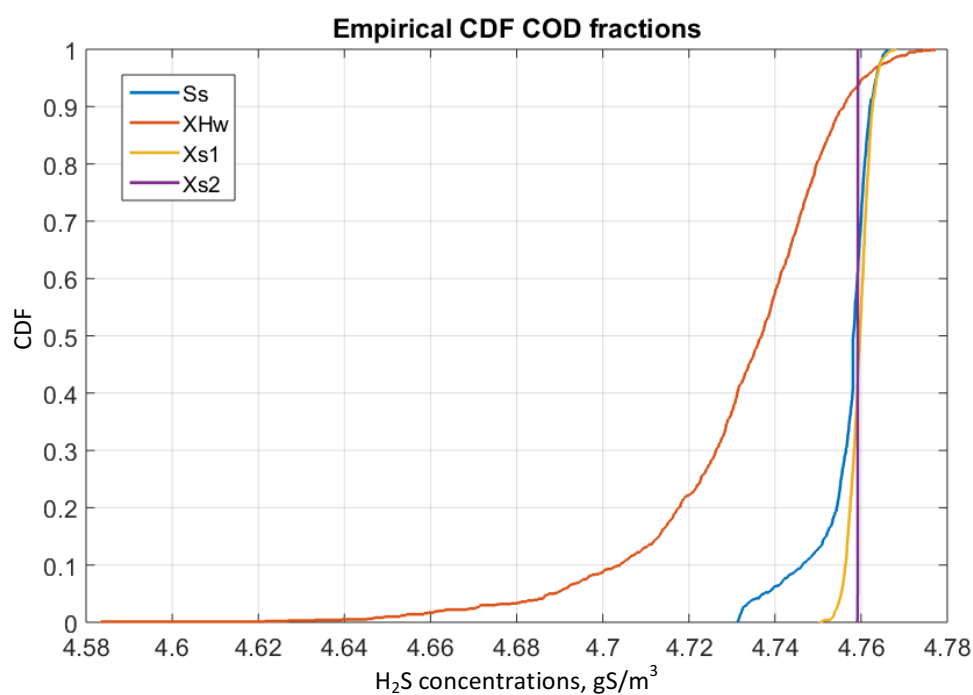


Figure 4.6, COD related hydrogen sulfide concentration distribution curves.

Figure 4.6 shows the COD related hydrogen sulfide concentration distribution curves. Apart from the coefficient parameters, it illustrates more fluctuations on hydrogen sulfide concentrations related to COD. It also indicates that heterotrophic biomass (X_{HW}) and fermentation products (S_S) are among the most influential COD fractions, the fast hydrolysable substrates (X_{S1}) also contributes to the change of hydrogen sulfide concentrations. The hydrogen sulfide concentration distribution curves of increased standard/average ratio to 0.5 are listed as following Figures 4.7 and 4.8, to have a clearer view.

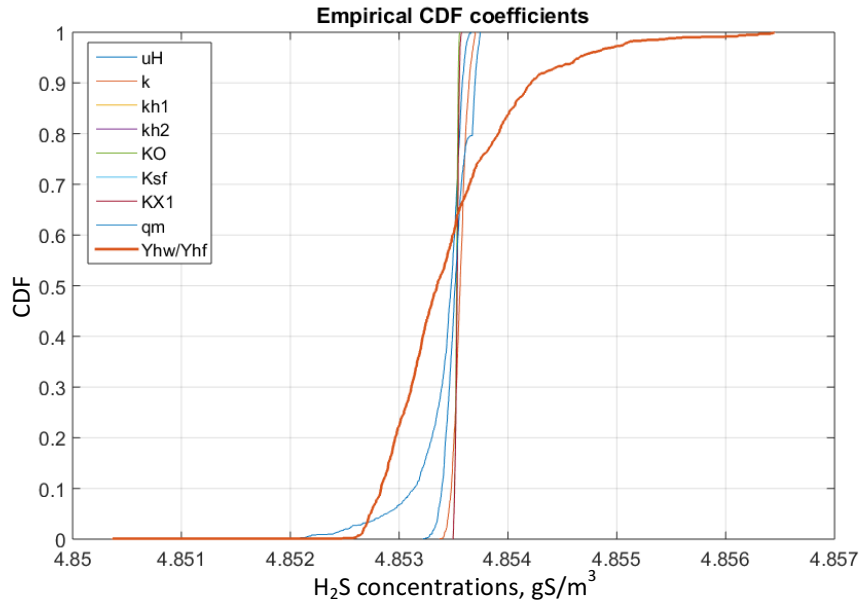


Figure 4.7, coefficient related hydrogen sulfide distribution curves

As similar to Figure 4.5, the increased standard deviation over average ratio coefficient parameters does not result in a significant change on hydrogen sulfide as well. The yield constant for biomass aerobic growth (Y_{hw}) is still the highest uncertain coefficient parameter.

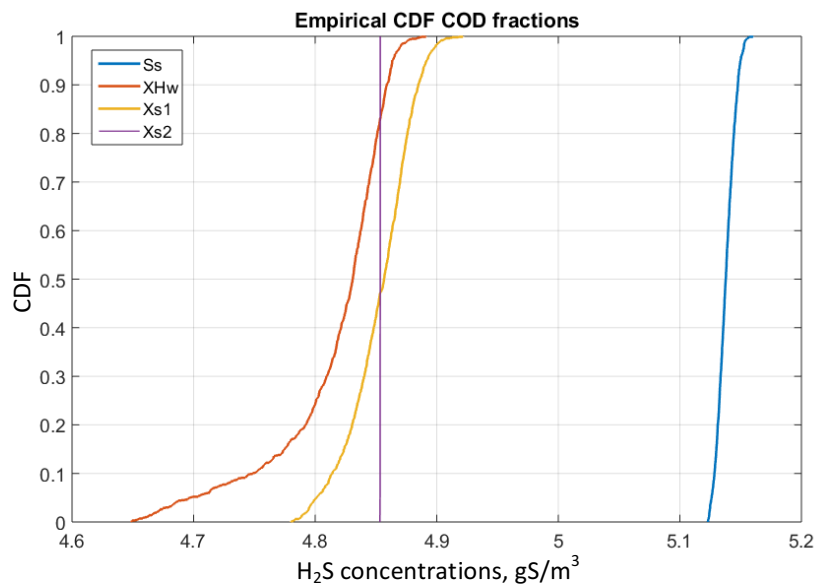


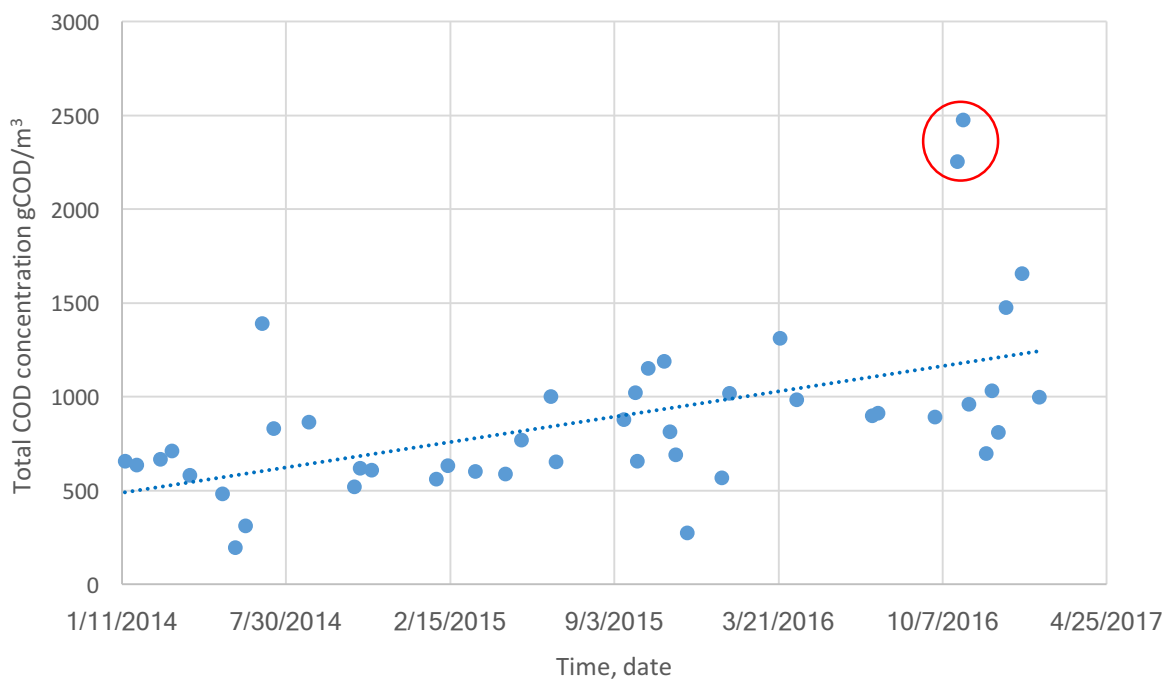
Figure 4.8, COD related hydrogen sulfide distribution curves

Follows the similar variation trend of Figure 4.6, Figure 4.8 shows the rank of COD fraction influence is heterotrophic biomass (X_{Hw}), the fast hydrolysable substrates (X_{S1}), and fermentation products (S_s). With the increased standard/average ratio shown in Table 4.2, X_{S1} increased from 0.08 to 0.5, while S_s decreased from 0.72 to 0.5, that's why X_{S1} came to the

second place at this run. The slow hydrolysable substrates (X_{S2}) still does not have a significant uncertainty and sensitivity compared to other three COD parameters.

4.3.2 Comparison between sampling data and literature dataset

Total COD is one of the five most influential factors on hydrogen sulfide formation, and the COD fractions all depends on total COD. While total COD varies significantly for different systems. The three-year long term wastewater sampling data was analysed and summarised on the change of total COD, change of weather and wastewater temperature and the change of flow rate. Figure 4.9 illustrates the change of total COD of wastewater collected in the wastewater treatment plant.



such as during heavy rains. The samples showed a lowest total COD of 195 g-COD/m³ on 29.05.2014, and a highest total COD of 2475 g-COD/m³ on 01.11.2016. The lowest COD record date was on a heavy rainy day with a very high inflow rate into the wastewater treatment plant. While the highest COD record date was next to the second highest COD date on 25.10.2016 with a total COD of 2253g-COD/m³. Both these two dates were on dry weather flow with a low inflow rate.

It is hard to find a trend or regulation on the change of COD relating to seasons or years. However, the sampling wastewater data showed a trend line that the wastewater total COD is increasing yearly. The change of total COD mostly related to the change of weather, temperature, and flow rate. COD increasing could also be due to more inhabitants, or and reduction of water consumption. Figure 4.10 shows the change of inflow rate into the wastewater treatment plant.

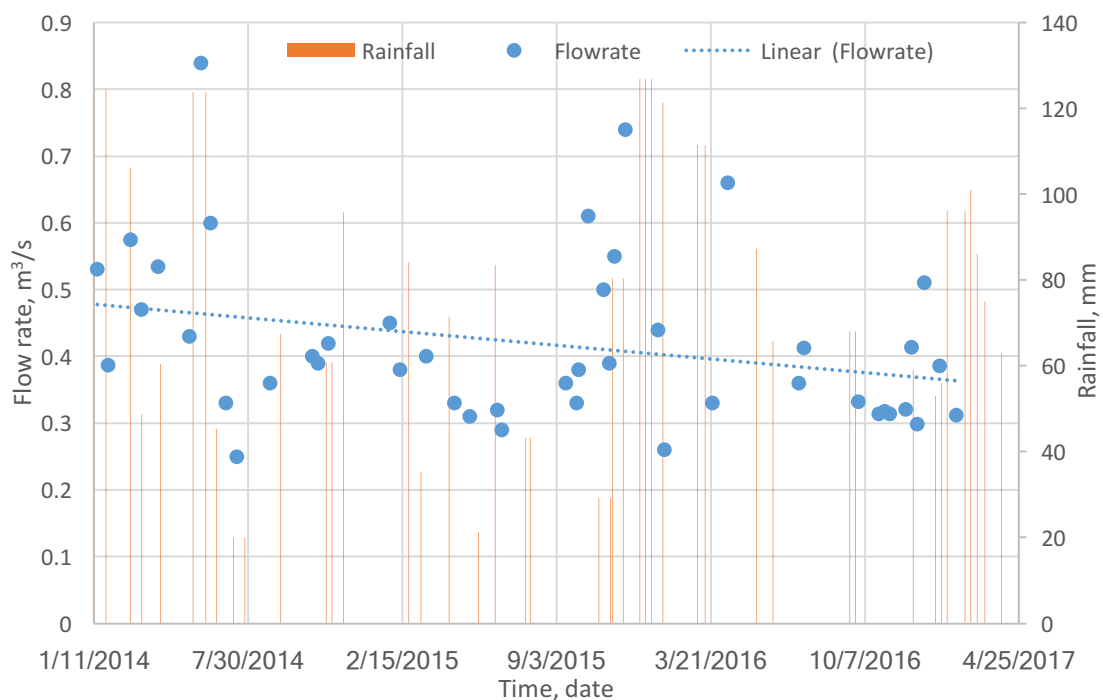


Figure 4.10, the annual variation of inflow rate and rainfall at the wastewater treatment plant.

Figure 4.10 shows the annual variation of inflow rate into the wastewater treatment plant. The flow was recorded by the inflow monitoring unit installed in the plant. The machine reads data from the inflow wastewater such as temperature, air pressure, pH, flow rate, flow velocity every 10 seconds. The flow data was recorded at the time during wastewater sampling. This wastewater treatment plant has an annual average flow rate of 0.42 m³/s. The

Highest flow rate recorded in three years was $0.84 \text{ m}^3/\text{s}$ on 29.05.2014, and the lowest was $0.25 \text{ m}^3/\text{s}$ on 15.07.2014. The rainfall data was from the UK Met Office. A COD-flow rate figure was also plotted as shown in Figure 4.11. It can be seen that the annual rainfall almost corresponds to the inflow rate especially the peak flows. It is interesting and noticeable that the variation on total COD exactly correlated to the change of flow rate. It was recorded the lowest total COD of $195 \text{ g}\cdot\text{COD}/\text{m}^3$ exactly on the highest flow rate day $0.84 \text{ m}^3/\text{s}$. Even though the highest COD $2475 \text{ g}\cdot\text{COD}/\text{m}^3$ was not on the lowest flow rate day, but the flow was relatively very low. It was also unusual for the two days 25.10.2016 and 01.11.2016 (red circled in Figure 4.9), the wastewater in the open channel flowing into the sedimentation tank was in very deep dark colour compared to the normal grey to brown colour.

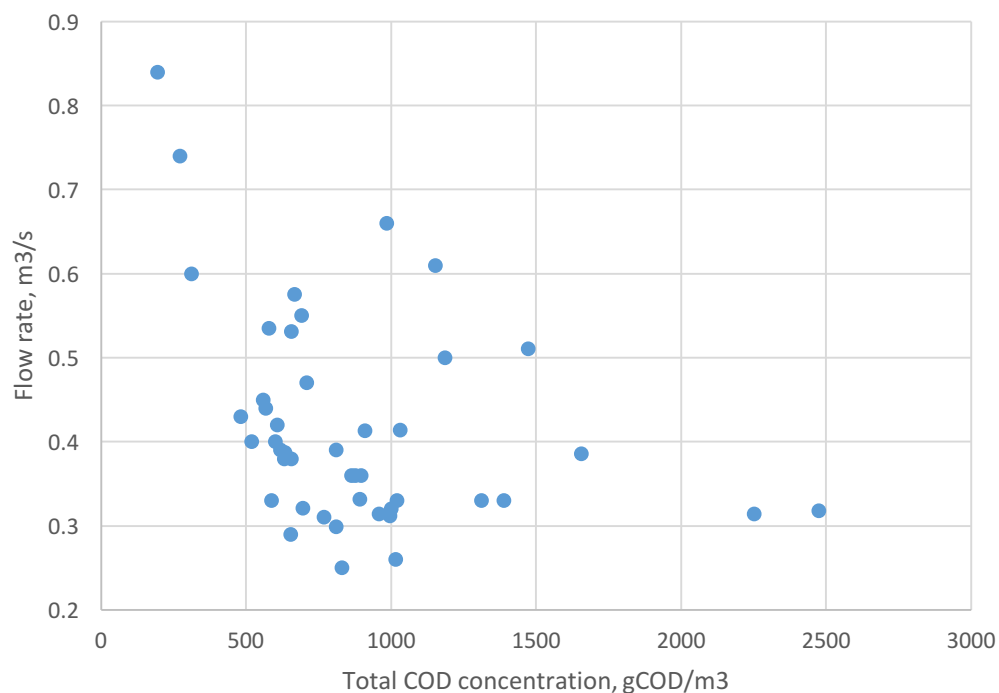


Figure 4.11, the annual variation of COD against flow rate in the WWTP.

It can be seen the whole trend from Figure 4.9, 4.10, 4.11 that the wastewater total COD had a continuous increase with a decrease of flow rate for more than three years data recording. Although there is no indication that the total water consumption in the UK is decreasing, it clearly shows that the reduced flow rate had a recognisable impact on the wastewater COD concentration, which furthermore on the in-sewer processes and sulfide formation. The increase of COD and decrease of flow rate could result from increased inhabitants and/or,

reduced water consumption, it could also be due to the introduction of SUDS which take road drainage out of the combined sewer system. This result follows the literature that the reduced water consumption or the SUDS or climate change has an impact on more concentrated wastewater and more sulfide production (Sun et al., 2015, Marleni et al., 2015, Shypanski et al., 2015).

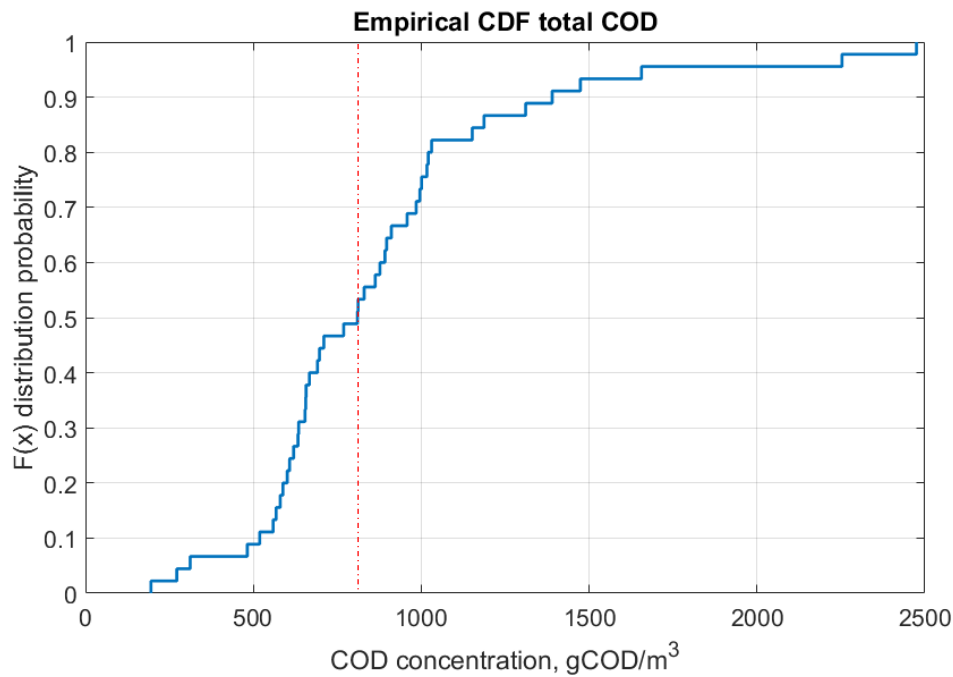


Figure 4.12, empirical cumulative distribution curve of the measured COD concentrations.

Figure 4.12 illustrates the cumulative distribution curve of those measured COD concentrations. The distribution curve is not so smooth due to the limited sampling numbers compared to the smooth curves within 1000 value dataset. The average (mean) and standard deviation of the sampling COD concentrations is 877.2 and 441.9 respectively. Extreme high and low COD is 2475 and 195 correspondingly (unit: gCOD/m³). The total COD, mean and standard deviation is larger than the literature dataset. It is also difficult to conclude whether the COD concentration is high or low due to lack of more comparison data, but over 24% of the samples exceed 1000 gCOD/m³ annually.

In order to compare the COD fraction between literature datasets and the sampling data, the theoretical COD fraction from WATS model was applied on the sampling dataset. The mean and standard deviation of each COD substrate fraction were calculated.

Table 4.3, Comparison of COD fractions between datasets.

Parameters (gCOD/m ³)	Dataset A (μ, σ)	Dataset B (μ, σ)	Sampling dataset (μ, σ)
S_S	N (13.5; 11)	N (32.4; 23.3)	N (52.6; 26.5)
X_{HW}	N (51; 16)	N (55; 16)	N (87.7; 44.2)
$X_{S, fast}$	N (63; 24)	N (124; 19)	N (122.8; 61.9)
$X_{S, slow}$	N (564; 163)	N (228; 83)	N (614.1; 309.3)
<i>Total</i>	N (691.5; 214)	N (439.4; 141.3)	N (877.2; 441.9)

Table 4.3 shows the comparison on COD fraction between literature datasets and sampling dataset. The COD fraction of sampling dataset was calculated by applying the WATS model COD fraction which is X_{HW} 10%, S_S 6%, $X_{S, fast}$ 14%, $X_{S, slow}$ 70%. From Table 4.3 it can be seen that compared to the dataset A and B, the mean and standard deviation of biomass (X_{HW}) and fermentable substrates (S_S) of sampling data are much higher than that in dataset A and B. Even the total COD of Dataset A and Sampling dataset is very close, the sampling X_{HW} and S_S are still much higher than dataset A. From the initial Monte Carlo simulation, it is notable that X_{HW} and S_S are among the top uncertain COD fractions, so it can be seen that the hydrogen sulfide variation would go up if the sampling dataset was the COD measured in the pipes.

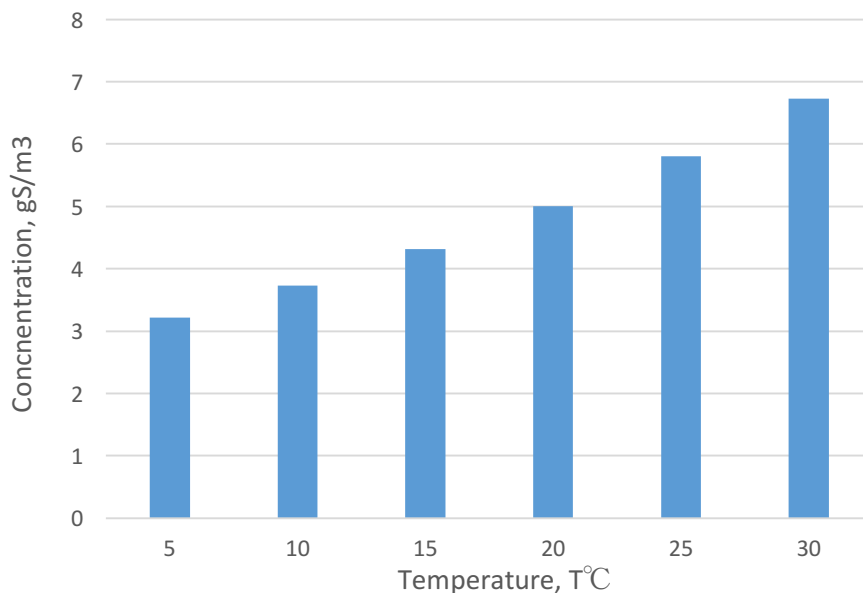


Figure 4.13, Hydrogen sulfide concentration as function of temperature variation.

The effect of water temperature variation on sulfide formation is shown in Figure 4.13. It is based on the WATS model results in rising main A for 6-hour transport with the temperature variation from 5 to 30°C, which represents one DWF day. Basically, the concentration of

hydrogen sulfide increases with the rising of temperature which also follows the mathematical way in the model equations. However, the change of temperature in this model is a single variable which only results in a simple linear relation between hydrogen sulfide and temperature. Thus, more comparison modelling should be simulated with more variables. Temperature is not only influencing and changing the sulfide formation rate equation, it also affects the sulfate reducing bacteria activities and biofilm growth. However, these processes could not be presented and expressed in the process models. The model simulation should be compared and validated with field measurements.

The change of weather and wastewater temperature was also measured for the three years sampling data. It is summarised in Figure 4.14.

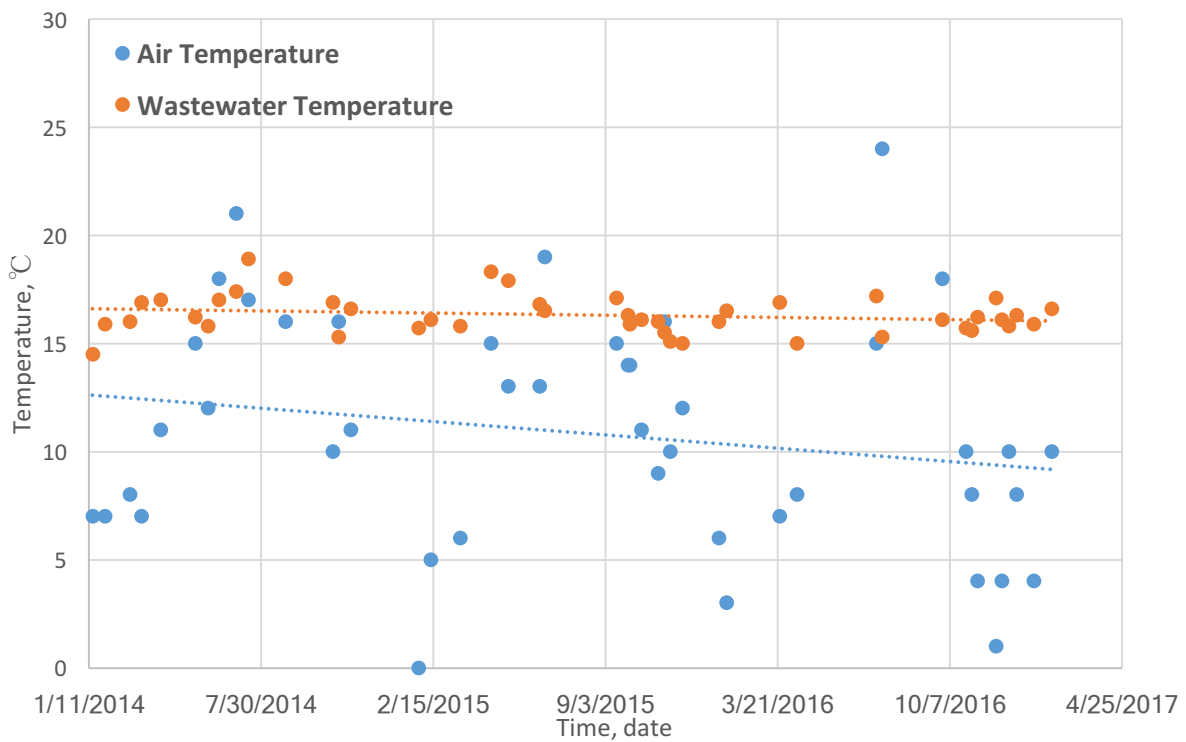


Figure 4.14, weather and wastewater temperature variations at the wastewater treatment plant.

The weather temperature (Atmosphere temperature) and wastewater temperature were measured on every sampling day. From Figure 4.14 it can be seen that both the weather and wastewater temperature had a drop trendline from the three years measurement data, which reflects the average climate is getting colder for the sampling period. It had an average weather temperature of 10.8°C, which is closed to the annual average temperature for South

Yorkshire of 10 °C between 1981 and 2010 provided by Met Office. The wastewater had an average temperature of 16.3 °C and there was not quite changes and fluctuations on the wastewater temperature. It looks like there was little dependency on weather temperature for wastewater temperature. From the data it shows the highest weather temperature was 24°C on 20.07.2016 when the wastewater temperature was 15.3°C; the lowest temperature recorded was 0 °C on 29.01.2015 while the wastewater temperature was 15.7 °C, which was even higher than the wastewater temperature on the hottest day. However, the average wastewater temperature in summer seasons was 1 – 2 °C higher than the temperature in winter seasons indeed. It can be concluded that the wastewater temperature is influenced by weather, but not very dependent on weather temperature. It maintained in a certain range annually.

4.4 Conclusions and Discussions

This chapter mainly summarized the global sensitivity analysis on selected WATS process model parameters. Monte Carlo simulations had been implemented on these parameters in the rising main A in Catchment A. Model results showed that the heterotrophic biomass (X_{HW}), readily biodegradable substrates (S_S) and fast hydrolysable substrates (X_{S1}) are the most sensitive COD fractions in terms of wastewater biochemical transformation and sulfide formation. The yield constant (Y_{HW} , Y_{HF}) is the most sensitive coefficient parameter. It also can be seen from the study that the importance of COD fraction for the definition of wastewater property and the transformation processes. Hence, the OUR (oxygen uptake rate) test is normally implemented for model studies involved with field measurements. The OUR) test and analysis is essential and necessary for detecting the COD fractions for wastewater samples. The OUR measurement must be implemented for dealing with new study and model validation.

The long-term wastewater sampling results as part of the sensitivity analysis also indicated the wastewater total COD with a mean COD concentration of 877 g·COD/m³ which is much higher than the literature database. The sampling data was collected at the downstream and the end of the sewer system, which means there would be even higher COD concentrations in the upstream system because low COD centration is normally found at the wastewater treatment plant due to the degradation of organic matter during transformations. The change

of COD concentration is corresponding with the change of flow rate. And the COD concentration had a continuous increase with a decreasing of inflow rate into the WWTP. This could result from the increasing of inhabitants, reduced water consumption, and also the introduction of SUDS in the systems. The temperature variation of wastewater seems to be quite stable, and it is not much involved with the weather and air temperature.

Chapter 5, Methane formation in sewers and the relative contribution from septic tanks and sewer pipes.

5.1 Introduction

Problems resulted from methane production in sewers has been introduced in Chapter 1. The formation and fate of methane in sewer systems have not received as much attention as hydrogen sulfide in sewers, and the methane production and release from sewer systems had not been investigated and reported until recent years (Guisasola et al., 2008). Significant methane production in sewers has been analysed and reported from both lab experiments and field tests (Liu et al., 2015c, Liu et al., 2016b). Field analysis showed the water phase methane concentration in rising mains can easily build up to 20 – 25 mg/l in Australia sewer systems, and up to 100 mg/L in lab conditions (Guisasola et al., 2008). Sewer pipe is not the only place for methane production, other sewer facilities such as in-line septic tanks and storage tanks are believed to be a substantial methane contributing source as well. However, few studies have investigated the transformation processes and methane formation in these facilities. Field measurements from 8 septic tanks in California US indicate methane and carbon dioxide production rate of 11 and 33 g capita⁻¹ day⁻¹, respectively (Diaz-Valbuena et al., 2011). And a 27.1 g capita⁻¹ day⁻¹ methane production rate was reported by the US. EPA (EPA, 2010).

5.1.1 Septic tanks

Septic tanks have been reported as one of the major GHG emission sources, which can contribute methane production as equal to 0.23 Tonnes carbon dioxide capita⁻¹ year⁻¹ (Pachauri et al., 2014). Septic tanks were firstly reported to be used in sewer systems in the Europe in the 19th century (Butler and Payne, 1995) as an important facility to treat waste disposal. In the recent decades, septic tanks have gradually not been used as the pre-treatments in urban drainage system with the development of modern wastewater treatment plants. For example, septic tanks are only used in small communities in remote areas in the UK (Butler and Payne, 1995). However, septic tanks are still commonly existed and playing an important role in many countries such as in the US and China. At the present time, around

20% of the US population relies on septic tanks and over 60% of the population in China depends on septic tanks for initial pre-treatment (Diaz-Valbuena et al., 2011, Jian-ling, 2011).

The most commonly used septic tanks today include single chamber and multi chamber tanks (Butler and Payne, 1995). There are normally three layers in septic tanks, namely the top scum layer which mainly consists of grease, oil and buoyant particles, the middle clear liquid layer, and the bottom sludge layer (Crites and Technobanoglous, 1998). The formation of methane gas mainly occurs in the bottom sludge layer is assumed within the same acidogenesis and methanogenesis microbial processes in anaerobic digestion (McCarty, 1964, Lawrence and McCarty, 1969). The acidogenesis is the hydrolysis and fermentation process in which large organic compounds are degraded to small compounds such as hydrogen, carbon dioxide and VFAs (e.g., acetate). The small organic compounds are further transformed to methane through methanogenesis process (McCarty, 1964).

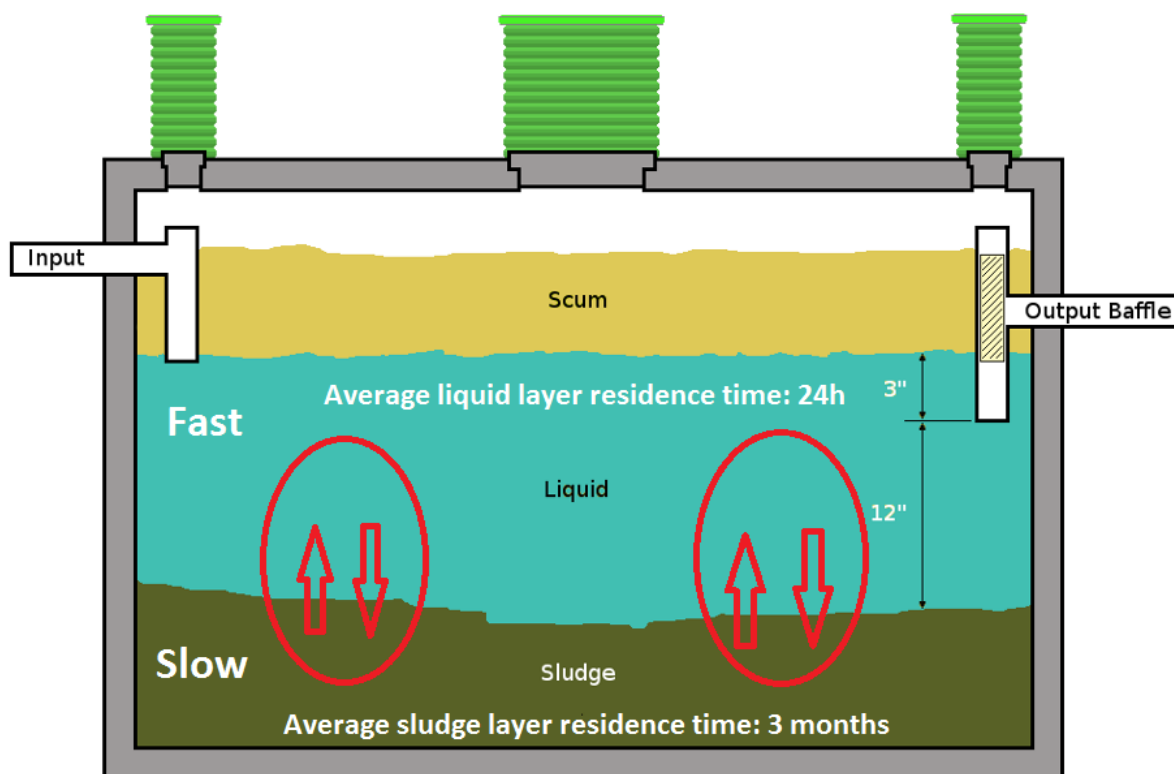


Figure 5.1, Schematic of septic tank layers, processes, and HRT.

Figure 5.1 illustrates the inside layout of typical single chamber septic tanks with three layers. The liquid layer has an average residence time of 24 hours, and the sludge layer has an

approximately 3 month's residence time (Zhou et al., 2013). The transformation processes in the liquid layer are relatively fast and are believed as similar to the processes in the sewer pipes. The transformation processes in the sludge layer are slow compared to the liquid layer. It is more a matter of the long residence time allows for some of the processes that are generally too slow to be significant in sewers to be important in the septic tanks. The septic tank emptying frequency depends on the dimension of tanks, influent, and temperature. The average emptying frequency for septic tanks in China is around 3 months, however, some small and remote septic tanks may take up to several years for one empty (Zhou et al., 2013). And the emptying of septic tanks in the Europe would normally occur only in every 1 – 5 years (Philip et al., 1993).

5.1.2 Anaerobic digestion and the anaerobic digestion model (ADM)

Anaerobic digestion is a series process of the decomposition of large particle hydrolysable and biodegradable organic materials by microorganisms and certain bacteria in the absence of oxygen (Gunnerson et al., 1986). The anaerobic digestion activities in natural environment commonly exist in lakes and oceanic basin sediments where as a source of greenhouse gases production; anaerobic digestion is also used in industries as a mean of waste management and food production (Koyama, 1963). The anaerobic digestion mainly consists of four stage processes: hydrolysis, acidogenesis, acetogenesis and methanogenesis (Gunnerson et al., 1986). The hydrolysis the first step of breaking down large organic substrates to smaller molecules such as sugar, ammonia acid and LCFA (long-chain fatty acids). The second stage acidogenesis which is also the fermentation stage. It is the further decomposition of hydrolysis products to VFAs (volatile fatty acids) and other products such as ammonia, carbon dioxide and hydrogen sulfide (Lettinga, 1995). The third stage is the formation of acetic acid along with more carbon dioxide and hydrogen. The last stage methanogenesis is the formation of methane by the uptake of acetate and hydrogen, with the production of carbon dioxide and water in the meantime (Gunaseelan, 1997).

The IWA anaerobic digestion model No 1 (ADM1) was first established by the IWA ADM task group in 1997 and published in 2002 (Batstone et al., 2002a, Batstone et al., 2002b). This model basically follows the four steps in the anaerobic digestion processes. It defines the organic materials as carbohydrates, proteins and lipids, and the methanogenesis as a separate

step from acetate and hydrogen. The ADM No 1 model has been used in many studies associated with anaerobic digestion (Blumensaat and Keller, 2005); to deal with high strength wastewater such as from farm and agriculture (Normak et al., 2015), and industrial waste such as olive mill and sugar production (Fezzani and Cheikh, 2008, Barrera et al., 2015). In these studies, the ADM No 1 model all showed very similar results compared to measurements.

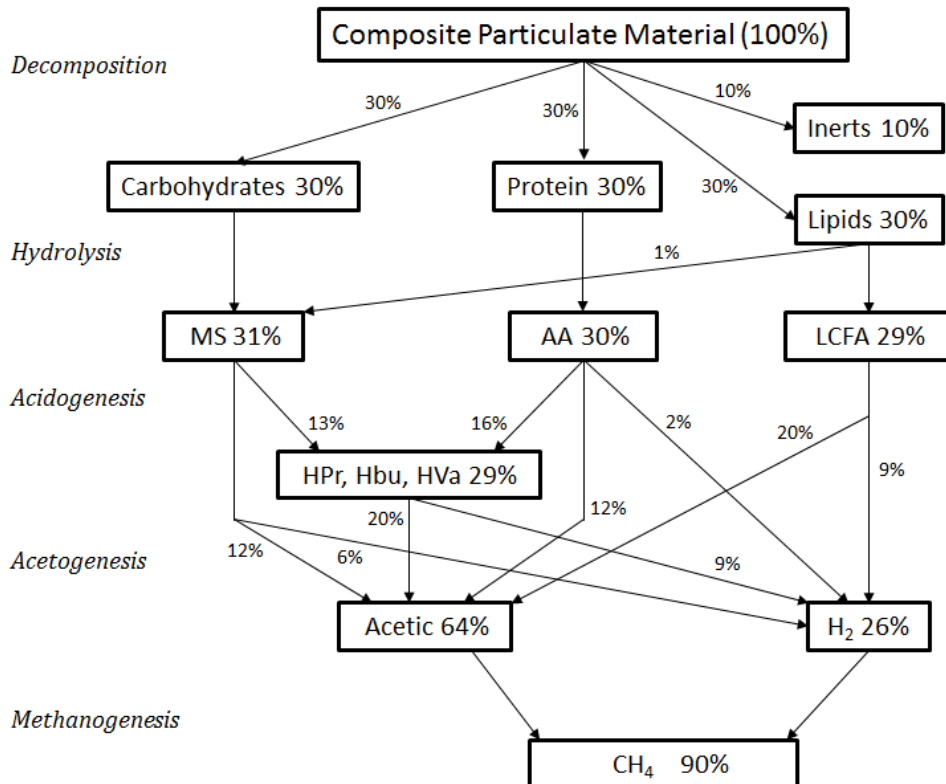


Figure 5.2, COD fraction and anaerobic digestion processes in ADM No 1 model (modified from (Batstone et al., 2002a)).

Figure 5.2 illustrates the composition of COD fractions and the anaerobic digestion processes expressed in the ADM No 1 model. The model defines the total COD consists of 30% carbohydrates, 30% protein, 30% lipids and 10% inerts. Acetate and hydrogen are produced through hydrolysis, acidogenesis and acetogenesis processes. Methane is produced from the final methanogenesis process through the uptake of acetate and hydrogen. The ADM model matrix of COD fractions is shown in Table 5.1. Symbols are referred to the nomenclatures in page 9 for an explanation.

Table 5.1, COD fractions in Anaerobic Digestion Model ADM No.1 (Batstone et al., 2002b, Batstone et al., 2002a)

Processes	S_{su}	S_{aa}	S_{fa}	S_{va}	S_{bu}	S_{pro}	S_{ac}	S_{h2}	S_{ch4}	X_c	X_{ch}	X_{pr}	X_{li}	X_{su}	X_{aa}	X_{fa}	X_{c4}	X_{pro}	X_{ac}	X_{h2}	Rates	
Disintegration										-1	$f_{ch,xc}$	$f_{pr,xc}$	$f_{li,xc}$								$K_{dis}X_c$	
Hydrolysis carbohydrates	1										-1											$K_{hyd,ch}X_{ch}$
Hydrolysis of proteins		1										-1										$K_{hyd,pr}X_{pr}$
Hydrolysis of lipids	1- $f_{fa,li}$		1- $f_{fa,li}$										-1									$K_{hyd,li}X_{li}$
Uptake of sugars	-1				(1- $Y_{su})f_{bu,su}$	(1- $Y_{su})f_{pro,su}$	(1- $Y_{su})f_{ac,su}$	(1- $Y_{su})f_{h2,su}$						Y_{su}								$K_{m,su} \frac{S_{su}}{K_s + S_{su}} X_{su} I_1$
Uptake of amino acids		-1		(1- $Y_{aa})f_{va,aa}$	(1- $Y_{aa})f_{bu,aa}$	(1- $Y_{aa})f_{pro,aa}$	(1- $Y_{aa})f_{ac,aa}$	(1- $Y_{aa})f_{h2,aa}$							Y_{aa}							$K_{m,aa} \frac{S_{aa}}{K_s + S_{aa}} X_{aa} I_1$
Uptake of LCFA			-1				(1- $Y_{fa})0.7$	(1- $Y_{fa})0.3$								Y_{fa}						$K_{m,fa} \frac{S_{fa}}{K_s + S_{fa}} X_{fa} I_2$
Uptake of valerate				-1		(1- $Y_{c4})0.54$	(1- $Y_{c4})0.31$	(1- $Y_{c4})0.15$									Y_{c4}					$K_{m,c4} \frac{S_{va}}{K_s + S_{va}} X_{c4} \frac{1}{1 + S_{bu}/S_{va}} I_1$
Uptake of butyrate					-1		(1- $Y_{c4})0.8$	(1- $Y_{c4})0.2$									Y_{c4}					$K_{m,c4} \frac{S_{bu}}{K_s + S_{bu}} X_{c4} \frac{1}{1 + S_{va}/S_{bu}} I_1$
Uptake of propionate						-1	(1- $Y_{pro})0.57$	(1- $Y_{pro})0.43$										Y_{pro}				$K_{m,pr} \frac{S_{pro}}{K_s + S_{pro}} X_{pro} I_2$
Uptake of acetate							-1		1- Y_{ac}										Y_{ac}			$K_{m,ac} \frac{S_{ac}}{K_s + S_{ac}} X_{ac} I_3$
Uptake of hydrogen								-1	1- Y_{h2}											Y_{h2}		$K_{m,h2} \frac{S_{h2}}{K_s + S_{h2}} X_{h2} I_1$
Decay of X _{su}										1				-1								$K_{dec,xsu}X_{su}$
Decay of X _{aa}										1					-1							$K_{dec,xaa}X_{aa}$
Decay of X _{fa}										1						-1						$K_{dec,xfa}X_{fa}$
Decay of X _{c4}										1							-1					$K_{dec,xc4}X_{c4}$
Decay of X _{pro}										1								-1				$K_{dec,xpro}X_{pro}$
Decay of X _{ac}										1									-1			$K_{dec,xac}X_{ac}$
Decay of X _{h2}										1										-1		$K_{dec,xh2}X_{h2}$

In ADM 1 there are two routes for the production of methane; via the uptake of acetate (Equation 5.1) and via the uptake of hydrogen (Equation. 5.2)

$$r_{ac} = K_{m,ac} \frac{S_{ac}}{K_s + S_{ac}} X_{ac} I_3 \quad (5.1)$$

$$r_{h2} = K_{m,h2} \frac{S_{h2}}{K_s + S_{h2}} X_{h2} I_1 \quad (5.2)$$

Where r_{ac} is the methane formation rate from the uptake of acetate, r_{h2} is the methane formation rate from the uptake of hydrogen. Equation 5.1 and 5.2 shows the methane formation rate equations for the uptake from acetate and hydrogen respectively. Where K_m is the specific Monod maximum uptake rate, K_s is the Monod half saturation constant, S_i is the soluble component concentration (kgCOD/m^3), X_i is the particulate component concentration (kgCOD/m^3), and I_i is the inhibition function. In ADM 1, it defines the liquid phase hydrogen was used for hydrogen inhibition. The acetoclastic methanogenesis is the major methanogenic step, in which methane and carbon dioxide is produced from acetate as Equation 5.3 shows:



5.1.3 SeweX model for methane production

The Australian SeweX model is the first published sewer process model that attempts an incorporation of methane production in the reaction matrix. It was further extended to describe the methane formation process after the sulfur cycle. This model defines the formation of hydrogen sulfide and methane in rising mains is a simultaneous process as long as the wastewater COD and sulfate concentration ratio is sufficient (Guisasola et al., 2009).

The SeweX model matrix describing the methanogenesis and sulfidogenesis processes is presented in Table 5.2.

Table 5.2, Stoichiometry and kinetics of SeweX model describing methanogenesis and sulfidogenesis processes – model matrix (Guisasola et al., 2009).

Processes	CH_4 (Methane)	$C_2H_4O_2$ (Acetate)	$C_6H_{12}O_6$ (Glucose)	$C_3H_6O_2$ (Propionate)	CO_2	H_2	H_2O	H_2SO_4	H_2S	Kinetics
Hydrogenotrophic methanogenesis	1				-1	-4	2			$k_{CH_4,H_2} \cdot \frac{S_{H_2}}{K_{H_2,MA} + S_{H_2}} \cdot \frac{A}{V} \cdot \alpha^{T-20}$
Acetoclastic methanogenesis	1	-1			1					$k_{CH_4,SAC} \cdot \frac{S_{AC}}{K_{SAC,MA} + S_{AC}} \cdot \frac{A}{V} \cdot \alpha^{T-20}$
Acetogenesis		2	-1		2	4	-2			$q_{ACETOG} \cdot \frac{S_F}{K_F + S_F} \cdot \frac{A}{V} \cdot \alpha^{T-20}$
Acidogenesis		2	-3	4	2		2			$q_{ACIDOG} \cdot \frac{S_F}{K_F + S_F} \cdot \frac{A}{V} \cdot \alpha^{T-20}$
Hydrogenotrophic sulfidogenesis						-4	4	-1	1	$k_{H_2S,H_2} \cdot \frac{S_{H_2}}{K_{H_2,SRB} + S_{H_2}} \cdot \frac{S_{SO_4}}{K_{SO_4} + S_{SO_4}} \cdot \frac{A}{V} \cdot \alpha^{T-20}$
Acetate-based sulfidogenesis		-1			2		2	-1	1	$k_{H_2S,SAC} \cdot \frac{S_{AC}}{K_{AC,SRB} + S_{AC}} \cdot \frac{S_{SO_4}}{K_{SO_4} + S_{SO_4}} \cdot \frac{A}{V} \cdot \alpha^{T-20}$
Propionate-based sulfidogenesis		1		-1	1		2	-3/4	3/4	$k_{H_2S,SPROP} \cdot \frac{S_{PROP}}{K_{PROP} + S_{PROP}} \cdot \frac{S_{SO_4}}{K_{SO_4} + S_{SO_4}} \cdot \frac{A}{V} \cdot \alpha^{T-20}$

In SeweX model, it defines the formation of methane in two routes, the hydrogenotrophic methanogenesis and the acetoclastic methanogenesis. Equation 5.4 and 5.5 shows the kinetics rate equations for methane formation from the uptake of hydrogen and acetate.

$$r_{ch4h2} = k_{ch4,h2} \frac{S_{h2}}{K_{h2ma} + S_{h2}} \frac{A}{V} \alpha^{T-20} \quad (5.4)$$

$$r_{ch4ac} = k_{ch4,ac} \frac{S_{AC}}{K_{ACma} + S_{AC}} \frac{A}{V} \alpha^{T-20} \quad (5.5)$$

Where r_{ch4h2} is hydrogenotrophic methanogenesis rate, r_{ch4ac} is the acetoclastic methanogenesis rate. In Equations 5.4 and 5.5, the k_{ch4i} is the maximum transformation rate, $K_{i\ ma}$ is the half saturation constant, S_{h2} and S_{AC} is the soluble concentration of hydrogen sulfide and acetate in wastewater, $\frac{A}{V}$ is the area volume ratio of sewer pipes. α^{T-20} is the temperature coefficient. Basically, it can be seen from Equation 5.4 and 5.5, the kinetic equations of methane formation is very similar to the methane formation rate equations described in Anaerobic Digestion Model shown in Equation 5.1 and 5.2. In SeweX model it added the area volume ratio of sewer pipes and the temperature coefficient into the equation. The particulate and inert organic matter is not included in the SeweX model adaptation, probably due to the relative short residence time in the sewer pipes compared to the HRT in septic/storage/retention tanks, and there is less particulates and solids accumulated in pipes compared to in tanks. The purpose of the application of SeweX model is to make a comparison between ADM 1 for the methane formation processes and relative contributions.

5.2 Methodologies

The aim of this chapter is to assess and compare the relative methane formation in septic tanks and sewer pipes. The objective also includes evaluating how well the model application and combination works and what future work would be needed. Few studies had investigated methane formation in septic tanks, and no literature has been found yet by applying the IWA Anaerobic Digestion Model on sewerage septic tanks. This model study is to give an adaptation on using the IWA ADM 1 model to investigate methane formation in septic tanks. It is also to illustrate a view on how to integrate the methane formation process in both the

sewer pipe model and septic tank model, and prepare the future model validation with field tests and measurements.

5.2.1 Field measurements on selected septic tank

In order to analyse the wastewater total COD removal rate of septic tanks, a field measurement was carried out by the Chinese collaborators on a selected residential septic tank in Lanzhou City, Northwest China. This septic tank is a typical one representing the septic tanks constructed in China in the last three decades. It is a single chamber tank with an approximately 10 m³ volume. It serves 160 households equivalent of roughly 500 residents. In order to compare the influence of weather and temperature. Four sampling periods had done in October, December 2013, and April, June 2014. Wastewater samples were collected at the inlet and outlet of the septic tank. Three-day samples were collected during each sampling period. Samples were collected at 7:00 – 9:00 am (three samples), 11:00 – 14:00 pm (three samples), and 17:00 – 21:00 pm (three samples) on each sampling day. The three samples collected at each time period were mixed for COD analysis. The effluent samples were collected 30 minutes later than the influent samples at each sampling time period, because the residence time in the tank is unknown, and it is hard to describe how the materials are transported in the tank processes. Thus, there were six samples a day for both influent and effluent, 18 samples a season, together 72 samples in total. The wastewater COD analysis was carried out within 30 minutes after samples were collected. The daily and annual COD removal rate were calculated and listed in Table 5.4.

5.2.2 COD analysis method (Potassium Dichromate Method)

The total COD of wastewater samples were analysed by potassium dichromate method. All the samples were analysed at the University lab following the Chinese National Standard Method (GB 11914 – 89). The instruments, reagents and methods used were listed below:

Table 5.3, Chemicals and instruments used in the COD analysis.

Chemicals	
Ag ₂ SO ₄	HgSO ₄
H ₂ SO ₄ (ρ=1.84g / mL)	Standard Ferroin indicator solution

Standard potassium dichromate solution ($C_{1/6} K_2Cr_2O_7 = 0.250 \text{ mol/L}$)

Standard ammonium ferrous sulfate solution ($C(NH_4)_2Fe(SO_4)_2 \cdot 6H_2O \approx 0.10 \text{ mol/L}$)

Instruments

500 mL Erlenmeyer flask

Reflux units

25mL/50mL acid burette

Heating facility (electric furnace)

transfer pipette

volumetric flask

Table 5.3 shows the chemicals and instruments used in the COD analysis experiments. The main Erlenmeyer flask and reflux units are shown in Figure 5.3.



Figure 5.3, potassium dichromate method COD analysis instruments

Figure 5.3 photo shows the reflux units for the condensation of heat vapour. The schematic of electric furnace and Erlenmeyer flask on the right is the main instrument for COD analysis. The detailed experiment step follows the standard method (GB 11914 – 89). The COD concentrations is calculated by Equation 5.6

$$COD_{Cr}(O_2, mg/L) = 8 \times 1000 (V_0 - V_1) \cdot C/V \quad (5.6)$$

In Equation 5.6, where 8 is the molar mass of oxygen (g/mol), V_1 is the volume of standard ammonium ferrous sulfate solution used for wastewater sample titration, V_0 is the volume of standard ammonium ferrous sulfate solution used for blank test of distilled water, V is the volume of wastewater sample, C is the concentration of standard ammonium ferrous sulfate solution.

5.2.3 Solids settlement experiment

Three layers are normally been found in a septic tank, that is the scum, liquid and sludge layer. Apart from the transformation processes occurs in each layer, there is also mass transfer and material exchange between layers. In order to apply the Anaerobic Digestion Model in the sludge layer, the COD inlet and transfer processes from liquid layer to the sludge layer was simulated by a series of simple solids settlement experiments. The experiment gives a general view on the mass transfer rate between liquid and sludge layer. However, these experiments could not be done by the Chinese collaborators due to their time schedule. Wastewater samples collected at the Woodhouse Mill wastewater treatment plant in South Yorkshire were used for the implementation. It is expected that the samples from the UK WWTP will have much lower COD concentration compared to the samples in the Chinese septic tank. The sampling site is located at the open channel after lifting and grids, before the sedimentation tanks. Four samples were collected within a month for comparison. The settlement experiments had done by using a 2-litre measuring cylinder.

Wastewater samples were transported to the lab immediately after sampling. Firstly, the sampling jerry can was shaken well before use; a 5 mL raw wastewater sample was taken using a pipette for the purpose of measuring raw wastewater COD and stored in the fridge for approximately 3 hours till the end of each settlement experiment. The wastewater jerry can was shaken well again before transferring to the 2L measuring cylinder. A stop watch was used to record time once the 2L wastewater was transferred to the cylinder. The change of the height of solids accumulated at the bottom of the cylinder was recorded every 10 seconds. The height was read by the measuring tape on the cylinder. The change of the heights was observed every 10 minutes after 30 minutes because almost all the solids were settled. After 1 hour and 30 minutes, wastewater samples from the top, middle and bottom of the cylinder were collected and stored in the fridge. Figures of solids layer height against time were

plotted, and the total COD of samples from raw, top, middle and bottom were analysed. The COD transfer rate (mass transfer rate) from liquid layer to sludge layer was calculated.

5.2.4 COD analysis method (spectrophotometric method)

The COD of wastewater samples were analysed using the spectrophotometric method here in the UK. It is a more simplified and convenient approach for COD measurement compared to the standard potassium dichromate method used in China in Section 5.2.2. The standard potassium dichromate method is more accurate compared to the spectrophotometric method which is an approximate reading by the absorption of light. And the standard potassium dichromate method is usually used to validate the spectrophotometer readings (Basavaiah and Somashekar, 2007).



Figure 5.4, Spectrophotometer and COD vials used for COD analysis (Hach-UK, 2017b).

Figure 5.4 shows DR3900 spectrophotometer and the COD vials from Hach Lange which was used for COD analysis. LCK514 and LCK014 COD vials were used in the experiments which have a measuring range of 100-2,000mg/L and 1,000-10,000mg/L, respectively. These COD vials are based on the standard method ISO 6060-1989, DIN 38409-H41-H44, which is dichromate chemical oxygen demand analysis method. The theory is the measurement of Cr^{6+} that remains in the solution or the measurement of Cr^{3+} which is produced in the solution after the sample was oxidized by potassium dichromate in a 50% sulfuric acid (Hach-UK, 2017a). The COD measurements procedure was simply summarised below:

Firstly, the vial was shaken well till all components dissolved, then 2 mL of wastewater sample was added into the pre-mixed solution in the vial, it was shaken to well mixed. Secondly, Heat the vials in the electric furnace at 150 °C for 2 hours, then vials were cooled down to room temperature. Lastly, the barcode and the absorbance of the vial and solution was read by the spectrophotometer automatically. The COD value reading displayed on the screen.

5.2.5 ADM model implementation on the septic tank

The IWA Anaerobic Digestion Model No 1 was implemented on the case study selected septic tank with which the influent and effluent total COD measurements were analysed. This septic tank has an inner volume of approximately 10 m³. The average daily flow was measured to be 1 m³/h. It can be expected the residence time in the septic tank is around 10 hours, although it seems very low for a septic tank. The initial composite particulate material of the septic tank in the ASM 1 was set to be the annual average total COD measured. And the units used in the ADM 1 model was all kg/m³·day. According to the COD fractions presented in the ADM model, the total COD 100% consists of 30% carbohydrates + 30% proteins + 30% lipids + 10% inerts, hence, the initial model parameters of COD fractions was assigned with the proportions described in the model. The mass transfer rate from liquid layer to sludge layer calculated by the solids settlement experiment in Section 4.2.3 was implemented in the ADM 1 model for the sludge layer inlet COD value. It is expected that the settlement rate calculated by the UK wastewater will be smaller than the actual rate of Chinese wastewater, because the Chinese wastewater has much higher COD concentrations. The rate was applied on the total COD at the influent of the septic tank. A series of time steps have been tested in the ADM model in order to compare the model stability and simulation running time. An optimal time step is selected for the balance of model stability and time cost. Last, the change of total COD measured in the septic tank was compared with the model results for further discussion.

5.2.6 SeweX model application for methane production

The SeweX model was used to simulate the methane formation in sewer pipes, the rising main in Chapter 2 was selected as study rising main pipe. The methane production in rising mains simulated by SeweX model was compared with the methane production simulated by ADM model in the septic tank. All the COD parameters used was taken from the measurements in

the Yorkshire wastewater treatment plant due to no field measurements has been taken on the COD concentrations in the study sewer pipes. This simulation was only for a theoretical comparison with the ADM model results for septic tanks. The transformation of COD fractions and the formation of methane in septic tanks and sewer pipes will be compared.

5.3 Results and Discussion

5.3.1 Septic tank COD removal rate

The seasonal and annual COD removal rate of the selected Chinese septic tank was summarised in Table 5.4. The total COD was analysed using the method in 5.2.2.

Table 5.4, the variation of wastewater quality before and after septic tank.

Seasons	Spring	Summer	Autumn	Winter	Annual
Temperature °C	12	24.6	9.8	-4.3	7.7
Influent (mg/L)	5398.5	5406.6	7511.1	3829.9	5536.5
Effluent (mg/L)	959.4	850.9	1001.0	822.4	908.4
Removal rate %	82.2	84.3	86.7	78.5	83.6

Table 5.4 summarised the total COD removal rate of the selected residential septic tank. It can be seen that this septic tank had an annual average COD of 5536.5 mg/L and an average COD removal rate of 83.6% with an annual average temperature of 7.7 °C. The total COD was analysed using the potassium dichromate method. Each of the four season's influent and effluent COD concentration was calculated by the average data collected in the three days in a season.

In general, the inlet wastewater total COD concentration was much higher than the COD concentrations collected in downstream sewer systems and wastewater treatment plant. This is because the toilets drainage sewer system is separated from the kitchen and bath sewers in this catchment. The septic tanks only receive wastes from the toilets, and the general wastewater is discharged to the sewer system directly (Literature shows the average total COD in septic tanks from public toilets in China is around 25,000 – 35,000mg/L, with 2% - 15% solids) (Zhang and Ni, 2005). From Table 5.4, it shows the autumn season had the highest

influent total COD (7511.1mg/L) and the highest COD removal rate (86.7%) even the temperature was relatively low compared to spring and summer. Winter season had the lowest influent and effluent total COD and the lowest COD removal rate, this is because the COD is removed by bacteria. The activity of bacteria is temperature dependent with low temperature leading to slow growth, hence the COD removal slows down in winter (Painter and Loveless, 1983). In theory, the COD removal rate in spring and summer season should be higher than autumn and winter because of the higher temperature and more active transformation processes. However, It was observed in the septic tank that especially in summer season, some sludge and solids particulate materials was taken up to the surface with the rising of gases produced at the bottom sludge layer due to the fast active biochemical transformations in the sludge layer. That is why the effluent COD concentration was higher than expected.

5.3.2 Solids settlement and mass transfer rate

The four wastewater samples termed sample 1,2,3,4 used for solids settlement experiment were collected on 29.11.2016, 08.12.2016, 14.12.2016, and 22.12.2016 respectively along with the routine wastewater sampling in the wastewater treatment plant in Yorkshire. COD analysis showed the four samples had original raw concentrations of 811mg/L, 1034mg/L, 810mg/L, and 1474mg/L. The solids settlement speed against time experiment was carried out in the cylinder. Figure 5.5 shows the solids settlement experiment results of the four samples:

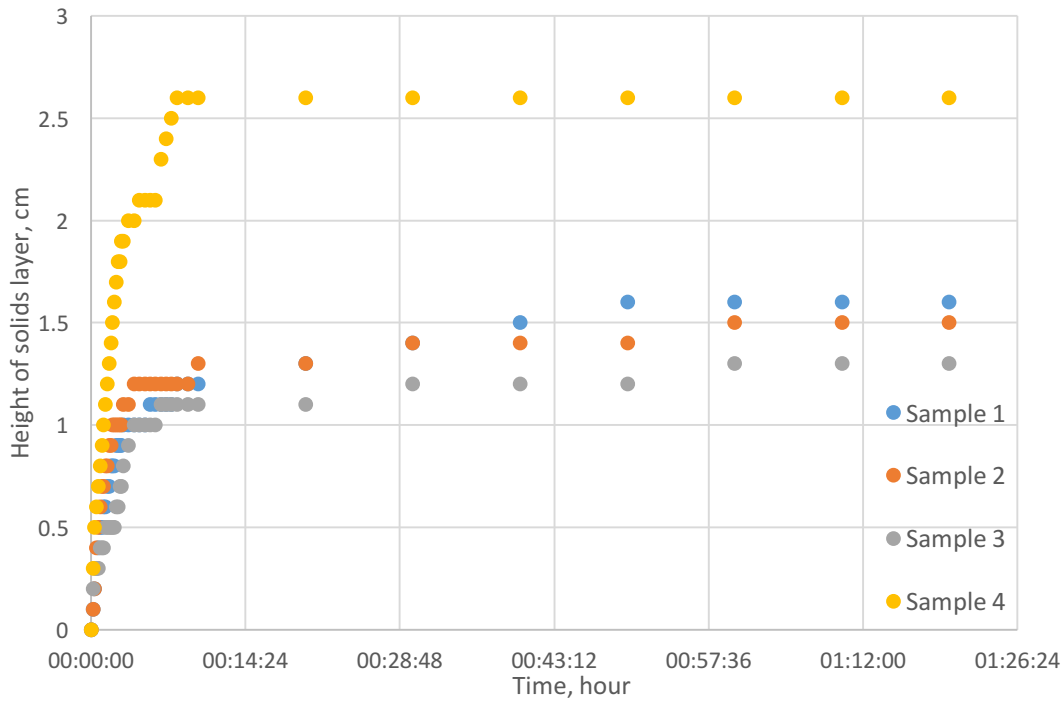


Figure 5.5, wastewater solids settlement experiments results.

Figure 5.5 illustrates the wastewater solids settlement experiments results, the change of solids layer height against time. It took nearly the same time for most of the solids to be settled for all four samples. Thus the solids settlement rate in wastewater is relatively fast. At the beginning, a trial experiment was carried out for 24 hours. It was measured the column height at the first 6 hours, then till the next day. It was found the solid layer height would no longer change after 1.5 hours, the height kept the same till the next day. Hence, the following comparing experiments were all only measured for 1.5 hours. Figure 5.6 shows the solids layer of four samples.

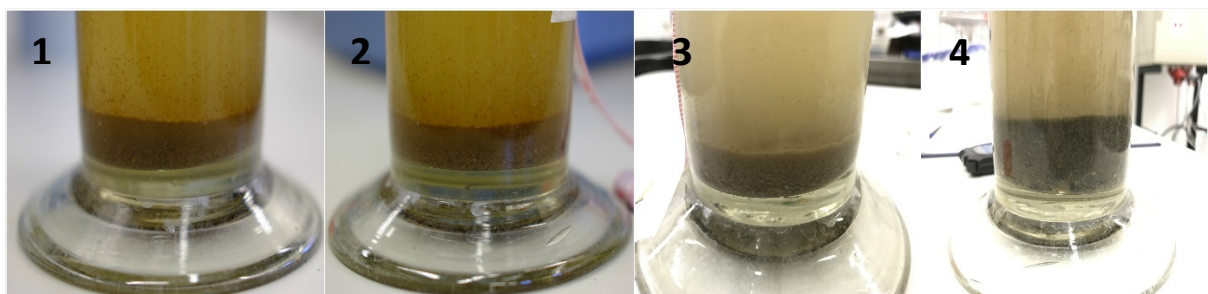


Figure 5.6, Solids layers of the four wastewater samples in the solids settlement experiments.

The four images in Figure 5.6 show the solids layer of the four wastewater samples in the solids settlement experiments. Sample 1,2,3 had a solids layer height of 1.6cm, 1.5cm, and 1.3 respectively corresponding to a raw COD concentration of 811mg/L, 1034mg/L, 810mg/L. Sample 4 had a solid layer height of 2.6cm with a raw COD of 1474mg/L. Both the COD concentration and solid height was much higher than the other three samples. From the results it can be concluded that the wastewater solids percentage reflects the total COD of wastewater. The total COD value is somehow related to the amount of solids, but not completely depends on the solids because only the organic compounds are accounted to the COD value. The wastewater solids and settlements also consist of inorganic particulate and inerts such as sands.

Table 5.5, Total COD analysis results of wastewater solids settlement samples.

COD (mg/L)	Sample 1	Sample 2	Sample 3	Sample 4
Raw	811	1034	810	1474
Top	555	384	579	730
Middle	533	441	693	752
Bottom	1861	1808	2511	2728
Height (cm)	1.6	1.5	1.3	2.6

Table 5.5 shows the COD analysis results of the four wastewater solids settlement samples.

Sample 1 and sample 3 had a similar raw COD concentration which was also close to the mean COD concentration collected at the wastewater treatment plant (877 mg/L). While sample 2 and sample 4 was much higher than average. The COD concentration of top and middle of the water column should be close, which only the middle layer COD of sample 1 was a bit lower than the top layer. The COD of middle layer in sample 2, 3 and 4 were all little higher than the top layer. Although sample 1 and 3 had the similar raw and top COD concentration, however, the bottom solids layer of sample 3 had a much higher COD concentration than sample 1. The height or the volume of solids layer of sample 3 was less than sample 1, which means sample 3 contained more particulate and settled organic matter in the solids layer. The COD of sample 4 was both high in raw and bottom layer, but it also had much more solids settled at the bottom. This probably means sample 4 contained not only high organic matter components but also high insoluble and inerts solids such as sands in the wastewater.

From the COD analysis results of different layers, the solids settlement and COD mass transfer rate can be calculated. For each of the experiment, wastewater was added to the 2L scale mark on the cylinder. From the reading of the measuring tape on the cylinder. It had a 50cm height. The inner diameter of the cylinder was measured by an electric micrometre which showed a result of 7.1cm. Thus the actual volume of wastewater column can be calculated as $0.002 \text{ m}^3 = \pi \cdot r^2 \cdot L$, where r was measured. The water column height was calculated to be $L = 0.5054 \text{ m}$ which was almost the reading of the measuring tape 0.5 m considering the error. Therefore, the volume of wastewater and the volume of solids can be calculated by the multiply of total volume with height ratio. For example, sample 1 had solids layer height of 1.6 cm, which means the solids volume can be calculated as $V = 0.002 \times (1.6/50) \text{ (m}^3\text{)}$. As the COD concentration for wastewater and solids was analysed, the organic matter COD related mass can be calculated. For sample 1, the raw wastewater COD concentration was 811 mg/l which was 811 g/m^3 , the raw wastewater COD mass should be $811 \times 0.002 = 1.622 \text{ gCOD (O}_2\text{)}$, the bottom COD mass was $1861 \times 0.002 \times (1.6/50) = 0.1191 \text{ gCOD (O}_2\text{)}$. The mass transfer rate would be $\frac{\text{Bottom}}{\text{Raw}} \times 100\%$. Where the mass transfer rate for sample one was calculated to be 7.34%. In the same way, the mass transfer fraction for the other three samples were calculated to be 5.25%, 8.06%, 9.62% respectively.

Table 5.6, wastewater COD mass transfer rates.

	Sample 1	Sample 2	Sample 3	Sample 4	Average
Rates (%)	7.34	5.25	8.06	9.62	7.6

It can be calculated that the four samples had an average mass transfer rate of 7.6%. However, all four samples were collected at the wastewater treatment plant, which is the end of the downstream sewer system. The samples were collected at the open channel after the lift and grid, this means the wastewater contained much fewer solids and sediments compared to the upstream. And the solids and particulate material percentage of influent to the septic tanks should be even higher due to the separate toilet system. It also can be seen from the wastewater samples collected in the septic tank in China. Hence, the mass transfer rate between liquid and sludge layer was set up to 10% as an assumption for the modelling of

septic tank processes. It can be expected the actual transfer rate in septic tank will probably be much higher than the WWTP.

5.3.3 ADM model results on the septic tank

The IWA Anaerobic Digestion Model No 1 was used to simulate the processes of the selected septic tank in China with field measurements. The septic tank has an approximately 10 m^3 volume. The inlet and outlet flow rate were measured to be roughly $1 \text{ m}^3/\text{h}$ for average during the sampling periods. The total COD was measured at the inlet of the septic tank, where the COD fraction carbohydrates, protein and lipids represented 30% respectively plus 10% of inerts. The starting point of total COD concentration for the ADM model was set to be the annual average total COD at the inlet due to no measurements inside the septic tank. A 10% COD mass transfer rate calculated from the solids settlement experiments was applied to the mass transfer process from the liquid layer to the sludge layer. Due to the processes described in the ADM model was relatively slow and the HRT in the septic tank was fairly long, different time steps were tested in the model to compare the model stability and simulation running time. A time step of 10 minutes results is shown below.

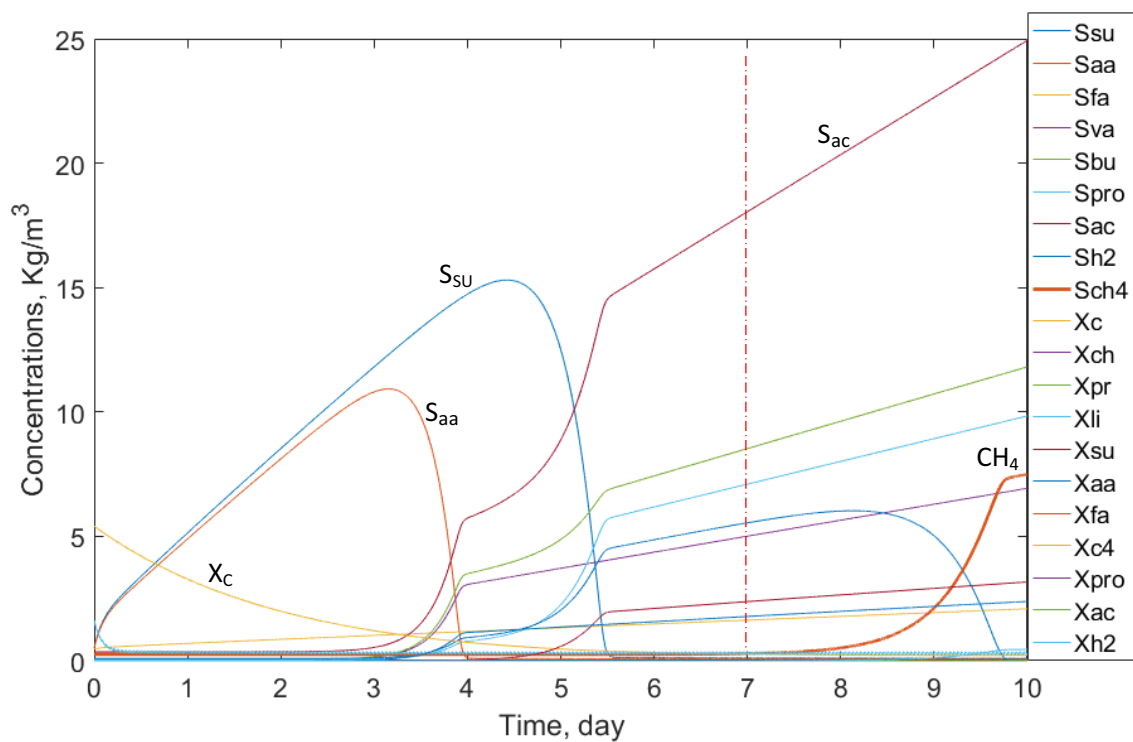


Figure 5.7, Change of COD fractions within 10 days of anaerobic digestion transformation in the sludge layer.

Figure 5.7 illustrates the variation of each COD fraction within 10 days of transformation, it can be seen from the figure that methane started to produce after approximately 7 days of transformations. The composite particulate material (X_c) had a steady decrease at the beginning, both sugars (S_{su}) and amino acids (S_{aa}) concentration experienced a growth and decay fluctuate in the first week. All other COD fraction components except the three mentioned above had a variable increase in the first 7 days.

The COD concentrations in the septic tank were different to the inlet COD before entering the tank. The difference on COD concentrations would be more significant than what in sewer pipes due to the much longer residence time. The COD concentration measured at the inlet of the septic tank was not the concentrations inside the septic tank due to the septic tank transformation process was occurring within intermediate concentrations when the transformations reached stable conditions. In order to get a closer look at the transformation processes after the first 7 days with a starting COD concentration for establishing the conditions, The COD fraction concentrations were selected around the 7th days when the concentrations became steady increasing. The selected time point is shown in Figure 5.7 as the red dash line indicates.

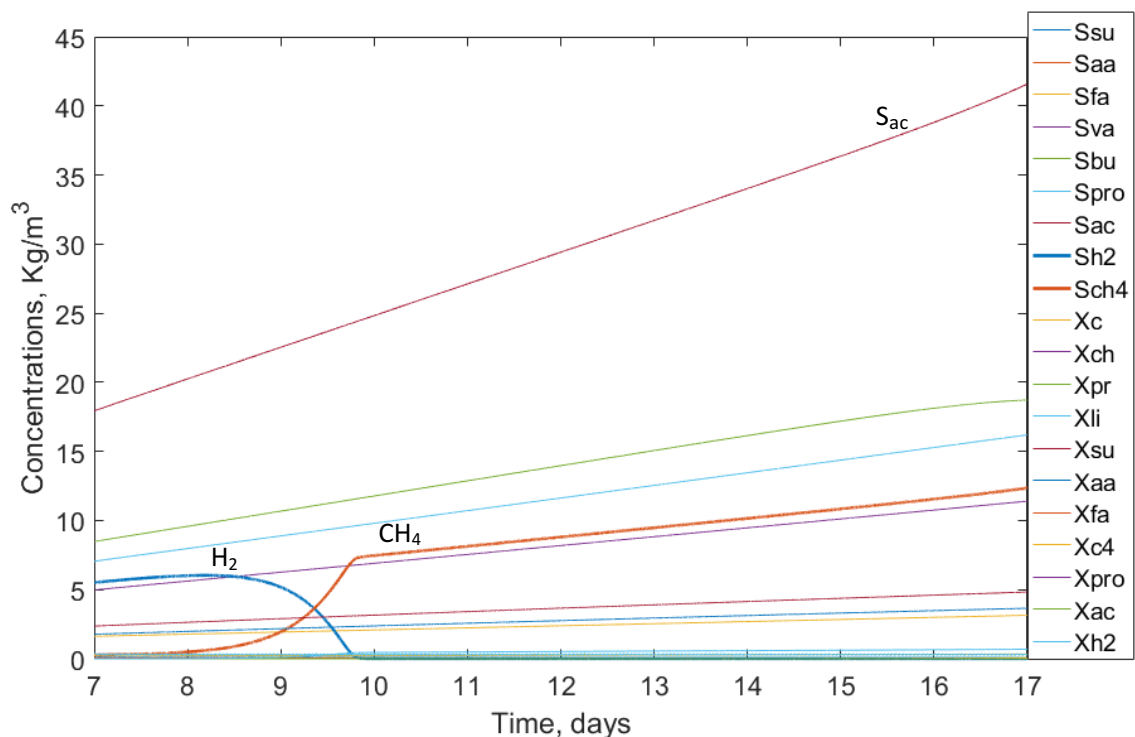


Figure 5.8, Change of COD fractions after first 7 days of transformations.

Figure 5.8 shows the transformation processes for 10 days with selected stabilized COD concentrations. It can be seen from the figure that apart from hydrogen and methane, all other fractions such acetate (S_{ac}), fatty acids (S_{fa}), valerate (S_{va}) and butyrate (S_{bu}) had steady growth. Methane started to be produced by the uptake of hydrogen, then methane reached steady growth when hydrogen was consumed. The major source for methane production comes from acetate after hydrogen. However, the production of acetate was higher than the consumption of acetate, hence, it still maintained growth. All the other constituents came from the decay of continuous inflow of composite particulate material (X_c). It also can be seen that the composite particulate material had a growth after the decomposition and consumption in the first week. The growth of composite particulate material came from processes such as the decay of sugars, amino acids and fatty acids but it was kept at a low concentration due to the lack of resources. For a further illustration, the model was running to simulate for another 15 days to see the variations in a month's time period.

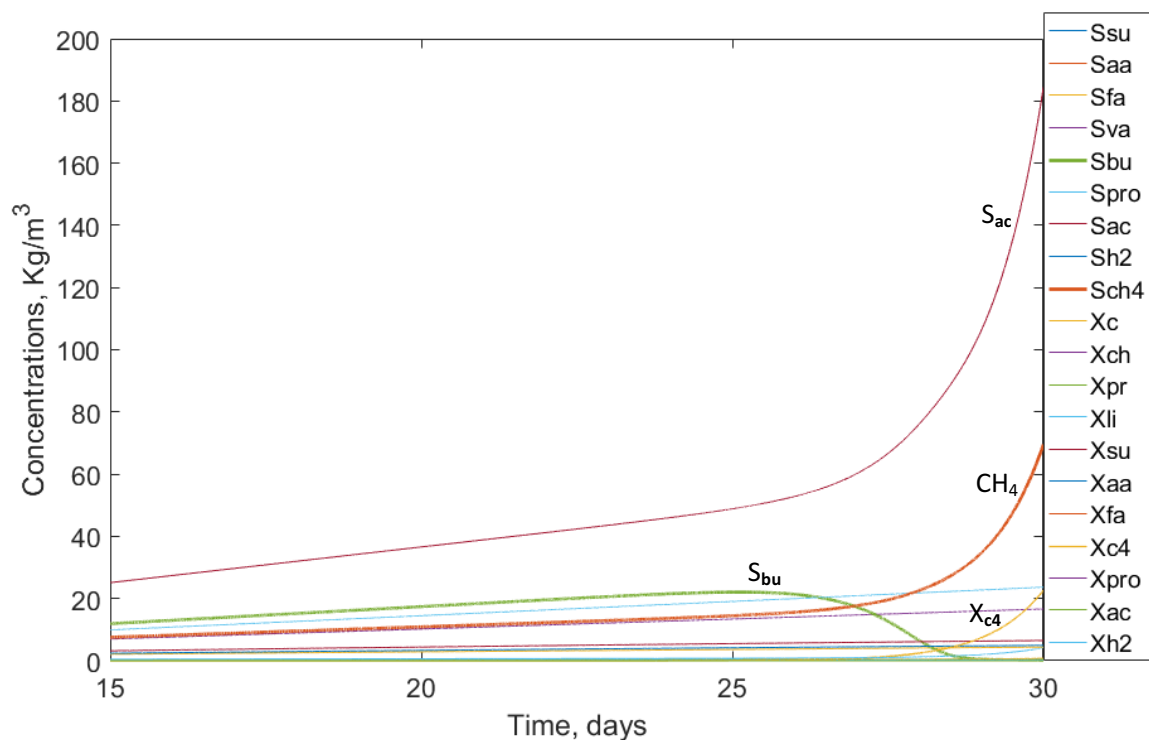


Figure 5.9, Variation of COD fractions after a stabilized concentration, 30 days transformation.

Table 5.9 shows the COD fraction variations within 30 days of transformation. It can be seen that there was a secondary fast growth of methane after approximately 27 days which was driven by the decrease of total butyrate (S_{bu}). The uptake of butyrate also contributed to the

increase of total acetate (S_{ac}) and valerate and butyrate degraders (X_{c4}). The model results showed the methane concentration was between 5 – 10 Kg/m^3 after the COD fractions became stable. The second growth could get up to 50 Kg/m^3 when the butyrate was used up. It is noticeable that the concentration of total acetate had a continuous growth from the beginning. The first large increase was the uptake of sugars and amino acids, and a second increase was the uptake of butyrate. In the Anaerobic Digestion Model expression, the only acetate consuming process is the uptake of acetate for methane formation. However, the uptake of sugars, amino acids, fatty acids, valerate, butyrate and propionate all contributes to the increase of acetate. That is why the acetate concentration kept growing all the time in the model results.

The field measurements of the influent and effluent COD of the septic tank indicated the annual average COD removal rate was 83.6%. The ADM 1 model calculated the removal rate of total COD, it took approximately 12.5 hours for the total COD removal rate reached 83.6%. The measurements were taken at the inlet and outlet of the septic tank. Which means the residence time of the liquid layer was simulated to be around 12 hours. If the septic tank was simply assumed to be fully mixed with the measured 10m^3 volume and $1\text{m}^3/\text{s}$ flow rate, then it would have the same order of magnitude as the 10 hours residence time compared to the modelled 12 hours. In order to calibrate and validate the ADM model for septic tank modelling, the change of COD fractions before and after the septic tank should be measured for future work. The gas phase methane concentration in the septic tank should also be measured to compare the total methane formation in the sewer system.

5.3.4 SeweX model results on methane formation in rising mains

The formation of methane in SeweX model methane section was simulated in the rising main in Catchment A introduced in Chapter 3. The wastewater COD used was the average concentration measured from the wastewater treatment sampling. Due to there was no measurement taken on COD fractions, where the acetate and readily biodegradable substrates (fermentation products) were calculated to be 50 g/m^3 using the fraction percentages as the initial concentrations respectively. Initial methane in wastewater before the rising main was set to be zero. Figure 5.10 shows the results of methane formation within 2.5 hours of residence time in the rising main A with the original diameter of 0.1m.

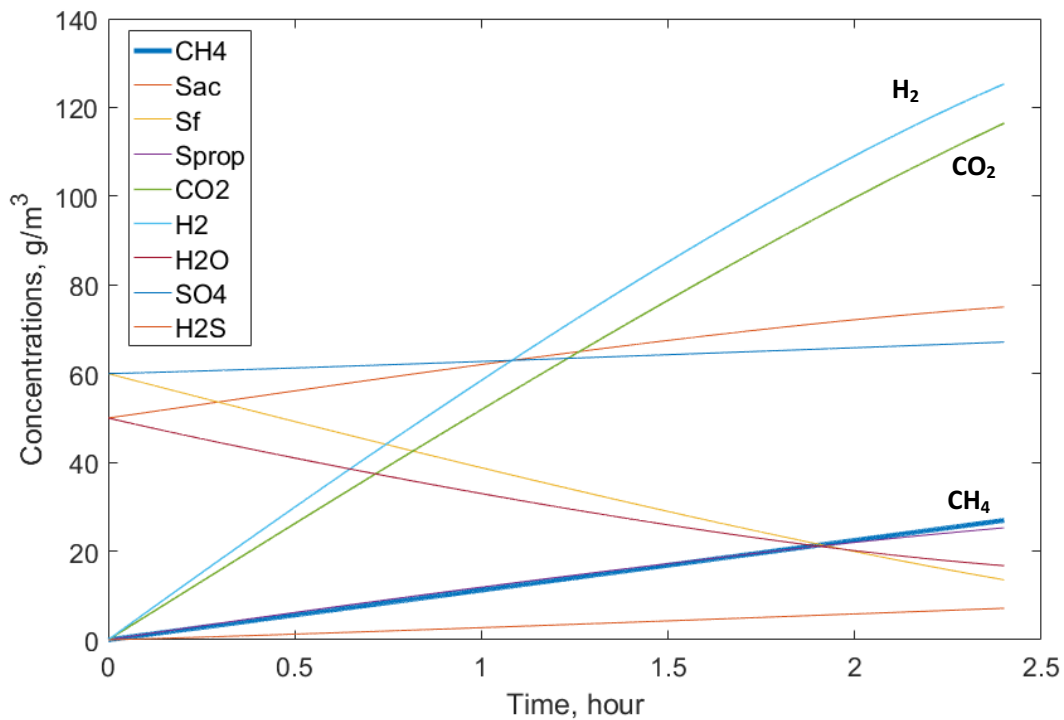


Figure 5.10, Methane production in wastewater in rising mains.

The variation of COD fractions and methane production in rising mains is shown in figure 5.10. It can be seen that there was a steady growth of methane in the rising main. There was also a large amount of hydrogen and carbon dioxide production. The concentration of acetate also increased during the anaerobic periods. (Rudelle et al., 2011) had done field measurements of the transformations of organic matter in 6 rising mains in Denmark, which indicated that total VFA, acetic acid and propionic acid all had significant growth during the anaerobic periods in the rising mains. After approximately 2.5 hours of transformation in the rising main, methane concentration increased to 25 g/m³ at the end of the rising main. It is similar to the field measuring results of methane concentration in rising mains in Australia around 20 – 25 mg/L (Guisasola et al., 2008). From the model results of ADM 1 and SeweX, the methane formation in septic tanks was much higher than that in the rising main pipes. However, there is no literature of the simulation of methane production in septic tanks. The American and Australian studies have already proved methane formation in sewer pipes and septic tanks, although literature summarised a lot of research conclude sewer system is not a considerable source for methane production. It can be concluded from the model simulation studies that septic tank is a substantial source for methane production in sewers compared to sewer pipes.

The methane concentration in septic tank can be built up to a significant concentration depending on the residence time. In order to validate the relative contribution from septic tank and sewer pipes, future field measurements should be carried out for the validation of ADM 1 model in septic tanks. Field measurements should be mainly focused on the inlet, outlet, and inside septic tank COD concentrations and COD fractions, the water phase methane concentration, and the gas phase methane concentration. The combination of ADM 1 and SeweX model can be used for the simulation of methane formation in sewer systems for catchment modelling.

5.4 Conclusions

This chapter mainly focused on the investigation of methane formation in septic tanks and sewer pipes. Due to the lack of literature on the methane formation in septic tanks, the model study approach provided a closer view on the processes in septic tanks. Field measurements showed a high strength wastewater COD at the inlet of the septic tank and relative high COD removal rate in the septic tank. The modelling approach of by using the Anaerobic Digestion Model on simulating the transformation processes in the septic tank illustrated the variation of the model defined COD parameters. The model results showed a high methane production due to the high COD concentration in the septic tank and the relatively long residence time. It provided a view that theoretically high methane production occurs in septic tanks. The field measurements in the US septic tanks, and the plenty of anecdotal evidence of methane explosions in China listed in Chapter 6 also strengthen the idea. More field measurements should be carried out for future work such as the COD fractions analysis and gas phase as well as water phase methane concentration testing in the septic tank. The using of ADM model on septic tank processes should be validated with field data for better description and prediction. The modelling of methane production in rising mains using SeweX model showed similar results in some previous studies. The utilization of both ADM and SeweX model can be combined with the simulation of methane formation in catchment modelling for future work.

Chapter 6, Field measurements and modelling approach of a sewer catchment in China.

6.1 Introduction

The sewer system is one of the most important urban infrastructures in China as similar to many other countries. The first ever well-designed drainage system in ancient China was constructed around 1800 – 1500 B.C. (Jianguo et al., 2007) It was specifically designed for the imperial palace of the Shang Dynasty. The closed conduit was originally built with wood boards then replaced with clay and pottery breaks. For over centuries, the drainage system was gradually spread to civil use from the royal exclusive use. The oldest existing ancient sewer system in China is called “Fushougou” located in Ganzhou City, southeast China. It was constructed in around 1068 - 1077 A.D. during Song Dynasty, and it is very well-preserved and still functioning well today (Rao et al., 2016).



Figure 6.1, The Fushougou ditch sewer system in Ganzhou City, China.

The name Fushougou ditch literally means “Happiness and Longevity Ditch”. It was the first combined sewer system in China which was specifically designed to tackle the local heavy rain weathers. It is one of the worlds’ renowned ancient sewer systems, and it is also a tourist site like the Paris sewer museum. The city had never been flooded over centuries since this system was constructed. Currently, this system is still serving roughly 300,000 residents in the city centre. The Fushougou system can be regarded as an ancient representative project

especially compared to some of the modern times sewer system in China which is vulnerable and cannot fulfil the demands of urbanization and population growth.

6.1.1 Impact of urban development and realities of sewer systems in China

China has been experiencing fast economic growth and urbanization as well as population growth since the opening of the market in the 1980s. Many cities had been through and still in the process of fast urbanization. However, the development of sewer system, as well as other underground infrastructures, has not kept up with the same pace as urbanization (Wang, 2008). The previous urban drainage system designed had not fully considered the speed of urbanization. Some newly constructed urban areas sewer systems are not well designed and managed to connect with the existing systems. The actual underground structure and layout of the sewer systems in some cities is even unclear and unknown (Jin, 2009). The sewer branch of some residential areas was randomly connected to a manhole or directly to the main trunk sewer. In some situations, renovated separate sewer pipes had been cross-connected with combined or storm sewer pipes which result in infiltration, inflow and pollution (Zhang et al., 2017).

Another significant existing problem is sewer flooding due to the inadequate sewer capacity and poor design. Many cities in China are facing severe flooding problem every year during rainy seasons in summer. On 21st July 2012, the flooding in the city centre of Beijing due to continuous heavy rain and flooded sewer system resulted in 79 dead and \$1.7 billion economic loss; the rainy season in May 2014 in Southern China caused sewer flooding in 23 cities of 5 provinces, 1.22 million people were seriously affected (Che et al., 2015). However, the sewer system is always surcharged even during dry weather flows. The photo in Figure 6.2 was taken in a residential sub-catchment for the field measurements in the TUSWMC. The manholes were all fully loaded on dry weather days, and this is a common phenomenon of many catchments in China.



Figure 6.2, Surcharged manholes on dry weather flow days in the study catchment in the TUSWMC.

These two manholes are in the branch sewer line of a small residential sub-catchment before the main trunk sewer pipe. Apart from fully loaded sewer systems, other common existing problems in the catchments include constantly pump operations and air presence in rising mains. Most of the small pumps in the system are always on in order to transport accumulated wastewater. For some large pumping stations there are stopping periods for the pumps because the dimension of the wet well is big enough. However, rising main is emptied due to the backflow of wastewater retained in it during the pump stopping period. When the pump turns back to operate again, a large amount of air is trapped in the rising main. It creates an aerobic condition for the biochemical transformations of wastewater and reduces hydrogen sulfide production. Meanwhile, it also reduces the pump efficiency and may cause damage to both the pump and the rising main pipe.

6.1.2 Methane induced sewer explosions

The formation of methane in sewer systems is not only a contribution to greenhouse gas emission, but also the most significant problem is the methane induced explosions in sewers. Sewer explosion due to the accumulation of methane gas has brought to serious attention in China in recent years. A large number of methane induced sewer explosions occurs in China every year which results in great personal and property losses. For instance, four security guards dead in a septic tank explosion during their regular security check at a residential community in Nanjing City on 1st December 2004; 21 dead in a gravity sewer explosion in Beijing on 24th March 2006; 6 dead and 22 severe injured in a series sewer explosion along a

sewer line in Chongqing City on 4th May 2010 (Su et al., 2011). All the three incidents had been investigated to be as the result of accumulated methane explosions. Hundreds of methane induced sewer explosions are being reported every year especially during the time period of Chinese New Year due to the set off of fireworks and crackers (Hua, 2014). CCTV footages showed the majority of these incidents were caused by young children playing with fireworks closed to manholes where methane gas was ignited. However, investigations also indicated the explosion can be triggered spontaneously such as the vibration from urban construction and underground electricity network (Li, 2007).



Figure 6.3, CCTV footage and the scenes photos of methane induced sewer explosions in China (Tencent, 2015, Sina, 2013).

Figure 6.3 shows some CCTV footages and photos taken at the scenes of explosion. The left two photos show two incidents of spontaneous methane explosion in manholes, where the explosive force blew up the manhole covers and pushed them away. The first manhole cover hits the kid who was badly injured, and the second manhole cover was pushed away for 50

meters and the car parked close to it was damaged but fortunately, no one was injured. In 2005, a series of regulatory frameworks have been made after several serious fatal accidents of sewer professional workers in Jinan City (Gao and Lu, 2006). 2 dead in a gravity sewer tunnel during their routine cleaning work of sediments and debris on 11th July 2005, only several days later, another 2 dead in cleaning a septic tank and the connecting gravity sewer pipe on 22nd July 2005. Investigations concluded that the first accident was caused by suffocation due to high concentration of methane, where the gas phase methane concentration was detected to be 18% volume percentage during the investigation. The second accident was caused by hydrogen sulfide poisoning after the anatomizing survey. Since then, the regulation requires at least one-hour ventilation with exhaust fan for man-accessed sewer work to avoid such tragedies happening again (Hua, 2014).

6.1.3 TU sustainable wastewater management centre

The Tsinghua University Sustainable Wastewater Management Centre (TUSWMC) is a specialised joint wastewater research centre founded by the Tsinghua University, Zhejiang University and the Yixing Institute of Water Research in 2009. The research centre is located in Yixing City, Jiangsu Province, Southeast China, in which inhabits 1.25 million population (Gov, 2015). Yixing has an annual average temperature of 15.7°C, annual precipitation of 1177mm, and annually 136.6 wet weather days. Figure 6.4 shows an example sub-catchment in the TUSWMC with currently selected case study pump stations.

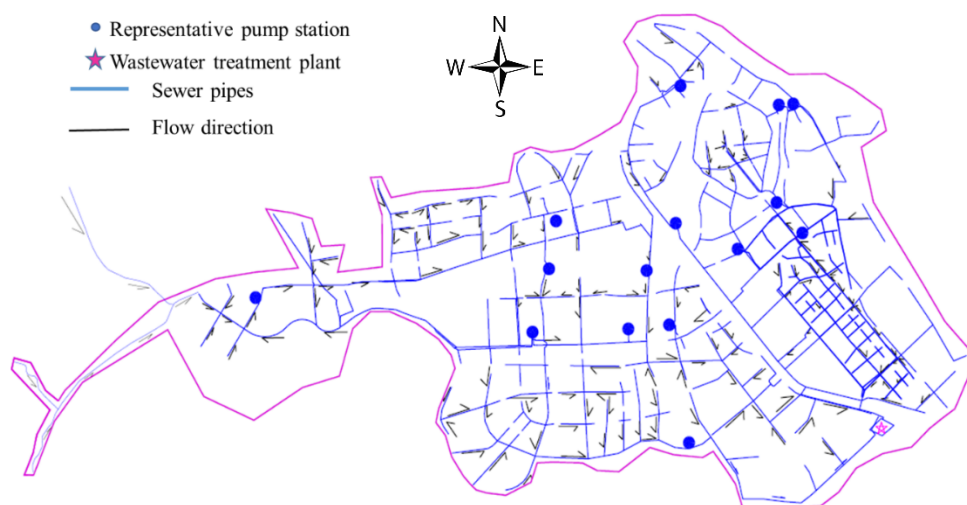


Figure 6.4, schematic of a selected catchment in the TUSWMC centre.

The case study gravity sewer system (figure 6.6) for gas monitoring in section 6.2.1 are located in the north of the catchment in Figure 6.4. At the southeast of the catchment where locates a WWTP. The flow rate and rainfall are being monitored and shown in Figure 6.5.

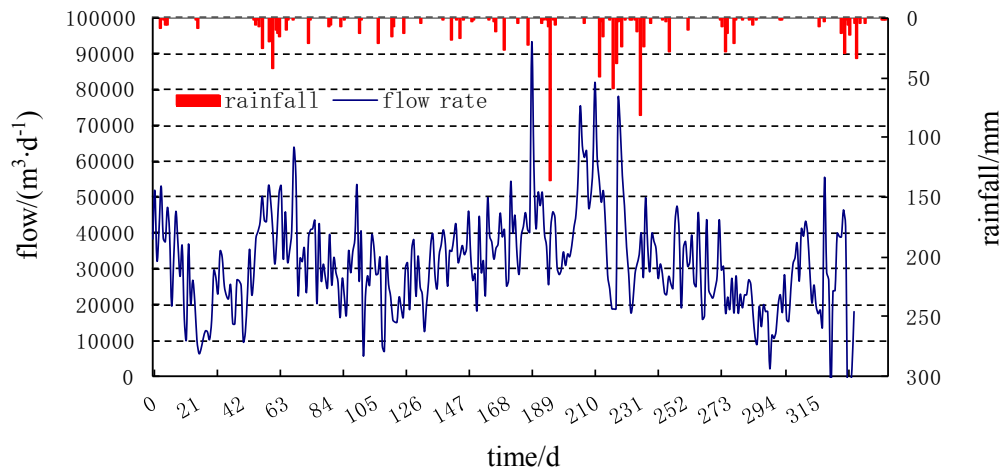


Figure 6.5, Change of the annual flow rate at the WWTP in the selected catchment.

The TUSWMC is located at the west of Yixing City centre. It includes a catchment area of roughly 40 km² with approximately 50,000 population. This sub-catchment area is newly constructed with the development of the city urban area, and it is dedicated to using for wastewater, sewers and the related researches for the TUSWMC. Unlike other common traditional sewer systems in China, this catchment was built with the modern urban drainage system regulations. There are no septic tanks existing in this catchment, and where only sewer pipe systems and wastewater treatment plants are presenting. Current studies and research carrying out in the catchment include such as flow monitoring, real time control, pump operations, bacteria growth and species investigation, sediment movement and transformations, gas movement, ventilation and detecting.

6.2 Methodologies

The aim of this chapter is to get a closer look at the operations and performances of the selected modern constructed Chinese sewer systems. All the sewer systems in the TUSWMC are newly build separated systems followed the design guidelines. No septic tank is presented in these catchments. And by far, the Chinese collaborators can only provide field work at their TUSWMC. Hence, it could not be selected a more typical septic tank involved system. By

monitoring the gas phase concentrations of hydrogen sulfide and methane, it aims to understand the hydraulic conditions, sulfide and methane formation and other problems in the sewer systems. The processes in gravity sewer systems and rising mains were investigated. In the meantime, it is going to investigate and analyse the possibility and capability of using sewer processes models developed based on the Europe and Australia sewer conditions such as the WATS and SeweX model to the Chinese sewer system with the local conditions. It is also important to look for solutions for the local sewer problems, and the essential future field measurements for model calibration and validation to meet the requirements by using these models under different conditions.

6.2.1 Gas monitoring in a residential gravity system

In order to investigate the typical range of hydrogen sulfide and methane concentrations in the Chinese sewer systems, a residential gravity sewer system and a residential rising main pumping system was selected to have gas phase sulfide and methane monitored respectively. The gravity system is located in the north of the sub-catchment shown in Figure 6.4.

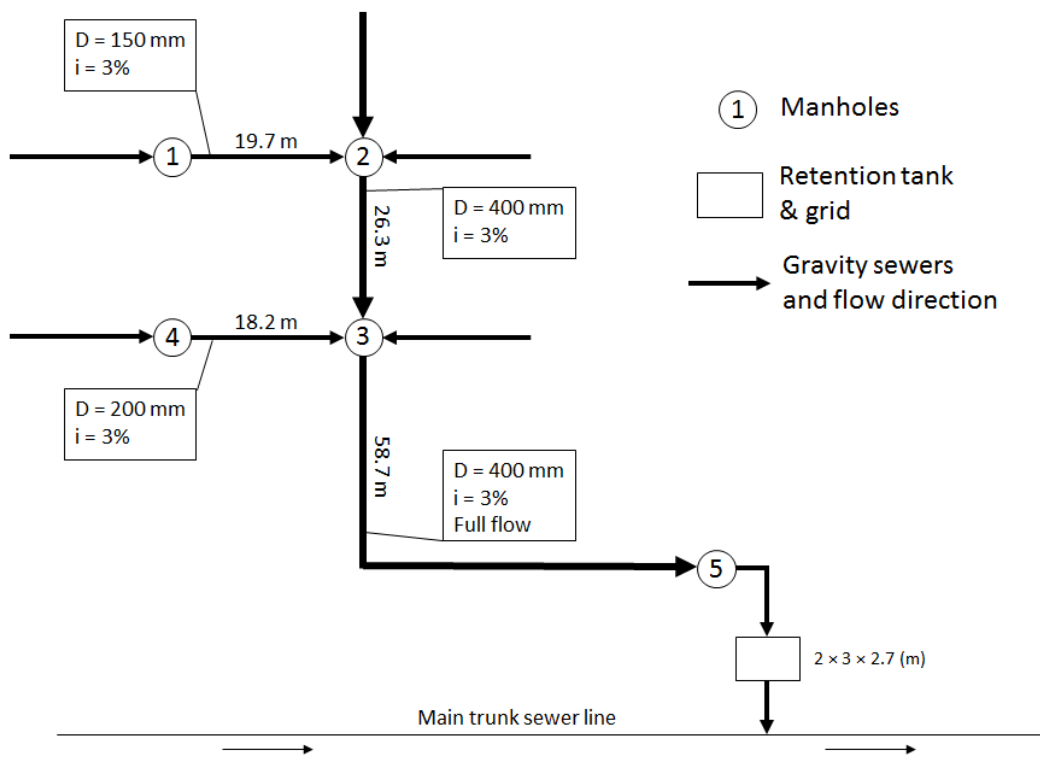


Figure 6.6, Schematic of the residential gravity sewer systems for gas monitoring.

Figure 6.6 shows the schematic layout of the gravity sewer systems in the residential community. The gravity system selected is part of the sub-catchment of a residential community in the TUSWMC. Manhole 1 and 4 is located on the branches of the sewer system, manhole 2, 3, 5 is situated on the main gravity sewer in the catchment. This intercepted gravity system serves 2580 residents in the catchment. The population was counted before manhole 5. The diameter, length, and the slope of the four gravity sewers between the 5 manholes were measured and illustrated in Figure 6.6. It is noticeable that the gravity sewer between manhole 3 and 5 was always full flow during the field measurements periods even it was on dry weather flow all time. This is a foul sewer as part of the separated system. It can be seen some interesting problems even in the newly constructed sewer systems.

The hydrogen sulfide and methane gas sensors were installed in each of the five manholes. The gas concentrations monitoring started on 3:45 pm 21.09.2016 and ended on 9:00 am 23.09.2016. The sensors recorded the gas concentrations and temperature at every 1 minute.



Figure 6.7, gas sensors and the installations in the manholes.

Figure 6.7 shows the photos of gas sensors and the installation places in the manholes. The installations of the gas sensors were carried out by 5 individual sewer practitioners. The recording of gas concentration and wastewater temperature for the five manholes was started at the same time. All the readings were saved in the internal memory storage.

6.2.2 Gas monitoring in two pumping-rising main systems

Two pumping-rising main systems with sufficient length and residence time were selected in the Yixing/TUSWMC catchment for hydrogen sulfide and methane measurements at the two ends of the rising mains. These two rising mains are downstream of two sub-catchments connecting to the wastewater treatment plant as shown in Figure 6.8. Rising main 1 is the catchment downstream pipe connecting to the WWTP shown in Figure 6.4.

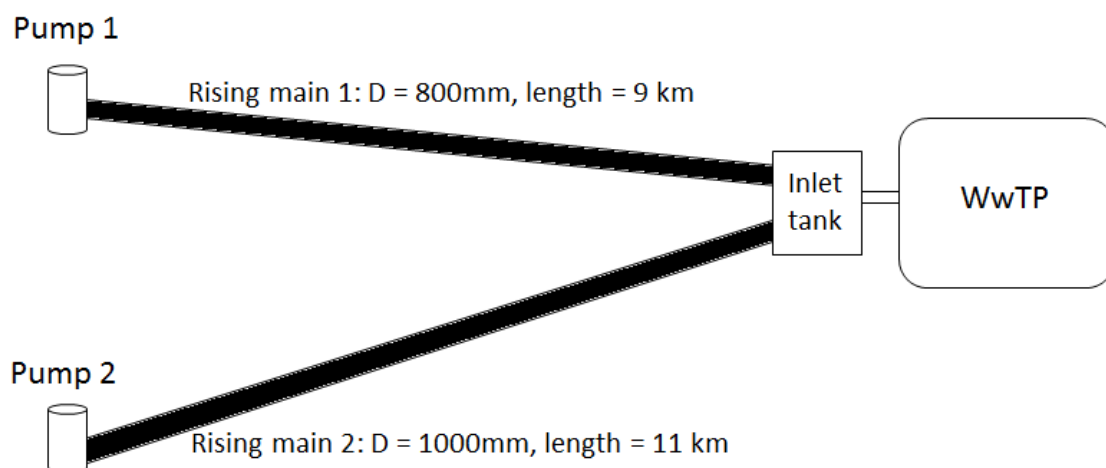


Figure 6.8, Schematic of two pumping rising main systems in the catchment.

Rising main 1 comes from the west of the catchment, and rising main 2 comes from the southwest. Both rising mains terminate at the inlet tank of the wastewater treatment plant. Rising main 1 has a diameter of 800mm and a length of 9 km. Assume the pumps are always on. The flow velocity in rising main 1 is 1.01 m/s, and the average residence time is 2.5h. Rising main 2 is 1000mm in diameter and 11 km in length. The flow velocity is 0.68 m/s, and the average residence time is 4.5h. Field investigation had confirmed both rising mains were full flow, no air was trapped and no backflow of wastewater during pump stopping periods.

The hydrogen sulfide and methane gas sensors were installed at the pumping stations and the inlet tank of the wastewater treatment plant. In pump 1 and 2, the gas sensors were hanged in the wet well just above the maximum water surface. Two sets of gas sensors were used at the inlet tank of the treatment plant. The distance between the outlets of two rising mains were approximately 2.5m. Data recorded was the average readings of the two sets of sensors.

6.2.3 Modelling approach on the gravity system

In order to apply the sewer processes models in the Chinese sewer systems for future work, the processes models must be validated and calibrated with field measurements. However, the hydraulic information and water phase COD concentrations have not been measured yet, and only the gas phase sulfide and methane concentration were available. The Chinese collaborators had measured some water phase COD concentrations in the main trunk sewer as shown in figure 6.6. The sampling location was approximately 500m downstream of the connecting point of the gravity system. Hence, a modelling approach by applying the SeweX model in the gravity system with very limited field data was conducted, to check the probable transformation processes and the reliability of the model.

The gas phase methane monitoring in Manhole 5 showed a time period of methane volume concentration exceeded 5% as shown in Figure 6.11. The volume percentage concentration can be converted to mass concentration based on the standard conversion method ISO 14912:2003 (Linde, 2017), in which 5% equals to 36mg/L. It is assumed equilibrium between the water phase and the gas phase which is rarely found in sewers because the air water mass transfer is generally slow. Then the water phase methane concentration can be calculated according to the gas phase concentration based on Henry's Law calculation.

$$\frac{C_g}{C_s} = H_u \quad (6.1)$$

Equation 6.1 is the unitless form of Henry's Law. Where C_g is the concentration of constituent in gas phase, mg/L. C_s is the saturation concentration of constituent in liquid, mg/L. H_u is

Henry's Law constant, unitless. The unitless Henry's constant for methane is 28.13 (Metcalf, 2003). Hence, the water phase methane concentration can be calculated as:

$$C_s = \frac{C_g}{H_u} = \frac{36}{28.13} = 1.28 \text{ mg/L} \quad (6.2)$$

No hydraulic information of the Chinese gravity system available yet, however, it can be estimated compared to the catchment in the UK introduced in Chapter 2. This is purely an estimation based on population, although the water consumption and lifestyle would be different in the two countries. The Chinese sub-catchment had total residents of 2580, while the UK catchment had a total population of 3600, and an average flow rate of 0.018 m³/s. The full flow gravity sewer pipes between Manhole 3 and 5 were 58.7m in length, 400 mm in diameter. Thus, the average flow rate and velocity in the Chinese system can be calculated to be 0.0129 m³/s and 0.1 m/s, respectively. Then the residence time can be calculated to be approximately 10min. The 0.1 m/s velocity is quite slow which can cause sediment build up. Maybe this is why this section of gravity sewer is always full flow, this may also result from the effects of backflows. This is a result of inappropriate design due to lack of information. And the flow rate data used from the UK catchment was from combined sewers, hence the actual flow rate in the Chinese system could be even slower. It has not been able to get the Chinese water samples and flow data measured. Information is provided as much as possible for the calculations and model simulations.

A 10 minutes residence time with the full flow pipe was programmed in the SeweX model in the gravity sewer. The transformation processes can be treated as the same as the processes in a rising main with anaerobic condition due to the gravity sewer was full flow. The initial wastewater COD concentration used was the average data from the UK sampling wastewater treatment plant. The SeweX model simulation aims to look at methane formation in sewer pipes with normal wastewater, not the toilet only septic tanks wastewater. Then the wastewater COD concentration can be estimated by the process model, and compared with the downstream wastewater COD measurements.

6.3 Results and Discussion

6.3.1 Gas concentrations in the gravity system

The gas phase hydrogen sulfide concentration in the gravity sewer systems was plotted in Figure 6.9. It was recorded 41 hours 15 minutes data in total from 21st to 23rd September 2016.

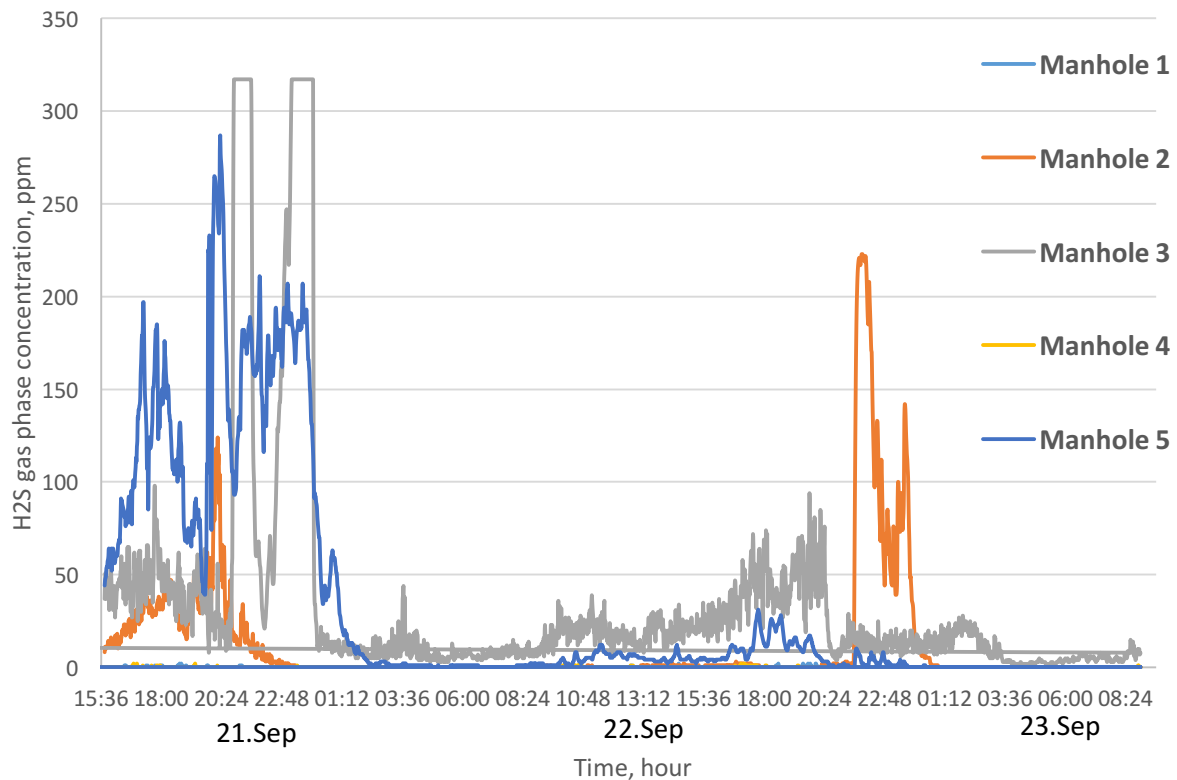


Figure 6.9, Gas phase hydrogen sulfide concentrations in the gravity sewer system.

Figure 6.9 illustrates the change of gas phase hydrogen sulfide concentrations at the five manhole sensor locations in the gravity sewer system. It can be seen from Figure 6.9 that the variation of hydrogen sulfide concentrations at five manholes followed a similar fluctuation pattern. The highest hydrogen sulfide concentrations appeared among late afternoon, evening and midnight for two days. It also can be seen that manhole 1 and 4 had the lowest hydrogen sulfide concentration detected. The sensor recorded the concentration was between 1 and 4 ppm which was almost in the sensor error range. However, manhole 2, 3, and 5 showed significant hydrogen sulfide gas concentration recorded. This is because manhole 1 and 4 was on the branch sewer lines where they were very close to the source from the buildings. While manhole 2, 3, 5 were all on the main sewer line with much higher

wastewater flow and longer transformation time since the upstream, because the gas phase movement is complex, hydrogen sulfide can come from anywhere, not only the 10 minutes residence time pipe, but also the upstream pipes with longer residence time. Also, the measured gas phase hydrogen sulfide concentration is much higher compared to some example sulfide concentrations in the Europe shown in Figure 3.12 in Chapter 3. The section of gravity sewer between manhole 3 and 5 was in full flow condition during the gas monitoring periods, even though it was reported by the site sewer practitioners that many gravity sewer pipes in the catchment were full flow all the time. This could also result in creating an anaerobic environment for the anaerobic transformation of wastewater and the formation of hydrogen sulfide.

The variation of wastewater temperature in the five manholes was also recorded as shown in Figure 6.10.

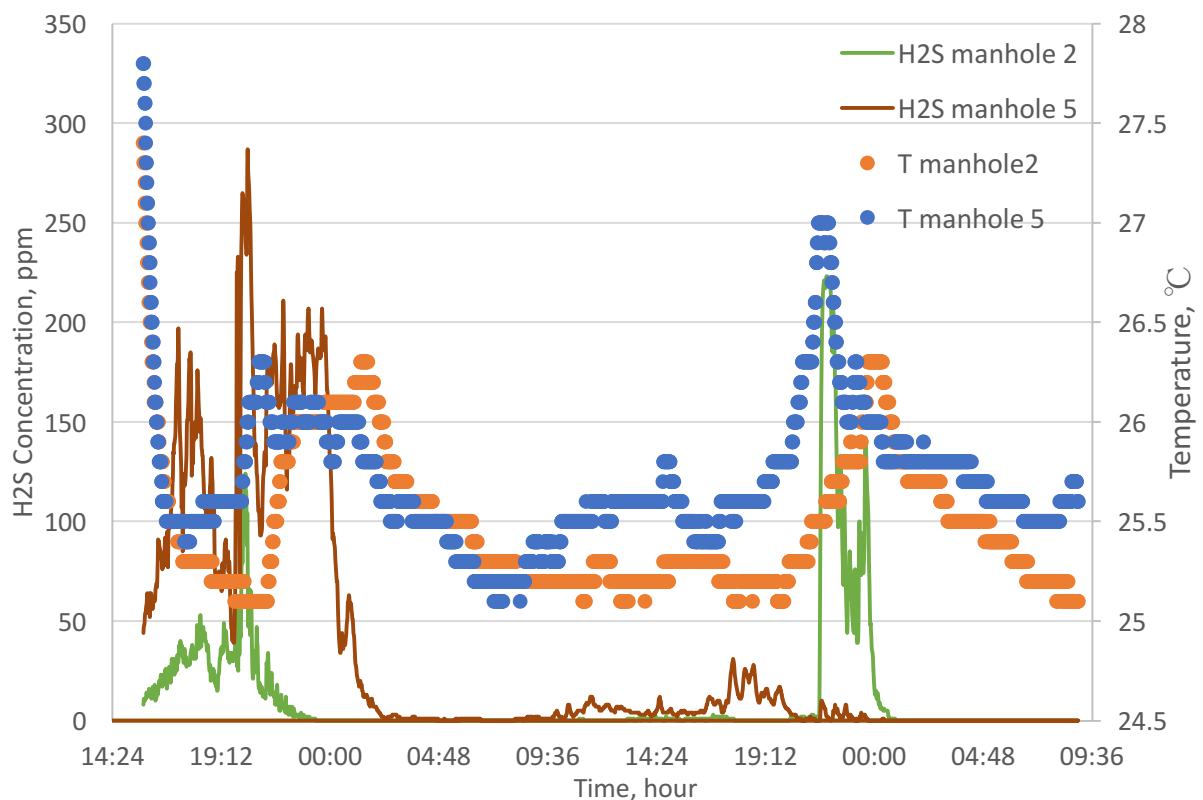


Figure 6.10, Wastewater temperature variations vs. sulfide concentration in the manholes.

Figure 6.10 illustrates the wastewater temperature variations in manhole 2 and 5. In general, the temperature of manholes on the main sewer pipe namely manhole 2, 5 which was slightly higher than the temperature of manholes on the branch lines. This was also related to the

higher sulfide gas concentrations in the three manholes on the main sewer line. All manholes recorded peak temperature between evening and mid-night periods for two days. This was related to the peak sulfide concentrations at this time periods again. The results showed that the hydrogen sulfide concentration is highly related to temperature. Even though the field measurements were gas phase concentration, which may not reflect the exact concentrations in the water phase. However, the peak sulfide concentrations associated with peak temperatures also reflects that higher temperature will result in more active air-water mass transfer and higher diffusion rate of hydrogen sulfide from the water phase.

The methane gas sensors in the manholes 1 - 4 all showed zero methane concentrations, not even trace methane concentration was detected. However, sensor number 5 which was installed in manhole 5 showed a significant concentration of methane since later afternoon on 22nd September till the recording ends on 23rd 9 am in the morning.

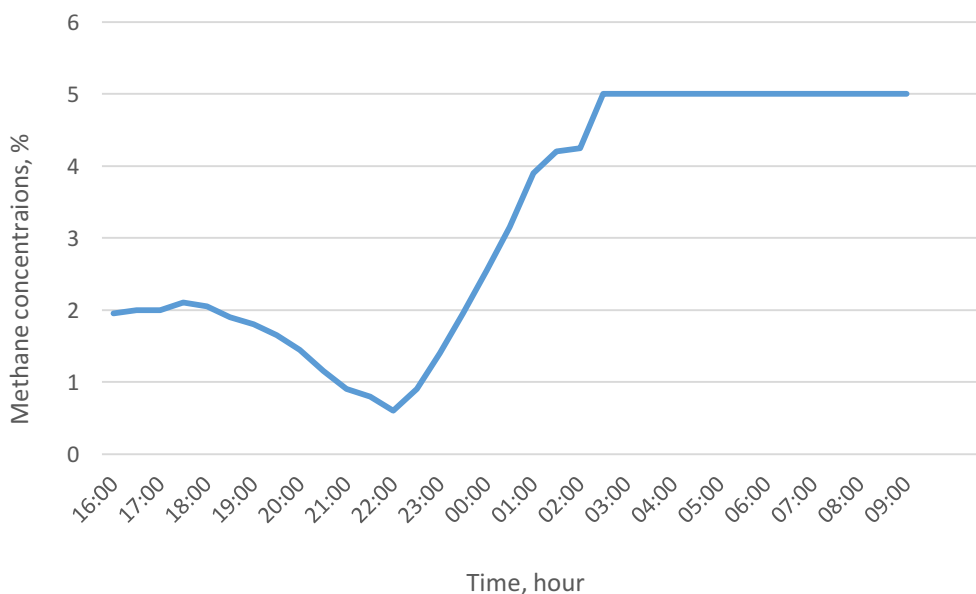


Figure 6.11, Methane concentrations in manhole 5.

The gas phase methane concentration started to appear in the afternoon on 22nd Sep, and started to build up during the mid-night to morning period on 23rd Sep. The concentration even exceeded the maximum value the sensor can read which is 5%. The methane concentration started to build up to more than 5% from 3 am. This was very dangerous because the methane volume percentage already exceeded the explosion limits. It was

interesting why manhole 5 also showed high hydrogen sulfide concentration during the same period in Figure 6.10. It was reported by the site sewer practitioners that the metal grid in the retention tank was partially blocked which resulted in wastewater retained in the retention tank. It was submerged all the connecting pipes, and the wastewater flow rate during night period was relatively slow. It gave rise to the formation of methane in the retention tank and the release of methane gas to the connecting pipes.

6.3.2 Gas concentrations in the pumping-rising main systems

The hydrogen sulfide and methane gas phase concentrations at pump 1, pump 2 and the inlet tank of wastewater treatment plant was monitored and recorded for three days. The measurements were carried out on 28th May, 1st June and 6th June 2016 respectively.

6.3.2.1 Hydrogen sulfide concentrations in the pumping-rising main systems

The three days gas phase hydrogen sulfide concentrations were recorded at the beginning and the end of the rising mains, which was in the pumping stations and the inlet tank of WWTP. Figure 6.12 shows the hydrogen sulfide gas concentrations at the wet wells in pump 1 and pump 2. It can be seen from Figure 6.12 that there were not significant hydrogen sulfide detected in the wet wells for three days. The average hydrogen sulfide concentrations in pump 1 were slightly higher than the concentrations in pump 2, because the average wastewater temperature in pump 1 was higher than that of pump 2. This may result in more hydrogen sulfide release from the water phase.

The hydrogen sulfide concentrations at the end of the rising mains which was the inlet tank were shown in Figure 6.13. Theoretically, hydrogen sulfide concentration at the end of the rising mains should be higher than the beginning of the pipes due to the anaerobic sulfide formation processes in the rising mains. However, the gas phase sulfide concentrations in the inlet tank were much lower than the concentrations in the pumping stations. This is because the outlet of the two rising mains was submerged in the inlet tank in the treatment plant. Less hydrogen sulfide was released into the air phase without turbulent flow or drop structures. That is why the sulfide concentrations in the inlet tank were even much lower than in the pumping stations. The submerged/surcharged discharge end of rising main is a technique for reducing of hydrogen sulfide releasing from the water phase. It is done on purpose to prevent

high hydrogen sulfide concentration occurring in the WWTPs. However, the methane concentration measured in the WWTP is relatively higher than the hydrogen sulfide concentration as shown in Figure 6.15. This is because methane has much lower water solubility compared to hydrogen sulfide. Hence, methane is easily released from water phase even with submerged pipes in the inlet tank.

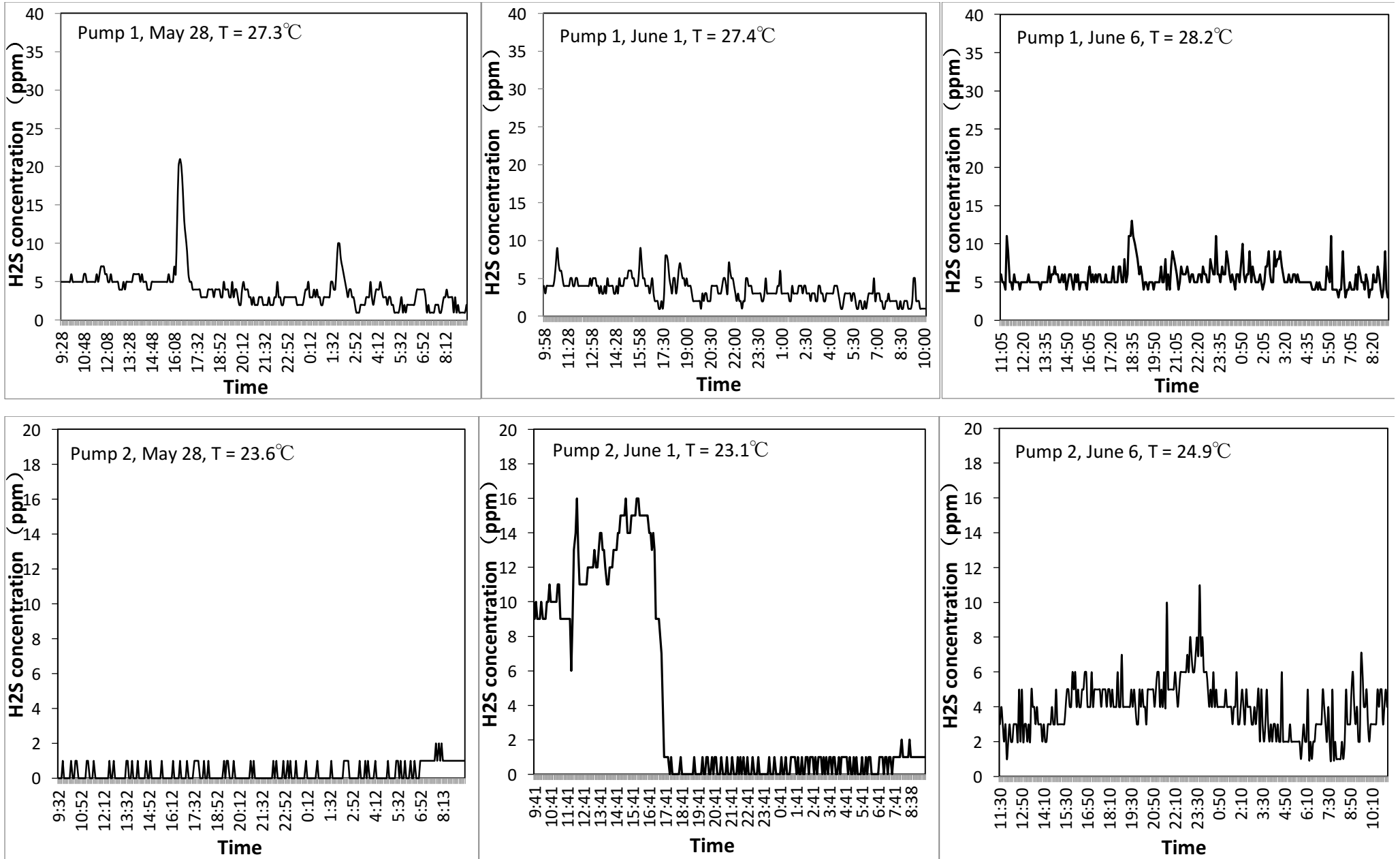


Figure 6.12, Hydrogen sulfide gas concentrations at the two pumping stations.

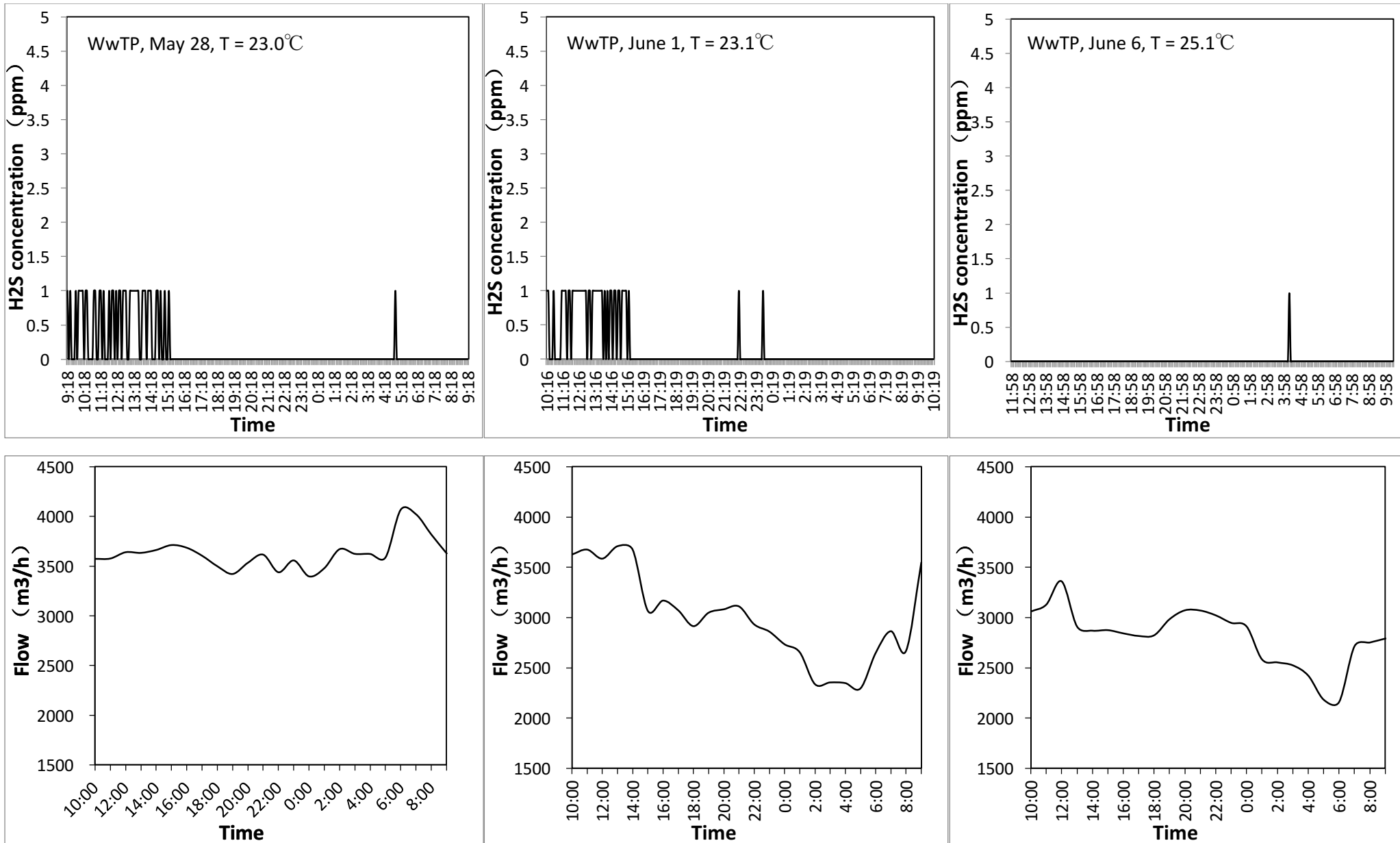


Figure 6.13, Hydrogen sulfide concentrations at the wastewater treatment plant and the flow rates.

6.3.2.2 Methane concentrations in the pumping-rising main systems

The methane gas concentrations in the pumping stations and the wastewater treatment plant were also recorded by the methane gas sensors. Figure 6.14 shows the variation of methane gas concentrations at the two pumping stations. There was no particular variation trend of methane concentrations in the three days. For instance, the methane concentration in pump 1 had a steady decreasing on 28th May, while it was increasing on 6th June. It is noticeable that the methane concentration (volume percentage) in pump 2 exceeded explosion limits on 1st June again. The methane concentration started to build up in the morning and exceeded the methane sensor maximum reading value 5% from 11 am to 5 pm. Pump 1 and pump 2 all showed higher methane concentrations than hydrogen sulfide concentration for three days, and pump 2 also reached critical condition on 1st June.

Figure 6.15 shows the variation of methane gas concentrations in the wastewater treatment plant. The methane gas concentrations in the inlet tank were relatively high even with submerged rising main outlets and steady flow condition compared to the hydrogen sulfide concentration which was very low. The methane concentration on 1st June had a sudden peak for roughly 1.5 hours, this might result from the methane built up from the upstream of rising main 2. To sum up, the hydrogen sulfide and methane gas concentration monitoring results indicated that both hydrogen sulfide and methane gas was detected at the pumping-rising main system. And the methane concentration was higher than the hydrogen sulfide which needs to take more concern on solving the methane problems for sewer system management.

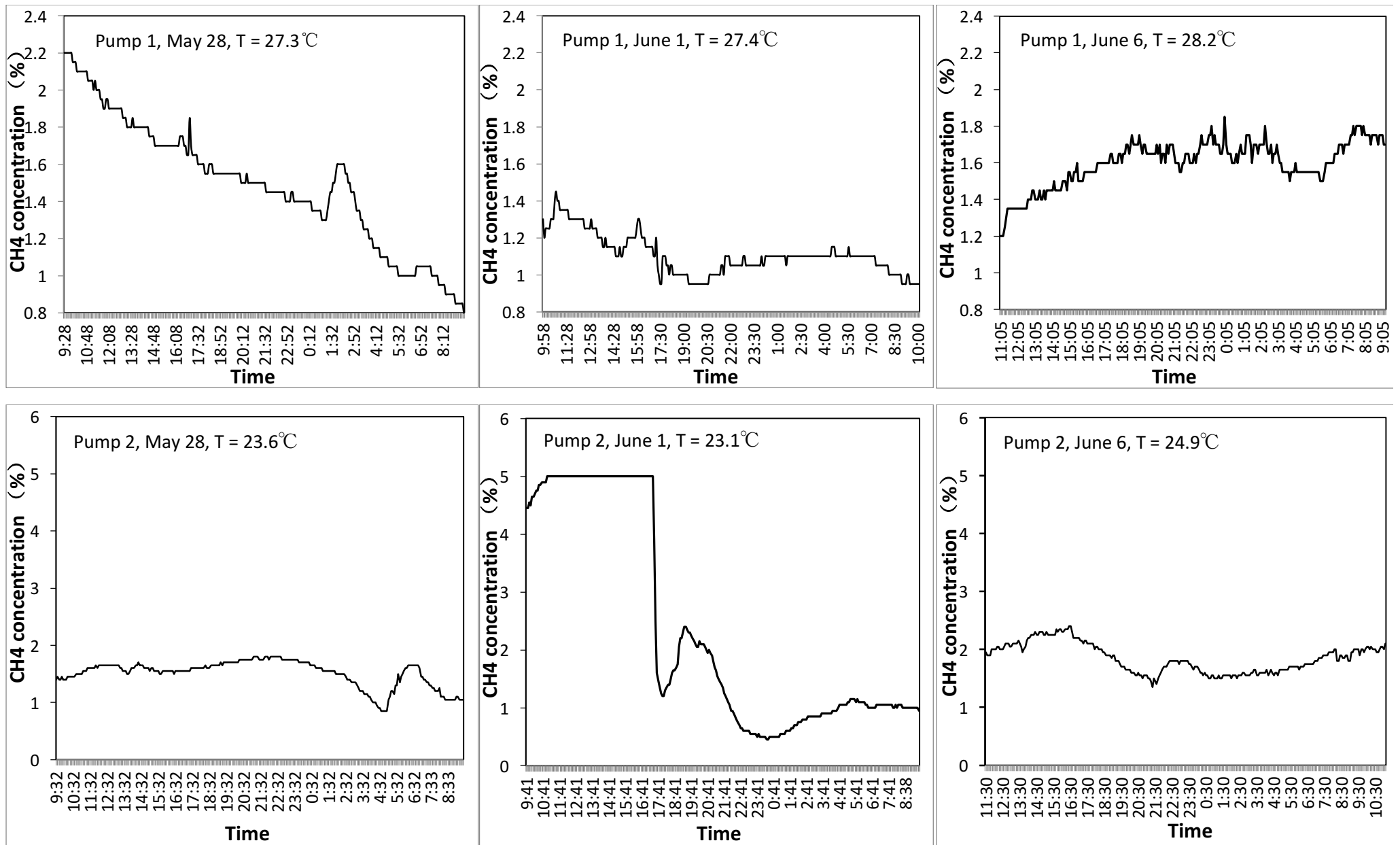


Figure 6.14, Methane gas concentrations in the two pumping stations.

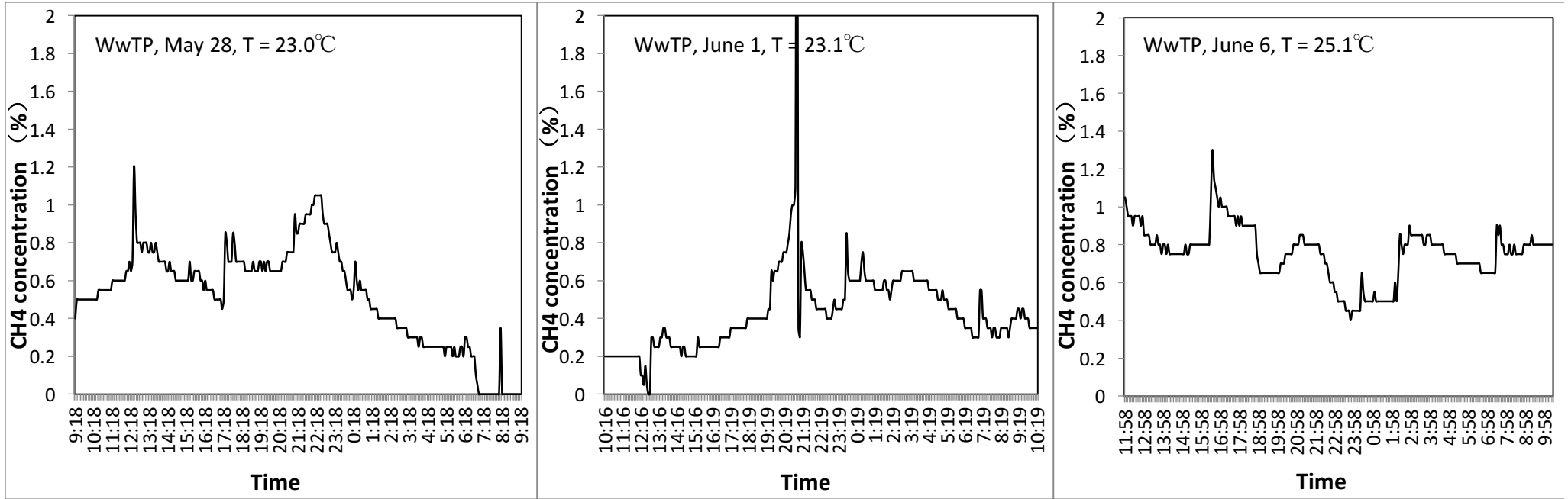


Figure 6.15, Methane gas concentrations at the wastewater treatment plant.

6.3.3 Modelling approach results on the gravity sewer pipe

The methane formation in the gravity sewer in SeweX model was shown in Figure 6.16:

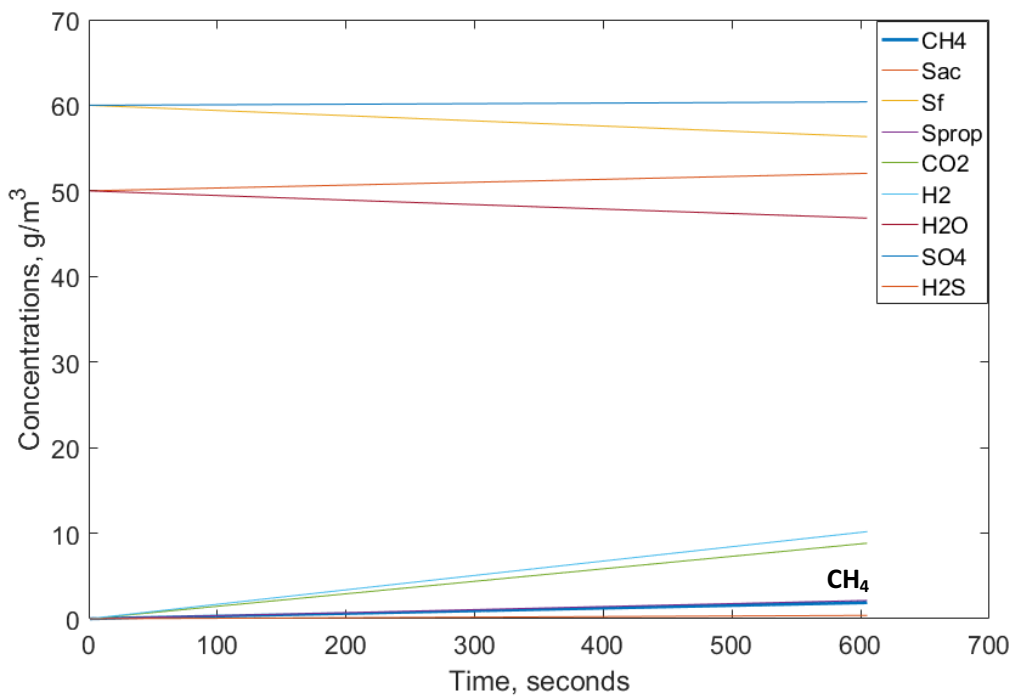


Figure 6.16, change of COD fractions in the gravity sewer pipe within 10 minutes.

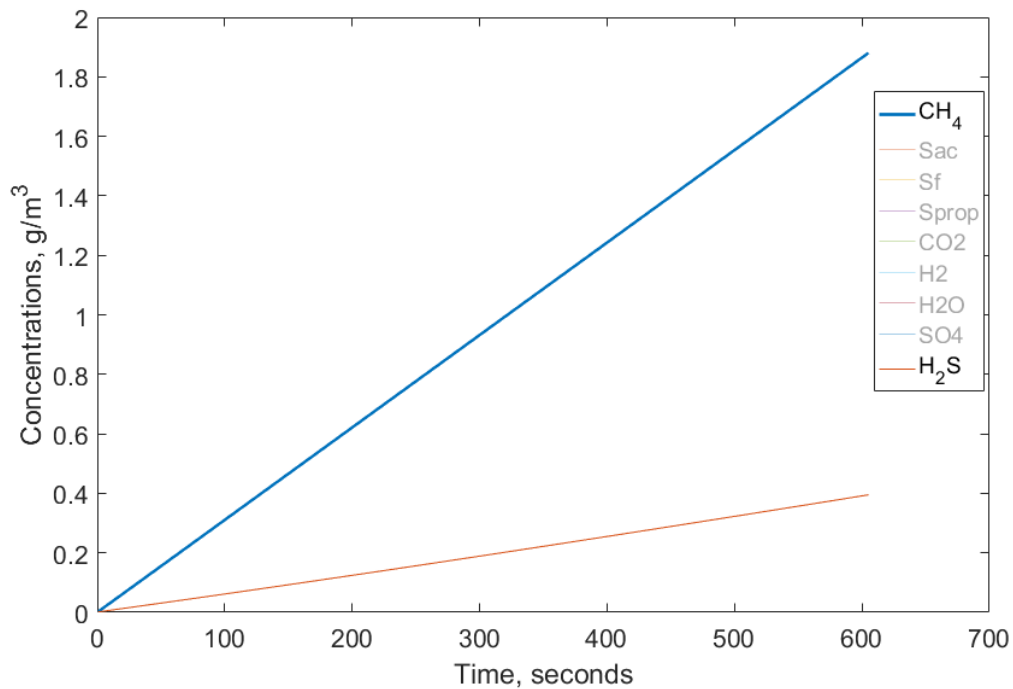


Figure 6.17, change of methane concentration in the gravity sewer pipe within 10 minutes.

Figure 6.16 and 6.17 illustrates the change of COD fractions and methane concentration in the gravity sewer within 10 minutes of residence time transformations. Methane concentration reached 1.8 mg/L after 10 minutes transformations. The model results indicated that if the methane concentration was 1.28 mg/L in the water phase, the initial wastewater COD concentration before the 10 minutes would be lower than 597.2 mg/L at manhole 3. Figure 6.16 shows the wastewater COD variations at the downstream main trunk sewer.

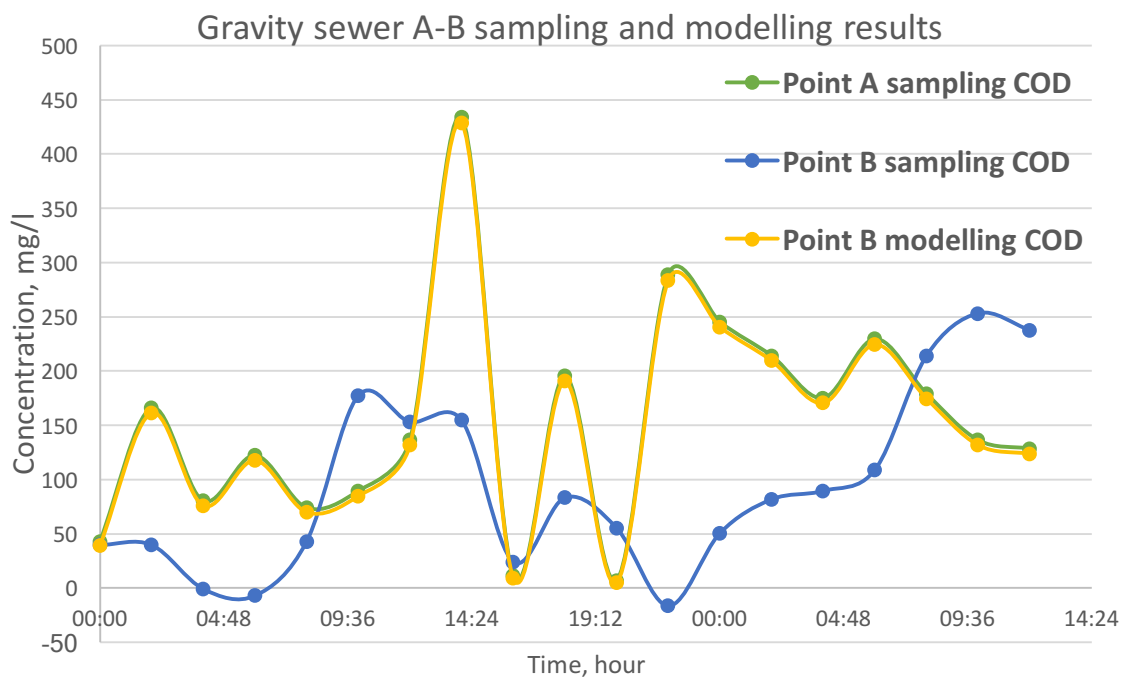


Figure 6.18, Sampling data of wastewater COD in the main trunk sewer pipe.

Figure 6.18 was the sampling data from the Chinese collaborators in Tsinghua University. Point A and B were both located on the main trunk sewer approximately 500 m downstream the sub-catchment. It can be seen that the total COD fluctuated in a day roughly between 50 to 450 mg/L. The fluctuation and variation were uncertain due to the unknown side connections between the sampling points. However, it can be used to compare the model simulation results for the upstream gravity sewer system, where the total COD was calculated to be lower than 597mg/L by model simulation. Although the comparison could not be specifically made between model results and the downstream sampling data. However, the model simulation results reflected the total COD range was closed to the COD measurements closed by, which means the high gas phase methane concentration was possible either

according to the model simulation or the sensor detection. It also needs to bring this back to the consideration by the operator that the methane build up was probably caused by downstream blockages, which means a septic tank, storage/buffer tank is also potential methane sources. Finally, a full comparison and conclusion can only be made with water phase parameters has been measured for future work.

6.4 Conclusions and Future Work

The field measurements of gas phase hydrogen sulfide and methane concentrations in the selected gravity sewer and rising main systems showed high hydrogen sulfide and methane concentrations in the systems. The hydrogen sulfide gas concentrations in the gravity sewer system ranged from 200 – 300 ppm during night periods, while the sulfide concentration in the rising main system was relatively low. High methane gas concentration was spotted at both the gravity sewer and rising main system. The methane gas was easily built up in the systems and exceeded 5% volume percentage which is the explosion limits. Methane concentration over 5% was recorded in the pump 2 wet well and even in the manhole 5 on the gravity sewer with full flow. The three days field gas monitoring indicated that the Chinese sewer system is high methane productive, which explains why so many methane induced sewer explosions occurring each year. Hence, the control and management of methane and its related problems will be the main objective when dealing with Chinese sewer systems. Investigations are still carrying on to understand why the Chinese sewer system is high methane productive. Septic tanks could be a major source as high methane production has been measured in the US septic tanks. Sewer pipes could also be a significant source as the Australian sewer pipes indicate high methane formation rate. Future work has also been proposed to look at if there would be any difference on the bacteria species in wastewater in different sewer systems in the world. The original source differences in different countries could also be a potential factor.

The characteristics of the selected gravity sewer system were typical in the Chinese catchments which represent surcharged full flow and in both high hydrogen sulfide and methane build up in the systems. The selection of the two large rising mains with large

pumping stations was to avoid those small pumping stations and rising mains with insufficient pump efficiency and partial full-flow in the rising main pipes. However, it was unexpected the outlet of the rising mains was submerged in the inlet tank in the wastewater treatment plant during the measuring days. The inlet tank pond was also well ventilated. That is why low hydrogen sulfide and methane concentrations were detected at the end of the rising mains. The field measurements of gas monitoring were good in figuring out and understanding the current problems and conditions of the systems. It was also a good start to conduct the following work. However, gas phase concentrations could not reflect the exact concentrations in the water phase at the measuring locations, because the ventilation and air space movement were complex in the sewer systems. Thus, wastewater samples measurements will be essential for further understanding of the processes in the systems.

The sewer processed models such as the WATS and SeweX model and the anaerobic digestion model ADM1 was developed based on the European and Australian sewer conditions. The characteristics of wastewater and local sewer and climate conditions vary a lot in different countries and regions. Hence, in order to apply the sewer processes models in the Chinese sewer system, model parameters such as/especially the COD fractions, temperature coefficient, formation rate coefficients should be adjusted to meet the Chinese sewer conditions. Good information on the hydraulics of the network is also needed in order to make a good estimate of transport. The analysis of wastewater samples is very important for model calibration and validation. Parameters such as the total COD and COD fractions are essential for starting a model simulation. The measurements of COD fractions can be achieved by using the OUR testing methods. Other parameters such as sulfate and organic matter are also important. It was already proposed to test the water phase hydrogen sulfide and methane concentration by using Gas Chromatography for the following work. A couple of rising mains with different diameter but the similar length is also being selected to test the influence of hydraulic condition and pipe dimension on the formation of hydrogen sulfide and methane in rising mains as discussed in Chapter 3. The related future work is being continuously proposing and implementing In China with Tsinghua University.

Chapter 7, Conclusions

The purpose of sewer process models is to help describe and manage real sewer systems. Process models can help predicting the specific and detailed locations and sewer conditions before taking actions and applying strategies. From the model studies in this thesis, it can be seen that for small scale system modelling, for example, the rising mains in Chapter 3, models can provide more accurate and precise results, but these models also require more detailed field measurements for model validation. For larger scale systems such as a large catchment or a city, model construction can be based on previous database, detailed field measurement is not necessary. Models can be used to predict hot spots such as high hydrogen sulfide and methane concentration locations. If field tests support it, the model results are reliable and can be trusted. Then the models can be used to larger scale systems to find out potential hot spots and problems instead of massive manual work of testing and measuring all around the locations.

The studies in chapter 3 provide a solution of integrating sewer hydraulic models with sewer process models. It indicates the importance of not only considering sewer hydraulic performance, but also sewer processes for the design of sewer systems. The models investigated the effect of pipe diameter, pumping settings, and COD availability on the formation of hydrogen sulfide in rising mains, which is the effect of A/V ratio, HRT and biofilm processes on sulfide formation. The model application can be potentially used to select optimal pipe diameter, pump operations and optimised chemical dosage for the downstream. The model results show that the effect of pipe diameter on sewer processes is very limited for small pipes. However, the effect is more significant for larger pipes in terms of total hydrogen sulfide production. It is also noticeable that different process models can result in very different model results. Hence, local model validation is very important when using a model at a new location. And the most important criteria is that the “self-cleaning” velocity should always be respected when designing sewer systems.

Global sensitivity analysis is very important to identify the most sensitive model parameters. Previous studies have discovered total COD as one of the most sensitive model parameters, however, the influence of individual COD fractions has not been investigated. The model

studies in Chapter 4 summarised the model sensitivity analysis on selected available WATS process model parameters, model results showed that the heterotrophic biomass, readily biodegradable substrates, and the fast hydrolysable substrates are the most sensitive COD fractions in terms of wastewater biochemical transformations and sulfide formation. Long term wastewater sampling in a WWTP in the UK showed a trend of increasing COD and decreasing flow rate. This could result from the increasing of inhabitants, reduced water consumption, and also the introduction of SUDS in the system.

Methane in sewer systems has aroused more concern in recent years as its GHG emission effect and explosive characteristics. Septic tanks have been proven to be a major source for methane production, however, very limited literature has been found in the area of sewer septic tank studies. By using the IWA ADM model on the septic tank is a first approach for simulating methane formation in Chapter 5. Septic tanks used in China are very different from Europe and US. They are integrated with the sewer systems as pre-treatment facilities. This study provides a new solution by using ADM and Sewer process models to simulate methane formation in both septic tanks and sewer pipes. Model study results indicate that significant methane production can occur in septic tanks, which means it is important to look at septic tanks as well as sewer pipes for the methane formation processes.

Methane is a serious concern in China as hundreds of explosions caused by it every year. The sewer processes models were used to the Chinese sewer systems in Chapter 6 even without validation and field data back-up, however, the model results can still explain some current existing problems in the system. The gas phase monitoring in the gravity system and the rising mains showed significant methane concentration and relatively moderate hydrogen sulfide concentration, which indicates the Chinese sewer system is certainly high methane productive. This provides a novel research area to look at methane formation in sewer systems in China. Future work has been proposed to investigate potential factors for the high methane productive Chinese sewer system such as the difference between bacteria species, methane oxidation and degradation in sewers, and the difference of original waste sources in different countries.

Publications

Conference Papers/Presentations

Moran Wang, W Shepherd, Rachel Smith, Henriette Jensen. “The effect of pipe diameter on hydrogen sulfide build-up in rising mains – model study”. 10th International Urban Drainage Conference. V II, pp 39-48. Quebec, Canada. September 2015.

Christian Akpan, Moran Wang, Catherine Biggs, Henriette Jensen. “Competition between anoxic hydrogen sulfide oxidation and the denitrification processes in wastewater”. 8th International Conference on Sewer Processes and Networks. Rotterdam, The Netherlands. August, 2016.

Appendices

Appendix A: Typical values for selected parameters in WATS model

Parameters	Description	Typical Value
X_{HW}	Heterotrophic active biomass in the water phase	20-100
X_{Hf}	Heterotrophic active biomass in the biofilm	~10
X_{S1}	Hydrolysable substrate, fast biodegradable	50-100
X_{S2}	Hydrolysable substrate, slowly biodegradable	300-450
S_F	Fermentable substrate	0-40
S_A	Fermentable products (i.e. VFAs)	0-20
S_S	Readily biodegradable substrates ($S_F + S_A$)	0-40
S_O	Dissolved oxygen	0-4
COD	Total COD	About 600
S_{H_2S}	Total sulfide	0-5
α_w	Temperature coefficient for heterotrophic, aerobic water phase processes	1.07
α_f	Temperature coefficient for aerobic biofilm processes	1.05
α_r	Temperature coefficient for reaeration	1.024
α_{sf}	Temperature coefficient for sulfide formation in the biofilm	1.03
μ_{HW,O_2}	Maximum specific aerobic growth rate for heterotrophic biomass in the water phase (day^{-1})	4-8
μ_{HW,NO_3}	Maximum specific anoxic growth rate for heterotrophic biomass in the water phase (day^{-1})	2-6
ϵ_f	Relative efficiency constant for hydrolysis of the biofilm biomass	01-02
k_{h1}	Hydrolysis rate constant, fraction 1 (fast) (day^{-1})	5
k_{h2}	Hydrolysis rate constant, fraction 1 (slow) (day^{-1})	0.5
K_O	Saturation constant for DO ($\text{g O}_2 \text{ m}^{-3}$)	0.01-0.5
K_{NO_3}	Saturation constant for nitrate (g N m^{-3})	0.5-1.0
K_{Sw}	Saturation constant for readily biodegradable substrates in the water phase (g COD m^{-3})	0.5-2.0
K_{X1}	Saturation constant for hydrolysis, fraction 1 (fast) ($\text{g COD (g COD)}^{-1}$)	1.5
K_{X2}	Saturation constant for hydrolysis, fraction 1 (fast) ($\text{g COD (g COD)}^{-1}$)	0.5
q_{m,O_2}	Maintenance energy requirement rate constant for aerobic respiration in the water phase (day^{-1})	0.5-1.0
Y_{HW,O_2}	Yield constant for aerobic growth of heterotrophic biomass in the water phase ($\text{g COD (g COD)}^{-1}$)	0.50-0.60
Y_{HW,NO_3}	Yield constant for anoxic growth of heterotrophic biomass in the water phase ($\text{g COD (g COD)}^{-1}$)	0.30-0.40
Y_{Hf,O_2}	Yield constant for aerobic growth of heterotrophic biomass in the biofilm ($\text{g COD (g COD)}^{-1}$)	0.50-0.60

Appendix B: Typical values for selected parameters in SeweX model

Parameters	Description	Value
q_{ACETOG}	Acetogenesis rate coefficient	12.2 ± 0.96
q_{ACIDOG}	Acidogenesis rate coefficient	2.14 ± 1.08
k_{H_2S,H_2}	Hydrogenotrophic sulfidogenesis rate coefficient	< 0.001
$k_{H_2S,AC}$	Acetate-based sulfidogenesis rate coefficient	1.36 ± 0.16
$k_{H_2S,PROP}$	Propionate-based sulfidogenesis rate coefficient	0.90 ± 0.41
k_{CH_4,H_2}	Hydrogenotrophic methanogenesis rate coefficient	1.92 ± 0.52
$k_{CH_4,AC}$	Acetoclastic methanogenesis rate coefficient	4.44 ± 0.30
K_F	Saturation constant for fermentable substrates	10
$K_{H_2,SRB}$	Saturation constant for hydrogen in Hydrogenotrophic sulfidogenesis	0.01
$K_{AC,SRB}$	Saturation constant for acetate in Acetate-based sulfidogenesis	5
K_{PROP}	Saturation constant for propionate	5
K_{SO_4}	Saturation constant for sulfate	1.8
$K_{SAC,MA}$	Saturation constant for acetate in acetoclastic methanogenesis	1
$K_{H_2,MA}$	Saturation constant for hydrogen in Hydrogenotrophic methanogenesis	0.002

Appendix C: Suggested values for selected parameters in ADM 1 model

Parameter	Mesophilic High-rate (35°C)	Mesophilic Solids (35°C)	Thermophilic Solids (55°C)
$K_{dis}(d^{-1})$	0.4	0.5	1.0
$K_{hyd_CH}(d^{-1})$	0.25	10	10
$K_{hyd_PR}(d^{-1})$	0.2	10	10
$K_{hyd_LI}(d^{-1})$	0.1	10	10
$t_{res,X}(d)$	40	0	0
$K_{dec_all}(d^{-1})$	0.02	0.02	0.04
$K_{S_NH3_all}(M)$	1×10^{-4}	1×10^{-4}	1×10^{-4}
$pH_{UL\ acet/acid}$	5.5	5.5	5.5
$pH_{LL\ acet/acid}$	4	4	4
$k_{m_su}(COD\ COD^{-1}d^{-1})$	30	30	70
$K_{S_su}(kgCOD\ m^{-3})$	0.5	0.5	0.5
$Y_{su}(COD\ COD^{-1})$	0.10	0.10	0.10
$k_{m_aa}(COD\ COD^{-1}d^{-1})$	50	50	70
$K_{S_aa}(kgCOD\ m^{-3})$	0.3	0.3	0.3
$Y_{aa}(COD\ COD^{-1})$	0.08	0.08	0.08
$k_{m_fa}(COD\ COD^{-1}d^{-1})$	6	6	10
$K_{S_fa}(kgCOD\ m^{-3})$	0.4	0.4	0.4
$Y_{fa}(COD\ COD^{-1})$	0.06	0.06	0.06
$K_{I,H2_fa}(kgCOD\ m^{-3})$	5×10^{-6}	5×10^{-6}	n/a
$k_{m_c4+}(COD\ COD^{-1}d^{-1})$	20	20	30
$K_{S_c4+}(kgCOD\ m^{-3})$	0.3	0.2	0.4
$Y_{c4+}(COD\ COD^{-1})$	0.06	0.06	0.06
$K_{I,H2_c4+}(kgCOD\ m^{-3})$	1×10^{-5}	1×10^{-5}	3×10^{-5}
$k_{m_pro}(COD\ COD^{-1}d^{-1})$	13	13	20
$K_{S_pro}(kgCOD\ m^{-3})$	0.3	0.1	0.3
$Y_{pro}(COD\ COD^{-1})$	0.04	0.04	0.05
$K_{I,H2_pro}(kgCOD\ m^{-3})$	3.5×10^{-6}	3.5×10^{-6}	1×10^{-5}
$k_{m_ac}(COD\ COD^{-1}d^{-1})$	8	8	16
$K_{S_ac}(kgCOD\ m^{-3})$	0.15	0.15	0.3
$Y_{ac}(COD\ COD^{-1})$	0.05	0.05	0.05
$pH_{UL\ ac}$	7	7	7
$pH_{LL\ ac}$	6	6	6
$K_{I,NH3}(m)$	0.0018	0.0018	0.0011
$k_{m_h2}(COD\ COD^{-1}d^{-1})$	35	35	35
$K_{S_h2}(kgCOD\ m^{-3})$	2.5×10^{-5}	7×10^{-5}	5×10^{-5}
$Y_{h2}(COD\ COD^{-1})$	0.06	0.06	0.06
$pH_{UL\ h2}$	6	6	6
$pH_{LL\ h2}$	5	5	5

Appendix D: Suggested stoichiometric parameters in ADM 1 model

Parameters	Description	Value
$f_{sl,xc}$	Soluble inerts from composites	0.1
$f_{xl,xc}$	Particulate inerts from composites	0.25
$f_{ch,xc}$	Carbohydrates from composites	0.20
$f_{pr,xc}$	Proteins from composites	0.20
$f_{li,xc}$	Lipids from composites	0.25
N_{xc}, N_I	Nitrogen content of composites and inerts	0.002
$f_{fa,li}$	Fatty acids from lipids	0.95
$f_{h2,su}$	Hydrogen from sugars	0.19
$f_{bu,su}$	Butyrate from sugars	0.13
$f_{pro,su}$	Propionate from sugars	0.27
$f_{ac,su}$	Acetate from sugars	0.41
$f_{h2,aa}$	Hydrogen from amino acids	0.06
N_{aa}	Nitrogen in amino acids and proteins	0.007
$f_{va,aa}$	Valerate from amino acids	0.23
$f_{bu,aa}$	Butyrate from amino acids	0.26
$f_{pro,aa}$	Propionate from amino acids	0.05
$f_{ac,aa}$	Acetate from amino acids	0.40

Appendix E: Matlab script for modelling the operation of pumping stations

```
clc;
clear;
close all;

Flow_Data = xlsread('Flow_Aver.xlsx'); % Read Excel into Matlab

V_water = 0.3;
T_start = [];
T_stop = [];
flag = 0;
Flags = [];
V_waters = [];
for ii = 1:length(Flow_Data)
    if flag == 0;
        if V_water >= 1.175
            flag = 1;
            V_water = V_water + Flow_Data(ii,2)*1e-3 - 9.72*1e-3;
            T_start = [T_start; ii];
        else
            V_water = V_water + Flow_Data(ii,2)*1e-3;
        end
    end

    if flag == 1;
        if V_water <= 0.3
            flag = 0;
            V_water = V_water + Flow_Data(ii,2)*1e-3;
            T_stop = [T_stop; ii];
        else
            V_water = V_water + Flow_Data(ii,2)*1e-3 - 9.72*1e-3;
        end
    end
    Flags = [Flags; flag];
    V_waters = [V_waters; V_water];
end

figure
stairs(Flags)
xlim([0 1500])
ylim([-0.1, 1.1])
TT_start = datestr(Flow_Data(T_start,1), 'HH:MM:SS');
TT_stop = datestr(Flow_Data(T_stop,1), 'HH:MM:SS');
figure;
plot(V_waters)
```

Appendix F: Matlab script of WATS model for rising main and gravity sewers

```

clc;clear;close all;

% Import Constants from Constants_Aerobic
Constants_Aerobic

dt = 1/(60*60*24);
Results = [];
for t0 = 0:dt:0.1*(60*60*24)
    rgrw = uHO2*(Ss)/(KSw+Ss)*SO/(KO+SO)*XHw*aw^(Temp-20);
    rgrf = k*SO^0.5*Yhf/(1-Yhf)*(Ss)/(Ksf+Ss)*AV*af*(Temp-20);
    rmaint = qm*SO/(KO+SO)*XHw*aw^(Temp-20);
    rhydr1 = kh1*(Xs1/XHw)/(KX1+(Xs1/XHw))*SO/(KO+SO)*(XHw+e*XHf*AV)*aw^(Temp-20);
    rhydr2 = kh2*(Xs2/XHw)/(KX2+(Xs2/XHw))*SO/(KO+SO)*(XHw+e*XHf*AV)*aw^(Temp-20);
    XHf = XHf+dt*rgrf;
    Xs1 = Xs1+dt*(-rhydr1);
    Xs2 = Xs2+dt*(-rhydr2);
    SO = SO-dt*(((1-Yhw)/Yhw)*rgrw)+((1-Yhf)/Yhf)*rgrf+rmaint);
    if Ss >= rmaint
        XHw = XHw+dt*(rgrw);
        Ss = Ss+dt*(((1-Yhw)*rgrw)+((1-Yhf)*rgrf)-rmaint+rhydr1+rhydr2);
    else
        XHw = XHw+dt*(rgrw-rmaint);
        Ss = Ss+dt*(((1-Yhw)*rgrw)+((1-Yhf)*rgrf)+rhydr1+rhydr2);
    end
    Results = [Results;t0 rgrw rmaint rgrf rhydr1 rhydr2 XHw Ss Xs1 Xs2 SO]];
    if SO <=0;
        SF = Ss*2/3;
        SA = Ss - SF;
        t1=t0;
        Constants_Aerobic2
        Constants_Sulfur_Cycle

dt = 1/(60*60*24);
Results2 = [];
R_aa = [];
for t = t1:dt:(t1+10/24)*(60*60*24)
    rferm = qferm*(SF/(kferm+SF))*(KO/(KO+SO))*(XHw+e*XHf*AV)*a^(Temp-20);
    rhydranal = Nhana*kh1*(Xs1/XHw)/(KX1+(Xs1/XHw))*(KO/(KO+SO))*(XHw+e*XHf*AV)*a^(Temp-20);
    rhydrana2 = Nhana*kh2*(Xs2/XHw)/(KX2+(Xs2/XHw))*(KO/(KO+SO))*(XHw+e*XHf*AV)*a^(Temp-20);
    rd = dHana*(KO/(KO+SO))*XHw*a^(Temp-20);
    XHw = XHw+dt*(-rferm);
    SF = SF+dt*(rhydranal+rhydrana2-rd);
    SA = SA+dt*rd;
    Xs1 = Xs1+dt*(-rhydranal);
    Xs2 = Xs2+dt*(rferm-rhydrana2);
    % sulfur cycle anaerobic part
    ra = aa*((SF+SA+Xs1)^0.5)*(KO/(KO+SO))*AV*a^(Temp-20);
    S_II = S_II+dt*ra;
    SSO4 = SSO4 + dt*(-ra);
    R_aa = [R_aa ; [t ra S_II SSO4]];
    Results2 = [Results2;t rferm rhydranal rhydrana2 rd XHw SF+SA Xs1 Xs2 0 SF SA ra S_II
SSO4]];
end
    break
end
end
RH2Send = R_aa(:, [1 3]);

L = (length(Results)+length(Results2)+length(Results3));
R_all = [(0:L-1)*dt [Results(:,7:11);Results2(:,6:10);Results3(:,7:11)]];

figure
plot(R_all(:,1),R_all(:,2),R_all(:,1),R_all(:,3),R_all(:,1),R_all(:,4),R_all(:,1),R_all(:,5),R_all(:,1),R_all(:,6));

```

Appendix G: Matlab script of SeweX model for rising main and gravity sewers

```

clc;clear;close all;

% Import Constants from Constants_Aerobic
Constants_Aerobic

dt = 1/(60*60*24);
Results = [];
for t0 = 0:dt:0.1*(60*60*24)
    rgrw = uHO2*(Ss)/(KSw+Ss)*SO/(KO+SO)*XHw*aw^(Temp-20);
    rgrf = k*SO^0.5*Yhf/(1-Yhf)*(Ss)/(Ksf+Ss)*AV*af*(Temp-20);
    rmaint = qm*SO/(KO+SO)*XHw*aw^(Temp-20);
    rhydr1 = kh1*(Xs1/XHw)/(KX1+(Xs1/XHw))*SO/(KO+SO)*(XHw+e*XHf*AV)*aw^(Temp-20);
    rhydr2 = kh2*(Xs2/XHw)/(KX2+(Xs2/XHw))*SO/(KO+SO)*(XHw+e*XHf*AV)*aw^(Temp-20);
    XHf = XHf+dt*rgrf;
    Xs1 = Xs1+dt*(-rhydr1);
    Xs2 = Xs2+dt*(-rhydr2);
    SO = SO-dt*((1-Yhw)/Yhw)*rgrw+((1-Yhf)/Yhf)*rgrf+rmaint);
    if Ss >= rmaint
        XHw = XHw+dt*(rgrw);
        Ss = Ss+dt*((-1/Yhw)*rgrw+((-1/Yhf)*rgrf)-rmaint+rhydr1+rhydr2);
    else
        XHw = XHw+dt*(rgrw-rmaint);
        Ss = Ss+dt*((-1/Yhw)*rgrw+((-1/Yhf)*rgrf)+rhydr1+rhydr2);
    end
    Results = [Results;t0 rgrw rmaint rgrf rhydr1 rhydr2 XHw Ss Xs1 Xs2 SO]];
    if SO <=0;
        SF = Ss^2/3;
        SA = Ss - SF;
        t1=t0;
        Constants_Aerobic2
        Constants_Sulfur_Cycle

    dt = 1/(60*60*24);
    Results2 = [];
    R_aa = [];

    for t = t1:dt:(t1+10/24)*(60*60*24)
        rferm = qferm*(SF/(kferm+SF))*(KO/(KO+SO))*(XHw+e*XHf*AV)*a^(Temp-20);
        rhydranal = Nhana*kh1*(Xs1/XHw)/(KX1+(Xs1/XHw))*(KO/(KO+SO))*(XHw+e*XHf*AV)*a^(Temp-20);
        rhydrana2 = Nhana*kh2*(Xs2/XHw)/(KX2+(Xs2/XHw))*(KO/(KO+SO))*(XHw+e*XHf*AV)*a^(Temp-20);
        rd = dHana*(KO/(KO+SO))*XHw*a^(Temp-20);
        XHw = XHw+dt*(-rferm);
        SF = SF+dt*(rhydranal+rhydrana2-rd);
        SA = SA+dt*rd;
        Xs1 = Xs1+dt*(-rhydranal);
        Xs2 = Xs2+dt*(rferm-rhydrana2);

        % sulfur cycle anaerobic part SeweX sulfide rate equation
        ra = kH2S*((SF+SA)/(Ksf+SF+SA))*(SSO4/(KSO4+SSO4))*(KO/(KO+SO))*AV*(SF/(SF+SA));
        SSO4 = SSO4 + dt*(-ra);
        S_II = S_II+dt*ra;

        R_aa = [R_aa ; [t ra S_II SSO4]];

        Results2 = [Results2;t rferm rhydranal rhydrana2 rd XHw SF+SA Xs1 Xs2 0 SF SA ra S_II SSO4]];
    end
        break
    end
end
RH2Send = R_aa(:, [1 3]);

```

Appendix H: Matlab script of hydraulic and process model integration

```

clc;
clear;
close all;

% RRestime = [];
% RH2S = [];
% WATS_Pro;
% RH2S = [Results2(:,1) Results2(:,end-1)];

load('RH2S.mat')
Flow_Data = xlsread('Flow_Aver_7hb.xlsx'); % Read excel into Matlab

V_water = 0.3;
T_start = [];
T_stop = [];
flag = 0;
Flags = [];
V_waters = [];
FlagsEx = ones(4*60*60,1);
XT = [];
for ii = 1:length(Flow_Data)
    ii
    if flag == 0;
        if V_water >= 1.175
            flag = 1;
            V_water = V_water + Flow_Data(ii,2)*1e-3 - 9.72*1e-3;
            T_start = [T_start;ii];
        else
            V_water = V_water + Flow_Data(ii,2)*1e-3;
        end
    end

    if flag == 1;
        if V_water <= 0.3
            flag = 0;
            V_water = V_water + Flow_Data(ii,2)*1e-3;
            T_stop = [T_stop;ii];
        else
            V_water = V_water + Flow_Data(ii,2)*1e-3 - 9.72*1e-3;
        end
    end

    Flags = [Flags;flag];
    FlagsEx = [FlagsEx;flag];
    V_waters = [V_waters;V_water];

    T_one = 0; % pump start times
    T_zero = 0; % pump stop times

    kk = ii + 4*60*60;
    while T_one < (4*60*60);
        if FlagsEx(kk) == 1;
            T_one = T_one + 1;
        else
            T_zero = T_zero + 1;
        end
        kk = kk - 1;
        [kk ii]
    end
    XT = [XT;T_zero];

end

RH2Send = [];
for ii = 1:length(XT)

    RH2Send = [RH2Send;[Flow_Data(ii,1) RH2S(abs(RH2S(:,1) - XT(ii)/24/60/60 - 4/24) <
1.1574e-05,2)]];
end

```

Appendix I: Matlab script of SeweX model for methane formation

```
clc; clear; close all;

Parameters;

dt = 1/(60*60*24);
Results = [];

for t = 0:dt:0.1;

    R1 = kch4h2*(H2/(Kh2ma+H2))*AV*a;
    R2 = kch4ac*(Sac/(Kacma+Sac))*AV*a;
    R3 = qacetog*(Sf1/(Kf+Sf1))*AV*a;
    R4 = qacidog*(Sf1/(Kf+Sf1))*AV*a;
    R5 = kh2sh2*(H2/(Kh2srb+H2))*(SSO4/(Kso4+SSO4))*AV*a;
    R6 = kh2sac*(Sac/(Kacsrb+Sac))*(SSO4/(Kso4+SSO4))*AV*a;
    R7 = kh2sprop*(Sf2/(Kprop+Sf2))*(SSO4/(Kso4+SSO4))*AV*a;

    CH4 =CH4+dt*(R1+R2);
    Sac = Sac+dt*((-R2)+R3+R4+(-R6)+R7);
    Sf1 = Sf1+dt*((-R3)+(-R4));
    Sf2 = Sf2+dt*((4*R4)+(-R7));
    CO2 = CO2+dt*((-R1)+R2+(2*R3)+(2*R4)+(2*R6)+R7);
    H2 = H2+dt*((-4*R1)+4*R3+(-4*R5));
    H2O = H2O+dt*((2*R1)+(-2*R3)+(2*R4)+(4*R5)+(2*R6)+(2*R7));
    SSO4 =SSO4+dt*(-R5+R6+(0.75*R7));
    H2S = H2S+dt*(R5+R6+(0.75*R7));

    Results = [Results;[t CH4 Sac Sf1 Sf2 CO2 H2 H2O SSO4 H2S]];
end
```

Appendix J: Matlab script of ADM 1 model for methane formation

```

%% Anaerobic Digestion Model
%% ADM 1 on septic tank processes
clc;clear;close all;

Constants_ADM1
% Constants_ADM1_2

dt = 60/(60*60*24);
Results = [];
flag = 0;
for t = 0:dt:10
%     if abs(t - 1/24*flag)<=1e-5
%     Xch = (10*Xch+1.6221)/11;
%     Xpr = (10*Xpr+1.6221)/11;
%     Xli = (10*Xli+1.6221)/11;
%     flag = flag+1
    if abs(t - 1/24*flag)<=1e-5
        Xch = 0.16221;
        Xpr = 0.16221;
        Xli = 0.16221;
        flag = flag+1;
    end
% Rates
Rdis = Kdis*Xc;
Rhydcar = Khydch*Xch;
Rhydpr = Khydpr*Xpr;
Rhydli = Khydli*Xli;
Rpsu = KMsu*(Ssu/(KSsu+Ssu))*Xsu*(Ssu/(Ssu+0.33));
Rupaa = KMa*(Saa/(KSaa+Saa))*Xaa*(Saa/(Saa+0.33));
Rupfa = KMfa*(Sfa/(KSfa+Sfa))*Xfa*I2;
Rupva = KMc4*(Sva/(KSva+Sva))*Xc4*(1/(1+(Sbu/Sva)))*(Sva/(Sva+0.33));
Rupbu = KMc4*(Sbu/(KSbu+Sbu))*Xc4*(1/(1+(Sva/Sbu)))*(Sbu/(Sbu+0.33));
Ruppro = KMpr*(Spro/(KSpro+Spro))*Xpro*I2;
Rupac = KMac*(Sac/(KSac+Sac))*Xac*I3;
Ruph2 = KMh2*(Sh2/(KSh2+Sh2))*Xh2*(Sh2/(Sh2+0.33));
RdeXsu = Kdec*Xsu;
RdeXaa = Kdec*Xaa;
RdeXfa = Kdec*Xfa;
RdeXc4 = Kdec*Xc4;
RdeXpro = Kdec*Xpro;
RdeXac = Kdec*Xac;
RdeXh2 = Kdec*Xh2;
% Contents concentrations
Ssu = Ssu+dt*(Rhydcar+((1-Ffali)*Rhydli)+(-1)*Rpsu);
Saa = Saa+dt*(Rhydpr+(-1)*Rupaa);
Sfa = Sfa+dt*((1-Ffali)*Rhydli+(-1)*Rupfa);
Sva = Sva+dt*((1-Yaa)*Fvaaa)*Rupaa+(-1)*Rupfa);
Sbu = Sbu+dt*((1-Ysu)*Fbusu)*Rpsu+((1-Yaa)*Fbuaa)*Rupaa+(-1)*Rupbu);
Spro = Spro+dt*((1-Ysu)*Fprosu)*Rpsu+((1-Yaa)*Fproaa)*Rupaa+(-1)*Ruppro);
Sac = Sac+dt*((1-Ysu)*Facsu)*Rpsu+((1-Yaa)*Faca)*Rupaa+((1-Yfa)*0.7)*Rupfa+((1-
Yc4)*0.31)*Rupva+((1-Yc4)*0.8)*Rupbu+((1-Ypro)*0.57)*Ruppro+(-1)*Rupac);
Sh2 = Sh2+dt*((1-Ysu)*Fh2su)*Rpsu+((1-Yaa)*Fh2aa)*Rupaa+((1-Yfa)*0.3)*Rupfa+((1-
Yc4)*0.15)*Rupva+((1-Yc4)*0.2)*Rupbu+((1-Ypro)*0.43)*Ruppro+(-1)*Ruph2);
Sch4 = Sch4+dt*((1-Yac)*Rupac+(1-Yh2)*Ruph2);
Xc = Xc+dt*((-1)*Rdis+RdeXsu+RdeXaa+RdeXfa+RdeXc4+RdeXpro+RdeXac+RdeXh2);
Xch = Xch+dt*(Fchxc*Rdis+(-1)*Rhydcar);
Xpr = Xpr+dt*(Fprxc*Rdis+(-1)*Rhydpr);
Xli = Xli+dt*(Flixlc*Rdis+(-1)*Rhydli);
Xsu = Xsu+dt*(Ysu*Rpsu+(-1)*RdeXsu);
Xaa = Xaa+dt*(Yaa*Rupaa+(-1)*RdeXaa);
Xfa = Xfa+dt*(Yfa*Rupfa+(-1)*RdeXfa);
Xc4 = Xc4+dt*(Yc4*Rupva+Yc4*Rupbu+(-1)*RdeXc4);
Xpro = Xpro+dt*(Ypro*Ruppro+(-1)*RdeXpro);
Xac = Xac+dt*(Yac*Rupac+(-1)*RdeXac);
Xh2 = Xh2+dt*(Yh2*Ruph2+(-1)*RdeXh2);

Results = [Results;t Ssu Saa Sfa Sva Sbu Spro Sac Sh2 Sch4 Xc Xch Xpr Xli Xsu Xaa Xfa
Xc4 Xpro Xac Xh2]];
end

```

References

- ABDUL-TALIB, S., HVITVED-JACOBSEN, T., VOLLERTSEN, J. & UJANG, Z. 2002a. Anoxic transformations of wastewater organic matter in sewers—process kinetics, model concept and wastewater treatment potential. *Water science and technology*, 45, 53-60.
- ABDUL-TALIB, S., HVITVED-JACOBSEN, T., VOLLERTSEN, J. & UJANG, Z. 2002b. Half saturation constants for nitrate and nitrite by in-sewer anoxic transformations of wastewater organic matter. *Water science and technology*, 46, 185-192.
- ABDUL-TALIB, S., UJANG, Z., VOLLERTSEN, J. & HVITVED-JACOBSEN, T. 2005. Model concept for nitrate and nitrite utilization during anoxic transformation in the bulk water phase of municipal wastewater under sewer conditions. *Water science and technology*, 52, 181-189.
- ALMEIDA, M., BUTLER, D. & DAVIES, J. 1999. Modelling in-sewer changes in wastewater quality under aerobic conditions. *Water science and technology*, 39, 63-71.
- ANDERSSON, K., ALLARD, B., BENGTSSON, M. & MAGNUSSON, B. 1989. Chemical composition of cement pore solutions. *Cement and Concrete Research*, 19, 327-332.
- ARTHUR, S. & ASHLEY, R. 1998. The influence of near bed solids transport on first foul flush in combined sewers. *Water Science and Technology*, 37, 131-138.
- ASHLEY, R. & CRABTREE, R. 1992. Sediment origins, deposition and build-up in combined sewer systems. *Water Science and Technology*, 25, 1-12.
- AUGUET, O., PIJUAN, M., BORREGO, C. M. & GUTIERREZ, O. 2016. Control of sulfide and methane production in anaerobic sewer systems by means of Downstream Nitrite Dosage. *Science of The Total Environment*, 550, 1116-1125.
- AUTHORITIES, W. 2013. Sewers for adoption- a design and construction guide for developers. *Water Research Centre(2013) plc. Medmenham, 7 rd edition, 2013.*
- BABAN, A. & TALINLI, I. 2009. Modeling of organic matter removal and nitrification in sewer systems—an approach to wastewater treatment. *Desalination*, 246, 640-647.
- BARCO, J., WONG, K. M. & STENSTROM, M. K. 2008. Automatic calibration of the US EPA SWMM model for a large urban catchment. *Journal of Hydraulic Engineering*, 134, 466-474.
- BARRERA, E. L., SPANJERS, H., SOLON, K., AMERLINCK, Y., NOPENS, I. & DEWULF, J. 2015. Modeling the anaerobic digestion of cane-molasses vinasse: extension of the Anaerobic Digestion Model No. 1 (ADM1) with sulfate reduction for a very high strength and sulfate rich wastewater. *Water research*, 71, 42-54.
- BASAVAI AH, K. & SOMASHEKAR, B. 2007. Quantitation of ranitidine in pharmaceuticals by titrimetry and spectrophotometry using potassium dichromate as the oxidimetric reagent. *Journal of the Iranian Chemical Society*, 4, 78-88.
- BASTVIKEN, D., EJLERTSSON, J. & TRANVIK, L. 2002. Measurement of methane oxidation in lakes: a comparison of methods. *Environmental science & technology*, 36, 3354-3361.
- BATSTONE, D., KELLER, J., ANGELIDAKI, I., KALYUZHNYI, S., PAVLOSTATHIS, S., ROZZI, A., SANDERS, W., SIEGRIST, H. & VAVILIN, V. 2002a. Anaerobic digestion model no. 1 (ADM1), IWA task group for mathematical modelling of anaerobic digestion processes. *London: IWA Publishing.*

- BATSTONE, D. J., KELLER, J., ANGELIDAKI, I., KALYUZHNYI, S., PAVLOSTATHIS, S., ROZZI, A., SANDERS, W., SIEGRIST, H. & VAVILIN, V. 2002b. The IWA anaerobic digestion model no 1 (ADM1). *Water Science and Technology*, 45, 65-73.
- BEGHI, S. P., SANTOS, J. M., REIS, N. C., DE SÁ, L. M., GOULART, E. V. & DE ABREU COSTA, E. 2012. Impact assessment of odours emitted by a wastewater treatment plant. *Water Science and Technology*, 66, 2223-2228.
- BLUMENSAAT, F. & KELLER, J. 2005. Modelling of two-stage anaerobic digestion using the IWA Anaerobic Digestion Model No. 1 (ADM1). *Water Research*, 39, 171-183.
- BOON, A. & LISTER, A. 1975. Formation of sulphide in rising main sewers and its prevention by injection of oxygen. *Prog. Wat. Tech*, 7, 289-300.
- BOON, A. G. 1995. Septicity in sewers: causes, consequences and containment. *Water Science and Technology*, 31, 237-253.
- BOON, A. G., VINCENT, A. J. & BOON, K. G. 1998. Avoiding the problems of septic sewage. *Water science and technology*, 37, 223-231.
- BOWKER, R., AUDIBERT, G., SHAH, H. & WEBSTER, N. 1992. Detection, control, and correction of hydrogen sulfide corrosion in existing wastewater systems. *Office of Wastewater Enforcement and Compliance, Office of Water, Washington, DC*.
- BRONGERS, M. 2002. Appendix K. Drinking water and sewer systems in corrosion costs and preventative strategies in the United States. *Rep. FHWA-RD-01*, 156.
- BURLINGAME, G. A. 1999. Odor profiling of environmental odors. *Water science and technology*, 40, 31-38.
- BUTLER, D. & DAVIES, J. 2010. *Urban Drainage, Third Edition*, CRC Press.
- BUTLER, D. & PAYNE, J. 1995. Septic tanks: problems and practice. *Building and Environment*, 30, 419-425.
- CANTONE, J. P. & SCHMIDT, A. R. 2009. Potential dangers of simplifying combined sewer hydrologic/hydraulic models. *Journal of Hydrologic Engineering*, 14, 596-605.
- CHADWICK, A., MORFETT, J. & BORTHWICK, M. 2013. *Hydraulics in civil and environmental engineering*, Crc Press.
- CHE, W., WU, Y. & YANG, Z. 2015. 海绵城市建设指南解读之城市雨洪调蓄系统的合理构建 The guidance for the construction of sponge city and stormwater management system). *中国给水排水 (China Water Supply & Drainage)*, 31 (8), 13 - 23.
- CHENG, X., PETERKIN, E. & BURLINGAME, G. 2007. Study of the effect of DMSO on VOS odour production in a wastewater plant. *Water science and technology*, 55, 327-333.
- CIPOLLA, S. S. & MAGLIONICO, M. 2014. Heat recovery from urban wastewater: Analysis of the variability of flow rate and temperature. *Energy and Buildings*, 69, 122-130.
- COLLETT, A. N., MILLS, T. & WOLSTENHOLME, P. 2011. When "Green" Really Isn't Greenest: A Design Employing Inorganic Biofilter Media Restores Confidence and Advances Biofilter Technology, While Saving Cost and Energy. *Proceedings of the Water Environment Federation*, 2011, 597-611.
- CRITES, R. & TECHNOBANOGLOUS, G. 1998. *Small and decentralized wastewater management systems*, McGraw-Hill.
- CZEPIEL, P. M., CRILL, P. M. & HARRISS, R. C. 1993. Methane emissions from municipal wastewater treatment processes. *Environmental science & technology*, 27, 2472-2477.
- DAELMAN, M. R., VAN VOORTHUIZEN, E. M., VAN DONGEN, U. G., VOLCKE, E. I. & VAN LOOSDRECHT, M. C. 2012. Methane emission during municipal wastewater treatment. *Water research*, 46, 3657-3670.

- DE BELIE, N., MONTENY, J., BEELDENS, A., VINCKE, E., VAN GEMERT, D. & VERSTRAETE, W. 2004. Experimental research and prediction of the effect of chemical and biogenic sulfuric acid on different types of commercially produced concrete sewer pipes. *Cement and concrete research*, 34, 2223-2236.
- DE LOMAS, J. G., CORZO, A., GONZALEZ, J. M., ANDRADES, J. A., IGLESIAS, E. & MONTERO, M. J. 2006. Nitrate promotes biological oxidation of sulfide in wastewaters: experiment at plant-scale. *Biotechnol. Bioeng*, 93, 801-811.
- DIAZ-VALBUENA, L. R., LEVERENZ, H. L., CAPP, C. D., TCHOBANOGLOUS, G., HORWATH, W. R. & DARBY, J. L. 2011. Methane, carbon dioxide, and nitrous oxide emissions from septic tank systems. *Environmental science & technology*, 45, 2741-2747.
- DONCKELS, B., KROLL, S., VAN DORPE, M. & WEEMAES, M. 2014. Global sensitivity analysis of an in-sewer process model for the study of sulfide-induced corrosion of concrete. *Water Science & Technology*, 69, 647-655.
- DUFRESNE, M., VAZQUEZ, J., TERFOUS, A., GHENAIM, A. & POULET, J.-B. 2009. Experimental investigation and CFD modelling of flow, sedimentation, and solids separation in a combined sewer detention tank. *Computers & Fluids*, 38, 1042-1049.
- DULEKGURGEN, E., DOĞRUEL, S., KARAHAN, Ö. & ORHON, D. 2006. Size distribution of wastewater COD fractions as an index for biodegradability. *Water research*, 40, 273-282.
- DÜRRENMATT, D. J. & WANNER, O. 2014. A mathematical model to predict the effect of heat recovery on the wastewater temperature in sewers. *Water research*, 48, 548-558.
- EIJO-RÍO, E., PETIT-BOIX, A., VILLALBA, G., SUÁREZ-OJEDA, M. E., MARIN, D., AMORES, M. J., ALDEA, X., RIERADEVALL, J. & GABARRELL, X. 2015. Municipal sewer networks as sources of nitrous oxide, methane and hydrogen sulphide emissions: A review and case studies. *Journal of Environmental Chemical Engineering*, 3, 2084-2094.
- ELLIOTT, A. & TROWSDALE, S. 2007. A review of models for low impact urban stormwater drainage. *Environmental modelling & software*, 22, 394-405.
- ELMALEH, S., DELGADO, S., ALVAREZ, M., RODRIGUEZ-GOMEZ, L. & AGUIAR, E. 1998. Forecasting of H₂S build-up in a reclaimed wastewater pipe. *Water science and technology*, 38, 241-248.
- EPA, U. 2010. Inventory of U.S. Greenhouse Gas Emissions and Sinks: 1990-2008. *U.S. Environmental Protection Agency: Washington, DC*, EPA 430-R-10-006.
- EUROPEAN COMMISSION, E. 2011. Joint Research Centre (JRC)/Netherlands Environmental Assessment Agency (PBL), Emission Database for Global Atmospheric Research (EDGAR), release version 4.2. *edgar.jrc.ec.europa.eu (last access: 2013)*.
- FEZZANI, B. & CHEIKH, R. B. 2008. Implementation of IWA anaerobic digestion model No. 1 (ADM1) for simulating the thermophilic anaerobic co-digestion of olive mill wastewater with olive mill solid waste in a semi-continuous tubular digester. *Chemical Engineering Journal*, 141, 75-88.
- FIRER, D., FRIEDLER, E. & LAHAV, O. 2008. Control of sulfide in sewer systems by dosage of iron salts: comparison between theoretical and experimental results, and practical implications. *Science of the total environment*, 392, 145-156.
- FLAMINK, C., LANGEVELD, J. & CLEMENS, F. 2005. Aerobic transformations in sewer systems: are they relevant? *Water science and technology*, 52, 163-170.

- FREUDENTHAL, K., KOGLATIS, J., OTTERPOHL, R. & BEHRENDT, J. 2005. Prediction of sulfide formation in sewer pressure mains based on the IWA Anaerobic Digestion Model No. 1 (ADM1). *Water Science & Technology*, 52, 13-22.
- GANIGUE, R., GUTIERREZ, O., ROOTSEY, R. & YUAN, Z. 2011. Chemical dosing for sulfide control in Australia: an industry survey. *Water research*, 45, 6564-6574.
- GAO, W. & LU, Y. 2006. 几起中毒窒息死亡事故分析 (Investigation on Several Fatal Accidents in Sewer Systems). *劳动保护杂志 (Journal of Labour Protection)*, 1, 65-66.
- GARSDAL, H., MARK, O., DØRGE, J. & JEPSEN, S.-E. 1995. Mousetrap: modelling of water quality processes and the interaction of sediments and pollutants in sewers. *Water science and technology*, 31, 33-41.
- GOV, Y. 2015. 中国宜兴市政务网 (www.yixing.gov.cn) (In Chinese only).
- GUDJONSSON, G., VOLLERTSEN, J. & HVITVED-JACOBSEN, T. 2002. Dissolved oxygen in gravity sewers—measurement and simulation. *Water science and technology*, 45, 35-44.
- GUIDOTTI, T. 1996. Hydrogen sulphide. *Occupational Medicine*, 46, 367-371.
- GUISASOLA, A., DE HAAS, D., KELLER, J. & YUAN, Z. 2008. Methane formation in sewer systems. *Water Research*, 42, 1421-1430.
- GUISASOLA, A., SHARMA, K. R., KELLER, J. & YUAN, Z. 2009. Development of a model for assessing methane formation in rising main sewers. *Water Research*, 43, 2874-2884.
- GUJER, W., HENZE, M., MINO, T., MATSUO, T., WENTZEL, M. & MARAIS, G. 1995. The activated sludge model No. 2: biological phosphorus removal. *Water Science and Technology*, 31, 1-11.
- GUJER, W., HENZE, M., MINO, T. & VAN LOOSDRECHT, M. 1999. Activated sludge model no. 3. *Water Science and Technology*, 39, 183-193.
- GUNASEELAN, V. N. 1997. Anaerobic digestion of biomass for methane production: a review. *Biomass and bioenergy*, 13, 83-114.
- GUNNERSON, C. G., STUCKEY, D. C., GREELEY, M. & SKRINDE, R. 1986. Anaerobic digestion: Principles and practices for biogas systems.
- GUTIERREZ, O., PARK, D., SHARMA, K. R. & YUAN, Z. 2009. Effects of long-term pH elevation on the sulfate-reducing and methanogenic activities of anaerobic sewer biofilms. *Water research*, 43, 2549-2557.
- GUTIERREZ, O., PARK, D., SHARMA, K. R. & YUAN, Z. 2010. Iron salts dosage for sulfide control in sewers induces chemical phosphorus removal during wastewater treatment. *Water research*, 44, 3467-3475.
- GUTIERREZ, O., SUDARJANTO, G., REN, G., GANIGUÉ, R., JIANG, G. & YUAN, Z. 2014. Assessment of pH shock as a method for controlling sulfide and methane formation in pressure main sewer systems. *Water research*, 48, 569-578.
- HACH-UK 2017a. COD reagent products. <https://uk.hach.com/quick.search-product.search.jsa>.
- HACH-UK 2017b. DR 3900 Spectrophotometer. <https://uk.hach.com/spectrophotometers/dr3900-benchtopy-spectrophotometer/family?productCategoryId=24821455103>.
- HAMILTON, J. T., MCROBERTS, W. C., KEPPLER, F., KALIN, R. M. & HARPER, D. B. 2003. Chloride methylation by plant pectin: an efficient environmentally significant process. *Science*, 301, 206-209.
- HENSHER, D. A. & BUTTON, K. J. 2003. *Handbook of Transport and the Environment*, Elsevier.

- HENZE, M. 2000. *Activated sludge models ASM1, ASM2, ASM2d and ASM3*, IWA publishing.
- HOUHOU, J., LARTIGES, B., HOFMANN, A., FRAPPIER, G., GHANBAJA, J. & TEMGOUA, A. 2009. Phosphate dynamics in an urban sewer: A case study of Nancy, France. *Water research*, 43, 1088-1100.
- HUA, N. 2014. 武汉沼气爆炸事故分析 (The Analysis on the Sewer Explosion in Wuhan). 2014 上海国际城市地下管网建设工程展览会 (*International Conference and Exhibition on Urban Underground Network Construction Engineering, Shanghai, 2014*).
- HUGHES, M. N., CENTELLES, M. N. & MOORE, K. P. 2009. Making and working with hydrogen sulfide: the chemistry and generation of hydrogen sulfide in vitro and its measurement in vivo: a review. *Free Radical Biology and Medicine*, 47, 1346-1353.
- HUISMAN, J. & GUJER, W. 2002. Modelling wastewater transformation in sewers based on ASM3. *Water science and technology*, 45, 51-60.
- HUISMAN, J. L., GASSER, T., GIENAL, C., KÜHNI, M., KREBS, P. & GUJER, W. 2004a. Quantification of oxygen fluxes in a long gravity sewer. *Water research*, 38, 1237-1247.
- HUISMAN, J. L., WEBER, N. & GUJER, W. 2004b. Reaeration in sewers. *Water research*, 38, 1089-1100.
- HVITVED-JACOBSEN, T., VOLLERTSEN, J. & MATOS, J. S. 2002. The sewer as a bioreactor—a dry weather approach. *Water Science and technology*, 45, 11-24.
- HVITVED-JACOBSEN, T., VOLLERTSEN, J. & NIELSEN, A. H. 2013. *Sewer processes: microbial and chemical process engineering of sewer networks*, CRC press.
- HVITVED-JACOBSEN, T., VOLLERTSEN, J. & NIELSEN, P. H. 1998a. A process and model concept for microbial wastewater transformations in gravity sewers. *Water Science and Technology*, 37, 233-241.
- HVITVED-JACOBSEN, T., VOLLERTSEN, J. & TANAKA, N. 1998b. Wastewater quality changes during transport in sewers—An integrated aerobic and anaerobic model concept for carbon and sulfur microbial transformations. *Water Science and Technology*, 38, 257-264.
- IPCC 2006. Guidelines for National Greenhouse Gas Inventories, Prepared by the National Greenhouse Gas Inventories Programme, Eggleston HS, Buendia L. *Publicado por: IGES, Japón*.
- ISA, Z., GRUSENMEYER, S. & VERSTRAETE, W. 1986. Sulfate reduction relative to methane production in high-rate anaerobic digestion: technical aspects. *Applied and Environmental Microbiology*, 51, 572-579.
- ISLAS-LIMA, S., THALASSO, F. & GOMEZ-HERNANDEZ, J. 2004. Evidence of anoxic methane oxidation coupled to denitrification. *Water Research*, 38, 13-16.
- JANG, S., CHO, M., YOON, J., YOON, Y., KIM, S., KIM, G., KIM, L. & AKSOY, H. 2007. Using SWMM as a tool for hydrologic impact assessment. *Desalination*, 212, 344-356.
- JEHLICKOVA, B., LONGHURST, P. J. & DREW, G. H. 2008. Assessing effects of odour: a critical review of assessing annoyance and impact on amenity. *Odours and VOCs: Measurement, Regulation and Control Techniques*, 31, 139.
- JENNEMAN, G. E., MCINERNEY, M. & KNAPP, R. M. 1986. Effect of nitrate on biogenic sulfide production. *Applied and environmental microbiology*, 51, 1205-1211.
- JENSEN, H. S., NIELSEN, A. H., HVITVED-JACOBSEN, T. & VOLLERTSEN, J. 2009. Modeling of hydrogen sulfide oxidation in concrete corrosion products from sewer pipes. *Water Environment Research*, 81, 365-373.

- JIAN-LING, Z. 2011. Discussion on application and development of septic tank [J]. *Shanxi Architecture*, 26, 083.
- JIANG, F., LEUNG, D. H.-W., LI, S., CHEN, G.-H., OKABE, S. & VAN LOOSDRECHT, M. C. 2009. A biofilm model for prediction of pollutant transformation in sewers. *water research*, 43, 3187-3198.
- JIANG, F., LEUNG, H. D., LI, S., LIN, G. & CHEN, G. 2007. A new method for determination of parameters in sewer pollutant transformation process model. *Environmental technology*, 28, 1217-1225.
- JIANG, G., KEATING, A., CORRIE, S., O'HALLORAN, K., NGUYEN, L. & YUAN, Z. 2013. Dosing free nitrous acid for sulfide control in sewers: results of field trials in Australia. *Water research*, 47, 4331-4339.
- JIANGUO, B., ANQUAN, D. & HONGDE, L. 2007. 市政管道工程施工 (Urban Drainage Engineering). 中国建筑工业出版社 (China Construction Industry Press) .
- JIN, J. 2009. 城市排水系统运行状况研究 (The Investigation and Analysis on the Current Operations of Urban Drainage system). 科技资讯 (Science & Technology Information), (15)27-35.
- JONES JR, D. E. Design and Construction of Sanitary and Storm Sewers. 1970. ASCE.
- KAEMPFER, W. & BERNDT, M. Polymer modified mortar with high resistance to acid to corrosion by biogenic sulfuric acid. Proceedings of the IXth ICPIG Congress, Bologna, Italy, 14th, 1998. 681-687.
- KALANTARI, Z., LYON, S. W., FOLKESON, L., FRENCH, H. K., STOLTE, J., JANSSON, P.-E. & SASSNER, M. 2014. Quantifying the hydrological impact of simulated changes in land use on peak discharge in a small catchment. *Science of the Total Environment*, 466, 741-754.
- KARAHAN, Ö., DOGRUEL, S., DULEKGURGEN, E. & ORHON, D. 2008. COD fractionation of tannery wastewaters—particle size distribution, biodegradability and modeling. *Water Research*, 42, 1083-1092.
- KHALIL, M. 1999. Non-CO2 greenhouse gases in the atmosphere. *Annual Review of Energy and the Environment*, 24, 645-661.
- KIENOW, K. E., POMEROY, R. D. & KIENOW, K. K. 1982. Prediction of Sulfide Buildup in Sanitary Sewers. *Journal of the Environmental Engineering Division*, 108, 941-956.
- KNOBLAUCH, A. & STEINER, B. 1999. Major accidents related to manure: a case series from Switzerland. *International journal of occupational and environmental health*, 5, 177-186.
- KOUDELAK, P. & WEST, S. 2008. Sewerage network modelling in Latvia, use of InfoWorks CS and Storm Water Management Model 5 in Liepaja city. *Water and Environment Journal*, 22, 81-87.
- KOYAMA, T. 1963. Gaseous metabolism in lake sediments and paddy soils and the production of atmospheric methane and hydrogen. *Journal of Geophysical Research*, 68, 3971-3973.
- LAHAV, O., BINDER, A. & FRIEDLER, E. 2006a. A different approach for predicting reaeration rates in gravity sewers and completely mixed tanks. *Water environment research*, 78, 730-739.
- LAHAV, O., LU, Y., SHAVIT, U. & LOEWENTHAL, R. E. 2004. Modeling hydrogen sulfide emission rates in gravity sewage collection systems. *Journal of environmental engineering*, 130, 1382-1389.
- LAHAV, O., SAGIV, A. & FRIEDLER, E. 2006b. A different approach for predicting H₂S (g) emission rates in gravity sewers. *Water research*, 40, 259-266.

- LAPLACE, D., BACHOC, A., SANCHEZ, Y. & DARTUS, D. 1992. Trunk sewer clogging development–description and solutions. *Water Science and Technology*, 25, 91-100.
- LAWRENCE, A. W. & MCCARTY, P. L. 1969. Kinetics of methane fermentation in anaerobic treatment. *Journal (Water Pollution Control Federation)*, R1-R17.
- LEBRERO, R., BOUCHY, L., STUETZ, R. & MUNOZ, R. 2011. Odor assessment and management in wastewater treatment plants: a review. *Critical Reviews in Environmental Science and Technology*, 41, 915-950.
- LEE, K., PARK, K., KHANAL, S. & LEE, J. 2013. Effects of household detergent on anaerobic fermentation of kitchen wastewater from food waste disposer. *Journal of hazardous materials*, 244, 39-45.
- LEE, S.-B., YOON, C.-G., JUNG, K. W. & HWANG, H. S. 2010. Comparative evaluation of runoff and water quality using HSPF and SWMM. *Water Science and Technology*, 62, 1401-1409.
- LETTINGA, G. 1995. Anaerobic digestion and wastewater treatment systems. *Antonie van leeuwenhoek*, 67, 3-28.
- LI, D. 2007. 城市下水道爆炸的原因及处置措施 (The analysis and management of sewer explosions in urban drainage system). *消防技术与产品信息(Fire Technology & Information)*, 4, 35-36.
- LI, H., LIU, L., LI, M. & ZHANG, X. 2013. Effects of pH, temperature, dissolved oxygen, and flow rate on phosphorus release processes at the sediment and water interface in storm sewer. *Journal of analytical methods in chemistry*, 2013.
- LINDE 2017. Gas concentraton units converter. http://hiq.linde-gas.com/en/specialty_gases/gas_concentration_units_converter.html.
- LIONG, S.-Y., CHAN, W. T. & SHREERAM, J. 1995. Peak-flow forecasting with genetic algorithm and SWMM. *Journal of Hydraulic Engineering*, 121, 613-617.
- LIU, Y., GANIGUÉ, R., SHARMA, K. & YUAN, Z. 2016a. Event-driven model predictive control of sewage pumping stations for sulfide mitigation in sewer networks. *Water research*, 98, 376-383.
- LIU, Y., NI, B.-J., GANIGUÉ, R., WERNER, U., SHARMA, K. R. & YUAN, Z. 2015a. Sulfide and methane production in sewer sediments. *water research*, 70, 350-359.
- LIU, Y., NI, B.-J., SHARMA, K. R. & YUAN, Z. 2015b. Methane emission from sewers. *Science of the Total Environment*, 524, 40-51.
- LIU, Y., SHARMA, K. R., FLUGGEN, M., O'HALLORAN, K., MURTHY, S. & YUAN, Z. 2015c. Online dissolved methane and total dissolved sulfide measurement in sewers. *water research*, 68, 109-118.
- LIU, Y., TUGTAS, A. E., SHARMA, K. R., NI, B.-J. & YUAN, Z. 2016b. Sulfide and methane production in sewer sediments: field survey and model evaluation. *Water research*, 89, 142-150.
- LIU, Y., WU, C., ZHOU, X., ZHU, D. Z. & SHI, H. 2015d. Sulfide elimination by intermittent nitrate dosing in sewer sediments. *Journal of Environmental Sciences*, 27, 259-265.
- LOWE, S. A. 2010. Sanitary sewer design using EPA storm water management model (SWMM). *Computer Applications in Engineering Education*, 18, 203-212.
- MADSEN, H. I., HVITVED-JACOBSEN, T. & VOLLERTSEN, J. 2006. Gas phase transport in gravity sewers—A methodology for determination of horizontal gas transport and ventilation. *Water environment research*, 78, 2203-2209.
- MAKOWSKA, M. & SPYCHAŁA, M. 2014. Organic compounds fractionation for domestic wastewater treatment modeling. *Polish Journal of Environmental Studies*, 23, 131-137.

- MANNINA, G., FRENI, G., VIVIANI, G., SÆGROV, S. & HAFSKJOLD, L. 2006. Integrated urban water modelling with uncertainty analysis. *Water Science and Technology*, 54, 379-386.
- MARLENI, N., GRAY, S., SHARMA, A., BURN, S. & MUTTIL, N. 2015. Impact of water management practice scenarios on wastewater flow and contaminant concentration. *Journal of environmental management*, 151, 461-471.
- MARLENI, N., GRAY, S. R., SHARMA, A., BURN, S. & MUTTIL, N. 2012. Impact of water source management practices in residential areas on sewer networks-a review. *Water Science and Technology*, 65, 624-642.
- MARSALEK, J., CISNEROS, B. J., KARAMOUZ, M., MALMQUIST, P.-A., GOLDENFUM, J. A. & CHOCAT, B. 2008. *Urban Water Cycle Processes and Interactions: Urban Water Series-UNESCO-IHP*, CRC Press.
- MATHIOUDAKIS, V. & AIVASIDIS, A. 2009. Effect of temperature on anoxic sulfide oxidation and denitrification in the bulk wastewater phase of sewer networks. *Water Science and Technology*, 59, 705-712.
- MATIAS, N., NIELSEN, A. H., VOLLERTSEN, J., FERREIRA, F. & MATOS, J. S. Modelling The Release Of Volatile Compounds At Sewer Drop Structures-Application Of New Findings. Proceedings of the 10th International Urban Drainage Modelling Conference, 2015. 10th International Urban Drainage Modelling Conference.
- MATOS, J. & AIRES, C. 1995. Mathematical modelling of sulphides and hydrogen sulphide gas build-up in the Costa do Estoril sewerage system. *Water Science and Technology*, 31, 255-261.
- MAY, R., BROWN, P., HARE, G. & JONES, K. 1989. Self-cleaning conditions for sewers carryign sediment.
- MCCARTY, P. L. 1964. Anaerobic waste treatment fundamentals. *Public works*, 95, 107-112.
- MELNICK, M. & MELNICK, R. A. S., A. 1994. Manhole covers. *MIT press*.
- METCALF, E. 2003. Inc., wastewater engineering, treatment and reuse. *New York: McGraw-Hill*.
- MICHIELS, A. & SALGAONKAR, J. 1994. A Computer Model for Estimation of Atmospheric Hydrogen Sulfide Concentrations in Sanitary Sewers. *Proc. Odor and Volatile Organic Compound Emission Control for Municipal and Industrial Wastewater Treatment Facilities, Jacksonville, FL,]-39*.
- MINAMI, K. & TAKATA, K. 1997. Atmospheric methane: sources, sinks, and strategies for reducing agricultural emissions. *Water Science and Technology*, 36, 509-516.
- MITCHELL, V., DUNCAN, H., INMAN, M., RAHILLY, M., STEWART, J., VIERITZ, A., HOLT, P., GRANT, A., FLETCHER, T. D. & COLEMAN, J. 2007. State of the art review of integrated urban water models. *Novatech Lyon, France*, 1-8.
- MMBW 1989. Melbourne and Metropolitan Board of Works-hydrogen Sulphide Control Manual-septicity, Corrosion and Odour Control in Sewerage Systems. *Technological Standing Committee on Hydrogen Sulphide Corrosion in Sewerage Works*.
- MONTENY, J., DE BELIE, N., VINCKE, E., VERSTRAETE, W. & TAERWE, L. 2001. Chemical and microbiological tests to simulate sulfuric acid corrosion of polymer-modified concrete. *Cement and Concrete Research*, 31, 1359-1365.
- MOURATO, S., MATOS, J., ALMEIDA, M. & HVITVED-JACOBSEN, T. 2003. Modelling in-sewer pollutant degradation processes in the Costa do Estoril sewer system. *Water Science and Technology*, 47, 93-100.

- MUNSON, B. R., ROTHMAYER, A. P. & OKIISHI, T. H. 2012. *Fundamentals of Fluid Mechanics, 7th Edition*, John Wiley & Sons, Incorporated.
- NGUYEN, L., SCHAELEI, B., SAGE, D., KAYAL, S., JEANBOURQUIN, D., BARRY, D. A. & ROSSI, L. 2009. Vision-based system for the control and measurement of wastewater flow rate in sewer systems. *Water Science and Technology*, 60, 2281-2289.
- NIELSEN, A., YONGSIRI, C., HVITVED-JACOBSEN, T. & VOLLERTSEN, J. 2005a. Simulation of sulfide buildup in wastewater and atmosphere of sewer networks. *Water Science & Technology*, 52, 201-208.
- NIELSEN, A. H., HVITVED-JACOBSEN, T. & VOLLERTSEN, J. 2006a. Recent findings on sinks for sulfide in gravity sewer networks. *Water science and technology*, 54, 127-134.
- NIELSEN, A. H., HVITVED-JACOBSEN, T. & VOLLERTSEN, J. 2012. Effect of sewer headspace air-flow on hydrogen sulfide removal by corroding concrete surfaces. *Water Environment Research*, 84, 265-273.
- NIELSEN, A. H., LENS, P., VOLLERTSEN, J. & HVITVED-JACOBSEN, T. 2005b. Sulfide-iron interactions in domestic wastewater from a gravity sewer. *Water research*, 39, 2747-2755.
- NIELSEN, A. H. & VOLLERTSEN, J. Monitoring the Startup of a Sacrificial Concrete Sewer for Odor Control. Proceedings of the 13th International Conference on Urban Drainage, 2014. The International Conference on Urban Drainage.
- NIELSEN, A. H., VOLLERTSEN, J. & HVITVED-JACOBSEN, T. 2006b. Kinetics and stoichiometry of aerobic sulfide oxidation in wastewater from sewers—Effects of pH and temperature. *Water environment research*, 78, 275-283.
- NIELSEN, A. H., VOLLERTSEN, J., JENSEN, H. S., MADSEN, H. I. & HVITVED-JACOBSEN, T. 2008a. Aerobic and anaerobic transformations of sulfide in a sewer system—field study and model simulations. *Water Environment Research*, 80, 16-25.
- NIELSEN, A. H., VOLLERTSEN, J., JENSEN, H. S., WIUM-ANDERSEN, T. & HVITVED-JACOBSEN, T. 2008b. Influence of pipe material and surfaces on sulfide related odor and corrosion in sewers. *Water research*, 42, 4206-4214.
- NIELSEN, P. H. 1987. Biofilm dynamics and kinetics during high-rate sulfate reduction under anaerobic conditions. *Applied and Environmental Microbiology*, 53, 27-32.
- NIELSEN, P. H. & HVITVED-JACOBSEN, T. 1988. Effect of sulfate and organic matter on the hydrogen sulfide formation in biofilms of filled sanitary sewers. *Journal (Water Pollution Control Federation)*, 627-634.
- NIELSEN, P. H., RAUNKJÆR, K. & HVITVED-JACOBSEN, T. 1998. Sulfide production and wastewater quality in pressure mains. *Water Science and Technology*, 37, 97-104.
- NIELSEN, P. H., RAUNKJÆR, K., NORSKER, N. H., JENSEN, N. A. & HVITVED-JACOBSEN, T. 1992. Transformation of wastewater in sewer systems—a review. *Water Science and Technology*, 25, 17-31.
- NORMAK, A., SUURPERE, J., SUITSO, I., JÕGI, E., KOKIN, E. & PITK, P. 2015. Improving ADM1 model to simulate anaerobic digestion start-up with inhibition phase based on cattle slurry. *Biomass and Bioenergy*, 80, 260-266.
- NYT 2012. One Dead and Several Others Are Injured In Blasts Of Ottawa Sewers. *The New York Times*
<http://query.nytimes.com/gst/abstract.html?res=940DE1D61330E33ABC4850DFB3668382639EDE&legacy=true>.
- OMIL, F., LENS, P., VISSER, A., HULSHOFF POL, L. & LETTINGA, G. 1998. Long - term competition between sulfate reducing and methanogenic bacteria in UASB

- reactors treating volatile fatty acids. *Biotechnology and Bioengineering*, 57, 676-685.
- ORHON, D., ATEŞ, E., SÖZEN, S. & ÇOKGÖR, E. U. 1997. Characterization and COD fractionation of domestic wastewaters. *Environmental Pollution*, 95, 191-204.
- OSTOJIN, S., MOUNCE, S., SINGERTON, D. & BOXALL, J. 2011. Autonomous fuzzy logic control of pumping in sewer systems.
- PACHAURI, R. K., ALLEN, M. R., BARROS, V. R., BROOME, J., CRAMER, W., CHRIST, R., CHURCH, J. A., CLARKE, L., DAHE, Q. & DASGUPTA, P. 2014. *Climate change 2014: synthesis report. Contribution of Working Groups I, II and III to the fifth assessment report of the Intergovernmental Panel on Climate Change*, IPCC.
- PAI, T.-Y., CHEN, C., CHUNG, H., HO, H. & SHIU, T. 2010. Monitoring and assessing variation of sewage quality and microbial functional groups in a trunk sewer line. *Environmental monitoring and assessment*, 171, 551-560.
- PAINTER, H. & LOVELESS, J. 1983. Effect of temperature and pH value on the growth-rate constants of nitrifying bacteria in the activated-sludge process. *Water research*, 17, 237-248.
- PARK, K., LEE, H., PHELAN, S., LIYANAARACHCHI, S., MARLENI, N., NAVARATNA, D., JEGATHEESAN, V. & SHU, L. 2014. Mitigation strategies of hydrogen sulphide emission in sewer networks–A review. *International Biodeterioration & Biodegradation*, 95, 251-261.
- PARKINSON, J., SCHÜTZE, M. & BUTLER, D. 2005. MODELLING THE IMPACTS OF DOMESTIC WATER CONSERVATION ON THE SUSTAIN ABILITY OF THE URBAN SEWERAGE SYSTEM. *Water and Environment Journal*, 19, 49-56.
- PATNAIK, P. 2007. *A comprehensive guide to the hazardous properties of chemical substances*, John Wiley & Sons.
- PERRIN, D. D. 2013. *Ionisation constants of inorganic acids and bases in aqueous solution*, Elsevier.
- PETTS, J. & EDULJEE, G. 1994. Integration of monitoring, auditing and environmental assessment: waste facility issues. *Project Appraisal*, 9, 231-241.
- PHILIP, H., MAUNOIR, S., RAMBAUD, A. & PHILIPPI, L. 1993. Septic tank sludges: accumulation rate and biochemical characteristics. *Water Science and Technology*, 28, 57-64.
- POMEROY, R. 1945. The pros and cons of sewer ventilation. *Sewage Works Journal*, 203-208.
- POMEROY, R. 1959. Generation and control of sulfide in filled pipes. *Sewage and industrial Wastes*, 31, 1082-1095.
- POMEROY, R. & PARKHURST, J. 1977. Forecasting of sulfide buildup rates in sewers. *Progress in water technology*, 9, 621-&.
- PRESCOTT, L. M., HARLEY, J. & KLEIN, D. 2005. *Microbiology*, 6th. McGrawHill Higher Education.
- RAO, J., ZHU, Y., LI, Q., LIU, Z. & XIAO, L. 2016. Revelation of Fushougou ditch's conception for the construction of modern sponge city. *Journal of Yangtze River*, 47, 32-37.
- RASKIN, L., RITTMANN, B. E. & STAHL, D. A. 1996. Competition and coexistence of sulfate-reducing and methanogenic populations in anaerobic biofilms. *Applied and Environmental Microbiology*, 62, 3847-3857.
- RAUNKJÆR, K., HVITVED-JACOBSEN, T. & NIELSEN, P. H. 1994. Measurement of pools of protein, carbohydrate and lipid in domestic wastewater. *Water Research*, 28, 251-262.

- READ, G. F. 2004. *Sewers: Replacement and New Construction: Replacement and New Construction*, Butterworth-Heinemann.
- REICHERT, P., BORCHARDT, D., HENZE, M., RAUCH, W., SHANAHAN, P., SOMLYÓDY, L. & VANROLLEGHEM, P. 2001. River water quality model no. 1 (RWQM1): II. Biochemical process equations. *Water Science and Technology*, 43, 11-30.
- REIFFENSTEIN, R., HULBERT, W. C. & ROTH, S. H. 1992. Toxicology of hydrogen sulfide. *Annual review of pharmacology and toxicology*, 32, 109-134.
- RICHARD, M., BROWN, S. & COLLINS, F. Activated sludge microbiology problems and their control. 20th Annual USEPA National Operator Trainers Conference, 2003. 1-21.
- RINZEMA, A. & LETTINGA, G. 1988. Anaerobic treatment of sulfate containing wastewater.
- ROMER, A. E. & KIENOW, K. K. 2004. Rubber Gasket Concrete Pipe Joints...: Eliminating the Smoke and Mirrors. *Pipeline Engineering and Construction: What's on the Horizon?*
- ROSSMAN, L. A. 2010. *Storm water management model user's manual, version 5.0*, National Risk Management Research Laboratory, Office of Research and Development, US Environmental Protection Agency Cincinnati, OH.
- RUBINATO, M., SHUCKSMITH, J., SAUL, A. J. & SHEPHERD, W. 2013. Comparison between InfoWorks hydraulic results and a physical model of an urban drainage system. *Water Science and Technology*, 68, 372-379.
- RUDELLE, E., VOLLERTSEN, J., HVITVED-JACOBSEN, T. & NIELSEN, A. H. 2011. Anaerobic transformations of organic matter in collection systems. *Water Environment Research*, 83, 532-540.
- RUDELLE, E., VOLLERTSEN, J., HVITVED-JACOBSEN, T. & NIELSEN, A. H. 2012. Modeling anaerobic organic matter transformations in the wastewater phase of sewer networks. *Water Science & Technology*, 66, 1728-1734.
- SAFONIUK, M. 2004. Wastewater Engineering: Treatment and Reuse. *Chemical Engineering*, 111, 10-12.
- SALTELLI, A., RATTO, M., ANDRES, T., CAMPOLONGO, F., CARIBONI, J., GATELLI, D., SAISANA, M. & TARANTOLA, S. 2008. *Global sensitivity analysis: the primer*, John Wiley & Sons.
- SANTRY, J. W. 1963. Hydrogen sulfide in sewers. *Journal of the Water Pollution Control Federation*, 35, 1580-1588.
- SARAH, S. & ALBERT LEA, T. 2012. Sewer gas blamed for southern Minnesota house explosion that injured man. *ChelanHomeWatch | articles*.
- SCHMITT, F. & SEYFRIED, C. 1992. Sulfate reduction in sewer sediments. *Water Science and Technology*, 25, 83-90.
- SCHREIBER, L., HOLLER, T., KNITTEL, K., MEYERDIERKS, A. & AMANN, R. 2010. Identification of the dominant sulfate - reducing bacterial partner of anaerobic methanotrophs of the ANME - 2 clade. *Environmental microbiology*, 12, 2327-2340.
- SENA, H. C., CARIOCA, J. M., 2013. odor control with application of calcium nitrate - case study in the municipalities of santos and divinolandia Brazil. *5th IWA conference on Odour and Air emissions. San Francisco USA*.
- SHARMA, K., CORRIE, S. & YUAN, Z. 2012. Integrated modelling of sewer system and wastewater treatment plant for investigating the impacts of chemical dosing in sewers. *Water Science and Technology*, 65, 1399-1405.
- SHARMA, K., DERLON, N., HU, S. & YUAN, Z. 2014. Modeling the pH effect on sulfidogenesis in anaerobic sewer biofilm. *water research*, 49, 175-185.

- SHARMA, K., GANIGUE, R. & YUAN, Z. 2013. pH dynamics in sewers and its modeling. *Water research*, 47, 6086-6096.
- SHARMA, K. R., YUAN, Z., DE HAAS, D., HAMILTON, G., CORRIE, S. & KELLER, J. 2008. Dynamics and dynamic modelling of H₂S production in sewer systems. *Water Research*, 42, 2527-2538.
- SHYPANSKI, A., YUAN, Z. & SHARMA, K. R. 2015. Evaluating impacts of demand management on sewer corrosion. *10th International Urban Drainage Conference*.
- SINA, N. 2013. Sewer Explosion in Wenzhou City. <http://zj.sina.com.cn/news/d/2013-12-04/0755147559.html>.
- SŁYŚ, D. & STEC, A. 2012. Hydrodynamic modelling of the combined sewage system for the city of Przemyśl. *Environment Protection Engineering*, 38, 99-112.
- SOUZA, C., CHERNICHARO, C. & MELO, G. 2012. Methane and hydrogen sulfide emissions in UASB reactors treating domestic wastewater. *Water Science and Technology*, 65, 1229-1237.
- SPENCER, A. U., NOLAND, S. S. & GOTTLIEB, L. J. 2006. Bathtub fire: an extraordinary burn injury. *Journal of burn care & research*, 27, 97-98.
- SU, X., MO, X., HUANG, Z. & YU, M. 2011. 试论化粪池设置的必要性 (The Discussion on the Necessity of Septic Tanks in Modern Urban Drianage System). *实用技术 (Operative Technology)*, 12 (4), 23 - 27.
- SUAREZ, J. & PUERTAS, J. 2005. Determination of COD, BOD, and suspended solids loads during combined sewer overflow (CSO) events in some combined catchments in Spain. *Ecological Engineering*, 24, 199-217.
- SUCKER, K., BOTH, R. & WINNEKE, G. 2009. Review of adverse health effects of odours in field studies. *Water Science and Technology*, 59, 1281-1289.
- SUN, J., HU, S., SHARMA, K. R., BUSTAMANTE, H. & YUAN, Z. 2015. Impact of reduced water consumption on sulfide and methane production in rising main sewers. *Journal of Environmental Management*, 154, 307-315.
- SWAMEE, P. K., BHARGAVA, R. & SHARMA, A. K. 1987. Noncircular sewer design. *Journal of Environmental Engineering*, 113, 824-833.
- SWAMEE, P. K. & SHARMA, A. K. 2013. Optimal design of a sewer line using linear programming. *Applied Mathematical Modelling*, 37, 4430-4439.
- SYDNEY, R., ESFANDI, E. & SURAPANENI, S. 1996. Control concrete sewer corrosion via the crown spray process. *Water environment research*, 68, 338-347.
- TANAKA, N., HVITVED-JACOBSEN, T. & HORIE, T. 2000. Transformations of carbon and sulfur wastewater components under aerobic-anaerobic transient conditions in sewer systems. *Water environment research*, 651-664.
- TENCENT, N. 2015. Several Sewer Methane Explosion Incidents Analysis. http://www.weixinyidu.com/n_77122.
- THINGLAS, T. & KAUSHAL, D. 2008. Three-dimensional CFD modeling for optimization of invert trap configuration to be used in sewer solids management. *Particulate Science and Technology*, 26, 507-519.
- THISTLETHWAYTE, D. K. B. 1972. *Control of sulphides in sewerage systems*, Ann Arbor Science.
- TING, C. & LEE, D. 2007. Production of hydrogen and methane from wastewater sludge using anaerobic fermentation. *International Journal of Hydrogen Energy*, 32, 677-682.
- TOMAR, M. & ABDULLAH, T. H. 1994. Evaluation of chemicals to control the generation of malodorous hydrogen sulfide in waste water. *Water Research*, 28, 2545-2552.

- TRANSFER, U. S. E. P. A. O. O. T. & POMEROY, R. D. 1974. *Process design manual for sulfide control in sanitary sewerage systems*.
- TSIHRINTZIS, V. A. & HAMID, R. 1998. Runoff quality prediction from small urban catchments using SWMM. *Hydrological Processes*, 12, 311-329.
- U.S. ENVIRONMENTAL PROTECTION AGENCY (EPA), W., D.C. 2004. Report to Congress on Impacts and Control of CSO's and SSO's. *August 2004. Document No. EPA-833-R-04-001*.
- USEPA 1991. Hydrogen sulphide corrosion in wastewater collection and treatment system. *Technical Report, 430/09-91-010*.
- VALENTINE, D. L. & REEBURGH, W. S. 2000. New perspectives on anaerobic methane oxidation. *Environmental Microbiology*, 2, 477-484.
- VAVILIN, V., FERNANDEZ, B., PALATSI, J. & FLOTATS, X. 2008. Hydrolysis kinetics in anaerobic degradation of particulate organic material: an overview. *Waste management*, 28, 939-951.
- VINCKE, E. 2009. *Biogenic sulfuric acid corrosion of concrete: microbial interaction, simulation and prevention*, Universiteit Gent.
- VOLLERTSEN, J., DO CÉU ALMEIDA, M. & HVITVED-JACOBSEN, T. 1999. Effects of temperature and dissolved oxygen on hydrolysis of sewer solids. *Water Research*, 33, 3119-3126.
- VOLLERTSEN, J. & HVITVED-JACOBSEN, T. 2000. Sewer quality modeling—a dry weather approach. *Urban Water*, 2, 295-303.
- VOLLERTSEN, J. & HVITVED-JACOBSEN, T. 2002. Biodegradability of wastewater—a method for COD-fractionation. *Water science and technology*, 45, 25-34.
- VOLLERTSEN, J., HVITVED-JACOBSEN, T. & NIELSEN, A. H. 2005. Stochastic modeling of chemical oxygen demand transformations in gravity sewers. *Water environment research*, 77, 331-339.
- VOLLERTSEN, J., NIELSEN, A. H., JENSEN, H. S. & HVITVED-JACOBSEN, T. 2008a. Modeling the formation and fate of odorous substances in collection systems. *Water Environment Research*, 80, 118-126.
- VOLLERTSEN, J., NIELSEN, A. H., JENSEN, H. S., RUDELLE, E. A. & HVITVED-JACOBSEN, T. Modeling the corrosion of concrete sewers. 12th international conference on urban drainage, 2011a.
- VOLLERTSEN, J., NIELSEN, A. H., JENSEN, H. S., WIUM-ANDERSEN, T. & HVITVED-JACOBSEN, T. 2008b. Corrosion of concrete sewers—the kinetics of hydrogen sulfide oxidation. *Science of the total Environment*, 394, 162-170.
- VOLLERTSEN, J., NIELSEN, L., BLICHER, T. D., HVITVED-JACOBSEN, T. & NIELSEN, A. H. 2011b. A sewer process model as planning and management tool—hydrogen sulfide simulation at catchment scale. *Water Science & Technology*, 64, 348-354.
- WAKI, M., SUZUKI, K., OSADA, T. & TANAKA, Y. 2005. Methane-dependent denitrification by a semi-partitioned reactor supplied separately with methane and oxygen. *Bioresource technology*, 96, 921-927.
- WALTRIP, G. D. & SNYDER, E. G. 1985. Elimination of odor at six major wastewater treatment plants. *Journal (Water Pollution Control Federation)*, 1027-1032.
- WANG, A. 2008. 城市排水系统建设中存在的问题及对策 (Current Problems and Solutions for the Construction of Urban Drainage System in China). *中国给水排水 (China Water Supply & Drainage)*, 19(3), 27.
- WANG, J., ZHANG, J., XIE, H., QI, P., REN, Y. & HU, Z. 2011. Methane emissions from a full-scale A/A/O wastewater treatment plant. *Bioresource Technology*, 102, 5479-5485.

- WAPUG 2002. Code of practice for the hydraulic modelling of sewer systems. [http://www.ciwem.org/groups/wapug/Modelling COP Ver 03.pdf](http://www.ciwem.org/groups/wapug/Modelling_COP_Ver_03.pdf).
- WARD, M., HAMER, G., MCDONALD, A., WITHERSPOON, J., LOH, E. & PARKER, W. 2011. A sewer ventilation model applying conservation of momentum. *Water Science and Technology*, 64, 1374-1382.
- WILLEMS, P. 2006. Random number generator or sewer water quality model? *Water Science & Technology*, 54, 387-394.
- WITHERSPOON, J., ALLEN, E. & QUIGLEY, C. 2004. Modelling to assist in wastewater collection system odour and corrosion potential evaluations. *Water Science and Technology*, 50, 177-183.
- XU, S. & HASSELBLAD, S. 1996. A simple biological method to estimate the readily biodegradable organic matter in wastewater. *Water Research*, 30, 1023-1025.
- YANG, W., VOLLERTSEN, J. & HVITVED-JACOBSEN, T. 2005. Anoxic sulfide oxidation in wastewater of sewer networks. *Water science and technology*, 52, 191-199.
- YODA, M., KITAGAWA, M. & MIYAJI, Y. 1987. Long term competition between sulfate-reducing and methane-producing bacteria for acetate in anaerobic biofilm. *Water Research*, 21, 1547-1556.
- YONGSIRI, C., HVITVED-JACOBSEN, T., VOLLERTSEN, J. & TANAKA, N. 2003. Introducing the emission process of hydrogen sulfide to a sewer process model (WATS). *Water Science and Technology*, 47, 85-92.
- YONGSIRI, C., VOLLERTSEN, J. & HVITVED-JACOBSEN, T. 2004a. Effect of temperature on air-water transfer of hydrogen sulfide. *Journal of Environmental Engineering*, 130, 104-109.
- YONGSIRI, C., VOLLERTSEN, J. & HVITVED-JACOBSEN, T. 2004b. Hydrogen sulfide emission in sewer networks: a two-phase modeling approach to the sulfur cycle. *Water Science and Technology*, 50, 161-168.
- YONGSIRI, C., VOLLERTSEN, J. & HVITVED-JACOBSEN, T. 2005. Influence of wastewater constituents on hydrogen sulfide emission in sewer networks. *Journal of environmental engineering*, 131, 1676-1683.
- ZABETAKIS, M. G. 1965. Flammability characteristics of combustible gases and vapors. DTIC Document.
- ZARRA, T., NADDEO, V., BELGIORNO, V., REISER, M. & KRANERT, M. 2008. Odour monitoring of small wastewater treatment plant located in sensitive environment. *Water Science and Technology*, 58, 89-94.
- ZHANG, B. & NI, G. 2005. 城市水环境工程 (Urban Water & Drainage Engineering) . 清华大学出版社 (Tsinghua University Press) .
- ZHANG, L., DE SCHRYVER, P., DE GUSSEME, B., DE MUYNCK, W., BOON, N. & VERSTRAETE, W. 2008. Chemical and biological technologies for hydrogen sulfide emission control in sewer systems: A review. *Water Research*, 42, 1-12.
- ZHANG, M., HE, J., LIU, Y. & SHI, H. 2017. Estimation and optimization operation in dealing with inflow and infiltration of a hybrid sewerage system in limited infrastructure facility data. *Frontiers of Environmental Science & Engineering*, 11:7.
- ZHOU, X. & ZHANG, Q. 2003. Measurements of odour and hydrogen sulfide emissions from swine barns. *Canadian Biosystems Engineering*, 45, 6.13-6.13.
- ZHOU, Y., HUANG, J., NING, P., YANG, L. & ZHOU, X. 2013. simulative experimental research of methane production in sewer systems in Kunming. *Chinese Journal of Environmental Engineering*, 1673-9108(2013).
- ZOPPOU, C. 2001. Review of urban storm water models. *Environmental Modelling & Software*, 16, 195-231.

